ISBN 0-612-15760-1

Canada

UNIVERSITÉ D'OTTAWA
UNIVERSITY OF OTTAWA

ABSTRACT

This study presents a strategy for position feedback control, a so-called self-adjusting adaptive sliding mode controller, to obtain a desired steady state error for a DC-motor servo in the presence of Coulomb friction and stiction. Sliding mode controllers are of the type of nonlinear controllers which have been studied extensively by Russian scientists, including V.I. Utkin and V. Itkis. The self adjusting sliding mode control method that this thesis is focused on is an adaptive discontinuous controller with an approximated sliding mode trajectory. The study is concerned with both analytical and experimental performances of such a class of control strategy and a PID (proportional integral and derivative) controller in the presence of dry friction for the purpose of comparison. The study also investigates the effect of nonlinear phenomenon such as torque saturation on the states of the variables of such a system. The result of the paper is finally based on the suitable performance of the suggested control methodology utilizing a new form of sliding mode controller for the second order class of systems, rather than the conventional forms from V. Itkis and V.I. Utkin.

ACKNOWLEDGEMENT

I would sincerely like to thank Dr. D. Necsulescu for this patience, efforts and valuable suggestions to me during the writing of this report.

I would also like to thank my parents, particularly my mother for her great support during my studies, and my uncle for this ongoing help.

TABLE OF CONTENTS

LIST OF FIGURES

GLOSSARY OF NECESSARY SYMBOLS

a_1 or a1	The exact(ideal) position-error parameter
a_2 or a2	The exact(ideal) velocity-error parameter
$\hat{a}_1$	The measured position error parameter
$\hat{a}_2$	The measured velocity error parameter
b	The ideal controller u parameter [bu]
$\hat{b}$	The measured controller u parameter [$\hat{}$bu]
c,C	The slope of switching line
C_o	The initial slop of switching line.
C_{max}	The slope of switching line resulting from the sliding condition for the initial point [equation II.2-40]
c(t),C(t)	The slope variable of switching line
C1,c_1	The variable resulting from the sliding condition [equations II.2-39 and III.2-11]
D	The Coulomb friction parameter [used in section III.2(S3-4) as Dsgn(x_2). The real value is D=dw_o^2]
Dec	Decimal (0-127).
D'	The stiction parameter [used in section III.2(S3-4) as D'sgn(x_2). The real value is D'=d'w_o^2]
d	The Coulomb friction coefficient [used in section II.3 as dw_o^2 sgn(x_2)]
d'	The stiction coefficient [used in section II.3 as d'w_o^2 sgn(x_2)]
G(s)	Transfer function in Laplace-transform
G(z)	Transfer function in z-transform
J	Total mass moment of inertia of the system
J_L	The mass moment of inertia of the load
J_M	The motor mass moment of inertia of the shaft

K	The gain of the sliding mode controllers
K^1	The gain of the sliding mode controller, type B [equation III.2-14]
k	The integer constant k=1,2...n
k1	The secondary gain of the controller, type B [equation III.2-14]
K_p	The proportional gain of the PID controller
m_T	The parameter, representing different saturation levels (ideal and actual saturation)
R	Resistor symbol
T	Sampling time
T_c	Coulomb friction torque
T_e	Effective torque
T_M	Motor torque
T_{sat}	Saturation torque
Ts or T_s	Sampling time
t	Time
t_c	Time constant of the system
t_o	Initial time
t_s	Settling time
V	Voltage
u	Controller [control law]
u^- or U^-	The bound of controller u, for the space of $\sigma<0$
u^+ or U^+	The bound of controller u, for the space of $\sigma>0$
x	2 x 1 matrix consists of variables of the system x1,x2
$\dot{x}$	2 x 1 matrix consists of derivatives of the variables of the system
x_1 or x1	The variable of position error

x_2 or x2	The variable of velocity error[x1=x2]
z	The symbol used for the z-transform
ZOH	Zero Order Hold.
δ or $\delta(t)$	The variable of the slope of switching line [equation II.2-41,42,43,44]
$\delta_e(x1,x2)$	The differences of the actual and measured parameters of the system [equation II.2-23]
$\delta_e^1(x1,x2)$	The differences of the actual and measured parameters of the system, which involves the term of the measured gain [equation II.2-30a]
ϵ	The magnitude of increase of slope of switching line [equation II.2-42]
Θ or Θ_o	Output angular position from DC-motor
Θ_d or Θ_i	Desired angular position
σ	Switching line
w	(Omega)Damped frequency of the system
w_o	(Omega)Natural frequency of the system
ξ	Damping coefficient
ξ_v	Damping coefficient because of viscous friction
ξ_T	Damping coefficient because of tachogenerator

Chapter I

INTRODUCTION

I.1 INTRODUCTION

"Variable structure system" or "Multivariable variable structure system[29]" is a series of nonlinear class system studies that systematically motivated many Russian scientists to design and find solutions. Among them who can be referred to here, are S.V. Emelyanov, V.I. Utkin, V. Itkis, V.A. Taran, N.E. Kostyleva, A.M. Shubladze, V.B. Yezerov, and E.N. Dubrovsky. The source of this motivation was the discontinuous systems which would not accept the conventional theories on the existence and uniqueness of a solution. A discontinuous system (reference[33]) is a system represented by differential equations with a discontinuous right-hand side. These equations can be approximated by a certain real system whose behaviour is unambiguously determined everywhere and a sliding mode is understood as a motion represented by the real system when its equations tend to the equations of an ideal system. The solution for this kind of system generally pertains to the verification of the existence of a sliding mode (regime) or surfaces [7,14,15,18,21,29,39,40,33] which can also be obtained by Lyapunov stability. The representation and analysis of such a class of dynamic is more popular using Andronov's phase-plane. This is the method that current notes has chosen for its analysis.

At this point, explanations are stated here to clarify the matter of differences between a discrete motion and a discontinuous motion. The discontinuity of this kind [7,14,15,18,21,29,39,40,33] is the characteristic of a dynamic system which defines the state of motion with different spaces of R, where discretization[26] is the piece-wise states of such

a motion using sampling time! On the other hand, a discrete motion can be discontinuous or continuous but it should not be misunderstood with a discontinuous motion. A discontinuous system of this class is nonlinear[39]. This explanation is given here, since the discontinuous motion of a system such as a DC-motor utilizing a sliding mode controller or the simulation of such a system and the analysis of the resulting phase-plane trajectory is not explained by the discrete term only.

In summary, the discontinuity of a dynamic system can result in a discontinuous solution using Variable Structure System Control defined in different spaces of R. This solution is applied to the outcome of the existence of the sliding regimes or the sliding conditions for such a class of systems as discontinuous controller. These conditions result in a function of the Lyapunov type.

The predecessor to the self-adjusting adaptive sliding mode controller[33,45...] is a discontinuous controller that in fact, copies such an ideal motion (trajectory) upon an approximated type (a curve rather than a line for a second order system) of sliding surfaces. In other words, the use of time variant switching surfaces is the main explicit characteristic of such a control methodology. This controller inherits such sliding surfaces based on the same verification of the existence of time-invariant switching surfaces. This class of controllers, for the second order systems, will be presented in this study, in a new form of control solutions rather than the conventional forms from V. Itkes and V.I. Utkin.

Coulomb friction [1,30,31,32,34,35,36] is a phenomenon that changes the dynamic regime of a system to a nonlinear type. The effect of such phenomenon and the various topics of accurate positioning in a feedback servo-system have been discussed in [30,31,35,38,...], specifically using Variable Structure Control system. The use of a self adjusting sliding mode controller to obtain a better dynamic performance, is one subject that

has not been considered by any other studies in the field of digital feedback servo-DC-motor control yet.

The present study, initially develops continuous controllers, specifically for the second order systems and then focuses on the side effect of such a class of solutions, called chattering. High frequency chattering of a system trajectory is the main problem of this class of controllers, which may excite the system dynamic model[28]. The second phase of the study is focused on the verification of the nonlinear phenomena such as Coulomb friction, stiction and torque saturation for a DC-motor model. In the third phase of this study, a PID controller is designed for such a system in order its results to be compared with the results of operation of the self-adjusting sliding mode controller in the presence of Coulomb friction and stiction. In the design phase of self-adjusting adaptive sliding mode controllers, simulations are performed initially in order to verify the performances and the necessary conditions of such a class of controllers and to simplify the experiments.

The present topic was proposed by my supervisor Dr. D. Necsulescu.

I.2 LITERATURE STUDY

The majority of the reference sources in Variable Structure Control System are in Russian. In this field, the most extensive studies are found in [6,7,8,9,17,18,24,29,33,39]. These sources study discontinuous systems with differential equations which have discontinuous right-hand side. The control solutions for various system dynamics are presented in these sources. English references on Variable Structure System have also been presented in [12,14,15,16,21,28,33,40,41,45]. In this field, the complexity of the methods of

solutions are considerably involved with the increase of the degree of the system order. Because of this, higher order systems are concerned with higher number of switching surfaces and more complex verifications of the existence of such sliding surfaces [21,33,39].

The studies of optimal sliding conditions are illustrated by [16,17,24,25,37]. As a solution to the width of chattering and the effect of high frequency chattering on the states of the variables of the system, Slotline and Sastry [28] propose the use of boundary layer approach. The result of this approach is illustrated by simulations for a two degrees of freedom robot, without considering the effect of any nonlinear phenomenon on the system actuators. This paper leaves this subject open for more investigation. This is a good study on the design of such a class of controllers, but they should be applied with caution.

On the field of Coulomb friction and multivariable control strategy references [22,41] should be referred to. Also, in the field of Coulomb friction and the error compensation of its effect, references [13,32,38], study the control solutions for the accurate positioning of the actuators. In addition to the study on the effect of some nonlinear phenomena on the analog motor model wherein the present study is using its results, the Coulomb friction and stiction with phase-plane analysis are presented in [31]. This topic has also been considered in [1,30,34,35,36].

In the study of servo feedback control systems and Variable Structure Control, references [11,22,35] should be referred to. Reference [11] considers the solution as a high-gain feedback in its definition of such a class of controllers. This reference considers this methodology of control, for both a digital and an analog system. The results of these experiments illustrate the adaptive operation of such a control method on the variable state of a servo-motor, even when high friction is applied to the system. This result is demonstrated by the insensitivity of the system to changes of the system parameters. A

constant switching line is proposed as the ideal trajectory for such a system. This paper does not provide conclusions relating to the difficulty in the accurate positioning of the servo-motor wherein Coulomb friction is present. Reference [22] presents this class of control methodology for a digital position feedback DC-motor using a Z80-microprocessor. Different controllers utilize system dynamic variables such as voltage, current and torque wherein the conclusions indicate on a satisfactory performance of such controllers (i.e. trajectory of the system ends at the origin of the phase-plane). This study evaluates such a class of controllers for a constant switching line. The result of this paper indicates on the poor performance of the controller for the large magnitude of the slope of switching line in the form of switch. The paper recommends the use of a self-adjusting sliding mode controller by the term of "time varying switching line" as a solution for the switching modes of the variable states of the system. Other applications of this class of controllers (such as Impedance control...etc) are considered by other studies with various topics that because of their irrelevancy to the present topic they are not followed further here.

Chapter II

THEORY OF PID AND DISCONTINUOUS CONTROLLERS IN SLIDING MODE

II.1 PID CONTROLLER

The basic principle of the PID control scheme is to act upon the variable to be manipulated through a proper combination of three control actions:

a) Proportional control action, where the control action is proportional to the actuating error signal (the difference between the desired input and the feedback signal).

b) Integral control action where the control action is proportional to the integral of the actuating error signal.

c) Derivative control action where the control action is proportional to the derivative of the actuating error signal.

II.1.1 Pulse Transfer Function of the Digital PID Controller

The PID control action in analog controllers is given by[26]:

$$u(t)=K_p\left[\, e(t)+(1/T_i)\int_0^t e(t)\,dt+T_d\left(\frac{de(t)}{dt}\right)\right] \qquad \text{(II.1-1)}$$

where:

$e(t)$	error input signal to the controller.
$u(t)$	output signal of the controller.
K_p	proportional gain of the controller.
T_i	integral time (or reset time).
T_d	derivative time (or rate time).

In order to obtain the pulse transfer function for the digital PID controller, we may discretize equation (II.1-1) by approximating the integral term by the trapezoidal summation and the derivative term by a two-point difference form. The PID controller in z-domain (from [26], equation 3-66), is:

$$U(z)=\left[K_{PP}+\frac{K_I}{1-z^{-1}}+K_D(1-z^{-1})\right]E(z) \qquad \text{(II.1-2)}$$

where:

$K_{PP}=K_P-(K_PT_S/2T_I)=K_P-(K_I/2)$	proportional gain (z-domain).
$K_D=(K_PT_d/T_s)$	derivative gain.
$K_I=(K_PT_S/T_i)$	integral gain.
$E(z)$	error input signal to the controller.
$U(z)$	controller output signal.
T_S	sampling time.

II.1.2 PID Transfer Function in *s*-Domain

From II.1-1, taking the Laplace transform, we obtain:

$$u(s)=\left[\ K_P+(K_I/s)+K_D s\ \right]e(s) \qquad \text{(II.1-3)}$$

where:

K_p	proportional gain.
$K_D=K_P T_d$	derivative gain.
$K_I=K_P/T_i$	integral gain.
e(s)	input error signal to the controller.
u(s)	output signal from the controller.

The block diagram of the system is shown in Figure (II.1-1).

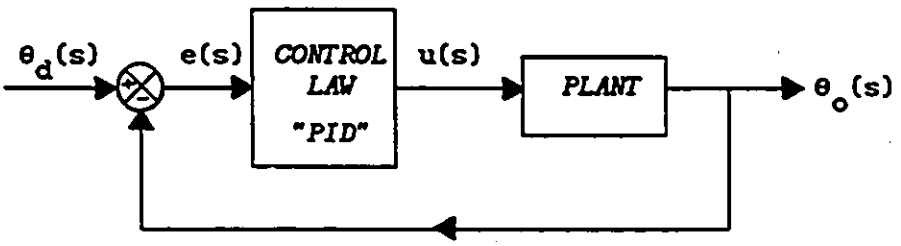

Figure II.1-1 Block diagram of a plant with PID controller.

II.2 DISCONTINUOUS CONTROLLERS IN SLIDING MODE

II.2.1 Discontinuous Control of A Second Order System in Sliding Mode Using Variable Structure System

The state space equation of a second-order system is:

$$\dot{x}=Ax \qquad \text{(II.2-1)}$$

where:

$$A=\begin{bmatrix} 0 & 1 \\ -a_1 & -a_2 \end{bmatrix}$$

$$x=[x_1 \; x_2]^T$$

a_1, a_2 are constants, representing process parameters.

x_1 positional error function

x_2 error velocity

We shall assume that the device (such as a DC-motor) is regulated by a controller providing a control signal u(t) through an amplifier with a positive gain b (constant). Thus the control system in state-space representation is described by:

$$\dot{x}=Ax+BU \qquad \text{(II.2-2a)}$$

where:

$$B=\begin{bmatrix} 0 \\ -b \end{bmatrix}$$

or:

$$\begin{cases} \dot{x}_1 = x_2 \\ \dot{x}_2 = -a_1 x_1 - a_2 x_2 - bu = f(x_1, x_2) - bu \end{cases} \qquad \text{(II.2-2)}$$

In the case of a variable structure controller, using sliding mode, u, the control law, is given by[21]:

$$u = \begin{cases} \alpha x_1 & \text{if } \sigma x_1 \geq 0 \quad \text{regions } \alpha^I, \alpha^{II} \\ \beta x_1 & \text{if } \sigma x_1 < 0 \quad \text{regions } \beta^I, \beta^{II} \end{cases} \qquad \text{(II.2-3)}$$

where

$$\sigma = x_2 + c x_1 \qquad \text{(II.2-4)}$$

α, β are called gains of the controller (constants).

c is constant, defining the slope of switching line $\sigma = 0$.

Figure (II.2-1) represents the regions in the phase-plane.

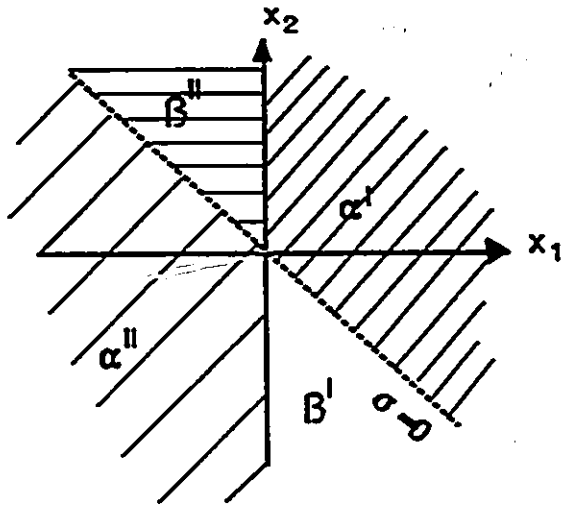

Figure II.2-1 A phase plane representation of the regions.

In figure II.2-1, $\alpha^{I},\alpha^{II},\beta^{I},\beta^{II}$, are the regions in the phase space of R, defined by two switches straight lines $x_1=0$, (coordinate axis) and $\sigma=0$. The four regions in this figure is defined by:

Region α^{I} $\quad x_1>0,\ \sigma>0.$
Region α^{II} $\quad x_1<0,\ \sigma>0.$
Region β^{I} $\quad x_1>0,\ \sigma<0.$
Region β^{II} $\quad x_1<0,\ \sigma>0.$

and:

σ, x_1 are called switching lines.

Figure II.2-2 shows the block diagram of such a system control.

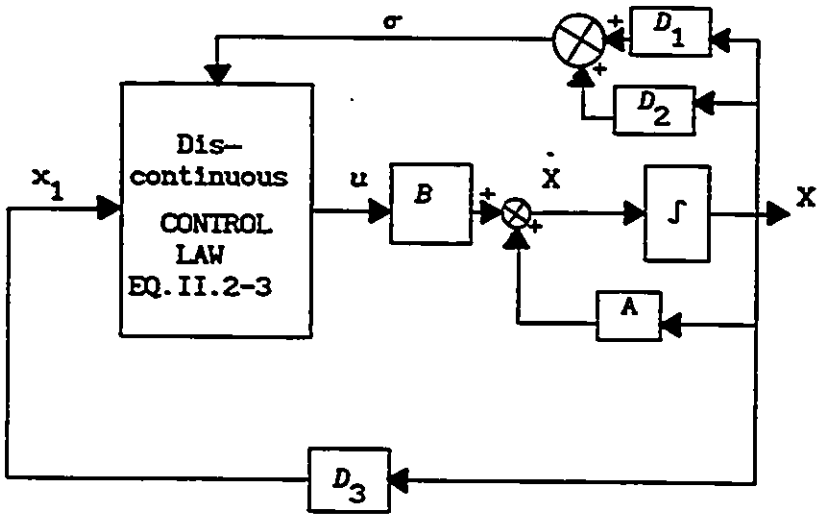

Figure II.2-2 Block diagram of a process with discontinuous controller.
$D_1=[c\ 0],\ D_2=[0\ 1],\ D_3=[1\ 0]$

First, the existence of sliding regime on the switching lines is verified. The sliding condition from [4] [relation:1.3.14] or [21,33,45] is given by:

$$\lim_{\sigma \to 0} \dot{\sigma}\sigma \leq 0 \qquad \text{(II.2-5)}$$

From II.2-4, taking the derivative, thus we can write:

$$\dot{\sigma} = c\dot{x}_1 + \dot{x}_2 \qquad \text{(II.2-6)}$$

and, on the switching line, since:

$$\sigma = cx_1 + x_2 = 0 \qquad \text{(II.2-7)}$$

or:

$$-cx_1 = x_2 \qquad \text{(II.2-8)}$$

thus, substituting II.2-2 and II.2-8 into II.2-6, gives:

$$\dot{\sigma} = -c^2 x_1 + a_2 c\, x_1 - a_1 x_1 - bu \qquad \text{(II.2-9)}$$

And substituting II.2-9 into II.2-5, will result :

$$\sigma x_1 [-c^2 + a_2 c - a_1 - b(u/x_1)] \leq 0 \qquad \text{(II.2-10)}$$

If $\sigma x_1 \geq 0$, from II.2-3 with $u = \alpha\, x_1$, we can write:

$$-c^2 + a_2 c - a_1 \leq b\alpha \qquad \text{(II.2-11)}$$

or:

$$[(-c^2 + a_2 c - a_1)/b\,] \leq \alpha \qquad \text{(II.2-12)}$$

If $\sigma x_1 < 0$, thus from II.2-3 with $u = \beta\, x_1$, and using II.2-10, we can write:

$$-c^2 + a_2 c - a_1 \geq b\beta \qquad \text{(II.2-13)}$$

or:

$$[(-c^2+a_2c-a_1)/b] \geq \beta \qquad \text{(II.2-14)}$$

Consequently, the necessary and sufficient sliding conditions are:

$$\begin{cases} (a_2c-c^2-a_1)/b \leq \alpha & \text{if } x_1\sigma \geq 0 \\ (a_2c-c^2-a_1)/b \geq \beta & \text{if } x_1\sigma < 0 \end{cases} \qquad \text{(II.2-15)}$$

Thus selections of the gains of α, β correspond to II.2-15 will generate discontinuous control laws similar to II.2-3, which cause system type of II.2-2, to operate in sliding mode.

To consider the uncertainties in this class of controllers which arise from the actual system model (changes of loads, measured parameters, effect of noise and delays...and other perturbations) in such a way that the controllers can be suitable for implementing self-adjusting adaptive sliding mode strategy for the computer programs, we change the sliding conditions II.2-15, into a general form of discontinuous control equation in sliding mode with sgn function. This will change the selections of switching values α and β into the choice of a constant K. To do so, we multiply both sides of equation II.2-15 by x_1. Then for $x_1>0$, we can write:

$$\begin{cases} (a_2c-c^2-a_1)x_1/b \leq \alpha x_1 & \text{if } \sigma \geq 0 \\ (a_2c-c^2-a_1)x_1/b \geq \beta x_1 & \text{if } \sigma < 0 \end{cases} \qquad \text{(II.2-16a)}$$

and for $x_1<0$, we can write:

$$\begin{cases} (a_2c-c^2-a_1)x_1/b \geq \alpha x_1 & \text{if } \sigma < 0 \\ (a_2c-c^2-a_1)x_1/b \leq \beta x_1 & \text{if } \sigma \geq 0 \end{cases} \qquad \text{(II.2-16b)}$$

The two inequalities II.2-16 a&b are similar (in the case of attraction of hyperplanes to sliding line) and we are able to interchange the two constants α and β with each other. The result for the conditions $x_1>0$ and $x_1<0$ can be represented by (II.2-16a). Satisfying the inequality II.2-16a, by adding $\pm K$, on the left hand side of the equation, and considering that $f(x_1,x_2)=-a_1x_1-a_2x_2$, we can write:

$$(f(x_1,x_2)-c^2x_1+K)/b=\alpha x_1 \qquad \text{if } \sigma\geq 0 \qquad \text{(II.2-17a)}$$

$$(f(x_1,x_2)-c^2x_1-K)/b=\beta x_1 \qquad \text{if } \sigma<0 \qquad \text{(II.2-17b)}$$

where: K is a positive constant.

This class of relations (II.2-17a&b) can be represented as (II.2-3, is substituted into II.2-17a&b and considering sgn function):

$$u=(1/b)\left[f(x_1,x_2)-c^2x_1+K\ \mathrm{sgn}(\sigma)\right] \qquad \text{(II.2-17)}$$

where if relation II.2-8 is also considered, II.2-17 can be represented by:

$$u=(1/b)\left[f(x_1,x_2)+c\ x_2+K\ \mathrm{sgn}(\sigma)\right] \qquad \text{(II.2-18)}$$

The use of sgn(σ) reduces the number of switching lines to one and also, because of the assumption of attraction of hyperplanes to switching lines, this will add a constraint to the V.I. Itkiss [21] parameter definition of a_1, a_2 as positive constants. The term $f(x_1,x_2)$ in this class of controllers, eliminates the term of its type in II.2-2 which results in the adaptive operation of the controller II.2-18 in the system. On the other hand, in terms of having exact knowledge of the system parameters a_1, a_2, controller can operate independently from the variable state of the system a_1x_1, a_2x_2.

We also follow the same contract from [33] as space u^+ belongs to $\sigma>0$, and u^- for $\sigma<0$. From this, space of $R^-(x,t)$ for the variable state of the system is defined by the states of $u^-(x,t)$ and $R^+(x,t)$, by $u^+(x,t)$.

To look for an appropriate controller out of its ideal state such as the type of candidate controller II.2.18 or those represented in [21,28,33], for a digital experiment, is not an easy task. The first step in this process is validation of such a class controller for its suitability and appropriateness for such a proposed system dynamic model (i.e. its performances from worst state to the best or its average state). In the literature study, we introduced this type of control methodology with extensive references wherein all had one piece of information in common, and that was ideal or if not, specific for the proposed processes. Regardless of such an idealistic mathematical analysis or such specific notations, the current study is focused on the results of simulations concerning with discrete motions for new form of represented sliding controllers. The discrete motion study from this point of view is considered here that a digital model is experienced and such simulations have similar results for a discrete system in order the performance and the robustness of the controller to be verified.

When controllers of the K sgn(σ) type, in the neighborhood of the origin of the phase-plane, are numerically simulated[1] for systems using solvers, chattering is observed in these systems trajectories (section II.2.2.1 and section III.2, simulation S4). Such a system motion is settled in a long time (in infinite time). This result in some cases, due to the choice of K, needed to be terminated in order to stop further chattering. To eliminate (notice here that in a digital system

---

1-Term of numerically simulation indicates here, the effect of round-off errors in estimation of the variables of the system using a solver. This term also represents the effect of magnitude of sampling time.

or discrete motion, the magnitude of sampling time is still one element which its effectiveness should not be forgotten in accurate positioning of the actuator for the following controller) this effect, controller II.2-18 can be reconfigured as follow:

$$u=(1/b)\left[f(x_1,x_2)+cx_2+K\ |x_1|\mathrm{sgn}(\sigma)\right] \qquad \text{(II.2-19)}$$

In this way, if $\lim_{t\to\infty}|x_1|=0$, consequently, x_2 will be zero. Multiplication of K in II.2-18 by $|x_1|$, does not change the sufficient and enough conditions of II.2-18 for having sliding mode, while the final chattering of the trajectory at the origin of the phase-plane will be dampened faster because of the effect of $|x_1|$.

Increasing K, in accordance with condition II.2-20, in the candidate controller II.2-19, may result in speeding the trajectory to reaching the switching line but from stability viewpoint, use of this condition is not compulsory [also consider 21]:

$$K > c^2 \qquad \text{(II.2-20)}$$

For the purpose of "reaching phase" study [28] of this controller, consider Figure II.2-3.

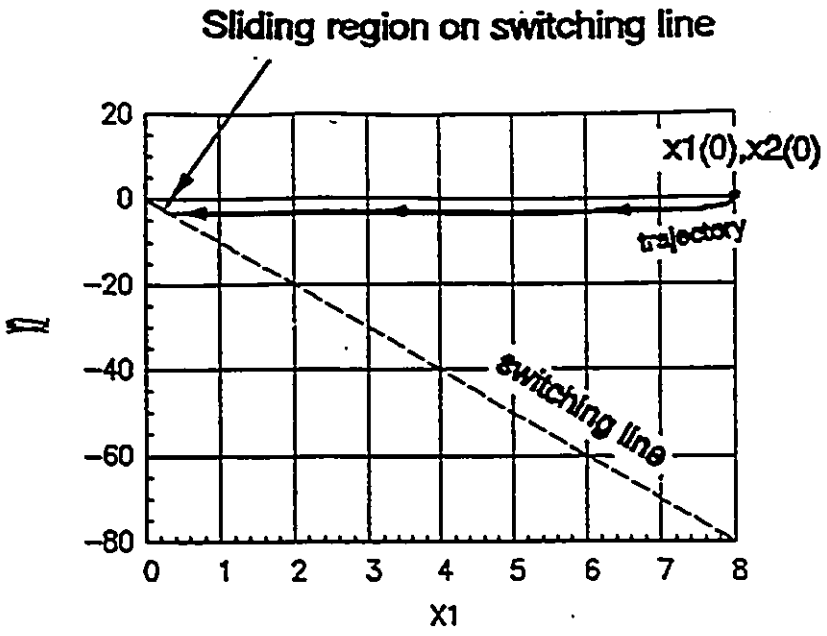

Figure II.2-3 A phase plane representation to the numerical simulation of II.2-2 and discontinuous controller II.2-19, c=10,K=30, $x_1(0)$=8 Rad, $x_2(0)$=0,sampling time=.01 Sec.

Choice of K in concerning with constraints and perturbations.

While using controllers with the characteristics shown in equation II.2-18 and 19, in actual system, we must select K cautiously. For instance, the actual parameters of a system in case of exact known, if it is shown by:

$$f(x_1,x_2)=-a_1x_1-a_2x_2 \qquad \text{(II.2-21)}$$

and when they are obtained by measurements, are represented by:

$$\hat{f}(x_1,x_2)=-\hat{a}_1x_1-\hat{a}_2x_2 \qquad \text{(II.2-22)}$$

Then, when controllers (II.2-18&19) are used on the system, an error (δ_e) is generated as:

$$\delta_e(x_1,x_2)=|f(x_1,x_2)-\hat{f}(x_1,x_2)| \qquad \text{(II.2-23)}$$

This error must be considered in choosing K. Taking this error into account, the controllers II.2-18&19 can be written as:

$$u=(1/b)\left[\hat{f}(x_1,x_2)+cx_2+K\ \mathrm{sgn}(\sigma)\right] \qquad \text{(II.2-24)}$$

$$u=(1/b)\left[\hat{f}(x_1,x_2)+cx_2+K\ |x_1|\mathrm{sgn}(\sigma)\right] \qquad \text{(II.2-25)}$$

To clarify the effect of uncertainties in the choice of K, equation II.2-24 is substituted into II.2-2, and we obtain:

$$\dot{x}_2=f(x_1,x_2)-\hat{f}(x_1,x_2)-cx_2-K\ \mathrm{sgn}(\sigma) \qquad \text{(II.2-26)}$$

with regard to δ_e from II.2-23, equation II.2-26 will be:

$$\dot{x}_2=\delta_e(x_1,x_2)-cx_2-K\ \mathrm{sgn}(\sigma) \qquad \text{(II.2-27)}$$

And if noise N(t) (assuming a white noise), is present in the system, then II.2-27 becomes:

$$\dot{x}_2=\delta_e(x_1,x_2)-cx_2-K\ \mathrm{sgn}(\sigma)+N(t) \qquad \text{(II.2-28)}$$

Therefore, the selection of K must be accomplished in such a way that (also, consider [4]-[relation 6-24, without the noise] and [22]):

$$K \geq \mathrm{Max}|\delta_e(x_1,x_2)| + \mathrm{Max}|N(t)| \qquad \text{(II.2-29)}$$

If the condition II.2-20 is also considered here, we can write:

$$K \geq \mathrm{Max}|\delta_e(x_1,x_2)| + \mathrm{Max}|N(t)| + c^2 \qquad \text{(II.2-30)}$$

Gain of the amplifier b, can also be a measurement($\hat{b}$) [4]. This term must be considered in II.2-29 or 30. Assuming :

$$\delta_e^I(x_1,x_2)=f(x_1,x_2)-b\ [\hat{b}]^{-1}\ \hat{f}(x_1,x_2)$$

Then:

$$K>[b^{-1}\hat{b}]\,[\max|\delta_e^I(x_1,x_2)|+\max|N(t)|] \qquad \text{(II.2-30a)}$$

In this way, the "reaching phase" is significantly concerned with the magnitude of $\delta_e^I(t)$. This problem is discussed in the section III.2.2.A, simulation S6 (consider the matter of natural frequency of the system and $\delta_e^I(t)$).

To show the system behavior during sliding motion, and the effect of K and c, a review of a simple double integrator system by phase plane analysis, is presented in the following section. This system analysis,

will help us to explain the strategy of the self adjusting adaptive control system in sliding mode, and will permit us to develop another form of discontinuous control law, in sliding mode, which is illustrated by the simulations of the system II.2-2 in the section III.2.1.A.

II.2.2 Discontinuous Control of A Double Integrator System

Consider a double integrator system as(from [27]):

$$\begin{cases} \dot{x}_1 = x_2 \\ \dot{x}_2 = -u \end{cases} \qquad \text{(II.2-31)}$$

Equation II.2-31, describes two families of parabolas in phase plane by defining control law as:

$$u = K\,\mathrm{sgn}(\sigma) \qquad \text{(II.2-32)}$$

For this purpose, consider Figure (II.2-4) and [27].

where:

C_n is a constant dependent on initial conditions, $x_1(0), x_2(0)$.
$n = 1,2,3\ldots n$

If we define a switching line of the form of II.2-4 $\{\sigma = cx_1 + x_2\}$, the motion trajectory of the system for any given initial condition, will be directed to the origin of the phase plane correspond to:

$$x_1(t) = x_1(t_o)e^{-c(t-t_o)} \qquad \text{(II.2-33)}$$

(Also consider [4,21,33])

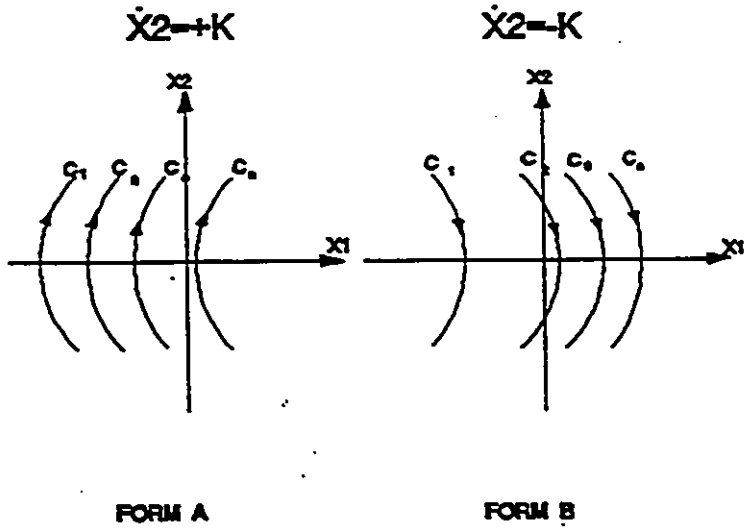

Figure II.2-4 Phase-plane representation of parabolas in the space of R^-, R^+, for the system II.2-31 and controller type of II.2-32.

where: t_o is the initial time.

This motion is accomplished in two modes:

a) switching mode represented in Figure II.2-5a.

b) sliding mode represented in Figure II.2-5b.

The system motion will be in the switching mode if the sliding conditions (section II.2.2.2) are not satisfied. These trajectories are given by:

$$\begin{cases} \dot{x}_2 = -K & \text{if } \sigma \geq 0 \\ \dot{x}_2 = +K & \text{if } \sigma < 0 \end{cases} \qquad \text{(II.2-34)}$$

The block diagram of this class of system model is represented in Figure (II.2-6).

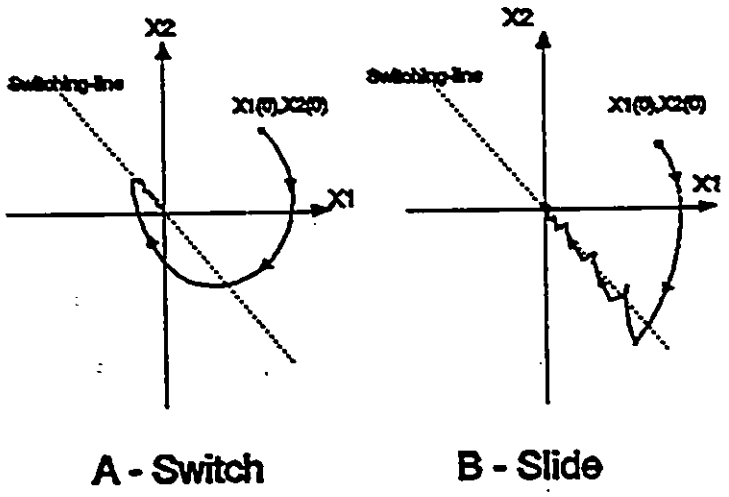

Figure II.2-5 Phase-plane representation of parabolas, in switching and sliding mode.

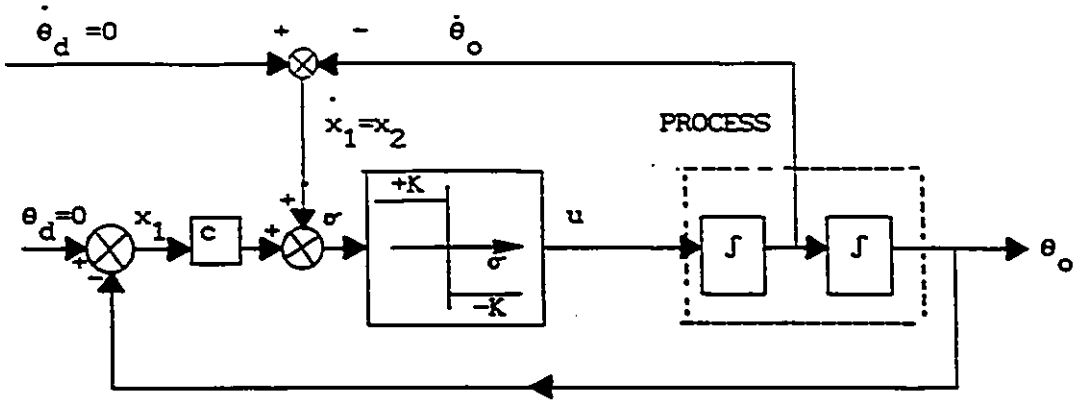

Figure II.1-6 Block diagram of a double integrator system and discontinuous control law represented by II.2-32 [$\sigma=cx_1+x_2$].

Figure II.2-7 shows a numerical simulation of the system II.2-34. This plot represents the behavior of such a system for a step initial change (angular position). The motion of the trajectory in the phase-plane is towards the origin by chattering upon sliding line $\sigma=0$.

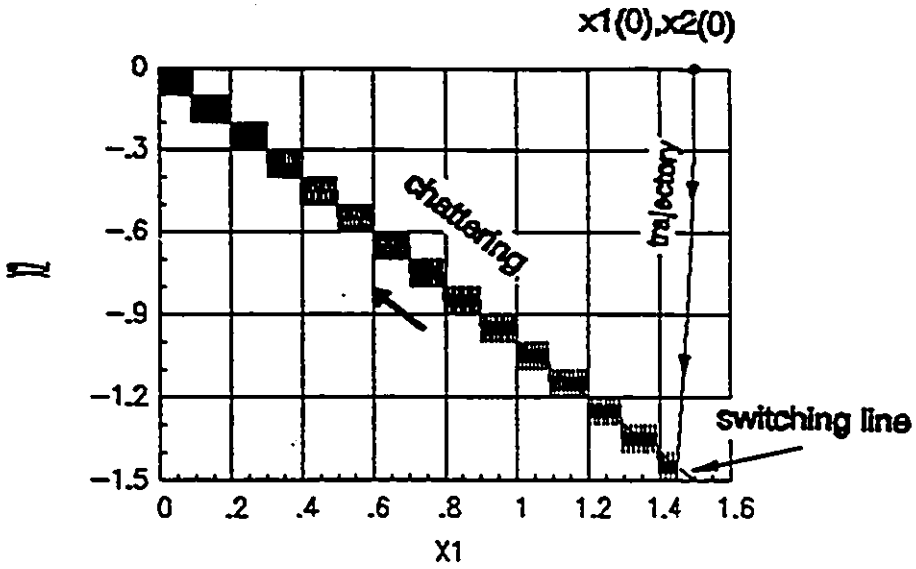

Figure II.2-7 Phase-plane representation of the system trajectory represented by: II.2-34 (a numerical simulation using Euler integration method), sampling time=.01 Sec., c=1, K=20, $x_1(0)=[\theta_o=1.5]$ Rad., $x_2(0)=0$ Rad/Sec.

II.2.2.1 The Effect of K-Gain of the Controller II.2-38 and Sampling Time

The magnitude of K of the discontinuous part as K sgn(σ) of the controller II.2-32, has the most significant role in the operation of the system in switching and sliding modes. The high values of K (defined in relation with the magnitude of sampling time and $|x_1(0)|$) has two favorable effects. First, if magnitude of K is increased, the span of parabolas will be increased (Figure II.2-8 and K_2 in this figure).

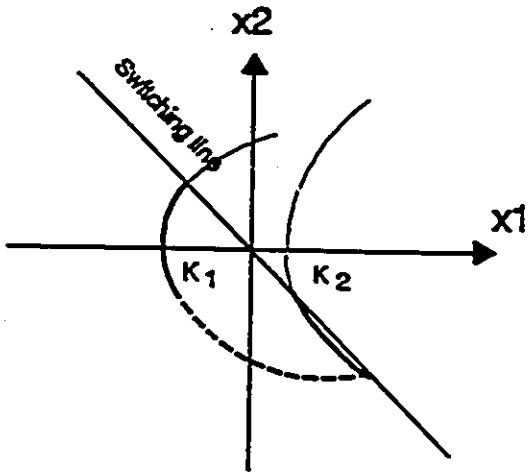

Figure II.2-8 Phase-plane representation of trajectories showing the effect of changes of the magnitude of K.

Type of parabolas with gain of K_2, leads to sliding states whereas parabolas with K_1 have a high tendency to switching mode (switching because of high consumption of time and the large range of changes of the position error is not desirable). The second favorable effect of the high magnitude of K is the possibility of the compensation of the resulting errors because of uncertainties which arise from the actual system dynamic model. This subject has been analyzed in the section II.2.1, by equations II.2-30 and 30a.

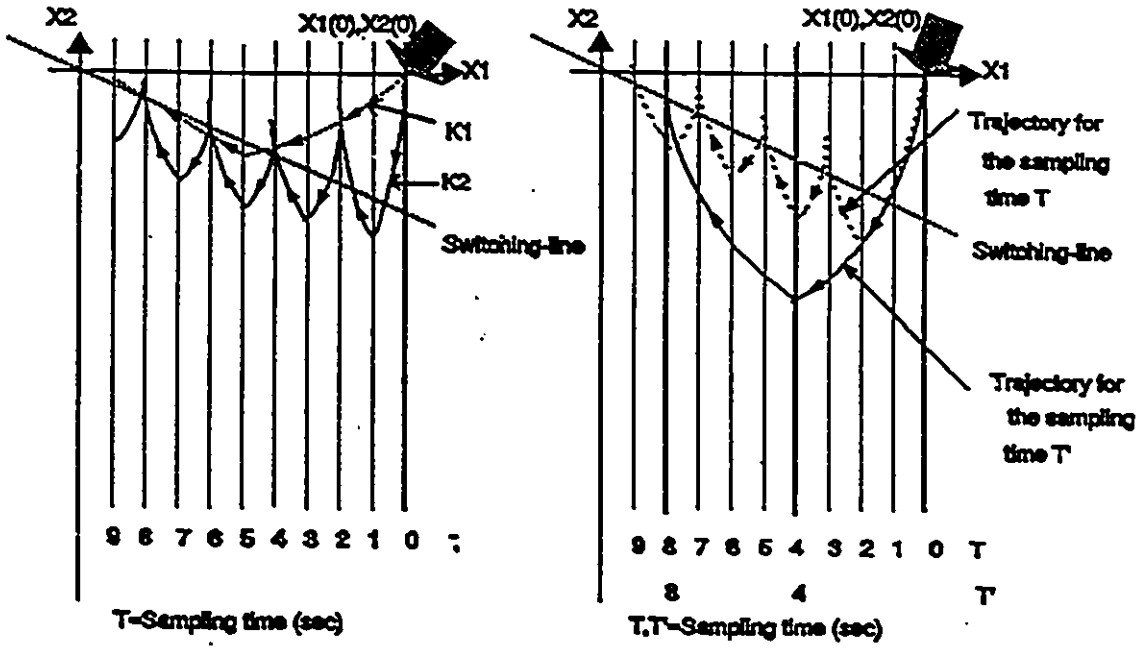

Figure II.2-9 Phase-plane representation of parabolas, in switching and sliding mode, showing effect of changes of the K and T_s.

The favorable effects of the large magnitude of K, may also cause side effects on the system. These become more complicated if it is accompanied by changes of the magnitude of sampling time. An unlimited increase of K will result in high frequency (from [28]) " **which may excite high frequency of the dynamics associated with the control system, which has been neglected in the course of modeling**" which means large span of parabolas here(Figure II.2-9(1)) and increase of the magnitudes of bounds of velocity-error, which increase the width of chattering. From Figure II.2-9(2), the decrease of sampling time, for any specific choices of K, reduces magnitudes of bounds of velocity-error which also results in the decrease of width of chattering and increase of the frequency of chattering. The effect of magnitudes of K and sampling time, on the system trajectory, from view point of width of chattering, are both in the same direction. This also implies that the increasing K, increases the size of closed-loop trajectory in the origin of the phase-plane. Similarly for the magnitude of sampling time this closed-loop can be large or small (contrary to II.2-33 and its mathematical result for the system ideal state (not discrete)). To observe these effects on the system trajectory represented by II.2-34, compare the following simulations of such a system in Figures II.2-11 through 14, for the changes of K and T_s. The closed-loop trajectory at the origin of the phase plane, which indicates on the presence of chattering of the position error $x_1(t)$, and velocity-error $x_2(t)$, in infinite time is represented in Figures II.2-13,15,17,18, for the simulations of such a system model. In this way, since the increase of K and sampling time will increase width of the chattering of x_1 and x_2 in infinite time, limiting x_1 (in order to reach the desired steady state error) or a termination condition for stopping further chattering will be necessary (when K and T_s are fairly large).

Large increase in K beyond a certain value, causes the velocity error to chatter between zero (small value near to zero. Or once sign of velocity-error changes), and a value (Figure II.2-18). Since K is very large, system trajectory, at the origin of the phase plane, will be of the form of a closed-loop (one of disadvantages of high gain

controllers of this class in discrete motion). In present digital feedback DC-motor model, the resulting motion in such a probable case will be in backward and forward rotation towards the target. In cases similar to figure II.2-17,18, where for any consecutive sampling time switch occurs, rules in Figure II.2-9 will be invalid. These are the cases that sampling frequency is equal to frequency of the chattering. On the other hand, for the large K in concerning with initial conditions, selection of the sampling time will describe the chattering frequency. In the actual model, these trajectories is also observed for such cases of the choices of T_s and K, when term $\delta_e^I(t)$ is small even if rule of $\omega_s >> 2\omega_o$ is considered for such discrete system.

Figure II.2-10 (A) and (B) are the representations of an ideal and actual state of a (discrete) system trajectory using, any class of discontinuous controllers in sliding mode for the second order systems.

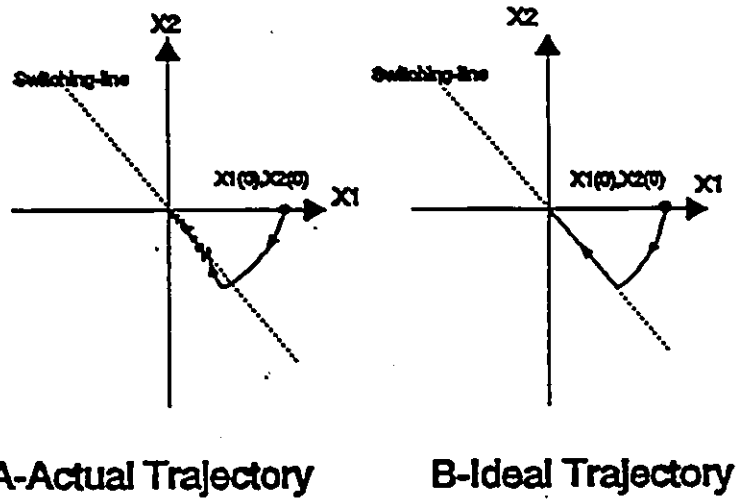

Figure II.2-10 Phase-plane representation of parabolas, representing actual sliding motion and an ideal motion in sliding mode.

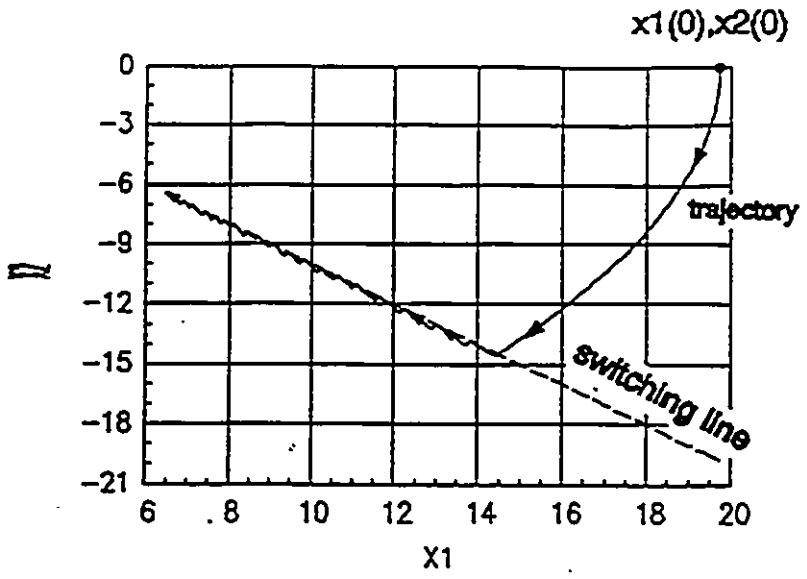

Figure II.2-11 Phase-plane representation of the trajectory of the system represented by II.2-34 (A numerical simulation by Euler integration method), sampling time=.01 Sec., c=1, K=20, $x_1(0)=[\theta_o]=19.74$ Rad., $x_2(0)=0$ Rad/Sec.

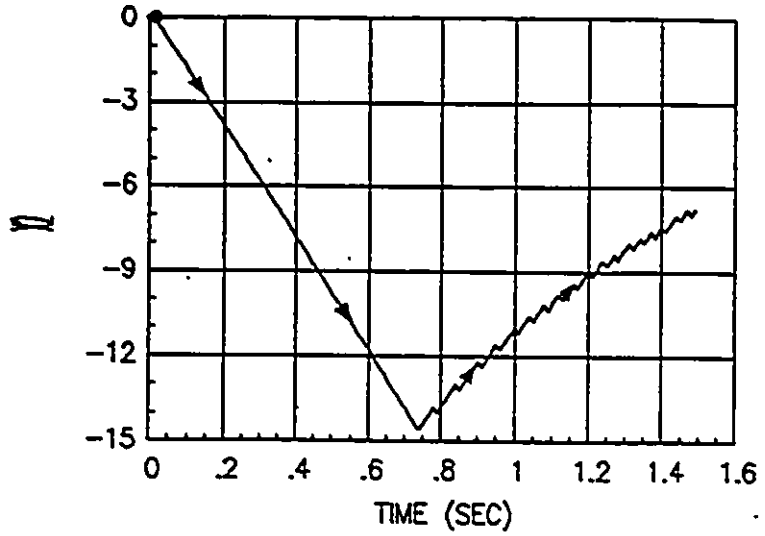

Figure II.2-12 Velocity error versus time. For the simulation of Figure II.2-11. (sampling time=.01 Sec., c=1, K=20, $x_1(0)=[\theta_o]=19.74$ Rad., $x_2(0)=0$ Rad/Sec.)

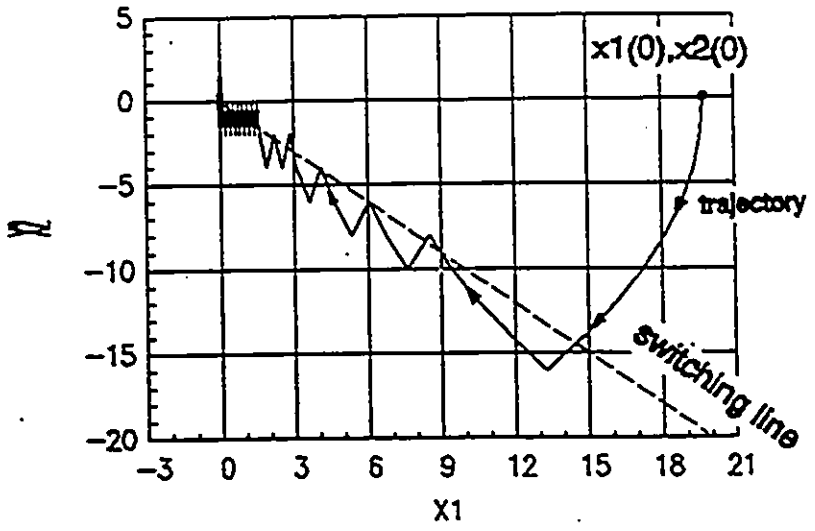

Figure II.2-13 Phase-plane representation of the trajectory of the system represented by II.2-34 (A numerical simulation by Euler integration method), sampling time=.1 Sec., c=1, K=20, $x_1(0)=[\theta_o]=19.74$ Rad., $x_2(0)=0$ Rad/Sec.

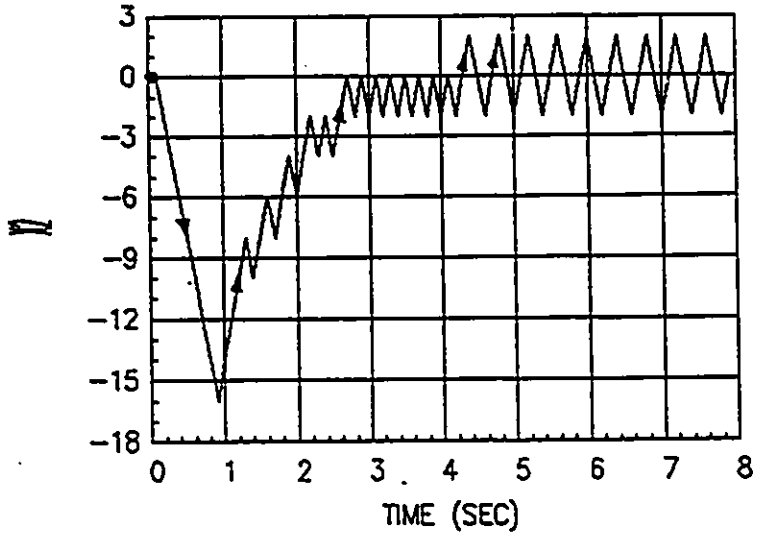

Figure II.2-14 Velocity error versus time. For the simulation of Figure II.2-13. (sampling time=.1 Sec., c=1, K=20, $x_1(0)=[\theta_o]=19.74$ Rad., $x_2(0)=0$ Rad/Sec.)

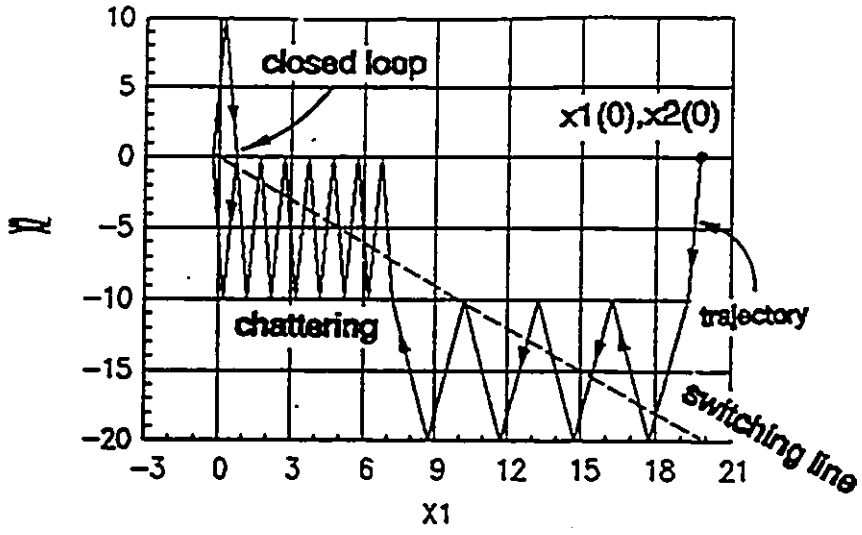

Figure II.2-15 Phase-plane representation of the trajectory of the system represented by II.2-34 (A numerical simulation by Euler integration method). SHOWING EFFECT OF INCREASE OF K. sampling time=.1 Sec., c=1, K=100, $x_1(0)=[\theta_o]=19.74$ Rad. ,$x_2(0)=0$ Rad/Sec.

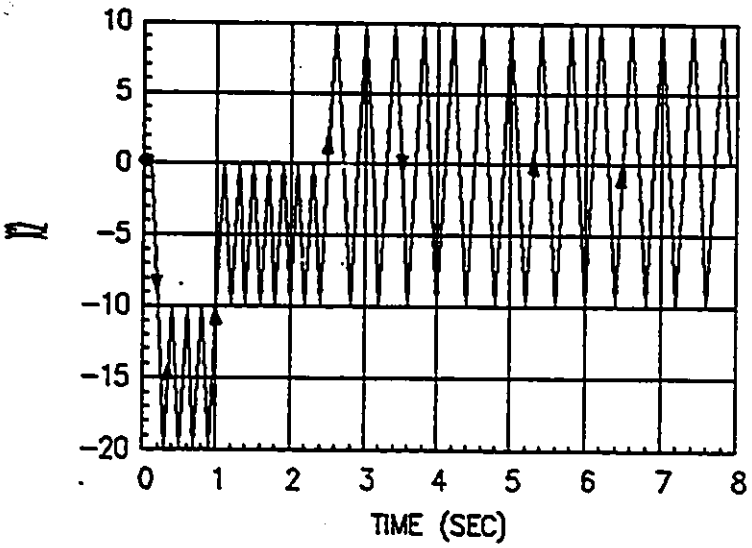

Figure II.2-16 Velocity error versus time. For the simulation of Figure II.2-15. (sampling time=.1 Sec., c=1, K=100, $x_1(0)=[\theta_o]=19.74$ Rad., $x_2(0)=0$ Rad/Sec.)

In order to show the effect of very large gains, system II.2-31 with controller II.2-32 has been simulated for the gains of K=100 and K=200. As these curves show, the closed-loop trajectory has grown and the frequency of chattering has been decreased.

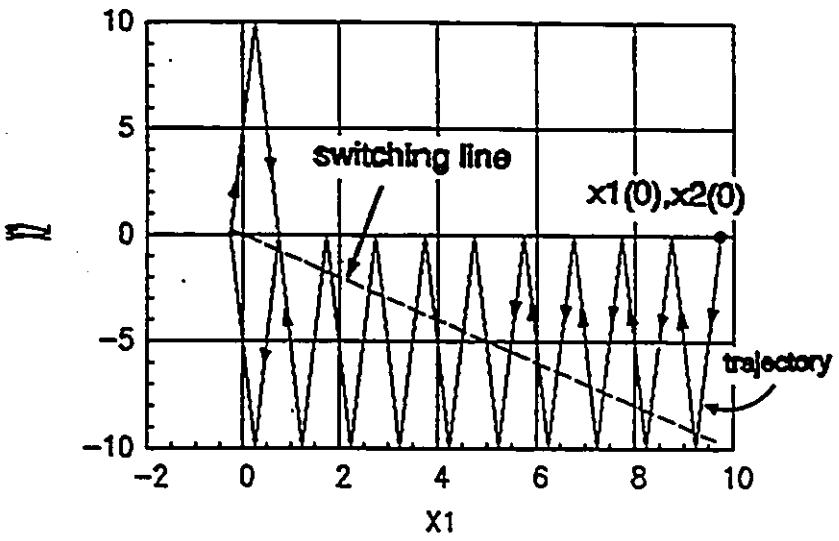

Figure II.2-17 Phase-plane representation of the trajectory of the system represented by II.2-34 (A numerical simulation by Euler integration method), sampling time=.1 Sec., c=1, K=100, $x_1(0)=[\theta_o]=9.74$ Rad., $x_2(0)=0$ Rad/Sec.

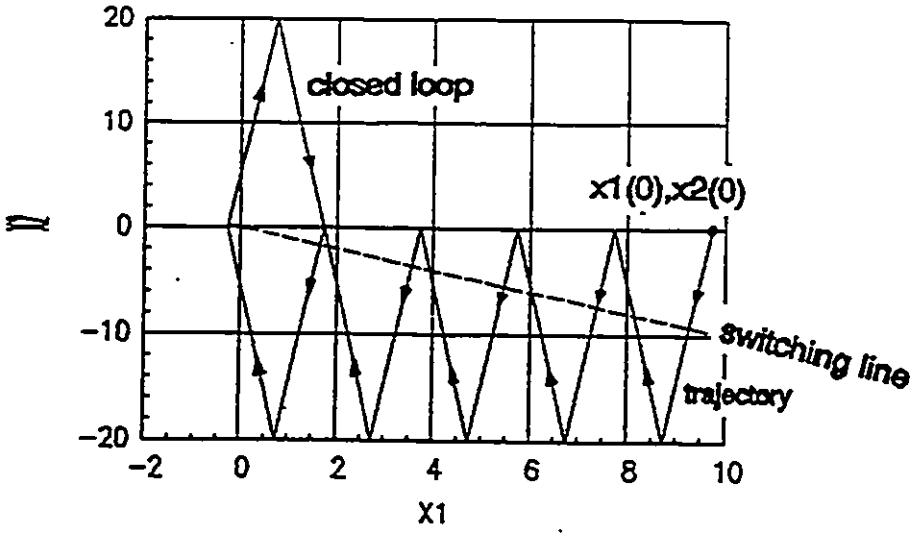

Figure II.2-18 Phase-plane representation of the trajectory of the system represented by II.2-34 (A numerical simulation by Euler integration method), sampling time=.1 Sec., c=1, K=200, $x_1(0)=[\theta_o]=9.74$ Rad., $x_2(0)=0$ Rad/Sec.

Meanwhile K, for this initial position error, is a large value(i.e. k=200 and Figure II.2-18).

II.2.2.2 The Sliding Conditions of A Double Integrator System

Recalling, sliding condition; equation II.2-5, as:

$$\lim_{\sigma \to 0} \dot{\sigma}\sigma \leq 0$$

and, equations II.2-6&8 as:

$$-cx_1 = x_2$$

$$\dot{\sigma} = c\dot{x}_2 + \ddot{x}_2$$

and from II.2-34, rewriting:

$$\begin{cases} \dot{x}_2 = -K & \text{if } \sigma \geq 0 \\ \dot{x}_2 = +K & \text{if } \sigma < 0 \end{cases}$$

we substitute II.2-34 into II.2-6, and we write:

$$\begin{cases} \dot{\sigma} = -K - c^2 x_1 & \text{if } \sigma \geq 0 \\ \dot{\sigma} = +K - c^2 x_1 & \text{if } \sigma < 0 \end{cases} \qquad \text{(II.2-35)}$$

Then, from II.2-35, with considering II.2-5, we conclude:

$$|x_1| \leq K/c^2 \qquad \text{(II.2-36)}$$

$$|x_2| \leq K/c \qquad \text{(II.2-37)}$$

Conditions II.2-36&37, must be both satisfied in order to force the system II.2-34 to operate in sliding mode. These inequities are described in Figure II.2-19.

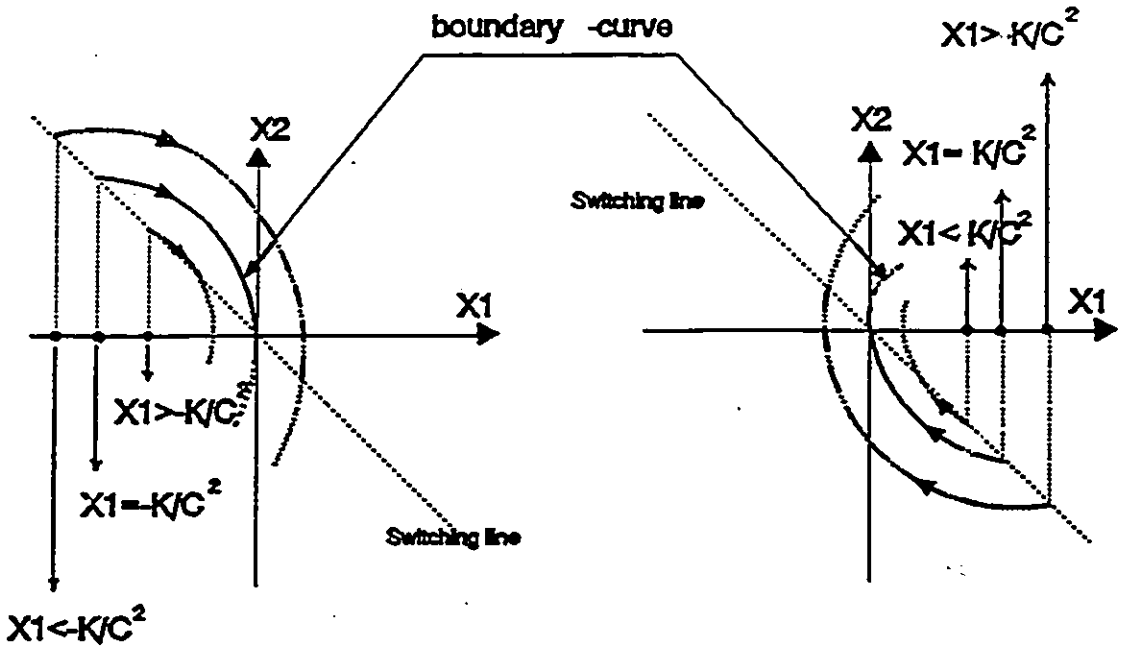

Sliding conditions in phase plane

Figure II.2-19 Phase-plane representation of parabolas, representing boundary switching curves.

These figures show that if one point is outside of the boundary curve, the motion of trajectory will be led to a switch to the opposite side, but once the point remains inside of the region (of the boundary switching curve), it must stay inside of the region by following the inner parabolas. For instance, the motion of the point D (Figure (II.2-20)) which is defined by x_1 and x_2, conditions of sliding mode, (II.2-36&37) can follow parabolas passing through the origin of the phase-plane. These parabolas are called boundary switching curves and are defined by substitution of II.2-36 into switching line (equation II.2-7), thus we can write:

$$Kx_1+|x_2|x_2=0 \qquad \text{(II.2-38)}$$

This curve in a complete state is depicted in Figure (II.2-20).

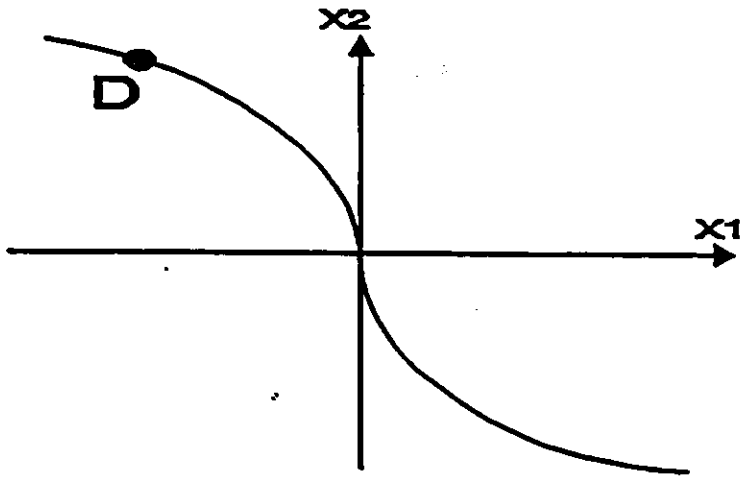

Figure II.2-20 Phase-plane representation of boundary switching curve represented by II.2-38.

II.2.2.3 Self-Adjusting Adaptive Sliding Mode Control Method

From[21][pages: 168-178] and [45][pages:205-229] and [12] [pages 57-60,169-180], a strategy is introduced as "Self Adjusting (Adaptive) Control System in Sliding Mode".

One of the problems in discontinuous control of systems in sliding mode with time-invariant switching surfaces is the adjustment of the slope of switching line (for a second-order type) so that system could operate in sliding mode. The self adjusting adaptive control system in sliding mode, is a recent method which can adjust the slope of switching line in the sliding regime by itself. This yields states of trajectory close to time-optimal response without the direct identification of the plant parameters.

As the author Zinober(1974)[45] states "for a linear system as:

$$\dot{z}=Az+bu$$

The basic self-adjusting adaptive sliding mode controller has the control law as (in our study we are presenting a new form of this class of controllers for the second order systems (II.2-19&18)):

$$u=-\ sgn(v)$$

where v is the linear switching function:

$$v= k^T z = q^{n-1}a_{n-1}z_1 + q^{n-2}a_{n-2}z_2+\ldots+a_o z_o \quad (q>0, a_i>0)$$

the z_i are the chosen state variables, q is the variable control parameter and the a_i are constants. The necessary conditions for sliding (or chattering) motion on v=0 with q constant have already been described (II.2-5,$\dot{v}v>0$). The self adjusting adaptive sliding mode controller is the strategy which changes q as a constant parameter to a time variant kind, by infinitesimal changes as:

$$q(t)=q(t)(1+\varepsilon)$$

consequently, v(t) as time-varying switching surface, will lead the states of variables of the system to the origin of the phase-plane by testing the sliding conditions for the next switching surface".

Consider the double integrator system described in section (II.2.2). Now, for an initial point $(x_1, 0)_o$, the slope of switching line is (for $x_2=0$, II.2-36, is ccnsidered here):

$$c^I=\left[\frac{K}{|x_1(t_o)|}\right]^{1/2} \qquad \text{(II.2-39)}$$

c^I is named as C_{max} at this point (which results sliding motion of the system). In this way, any selection less than C_{max}, guarantees the sliding motion of the system. For this purpose, C_o is selected in such a way that:

$$C_o < C_{max} \qquad \text{(II.2-40)}$$

And is initialized to the first slope of switching line (δ_1) as:

$$\delta_1=\delta(t=0)=C_o \qquad \text{(II.2-41)}$$

At this point, the strategy describes the motion of the trajectory in the phase-plane based on small (ε) increases of the slope of switching lines as:

$$\delta(t_n)=\delta(t_{n-1})+\varepsilon \qquad \text{(II.2-42)}$$

or:

$$\delta_n=\delta_{n-1}+\varepsilon \qquad \text{(II.2-43)}$$

where switching line by itself can be defined by:

$$\sigma_n=\delta_n x_1+x_2 \qquad \text{(II.2-44)}$$

Now, for this purpose, consider figure II.2-21.

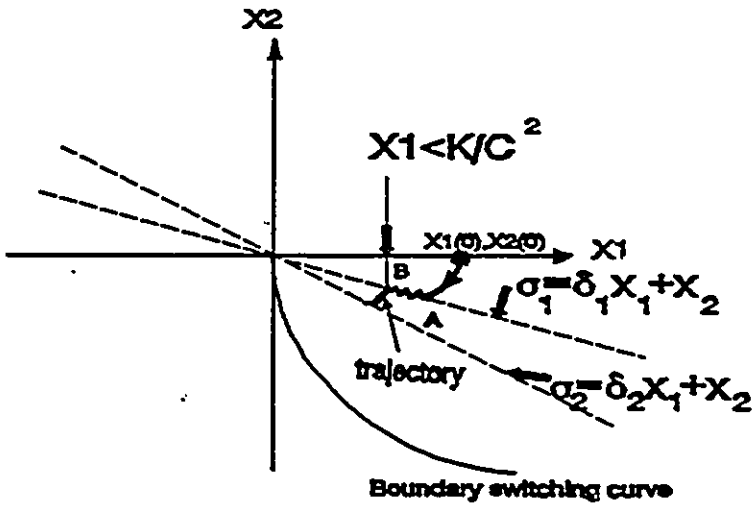

Figure II.2-21 Phase-plane representation of trajectory using self adjustable adaptive control strategy in sliding mode.

From the initial condition to point A, the system will follow trajectory, defined by II.2-34 ($u^+(x,t)$). In order to follow trajectory from point A, sign of σ_1 is tested and the states of variables of the system will be directed to point B, by II.2-34, where point B, is the point which satisfies the sliding condition II.2-36, for the next switching line (II.2-44) as:

$$\sigma_2=\delta_2 x_1+x_2$$

where δ_2 is computed by II.2-43.

Maintaining this strategy and increasing $\delta(t)$ by ε, the trajectory paths will be forced to reach to the origin of the phase-plane on an approximated switching curve.

In section III.2 this method is presented with the algorithms and simulations for the various conditions.

The next section is dedicated to the effect of nonlinear elements such as Coulomb friction, stiction and torque saturation for the linear feedback control of systems such as a DC-motor model.

II.2.3 Section Summay and Conclusions

In summary, three types of discontinuous controllers for linear second order systems were developed and reviewed here. These controllers will be tested with "Self-Adjusting Adaptive Sliding Mode Control Method".

The effects of K-gain of the controller (specifically) II.2-32, which has similar effects for II.2-18 and rather II.2-19 on the control of the states of variables of a second-order system, were analyzed. Also, the effects of changes of the magnitude of sampling time on such a system, specifically for the controller of the type of II.2-32, which has similar effects for the II.2-18 & 19, were investigated. The results of simulations for II.2-19 and II.2-32 which have been obtained for a time-invariant switching line indicate the existence of lag phase in reaching state and closed loops at the origin of the phase-plane (for only type "A" (i.e. having K $\text{sgn}(\sigma)$ term)). Regardless of some choices of K and T_s, it will be shown that the proposed time-varying switching line controller in sliding mode has better performance for similar selections of such elements in the control of a second-order system in comparing with time-invariant type. These results will be presented in section III.2 and in the final conclusions, section VI.

II.3 MODEL OF A DC-MOTOR SYSTEM

(The effects of some nonlinear phenomena on the step response of a position control system)

A position control system can often be approximated by a second order differential equation with the result that its responses to step inputs can be studied using the phase plane.

The approach is used below to illustrate the effect of some nonlinear phenomena such as Coulomb friction, stiction and torque saturation on the performance of an analog position control of a DC-motor from [5]. These results are specifically illustrated here for understanding the discrete motion of such a system by simulations which have not been considered anywhere yet.

Referring to Atherton's study, the block diagram of a system feedback DC-motor model in terms of the parameters ω_o, ξ_v and ξ_T can be shown as Figure (II.3-1).

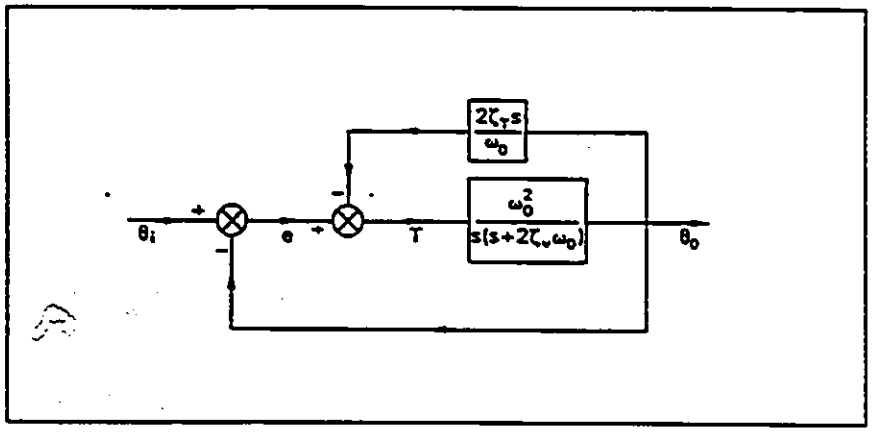

Figure II.3-1 A block diagram of the system

The figure has been purposely drawn to show the separate effects of

ξ_v and ξ_T , since the system can not be analyzed in terms of their sum ξ when nonlinearity occurs between the operational amplifier and the motor output[5].

II.3.1 The Effect of Coulomb Friction

When Coulomb friction on the motor shaft is taken into account (such as DC-motor), the variable state of the system can be described by (from [5]):

(With $\theta_1=0$, $x_1=\theta_o$ and $x_2=\dot{\theta}_o$)

$$\begin{cases} \dot{x}_1 = x_2 \\ \dot{x}_2 = -\omega_o^2 x_1 - 2\xi\omega_o x_2 - d\omega_o^2 \operatorname{sgn}(x_2) = f(x_1,x_2) - d\omega_o^2 \operatorname{sgn}(x_2) \end{cases} \qquad \text{(II.3-1)}$$

where:

$\xi=\xi_v + \xi_T$

$T_c=Jd\omega_o^2 \operatorname{sgn}(x_2)$ equivalent Coulomb friction torque.

The motion in the phase-plane is thus described by two linear differential equations, one valid for x_2 positive and the other for x_2 negative. The line $x_2=0$, is referred to as switching line. In both cases the phase portraits about an origin are shifted to the singular point $O_1(-d,0)$ for $x_2>0$ or $O_2(d,0)$ for $x_2<0$. Further more, any point on the x_1 axis between these singular points is an equilibrium point at which trajectories terminate [5](Figure (II.3-2)).

For the initial conditions $x_1(0)=-u_o$, and $x_2=0.$, and with a selection of $u_o >> d$, the phase-plane trajectory will terminate at O_1,

when $\xi \geq 1$, since the linear response has no over-shoot. With $0 \leq \xi < 1$, however the trajectory will terminate anywhere between O_1 and O_2, and the exact point depends upon ξ and the magnitude of u_o.

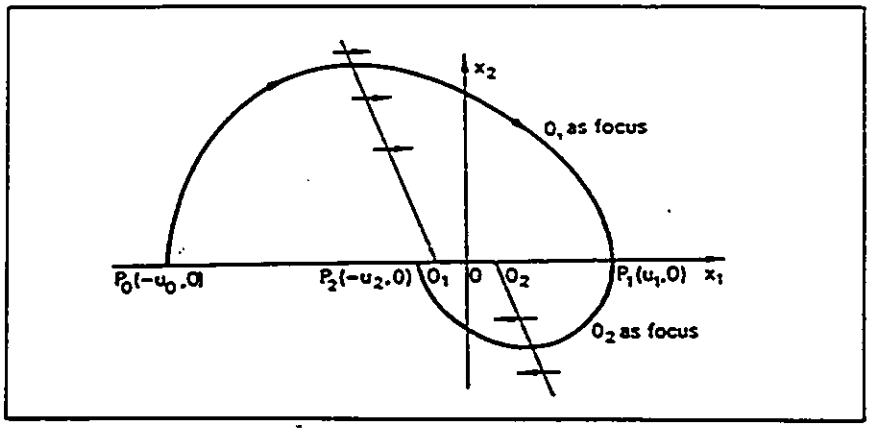

Figure II.3-2 Phase plane with effect of Coulomb friction

We also note[31] that when two surfaces are rubbing, or in sliding contact, a finite force is required to initiate motion and the surfaces are said to stick. The magnitude of the sticking force in stiction is larger than the Coulomb friction force. Its value depends on the specific materials in contact, their surfaces finishes, the normal force, and usually can only be determined by testing. Thus, the force used to accelerate the mass must exceed the stiction force to initiate motion. Once the motion starts the stiction force decreases (as a function of velocity) and normally approaches the Coulomb level at relatively low velocities.

The effect of stiction can be modeled in the same way as the term of Coulomb friction in the system represented by II.3-1. The coefficient of this model, because of the different magnitude, will be represented here in d'.

Numerical simulations of the system model II.3-1

The following simulations are performed in order to show the effect of Coulomb friction on the system represented by II.3-1, in a discrete motion in comparing with the results from [5].

Figures (II.3-3,4) are the results of computer simulati· , ·f the system represented by equation II.3-1 when Coulomb friction is considered in the system. Figure (II.3-5) represents an ideal trajectory of the equation II.3-1 when d=0. In this simulation Euler-integration method was used to solve the nonlinear system.

From Figures (II.3-3 and 4), since ξ=.7, system trajectories crosses the axis x_1, at point B (between origin and (+d,0)). The resulted error for the different magnitudes of the sampling time (compare distances 'a' in these figures) is the effect of following factors:

a- Method of solution of the nonlinear system .

b- Numerical values (round-off errors).

c- Sampling time.

Where the magnitude of sampling time plays the major role if it is selected a fairly large (with respect to the choice of $\omega_s >> 2\omega_o$). Consequently, for a digital feedback linear control system the resulting trajectory is mainly related to the magnitude of sampling time and precision of the digital processors. For instance, enormous simulations for different magnitudes of ξ, x_1 and sampling time implemented where the results showed that the point A may not be obtained for a discrete system if the choice of sampling time is not in an acceptable range, for $\xi \geq 1$ and for an appropriate selection of the magnitude of $x_1(0)$.

Also, considering both Figures (II.3-3 & 4), a similar motion trajectory is noticeable. As these two figures show, the states of variables of the system after point B, still remains active until the origin of the phase-plane is reached. As a matter of fact, this class of motion in an actual model of such a system does not exist, and once point B is reached, motion is terminated, and since the equation of II.3-1, by itself, is a model to represent the effect of the dissipative

Coulomb torque (as $T_c=J\ d\omega_o^2 sgn(x_2)$), the effect of numerical round-off errors and mainly the magnitude of sampling time must be considered here as the reasons for such a erratical motion. In other words, these results should not confuse us with a wrong trajectory representation of such a system dynamic model in reaching point B. The effects of elements introduced above (in simulation) cause the term $d\omega_o^2 sgn(x_2)$ to act as an error compensator upon the variables of the system model (II.3-1) where finally results in a sliding motion towards the origin of the phase-plane (similar to a sliding controller with relay amplitude of $d\omega_o^2$, and a switching line $\sigma=x_2$). The sliding motion after point B as the result of present simulations, is a noticeable point in recognizing the point of the affect of Coulomb friction torque on the state of system trajectory, which are used in simulations of the section III.2.2.

To show how such a trajectory slides (this is beyond the scope of the present study to discuss the proof of such a motion, but as an explicit explanation of such a phase of system in order not to be alias with the result of an error compensator such as sliding mode controller, these notes are followed) upon x_1 axis (recalling again; of a numerical simulated model type of II.3-1), when a singular point such as A or B does not exist (as end of the motion), equation II.2-32, and Figure (II.2-7), where; $c=0$, $K=d\omega_o^2$, are recalled here. We know that from equation II.3-1 the effective torque of the DC-motor is modeled by: $J\ f(x_1,x_2)$, and we also know once, $|f(x_1,x_2)| < d\omega_o^2$ (equation II.3-1), point B is reached and system trajectory must be terminated here. But since, $x_2<0$ ($\sigma<0$), the trajectory is defined by:

$$\dot{x}_2=+\alpha(t)$$

and when $x_2\geq 0$ ($\sigma\geq 0$), the trajectory is defined by:

$$\dot{x}_2=-\beta(t)$$

where α, β are positive

and since $\alpha(T_s+\Delta T_s)<\beta(T_s+\Delta T_s)$ [33,sec.2](for $x_1>0$ and the reverse for $x_1<0$) (singularities will occur if $\alpha(t)\geq\beta(t)$ in the form of closed-loops (case of existence of point A or B], thus according to Figure (II.2-8),

these differences results in different spans of parabolas (which cause the motion to be towards the origin), and since switch occurs between two plus and minus values, result will be a sliding motion (chattering) similar to a resulting trajectory of the dynamic model represented by II.2-34. Thus, system trajectory by chattering, moves towards the origin of the phase plane (Figure (II.3-3 & 4)).

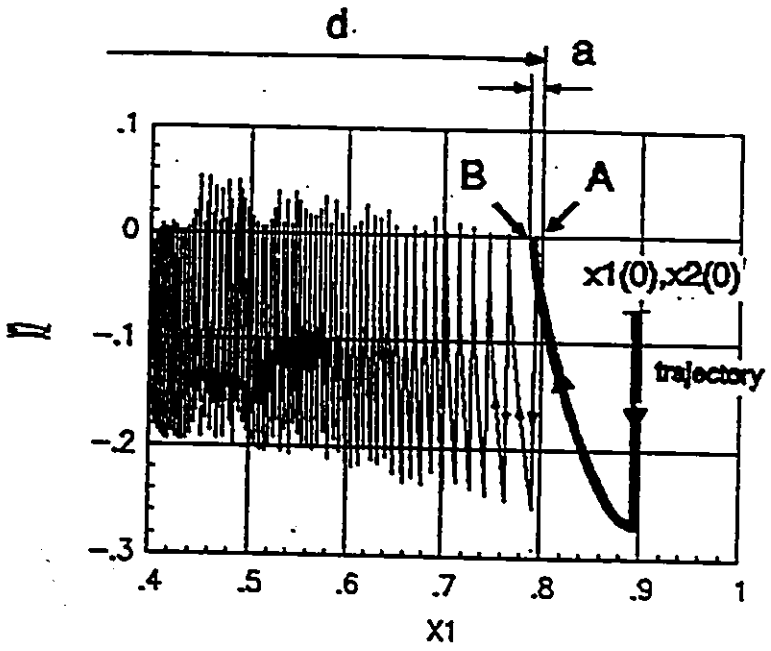

Figure II.3-3 A computer simulation of the EFFECT OF COULOMB FRICTION represented by equation II.3-1. ω_o=4 Rad/Sec, ξ=.7, d=.8 Rad, $x_1(0)$=.9 Rad, $x_2(0)$=-.07 Rad/Sec, Sampling Time T=.01 Sec,

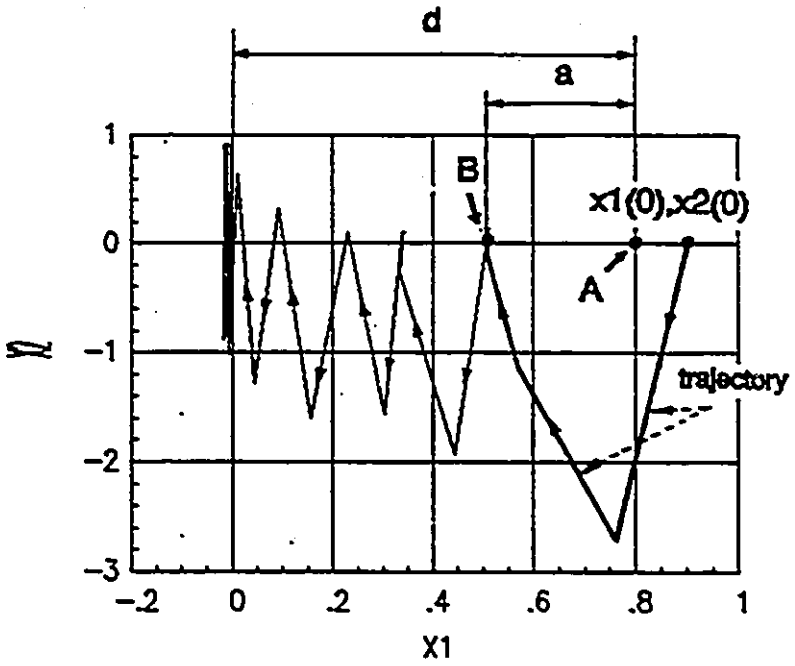

Figure II.3-4 A computer simulation of the EFFECT OF COULOMB FRICTION represented by equation II.3-1. ω_o=4 Rad/Sec, ξ=.7, d=.8 Rad, $x_1(0)$=.9 Rad, $x_2(0)$=-.07 Rad/Sec, Sampling Time T=.1 Sec,

$[f(x_1,x_2)=-2\xi\omega_o x_2-\omega_o^2 x_1]$J=Effective torque

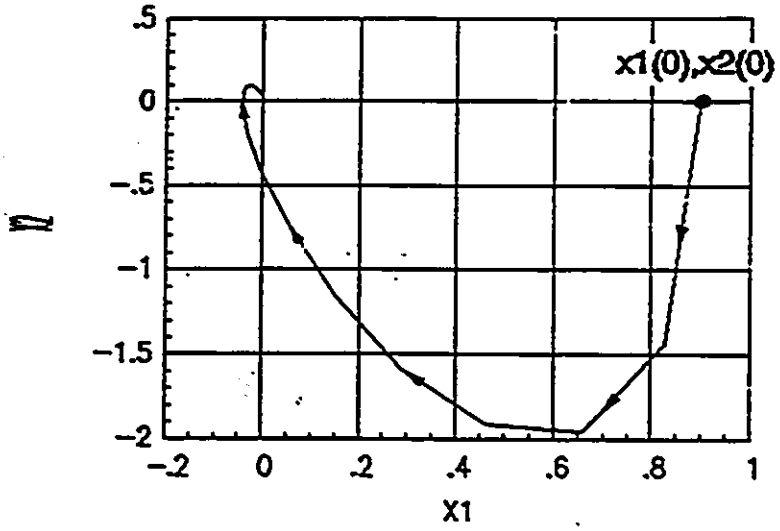

Figure II.3-5 A computer simulation WITHOUT COULOMB FRICTION represented by equation II.3-1. ω_o=4 Rad/Sec, ξ=.7,d=0 Rad,$x_1(0)$=.9 Rad,$x_2(0)$=-.07 Rad/Sec, Sampling Time T=.1 Sec,

II.3.2 The Effect of Torque Saturation

When a nonlinear operation takes place in the power amplifier or the motor, the equation of the motion has to be modified as follows[5]:

$$\ddot{\theta}_o+2\xi_v\omega_o\dot{\theta}_o=\omega_o^2 f_T(\theta_i-\theta_o-2\xi_T\dot{\theta}_o/\omega_o) \qquad \text{(II.3-2)}$$

Assuming that $\theta_i=0$, and the nonlinearity to be ideal saturation with limit levels $\pm h_T$, occurring at input levels of $\pm\delta_T$, the phase-plane can be divided into three regions, by two switching lines defined by:

$$\sigma_1=\sigma+\delta_T$$
$$\sigma_2=\sigma-\delta_T$$
$$\sigma=\theta_o+2\xi_T\dot{\theta}_o/\omega_o$$

the function f_T in II.3-2 is:

$$f_T=\begin{cases} +h_T & \text{when} \quad \sigma<-\delta_T & \text{region I} \\ -m_T\sigma & \text{when} \quad |\sigma|<\delta_T & \text{region II} \\ -h_T & \text{When} \quad \sigma>\delta_T & \text{region III} \end{cases}$$

where:

$$m_T=h_T/\delta_T .$$

(m_T, actually represents different saturation levels of the actual and ideal system. This magnitude can normally be assumed to be one).

Models of the motions of the system in these regions can be represented by the following differential equations:

$$\begin{cases} \dot{x}_2=-2\xi_\nu\omega_o x_2+\omega_o^2 h & \text{if} \quad \sigma<-\delta_T & \text{region I} \\ \dot{x}_2=-2\omega_o x_2(\xi_\nu+m_T\xi_T)-\omega_o^2 m_T x_1 & \text{if} \quad |\sigma|<\delta_T & \text{region II} \\ \dot{x}_2=-2\xi_\nu\omega_o x_2-\omega_o^2 h & \text{if} \quad \sigma>\delta_T & \text{region III} \end{cases} \qquad \text{(II.3-3)}$$

Fig.II.3-6, shows these regions.

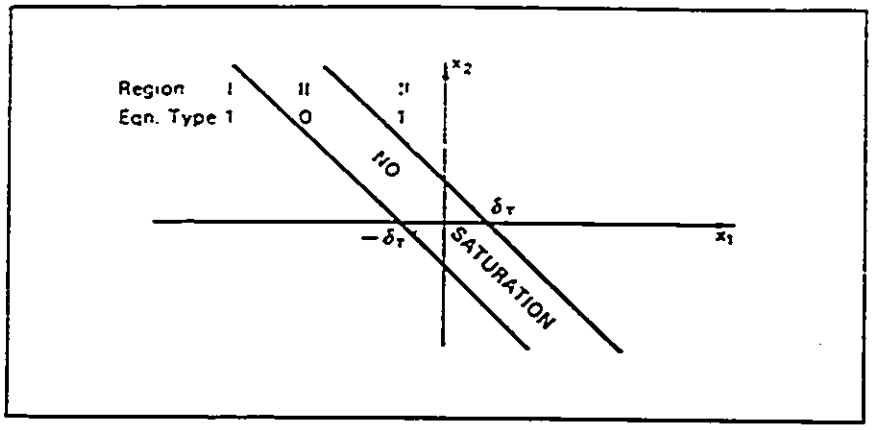

Figure II.3-6 Phase plane with regions.

To show the system behavior represented by II.3-3, first, we have to specify the types of trajectories in the above three regions. The trajectories of the regions I and III, are similar to a double integrator system trajectory represented by II.3-34, and are of the forms of parabolas depicted in Figure (II.2-4) as: FORM-A and FORM-B. For the region II, the poles of the system are (assuming $\theta_1=0$):

$$x', x''=\theta', \theta''=-\xi'\omega_o \pm \omega_o\left[\xi'^2 - m_T\right]^{1/2} \qquad \text{(II.3-4)}$$

where:

$$\xi'=\xi_v+m_T\xi_T \qquad \text{(II.3-5)}$$

When ξ_v , ξ_T are zero, the system will have two imaginary poles and if

$$\xi'^2 - m_T > 0$$

or:

$$[m_T]^{1/2} < \xi' = \xi_v + m_T \xi_T \qquad \text{(II.3-6)}$$

the trajectory will be of the form of FORM-D (Figure (II.3-7)), which represents an overdamp stable system. If

$$[m_T]^{1/2} > \xi' = \xi_v + m_T \xi_T \qquad \text{(II.3-7)}$$

then, the trajectory can be configured as FORM-C as Figure (II.3-7), and the system will be an underdamp system with complex conjugate poles.

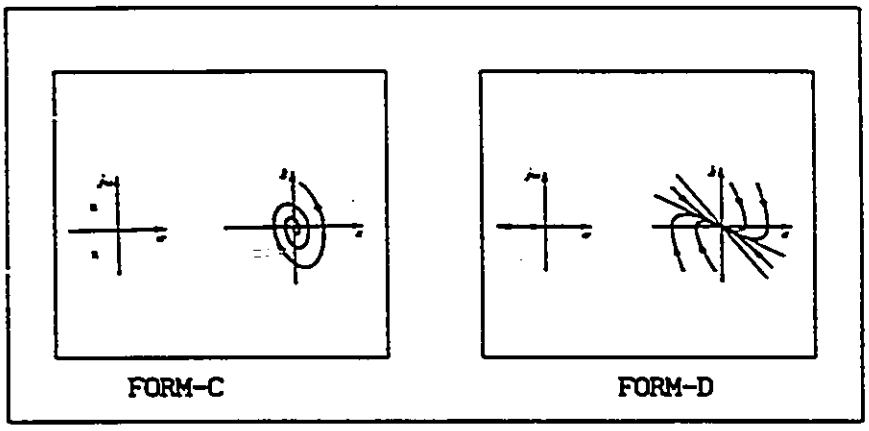

Figure II.3-7 Phase-plane representation of trajectories and s-plane of second-order type defined by II.3-6 & 7

The Simulations of the Model II.3-3

To clarify the effect of torque saturation on a DC-motor behavior under linear feedback control, numerical simulations have been implemented by the Euler integration method for the solution of nonlinear system represented by II.3-3. These simulations are performed here for different values of ξ_T, ξ_v and δ_T, and the results are depicted in the following figures. The parameters of the relation II.3-3, are

initialized as:

$$\begin{cases} h_T = 5.\ \text{Rad/Sec}^2 \\ \omega_o = 4\ \ \text{Rad/Sec} \end{cases}$$

ξ_v =0.0, $\theta_o(0)$=-2.8 Rad, $x_1(0)=\theta_o(0)-\theta_1=\theta_o(0)$ Rad,

$x_2(0)=\dot{\theta}_o(0)-\dot{\theta}_1=\dot{\theta}_o(0)$=0 Rad/Sec, and the sampling time is selected to be T_S=.01 Sec (in order to obtain $\omega_S >> 2\omega_o$).

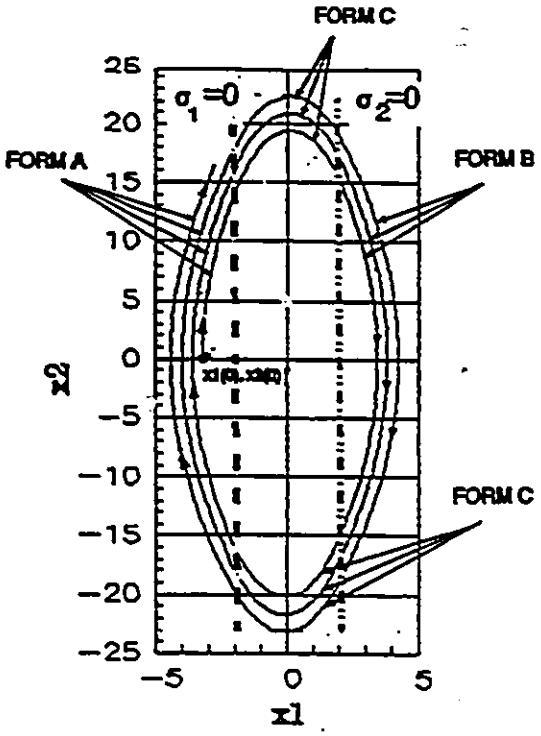

Figure II.3-8
ξ_T =1x10^{-7}, δ_T =2

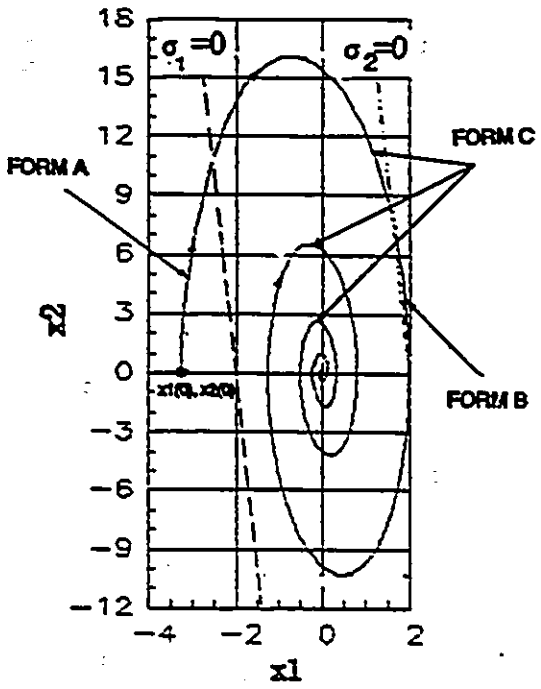

Figure II.3-9
ξ_T =.1, δ_T =2

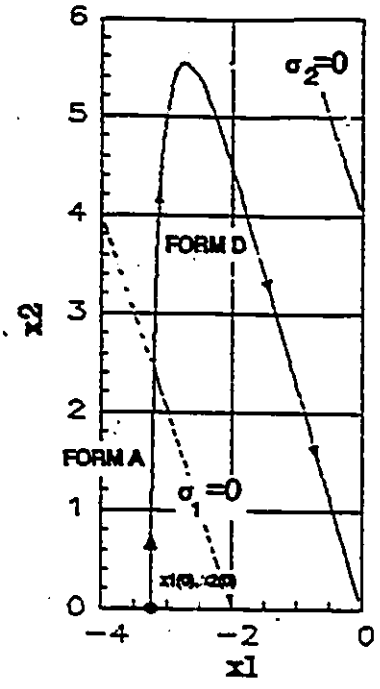

Figure II.3-10
ξ_T =1.0, δ_T =2

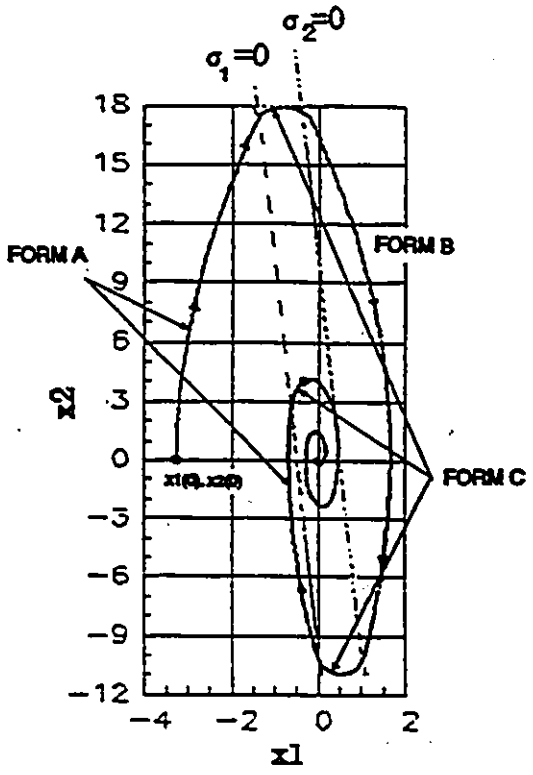

Figure II.3-11
ξ_T =.1, δ_T =.5

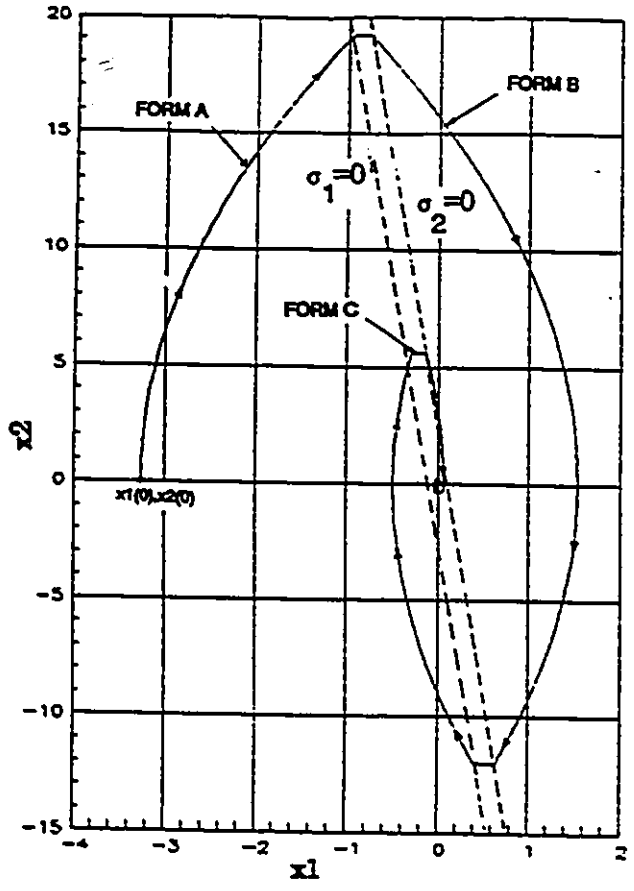

Figure II.3-12
ξ_T =.1, δ_T =.1

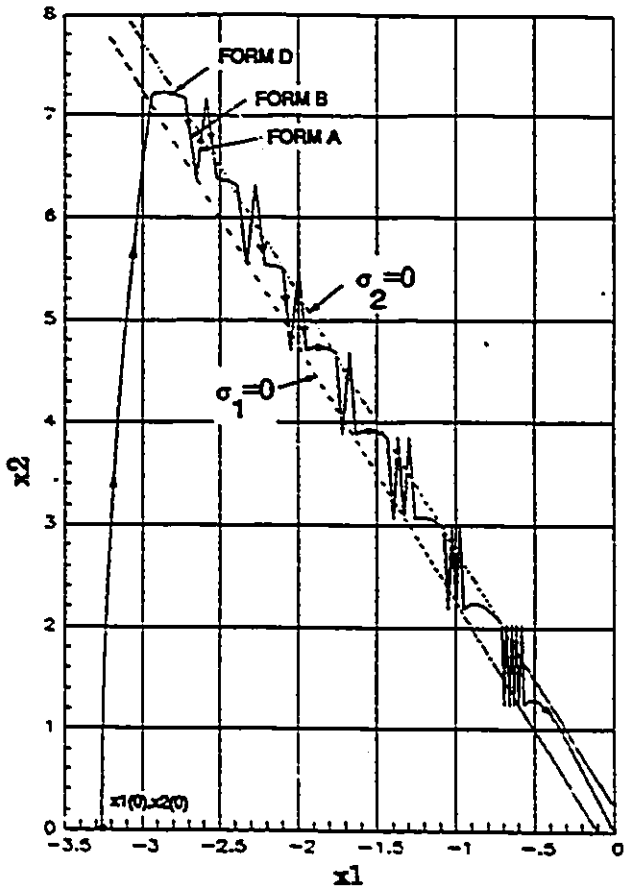

Figure II.3-13
ξ_T =.8, δ_T =.1

SIMULATIONS ANALYSIS.

To analyze the results of the simulated system II.3-3, for the changes of ξ_T and δ_T, the damping coefficient due to viscous friction, has been kept zero (ξ_v=0) in Figures (II.3-8,9,10,11, 12, 13).

Maintaining δ_T =2 in Figures (II.3-8,9,10), the effect of changes of the damping coefficient ξ_T (due to the velocity feedback from the tachogenerator) , from almost zero (Figure (II.3-8)), to one (Figure (II.3-10)), are shown. The responses of such a system are analyzed as:

a- An almost unstable motion (Figure (II.3-8) and marginal stability) with trajectories of the types of: FORM A & B & C.

b- Stable motion (Figure (II.3-9)) with trajectories of the types of: FORM A & B & C(for such system which is overdamp in region II).

c- Stable motior (Figure (II.3-10)) with represented trajectories of the forms of: FORM A & D (which is underdamp in region II).

By further increases of ξ_T, the system behavior will remain unchanged as Figure (II.3-10) shows (Consider II.3-6).

Results from Figures (II.3-8,9,10), imply that, only for very small magnitudes of ξ_v and ξ_T, the system can be unstable (effect of round-off numerical values of the states of variables of the system and the sampling time) or for even $\xi_v \cong 0$ and $\xi_T \cong 0$ system stays in a limit cycle (sinosoidal motion of the position-error for infinite time).

Maintaining ξ_T = 0.1 and decreasing the distance of the two switching lines (σ_1=0, σ_2=0) from δ_T =0.5 in Figure (II.3-11), to δ_T =0.1 in Figure (II.3-12), system responses will be stable motions (Figure (II.3-11&12)) with the representative trajectories of the types of: FORM-A, FORM-B, FORM-C. These results clarify that for $0 < \xi_T < (m_T)^{-1/2}$, changes of the distance of switching lines do not change the forms of such trajectories in the region II (i.e. Forms A,B,C, and stable motion).

Keeping δ_T =0.1 (Figure (II.3-13)), and increasing damping coefficient ξ_T, the response of the system will be a stable motion with

trajectories of the types of:FORM-A, FORM-B and FORM-D. Therefore, when $\xi' > (m_T)^{1/2} > 0$, the forms of A & B are accompanied by FORM-D into region II which shows that for the small magnitudes of δ_T, when ξ' is high, the system is able to ignore this region(i.e. by demonstrating trajectories of the types of FORM-A and FORM-B in region II). This is not only because of the effect of numerical round-off errors of the solver, but also the magnitude of sampling time is not small enough (in this case $T_o = 60T_S$) in order to have a similar ideal trajectory (i.e. having only FORM-D trajectory) in region II. By selecting a smaller δ_T or changing the magnitude of sampling time, state of motion will be of sliding type with demonstrating chattering. These forms of parabolas in region II are much closer to the actual system behavior if a digital feedback control system is used (A discrete system).

At this point, it is completely evident if ξ_T increases, trajectories emerge of the type of FORM-D, and it should not surprise us (Consider condition II.3-6 (When this condition is satisfied, form of the trajectory in region II is configured as FORM-D)).

Relation II.3-5 show that the system behavior is more sensitive to the changes of ξ_T rather than changes of ξ_v if only $m_T > 1$. And the reverse is true for $m_T < 1$. In other words, differences of the actual and ideal saturation levels are effective in the states of the motion of the system DC-motor (i.e. exact measurements of the levels of T_{Sat} are important here). Also, changes of the parameters of the system (different parameter measurements) result in different states of the system motion. Consequently, system motion (forms of the trajectories) is sensitive to parameter variation (Also effect of dust, temperature, corrosion,...etc. which may result a time-variant system).

From the equation II.3-3, the magnitudes of slopes of switching lines, are related to the magnitude of ξ_T. If ξ_T, becomes zero, these lines will be vertical. In this way, for the large distance of the switching lines, if $\xi_v = 0$, result will be comparable with the result of the simulation in Figure (II.3-8) (or having limit cycle), and if ξ_v, increases ($\xi_v > 0$), system variable state will be in a stable condition with trajectories of the types of FORM-D and FORM-C. But, if the

distance of the switching lines becomes very small, system variable state is in a sliding mode towards the origin of the phase plane.

II.3.3 Section Summary and Conclusions

What is the goal of these notes? To collect these results for a feedback control DC-motor system, using a discrete PID controller, without tachogenerator (no damping effect because of this), following conclusions are obtained:

1. Coulomb friction results in steady state errors. Contrary to the result for an analog DC-motor system model, the magnitude of such final error is dramatically related to the magnitude of the sampling time (rather than resulting final error as $x_1(t=\infty)=d$). Such resulting error is also observed for PID controller (Consider section III.1 and the effect of Coulomb friction).

2. If the viscous friction coefficient is small that it can be assumed to be zero, the state of the motion of the system with torque saturation limits is in unstable condition and depends upon T_s, may result in oscillation for long time. This result does not differ for any magnitude of such limits (distance of switching lines)[for the initial conditions in the saturated regions]. Similar result can also be observed from PID control system of this type.

3. The levels of the torque saturation result in different states of motion of the system relating to the magnitude of viscous coefficient and mainly the magnitude of sampling time. These states can be represented by sliding, underdamp and overdamp ed phases for $\xi>0$. If these limits (i.e. T_{sat}) are very small, the DC-motor dynamic model can no longer be represented by a continuous second order system. Such motion follows the state of sliding mode. Similar system behavior can be observed from PID controller used in feedforward of such a system.

4. The Differences in the measurements of the system parameters result in different system motions. From high oscillatory kind to... In

this way, the system behavior is sensitive to its exact measured parameters. This result is also obtained when a PID controller is present in feedforward loop.

5. Consequently, torque saturation in a DC-motor system changes the continuous state of the feedback control model to a discontinuous system. The state of the initial conditions of such model are effective elements in modifying the resulted motion.

Chapter III

CONTROLLER DESIGN AND COMPUTER SIMULATIONS OF THE DC-MOTOR MODEL WITH PID AND SELF-ADJUSTING ADAPTIVE SLIDING MODE CONTROLLER

III.1 PID CONTROLLER

The dynamic equation of the present DC-motor system with known parameters (this will be calculated in the section IV.1.5 (equation IV.1-2)), can be represented in state space as:

$$\dot{\theta} = \begin{bmatrix} 0 & 1 \\ 0 & 1 \end{bmatrix} \theta + \begin{bmatrix} 0 \\ 38.86 \end{bmatrix} u \qquad \text{(III.1-1)}$$

where u, is the equivalent input control voltage to the DAC-08C in Dec.(decimal) and θ is the sensory position in number of holes of the rotary disk. The transfer function of the system, thus, is given by:

$$G_p(s) = \frac{\theta(s)}{u(s)} = \frac{38.860}{s\,(s+1)} \qquad \text{(III.1-2)}$$

Assuming that the system is under unit feedback position control and G_P is the open loop transfer function of the system, The time constant (t_c), and the settling time (t_{ss}) of the closed-loop system are:

$$t_c = (1/2)^{-1} = 2 \text{ Sec}$$
$$t_{ss} = 4t_c \text{ (2\% criterion, } 0<\xi<.9) = 8 \text{ Sec}$$

The block diagram of the position control of the system with PID controller is depicted in Figure (III.1-1) with a ZOH (Zero Order Hold).

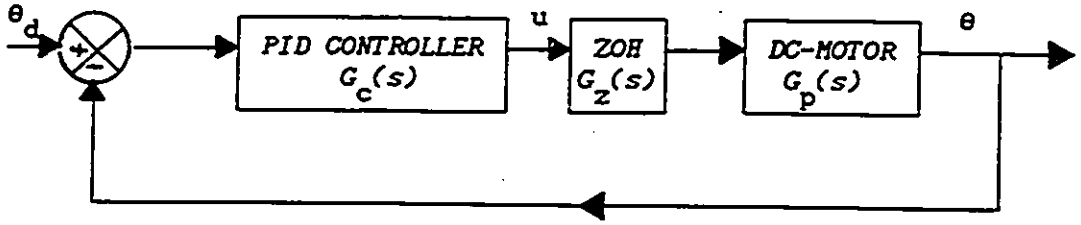

Figure III.1-1 A block diagram of a PID controller with ZOH .

Taking into account the settling time of the unit feedback closed loop system and the selection criterion of $T_s << t_c$), we select the sampling time as:

a) T_s=.03 Sec

b) T_s=.1 Sec

Now, considering the transfer function of ZOH as:

$$G_Z(s)=\frac{(1- e^{-Ts})}{s} \qquad \text{(III.1-3)}$$

where $T=T_s$.

The combined transfer functions of ZOH and DC-motor, can be written as:

$$G_{p\&zoh}(s)=\frac{(1 - e^{-Ts})(38.860)}{s^2\,(s+1)} \qquad \text{(III.1-4)}$$

Z-transformation of $G_{p\&zoh}$ (equation III.1-4), for each sampling time is:

for T_s=.03 Sec

$$G_{p\&zoh}(z)=\frac{.0173\ \ (Z+.9900)}{(Z-1)(Z-.9704)} \qquad \text{(III.1-5a)}$$

for T_s=.1 Sec

$$G_{p\&zoh}(z)=\frac{.188\ \ (Z+.9672)}{(Z-1)(Z-.9048)} \qquad \text{(III.1-5b)}$$

Considering the PID transfer function equation II.1-2 in z-domain and $G_{P\&ZOH}$ and considering block diagram of the Figures (III.1-1 and 2), we can obtain the PID controllers in discrete form as (method of solution from [26]):

For the case (a) as T_s=.03 Sec

$$u(k)=u(k-1)+11.1e(k)-20.7649e(k-1)+ 9.6948e(k-2) \qquad \text{(III.1-6a)}$$

For the case (b) as T_s=.1 Sec

$$u(k)=u(k-1)+1.1e(k)-1.9853e(k-1)+0 .8958e(k-2) \qquad \text{(III.1-6b)}$$

where u is the output from the PID controller in Dec.[0-127] and e.is the error signal ($e=\theta_d-\theta$ [hole], input signal to PID controller).

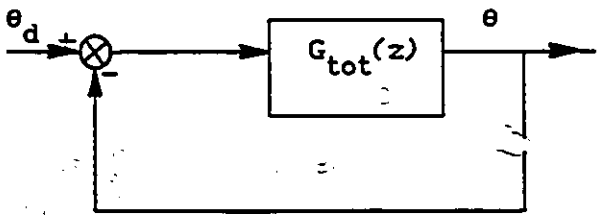

Figure III.1-2 The block diagram of the DC-motor servo system.

In this design , the $G_{tot}(z)$ (the open-loop transfer function of the Figure (III.1-1)) and the $G_{cl}(z)$ (the closed-loop transfer function of the Figure (III.1-2)), for the two above selections of the sampling time are:

for T_s=.03 Sec

$$G_{tot}(z)=\frac{.0173z^2+.0016z-.0154}{z^3-2z^2+1} \qquad \text{(III.1-7a)}$$

$$G_{cl}(z)=\frac{\theta(z)}{\theta_d(z)}=\frac{.1922z^2+.0173z-.1712}{z^3-1.8096z^2+1.0171z-.1697} \qquad \text{(III.1-8a)}$$

for T_s=.1 Sec

$$G_{tot}(z)=\frac{.1880z^2+.0126z-.1636}{z^3-2z^2+1} \qquad \text{(III.1-7b)}$$

$$G_{cl}(z)=\frac{\theta(z)}{\theta_d(z)}=\frac{.2068z^2+.0139z-.1800}{z^3-1.7932z^2+1.0139z-.1800} \qquad \text{(III.1-8b)}$$

where θ_d is in number of holes.

and the closed-loop damping coefficient, time constant and the poles are:

for T_s=.03Sec:
$$\begin{cases} t_c = .1672 \text{ Sec} \quad [t_{ss}=.6687 \text{ Sec}], \ \xi=1 \\ z_1 = .309 \\ z_2 = .6631 \\ z_3 = .8357 \end{cases}$$

for T_s=.1Sec:
$$\begin{cases} t_c = .6042 \text{ Sec} \quad [t_{ss}=2.417 \text{ Sec}], \ \xi=1 \\ z_1 = .3670 \\ z_2 = .5788 \\ z_3 = .8474 \end{cases}$$

The two Figures (III.1-3a and 3b), show the root locus of the block digram represented in the Figure (III.1-1) in z-plane. These figures show the representative roots for the choices of the proportional gain K_p.

Figures (III.1-4 and 5), show the response of the system III.1-7b (III.1-8b) for the desired input θ_d=3 Holes. Figures (III.1-6 and 7), show the response of the system III.1-7a (III.1-8a), for the same desired input. In these simulations, because of the discrete motion, system naturally shows overshoot. These overshoots are shown in both phase-plane representations of the system (Figures (III.1-4 and 6)). The magnitude of overshoot because of this, is increased if desired input increases (even for $\xi \geq 1$). For instance: simulating the system with sampling time .03 Sec, for desired input θ_d=15 Holes, resulted in an maximum overshoot as M_p=-2 Holes. The two Figures (III.1-5 and 7) show the output control signal to the DAC-08C. In the actual model, since the magnitude of Coulomb friction is high (equivalent 20 Dec.), for this desired input, system may not show any motion for the sampling time .1 Sec (control signal can not exceed a maximum 3 Dec. (Figure (III.1-5)). These simulations are (purposely) performed for the following conditions:

$x_1(-2)=0$, $x_1(-1)=0$, $x_1(0)=\theta_d-\theta=3$ Holes, (x_1=e), $u(-1)=0$

Also consider the simulations in APPENDIX-E, for different initial conditions.

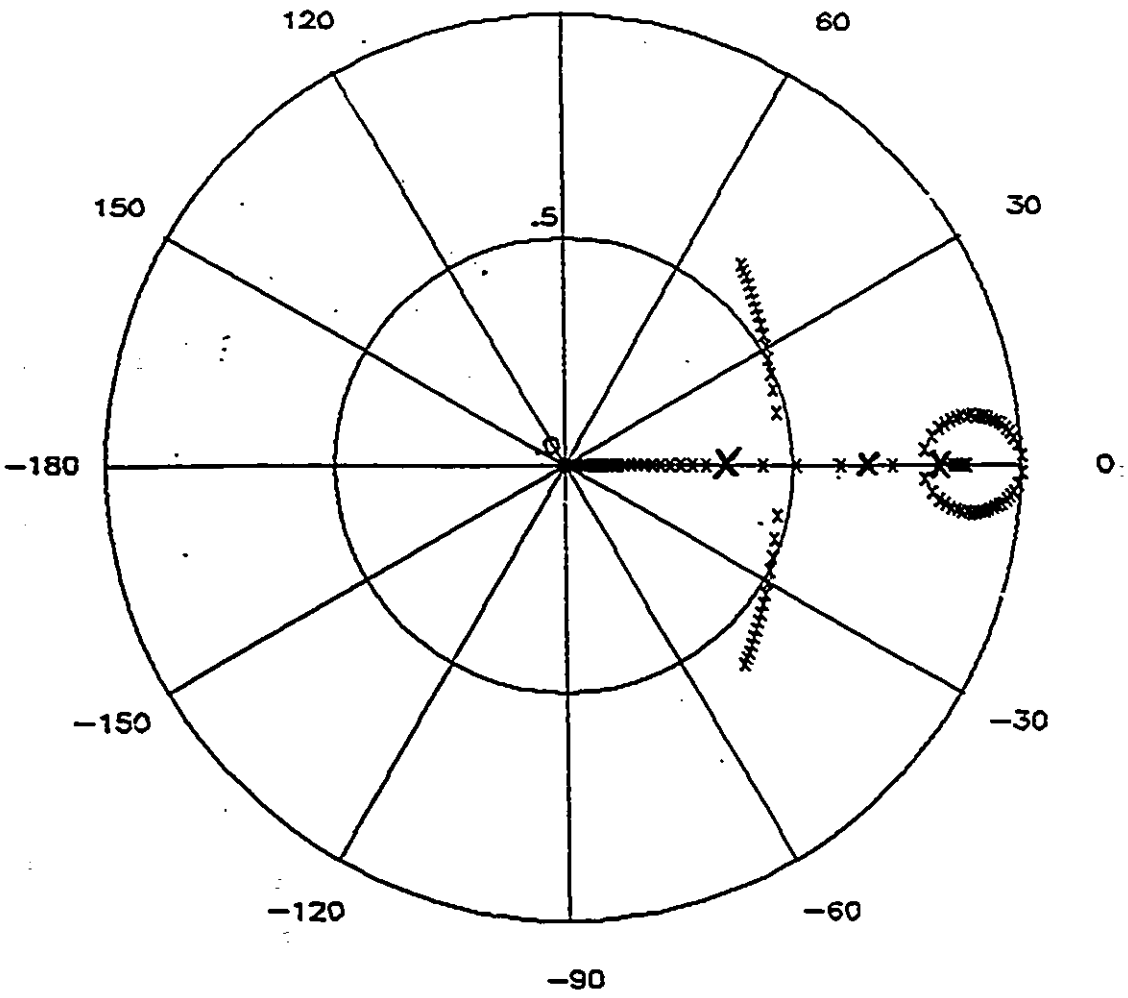

Figure III.1-3a The root locus of the system represented by Figure (III.2-1), and the representation of the roots of characteristic equation for the proportional gain of K_p=11 and sampling time T_s=.03 Sec

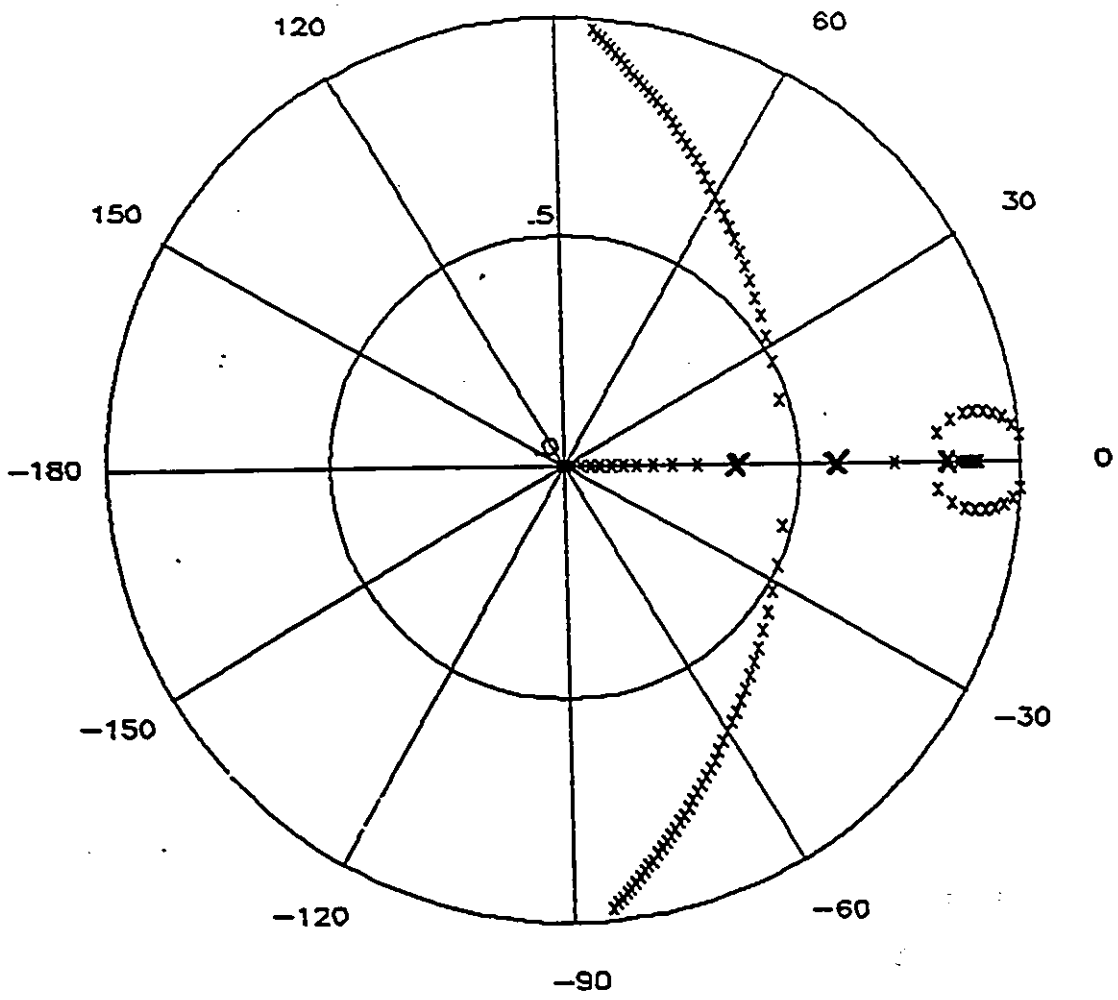

Figure III.1-3b The root locus of the system represented by Figure (III.2-1), and the representation of the roots of characteristic equation for the proportional gain of K_p=1.1 and the sampling time T_s=.1 Sec

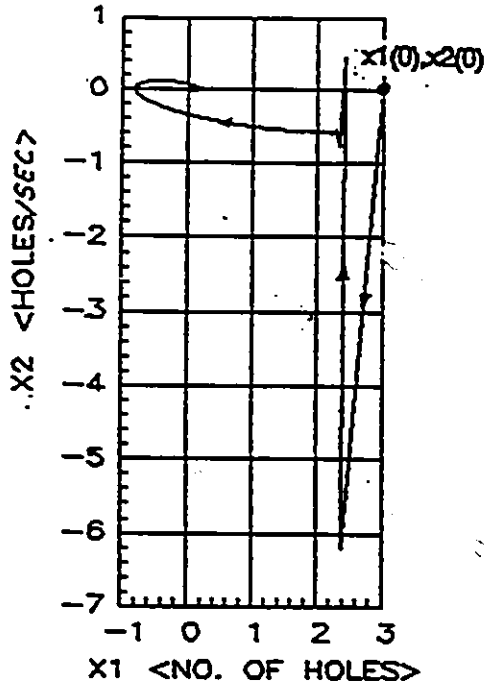

Figure III.1-4 Phase-plane representation of the system (case (a)).

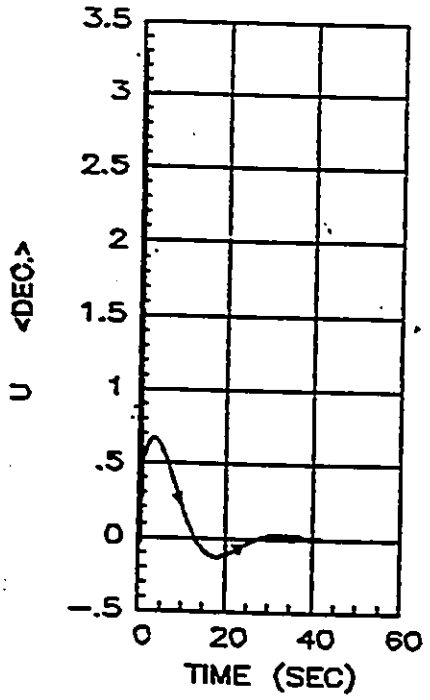

Figure III.1-5 Control output signal versus time(Sec).

(A numerical simulation of the experimental DC-motor model for the T_s=.1 Sec)

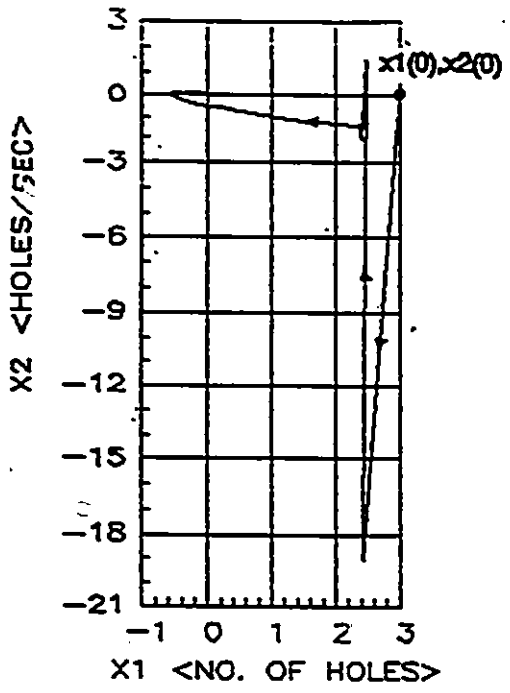

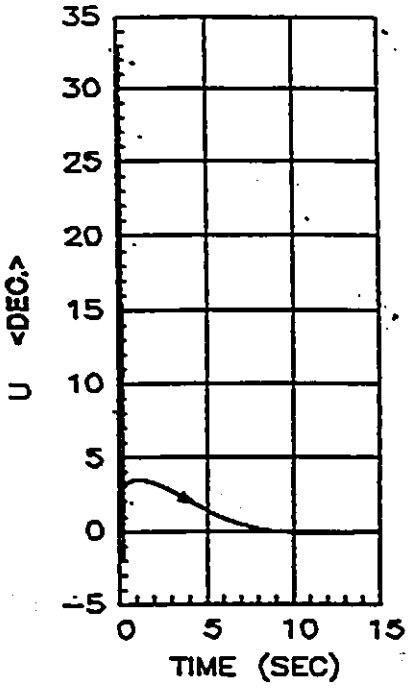

Figure III.1-6 Phase-plane representation of the system (case (b)).

Figure III.1-7 Control output signal versus time(Sec).

(A numerical simulation of the experimental DC-motor model for the T_s=.03Sec)

III.1.1 The Effect of Coulomb Friction

As it is studied in section II.2, for a system motion such as DC-motor system under linear feedback control (A "P" controller), in the presence of Coulomb friction, the final position error in the neighborhood of the origin of the phase plane can be observed (consider d'≥d). For a desirable resulting error by conditioning or adapting the controller, constraints may be subjected to the desirable dynamic.

To show this effect, we assume a PID controller operates in a feedforward loop shown in the block diagram of the Figure (II.3-1) (after first comparator). Similar to Figure (II.3-3), the state of variables of the system will be towards point $A'^{(3a)}$ and once Coulomb friction torque causes the termination of the motion, the velocity-error becomes zero, and the control output voltage from PID , given by II.1-1, as:

$$U=K_p x_1+K_d x_2+K_i \int x_1 dt$$

will be changed into:

$$U=K_p x_1+K_i \int x_1 dt$$

Or

$$U\cong x_1(t=\infty)\ (K_p+T_s K_i)$$

From this point, since x_1 remains unchanged for each sampling time, the above input signal U, for the restart of the motion of the system can not compensate, resulting error(if d'>d, section II.3) and DC-motor sticks at this point (point A (ideally), Figure (II.3-3)). The same input voltage in each sampling time is applied but no motion occurs and the position error remains at $x_1(t=\infty)$ (consequently a constant dependant upon ξ, T_s and $x_1(0)$). The resulting error may be reduced by the changes of the gains of the controller, but this may result in changes of the system trajectories. These kind of adaptations may result in undesirable dynamic of the system.

III.1.2 Section Summary and Conclusions

Since the characteristic polynomial of the PID control of the DC-motor is of third degree, analytically, the step response of the system, for different ranges of inputs (In the absence of external forces and frictions), should not vary too much in the term for the magnitude of overshoot, but use of a discrete system may cause overshoot even for $\xi>1$. Dependant upon the increase of the magnitude of the desired input the resulting overshoot will be increased.

Constraints in a structure of a digital process of a plant, some times does not permit the PID controllers to be designed for $\xi=1$ and even existence of round-off errors and precision of the digital signal processors (D/A, A/D, filters and op-amps...) and discretization may cause overshoot of the PID control trajectory. Consequently if the task of the system is path tracking (such as spot welders and gas cutters [4,23]) , PID controller, by itself will not be a good choice.

The response of this type of controllers in the presence of Coulomb friction and stiction on the system, is usually accompanied by steady state errors. This response is the effect of continuous control operation of the controller in the neighborhood of the origin of the phase plane in where equilibrium zone of the Coulomb friction starts.

Variable states of the system with PID controller is influenced by torque saturation (similar to Figures (II.3-8 to 13). Consider the results of the simulations at the end of the section III for this purpose).

III.2 SELF-ADJUSTING ADAPTIVE CONTROLLER IN SLIDING MODE

This section is divided into two parts. The first part presents the design of control algorithms. The second part presents the results of the performances of the controllers with the computer simulations. Because the results from mathematical analysis, are in fact not normally comparable with the results from the actual system (particularly a digital system (discrete system)), the following simulations are performed in order to help us in the analysis of the results of the experiment. Note that these results were obtained for the case of having exact knowledge of the parameters of the system (i.e. $\delta_e(t)=0$), except for the simulation S6. In this section two controllers in sliding mode as; type-A:with the term [Ksgn(σ)], and type-B:with the term [K $|x_1|$sgn(σ)] are tested for the following purposes:

1) Comparing performances of the controllers in the presence of Coulomb friction and stiction.

2) Investigating the performances of the controllers for various initial conditions if it is proved there is a switch in the system.

3) Studying the various magnitude of K and resulting frequency of the chattering.

4) Obtaining the conditions for the controllers in order to eliminate the effect of Coulomb friction and stiction.

5) Investigating the sensitivity of the controllers for the various magnitudes of K and ε for the states of switches and obtaining their limits.

6) Studying the effect of saturation on the performance of the controllers.

7) Investigating the effect of uncertain parameters of the system.

8) Investigating the effect of noise on the performance of the controller.

9) Verifying the solutions for increasing the performance of the controllers and their robustness.

10) Introducing candidate controllers for the compensation of the steady state error, resulting from Coulomb friction and stiction.

Since the volume of the results of the simulations does not permit us to present all of them here, therefore, only the parts conveying the main conclusions, will be illustrated.

III.2.1 Alternatives for Control Algorithm

Two algorithms for the implementation of the self adjusting (adaptive) controller in sliding mode, are presented here. One for a controller type of $\left[K\ \mathrm{sgn}(\sigma)\right]$, and second, for the controller type of $\left[K\ |x_1|\ \mathrm{sgn}(\sigma)\right]$.

III.2.1.A Controller Type A (with the term K sgn(σ))

In order to model the system for numerical computations, a solution for the nonlinear discontinuous system must be present. For the initial conditions as:

$$\begin{aligned} \theta(0)&=\theta_o \\ \dot{\theta}(0)&=0. \\ \ddot{\theta}(0)&=0. \end{aligned} \qquad \text{(III.2-1)}$$

The Euler integration method is used to solve the nonlinear system. This method is described by the following equations:

$$\dot{\theta}(t+\Delta t)=\dot{\theta}(t)+\Delta t\ddot{\theta}(t) \qquad \text{(III.2-2)}$$

$$\theta(t+\Delta t)=\theta(t)+\Delta t\dot{\theta}(t)+(1/2)\Delta t^2\ddot{\theta}(t) \qquad \text{(III.2-3)}$$

In order to find a suitable controller, the following control law is selected:

$$u=(1/b)[f(x_1,x_2)+K\ sgn(\sigma)] \qquad \text{(III.2-4)}$$

If III.2-4, is substituted into equation II.2-2, it gives:

$$\dot{x}_2=-K\ sgn(\sigma) \qquad \text{(III.2-5)}$$

The equation III.2-5, represents a double integrator system (section II.2.2). where for a step change in position, the errors (position, velocity, acceleration) will be computed as (assuming $\theta_d=0$):

$$\begin{aligned} x_1(t)&=\theta(t)\\ x_2(t)&=\dot{\theta}(t)\\ \dot{x}_2(t)&=\ddot{\theta}(t) \end{aligned} \qquad \text{(III.2-6)}$$

The flow-chart of this algorithm is presented in APPENDIX-A.

For the ease of studying the changes of the slope of switching lines, the curve of $l(t)$ versus $x_1(t)$, is introduced here as the representative motion of the switching line. This curve is given by:

$$l(t)=-c(t)x_1(t) \qquad \text{(III.2-7)}$$

$l(t)$ is shown in the phase-plane in the Figure (III.2-1). As this figure shows, the broken curves in the form of lines towards the origin of the phase-plane represent switching lines.

To distinguish this curve from the trajectory of the system, this curve is showed by a dashed-dotted curve and system trajectory is represented by a solid curve in all phase-plane representations.

To read graphs easier, the following chart is also presented here:

(from II.2-39)	$C_{max}=\left[K / \lvert x_1(t_o) \rvert \right]^{1/2}$	(III.2-8)
(from II.2-40&41)	$\delta_1=C_o =[C_{max}]/nn$	(III.2-9)
(from II.2-42)	$\varepsilon=[C_o]/n$	(III.2-10)
(from II.2-36) Magnitude of cond.	$C1(t+\Delta t)=K / [\delta(t+\Delta t)+\varepsilon]^2$	(III.2-11)

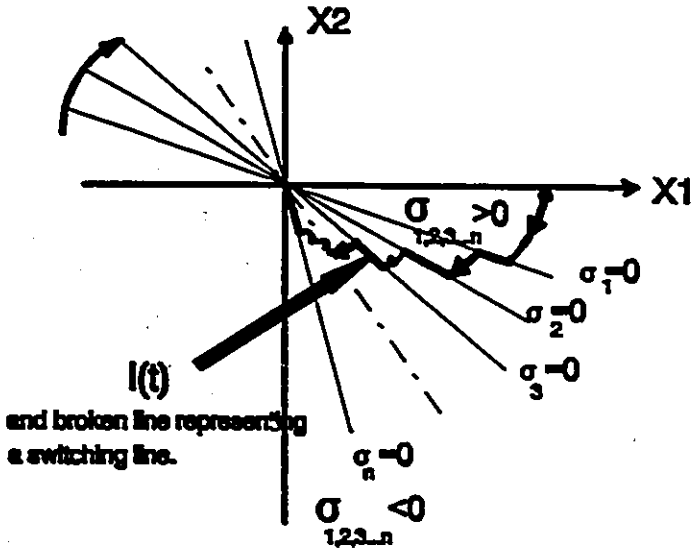

Figure III.2-1 Phase portrait of the curve of l(t), demonstrating the motion of the switching line.

III.2.1.B Controller Type B (with the term $K \mid x_1 \mid sgn(\sigma)$)

The second control law is selected from section II.2.2 (equation II.2-19):

$$u=(1/b)[f(x_1,x_2)+Cx_2+K^I \mid x_1 \mid sgn(\sigma)]$$

Substituting into equation(II.2-2), gives:

$$\begin{cases} \dot{x}_2=-Cx_2-K^I\mid x_1\mid & \text{if } \sigma\geq 0 \\ \dot{x}_2=-Cx_2+K^I\mid x_1\mid & \text{if } \sigma<0 \end{cases} \qquad \text{(III.2-12)}$$

Comparing with equation II.2-34 (for the double integrator dynamic equation), III.2-12 can be represented as:

$$\begin{cases} -K=-Cx_2-K^I\mid x_1\mid & \text{if } \sigma\geq 0 \\ +K=-Cx_2+K^I\mid x_1\mid & \text{if } \sigma<0 \end{cases} \qquad \text{(III.2-13)}$$

Considering, the condition of $K^I>C^2$, then we can define K^I as:

$$K^I=C^2+k1 \qquad \text{(III.2-14)}$$

where k1 can be selected to be a small positive value.

The two algorithms of the controllers of the types A and B can be seen in APPENDIX-A. In this algorithm for the condition of III.2-11, the information about the states of variables of the system for the last sampling time are used (a similar Gaussian approach has been applied (a sampling time behind)).

In order the system to reset itself when its trajectory crosses axis x_2, this condition is also added to this algorithm (type B):

$\delta(t)=\delta_1$ if $sgn(x_1)$ changes and the error-position is in acceptable range.

(reset of the system can also be possible by condition II.2-36)

III.2.2 The Results of Simulations

III.2.2.A Type A Controller Simulation

(for the sampling time T_s=.01 sec.)

SIMULATION-S1: The case of an arbitrary initial position-error. ($\delta_e(t)=0$)

$$\begin{cases} K=10 \\ n=3 \\ nn=8 \\ x_1(0)=2.00 \text{ Rad}, \; x_2(0)=0 \text{ Rad/Sec} \end{cases}$$

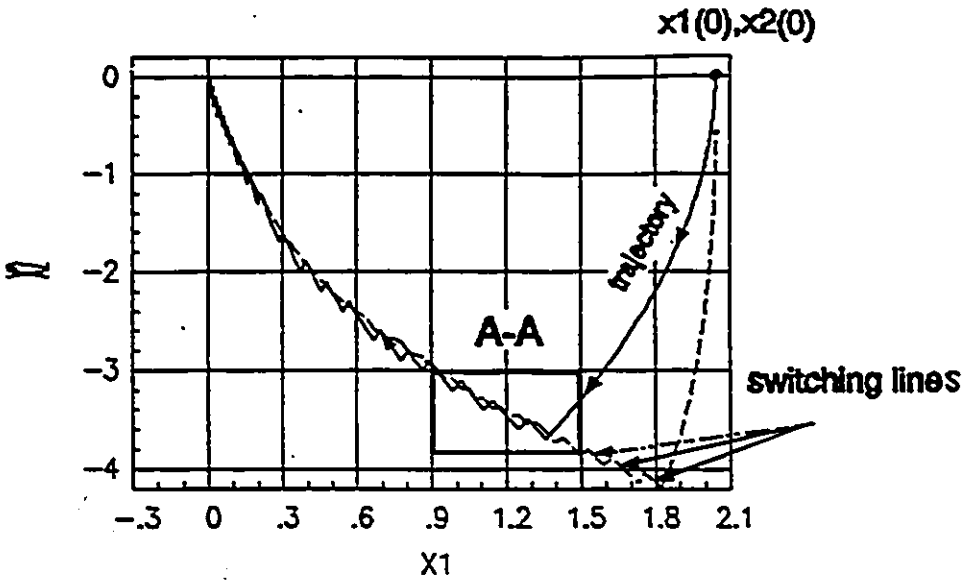

Figure III.2-2 Phase-plane representation of the trajectory.

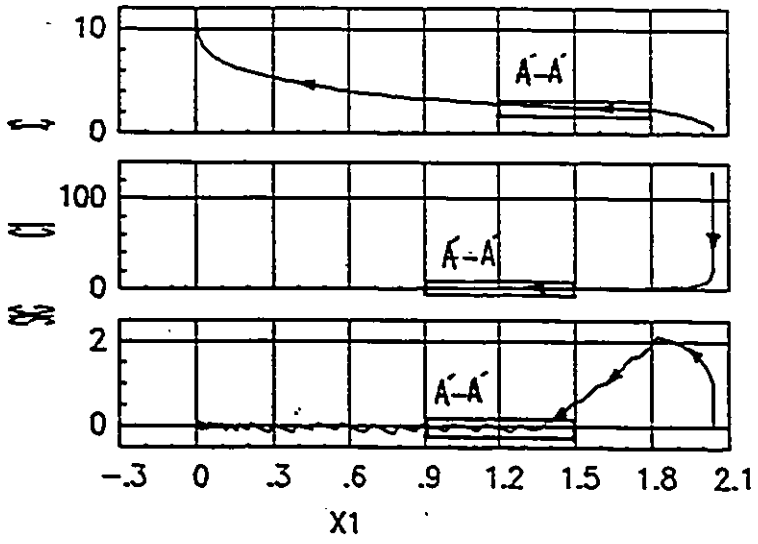

Figure III.2-3 c,c1,s versus position-error.

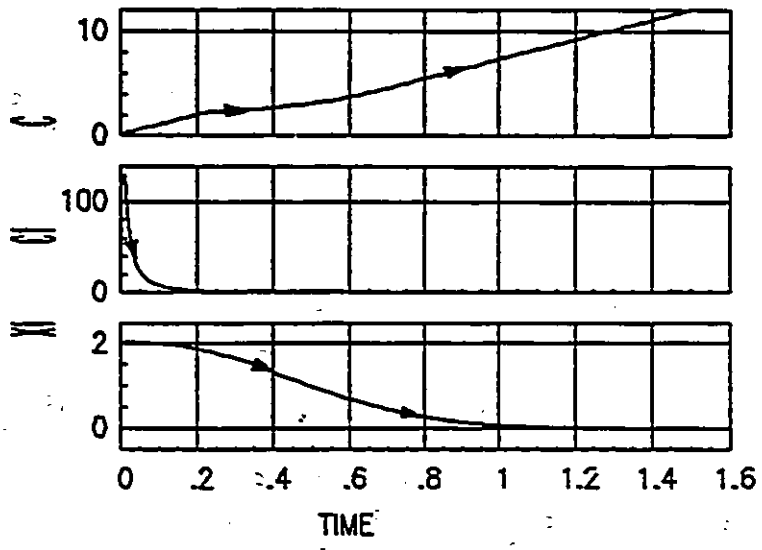

Figure III.2-4 c,c1,position-error versus time (Sec).

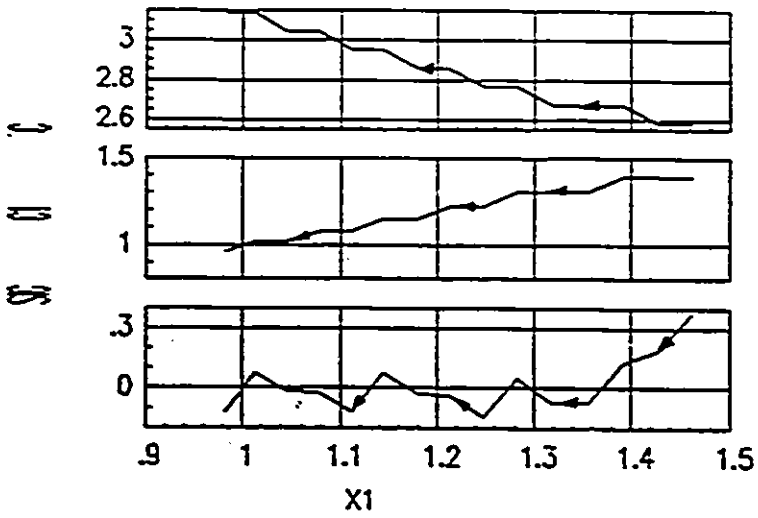

Figure III.2-5 c,c1,s versus $x_1(t)$ (detail rectangle A'-A').

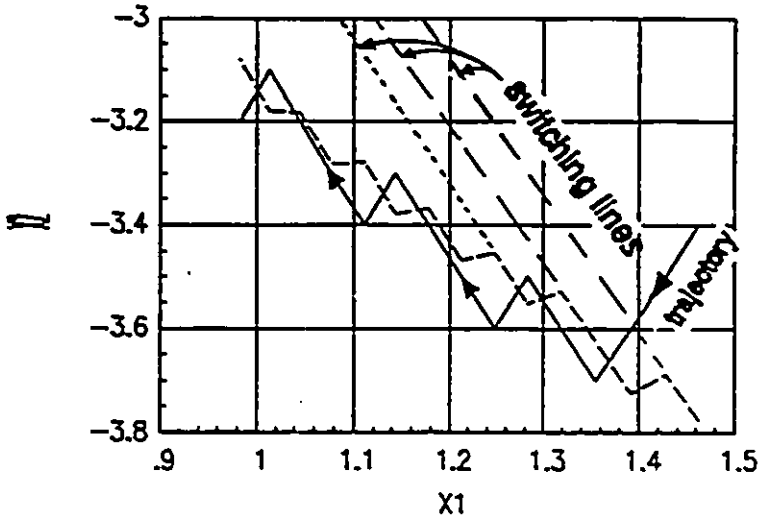

Figure III.2-6 Phase plane representation of the trajectory (detail rectangle A-A).

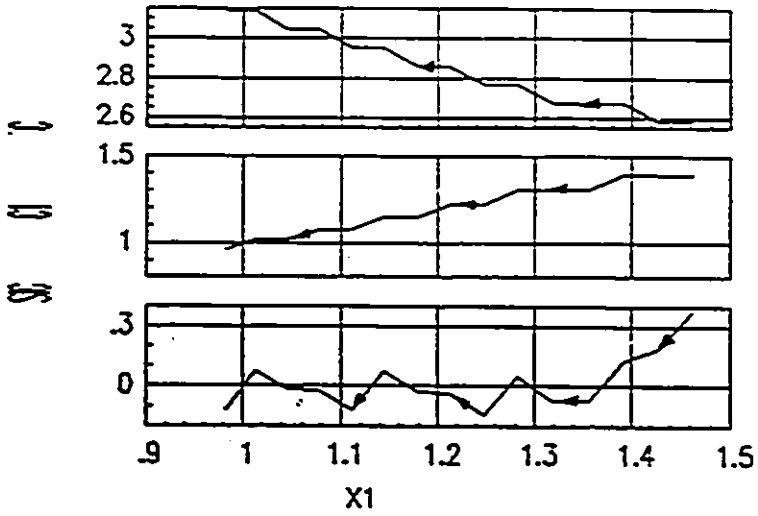

Figure III.2-5 c,c1,s versus $x_1(t)$ (detail rectangle A'-A').

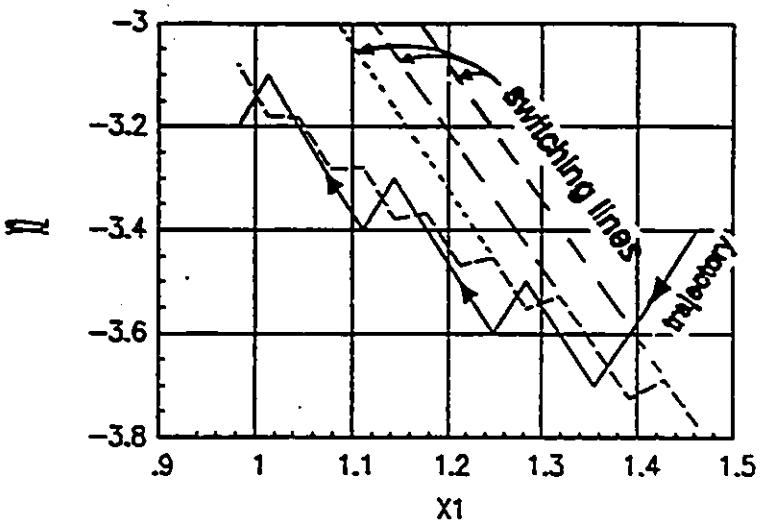

Figure III.2-6 Phase plane representation of the trajectory (detail rectangle A-A).

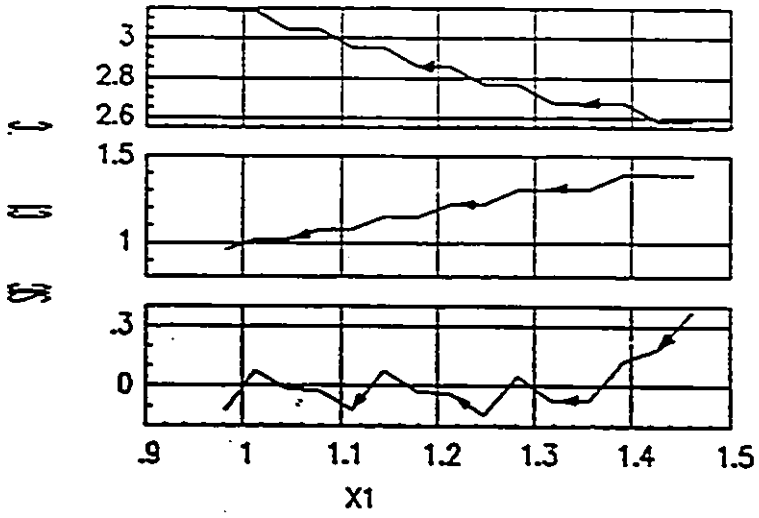

Figure III.2-5 c,c1,s versus $x_1(t)$ (detail rectangle A'-A').

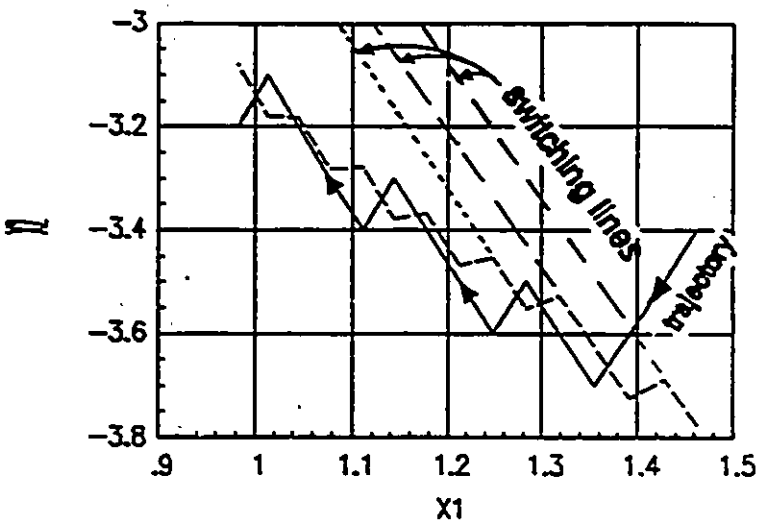

Figure III.2-6 Phase plane representation of the trajectory (detail rectangle A-A).

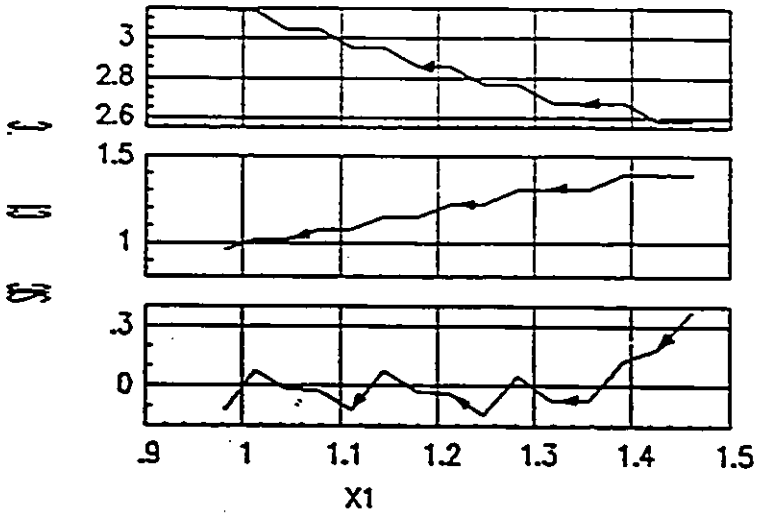

Figure III.2-5 c,c1,s versus $x_1(t)$ (detail rectangle A'-A').

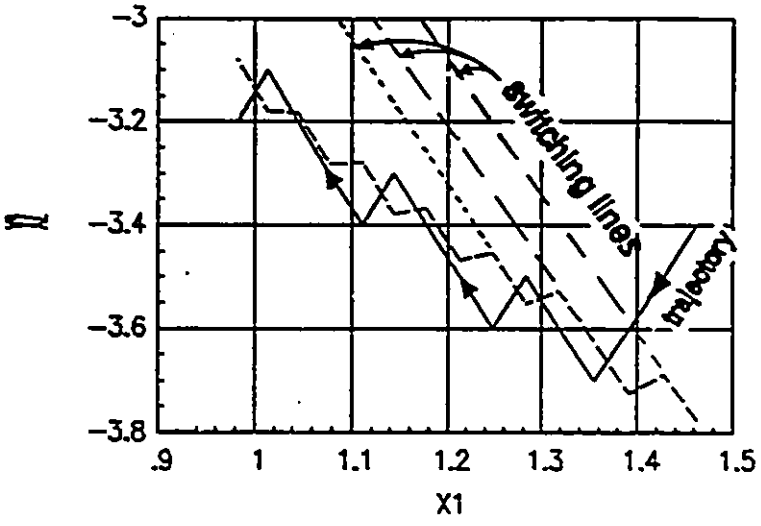

Figure III.2-6 Phase plane representation of the trajectory (detail rectangle A-A).

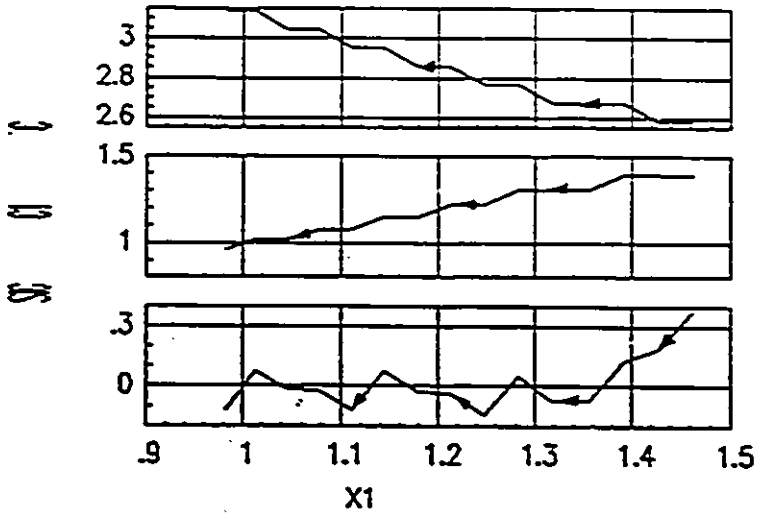

Figure III.2-5 c,c1,s versus $x_1(t)$ (detail rectangle A'-A').

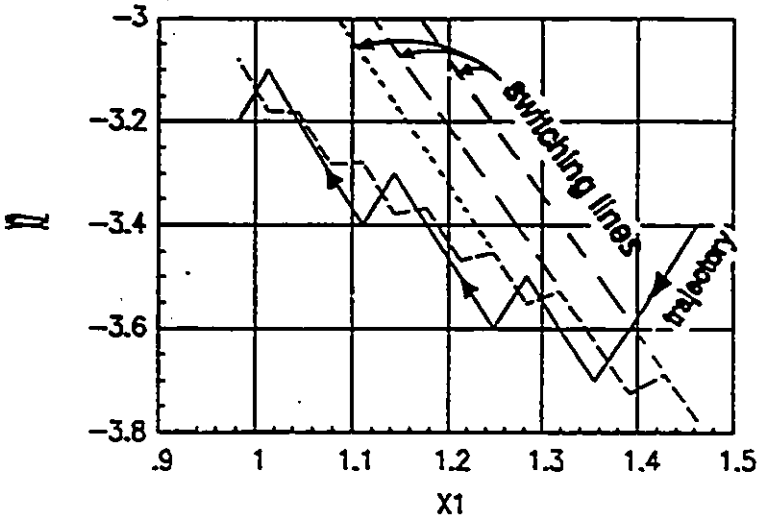

Figure III.2-6 Phase plane representation of the trajectory (detail rectangle A-A).

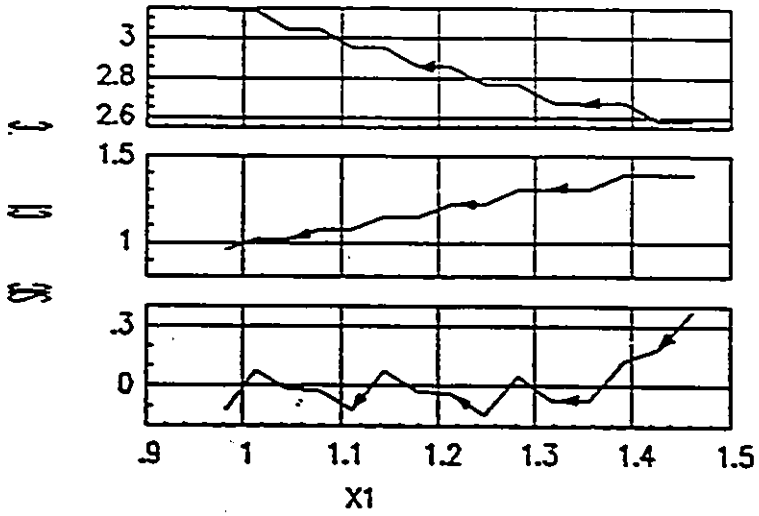

Figure III.2-5 c,c1,s versus $x_1(t)$ (detail rectangle A'-A').

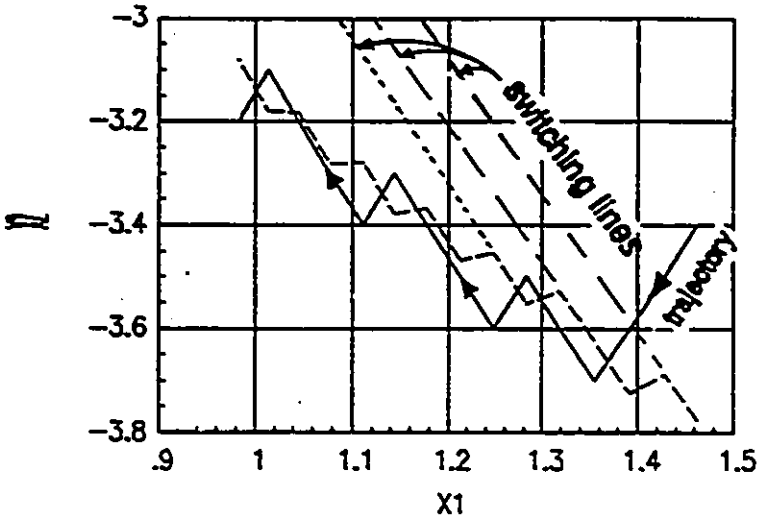

Figure III.2-6 Phase plane representation of the trajectory (detail rectangle A-A).

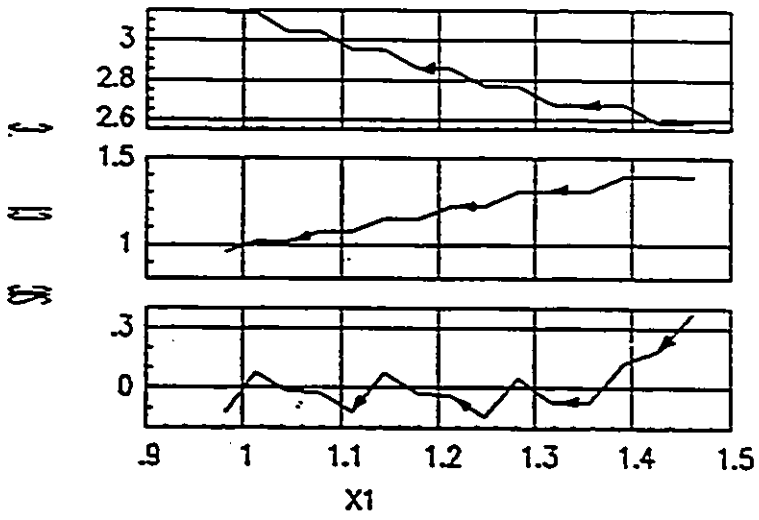

Figure III.2-5 c,c1,s versus $x_1(t)$ (detail rectangle A'-A').

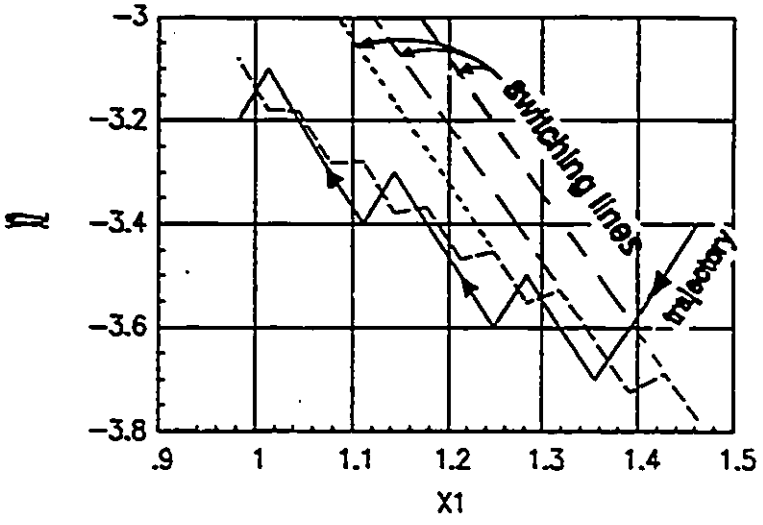

Figure III.2-6 Phase plane representation of the trajectory (detail rectangle A-A).

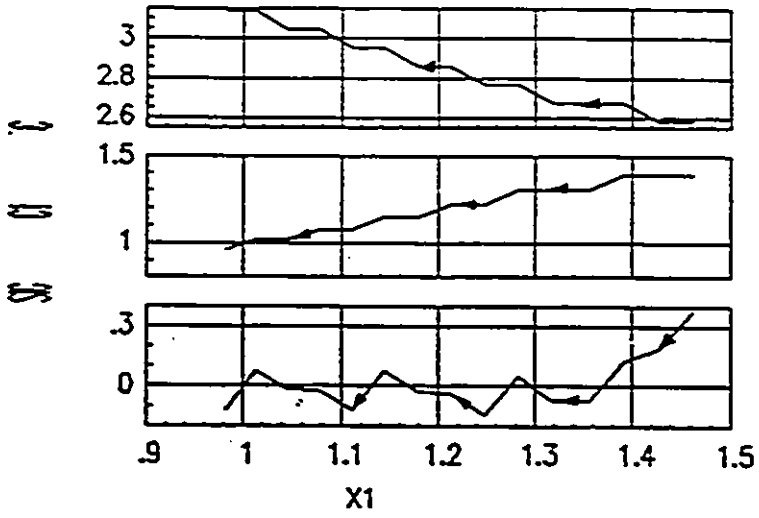

Figure III.2-5 c,c1,s versus $x_1(t)$ (detail rectangle A'-A').

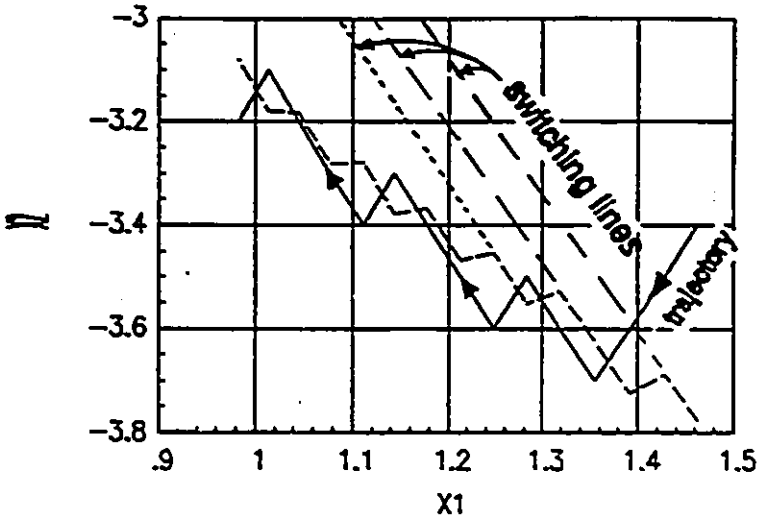

Figure III.2-6 Phase plane representation of the trajectory (detail rectangle A-A).

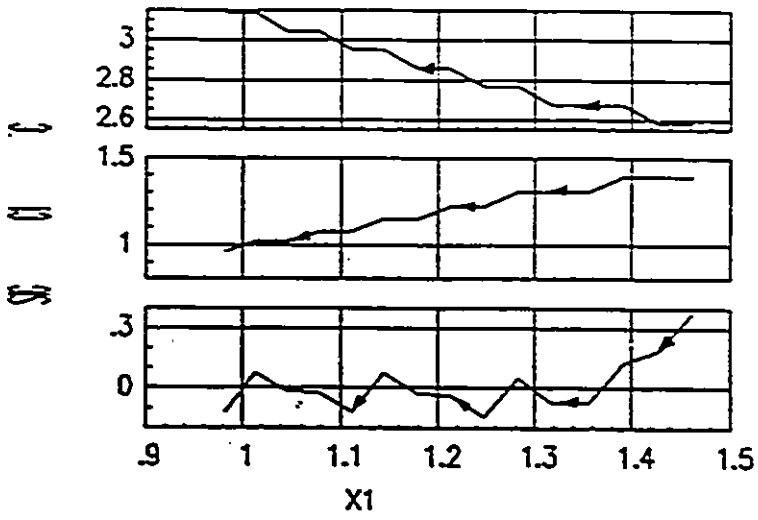

Figure III.2-5 c,c1,s versus $x_1(t)$ (detail rectangle A'-A').

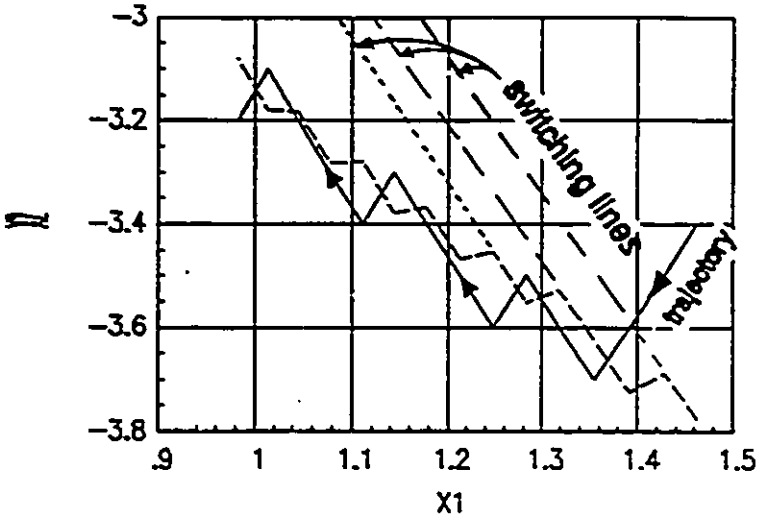

Figure III.2-6 Phase plane representation of the trajectory (detail rectangle A-A).

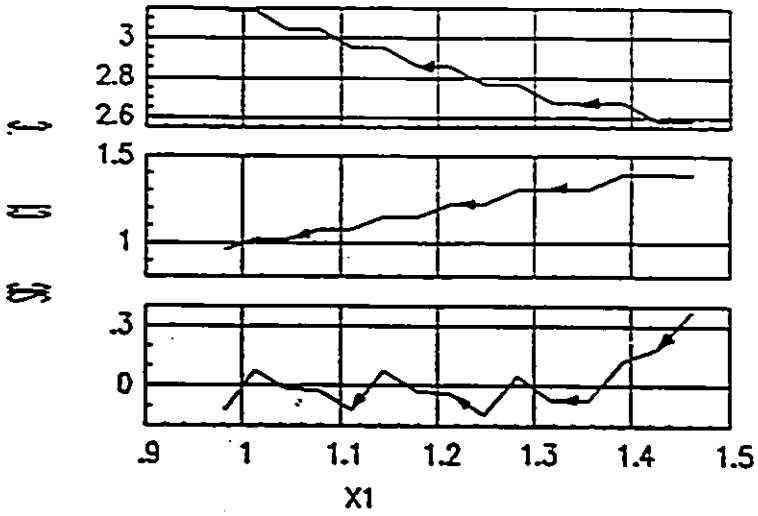

Figure III.2-5 c,c1,s versus $x_1(t)$ (detail rectangle A'-A').

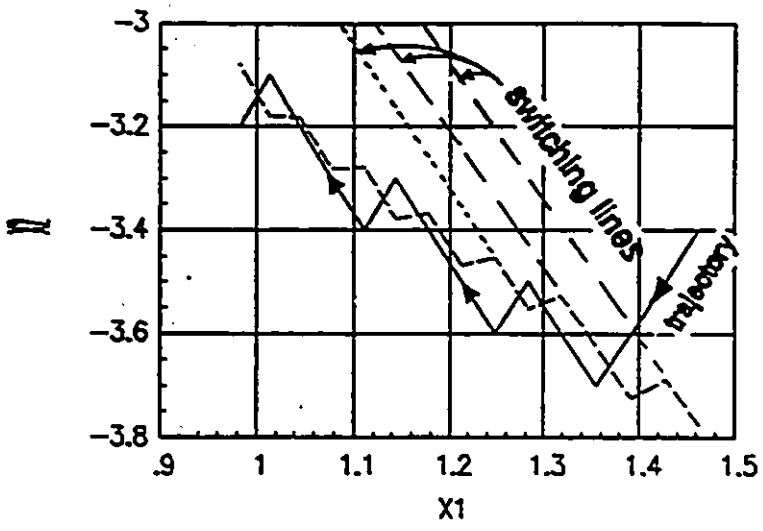

Figure III.2-6 Phase plane representation of the trajectory (detail rectangle A-A).

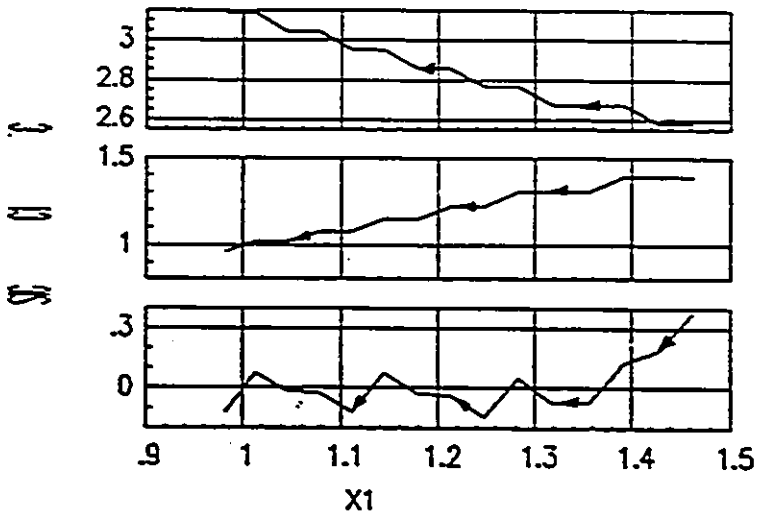

Figure III.2-5 c,c1,s versus $x_1(t)$ (detail rectangle A'-A').

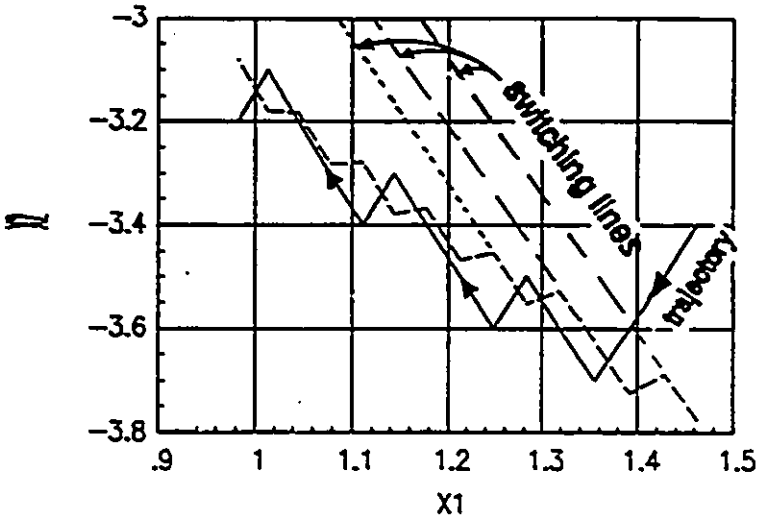

Figure III.2-6 Phase plane representation of the trajectory (detail rectangle A-A).

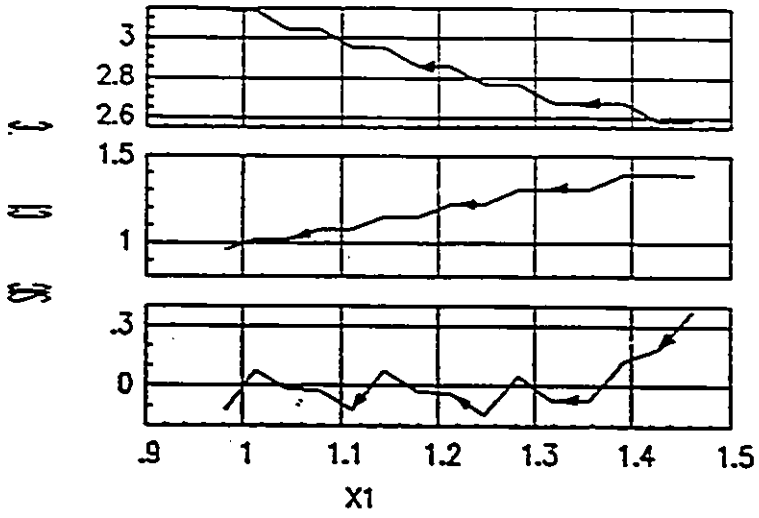

Figure III.2-5 c,c1,s versus $x_1(t)$ (detail rectangle A'-A').

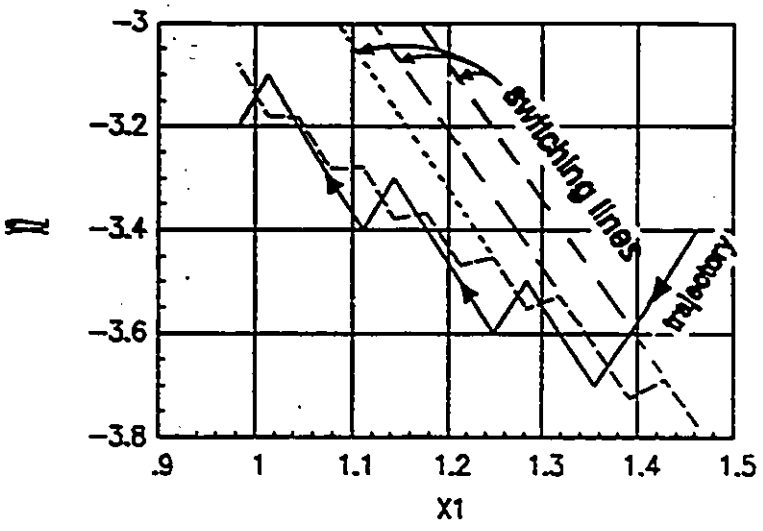

Figure III.2-6 Phase plane representation of the trajectory (detail rectangle A-A).

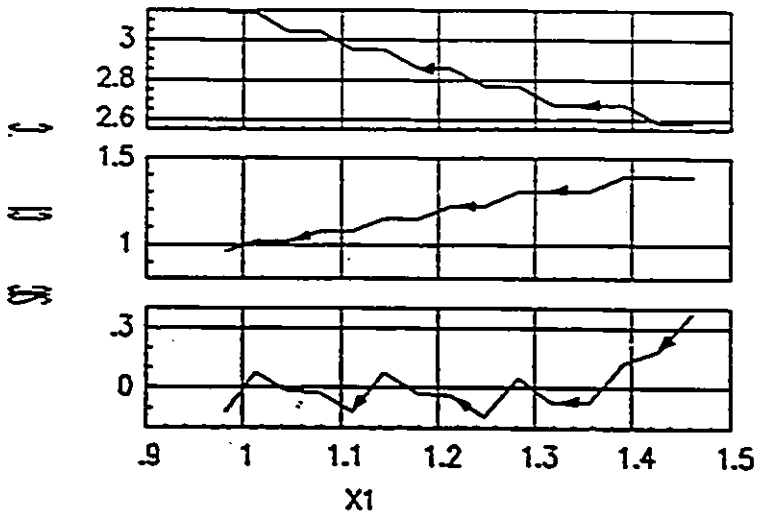

Figure III.2-5 c,c1,s versus $x_1(t)$ (detail rectangle A'-A').

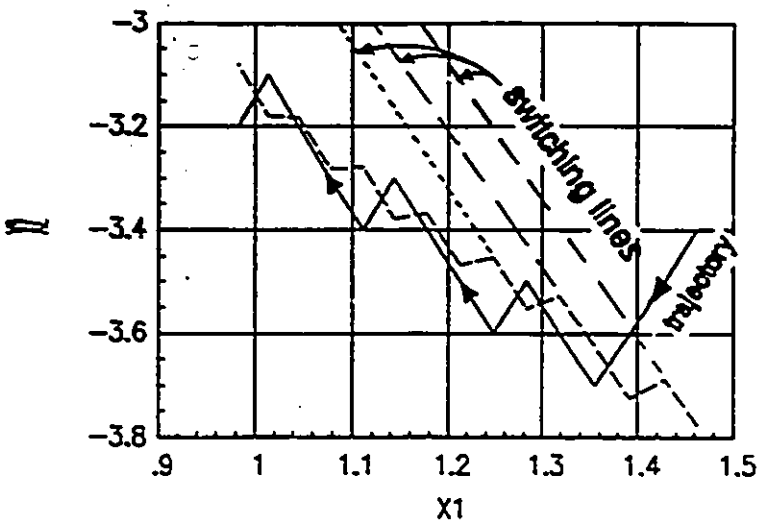

Figure III.2-6 Phase plane representation of the trajectory (detail rectangle A-A).

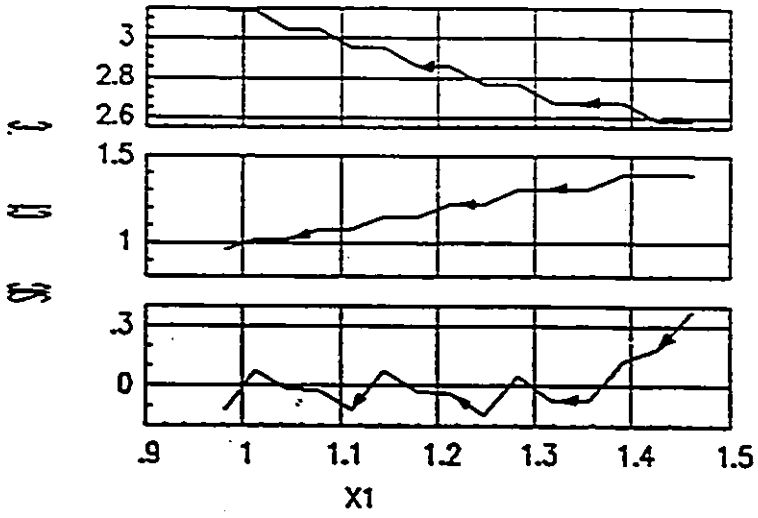

Figure III.2-5 c,c1,s versus $x_1(t)$ (detail rectangle A'-A').

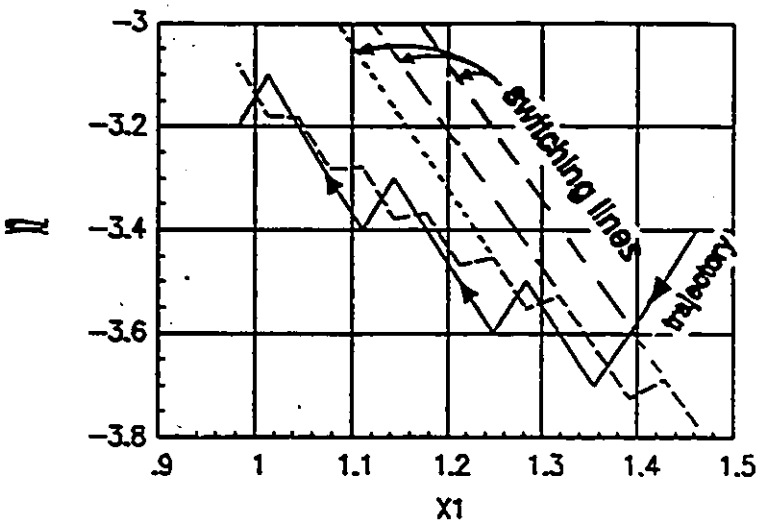

Figure III.2-6 Phase plane representation of the trajectory (detail rectangle A-A).

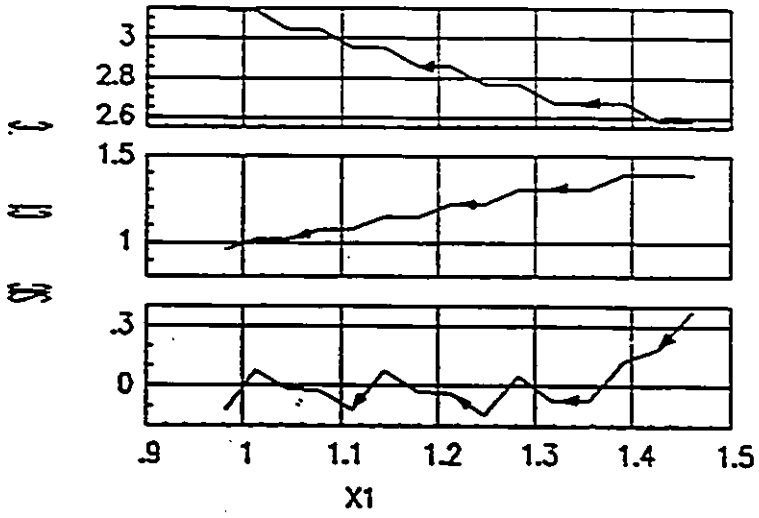

Figure III.2-5 c,c1,s versus $x_1(t)$ (detail rectangle A'-A').

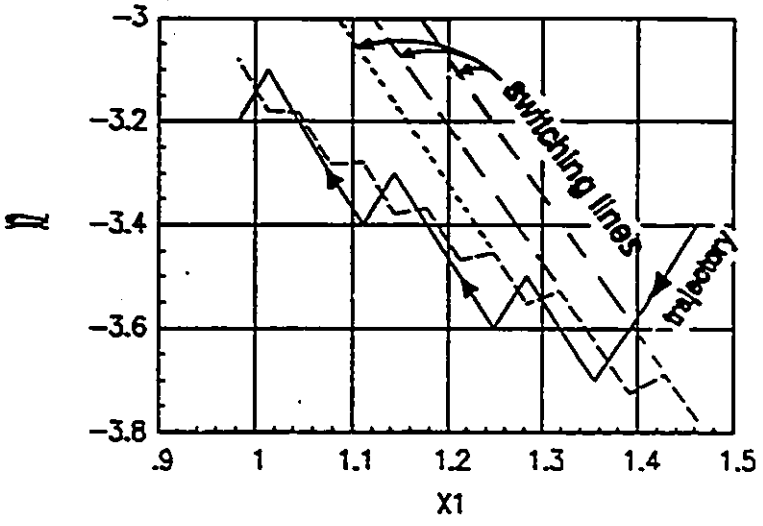

Figure III.2-6 Phase plane representation of the trajectory (detail rectangle A-A).

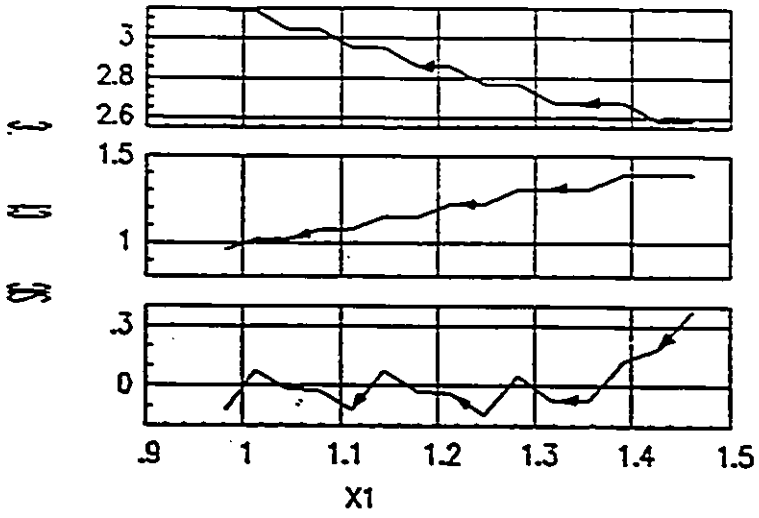

Figure III.2-5 c,c1,s versus $x_1(t)$ (detail rectangle A'-A').

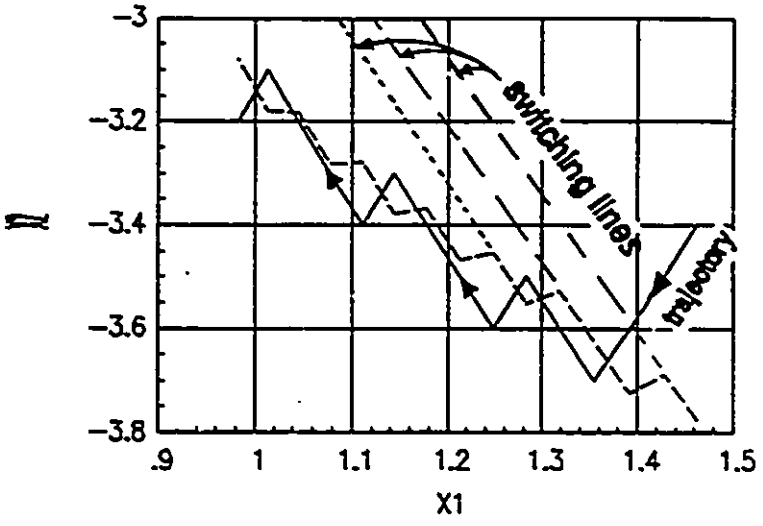

Figure III.2-6 Phase plane representation of the trajectory (detail rectangle A-A).

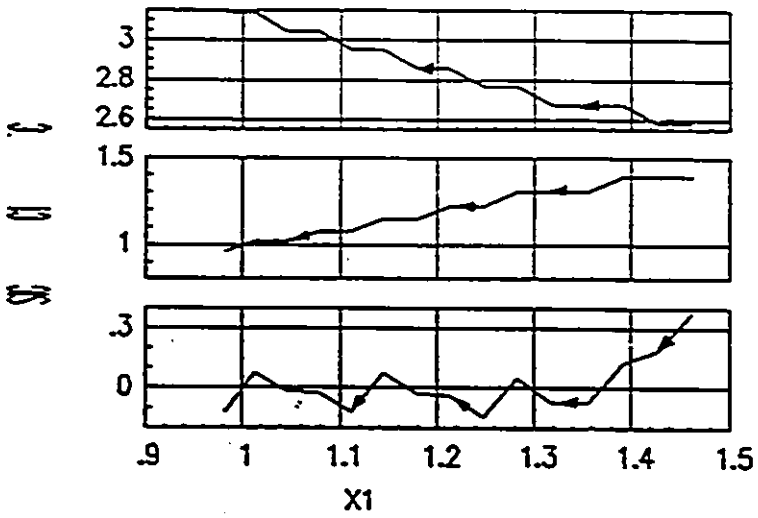

Figure III.2-5 c,c1,s versus $x_1(t)$ (detail rectangle A'-A').

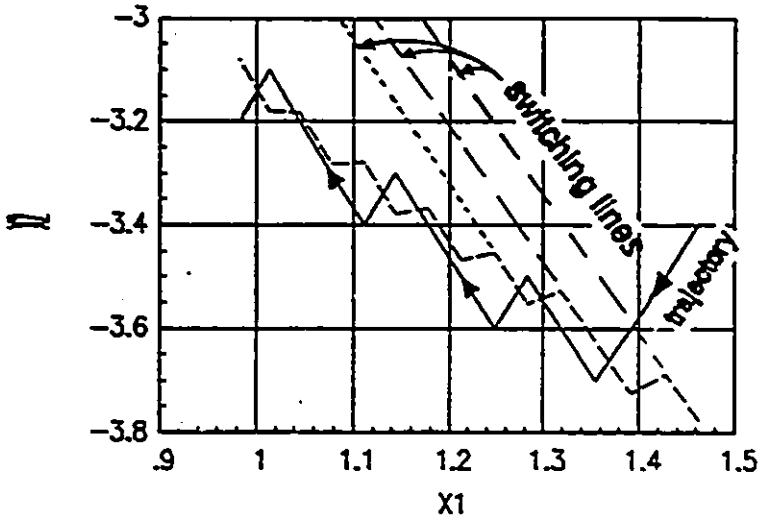

Figure III.2-6 Phase plane representation of the trajectory (detail rectangle A-A).

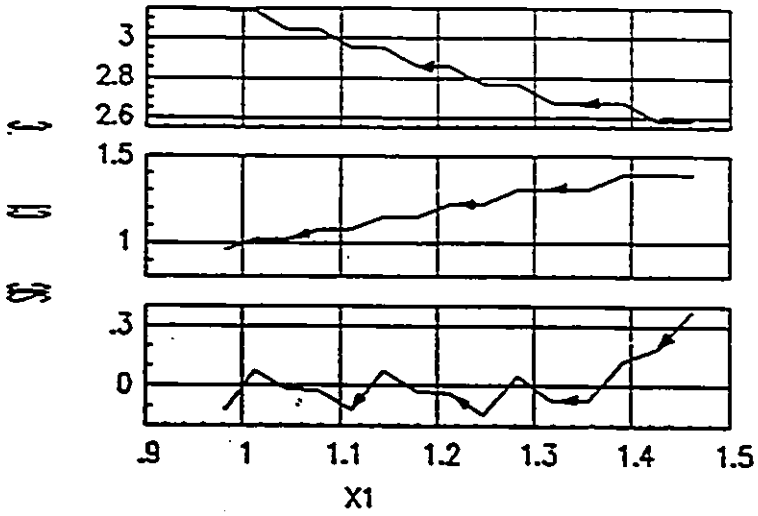

Figure III.2-5 c,c1,s versus $x_1(t)$ (detail rectangle A'-A').

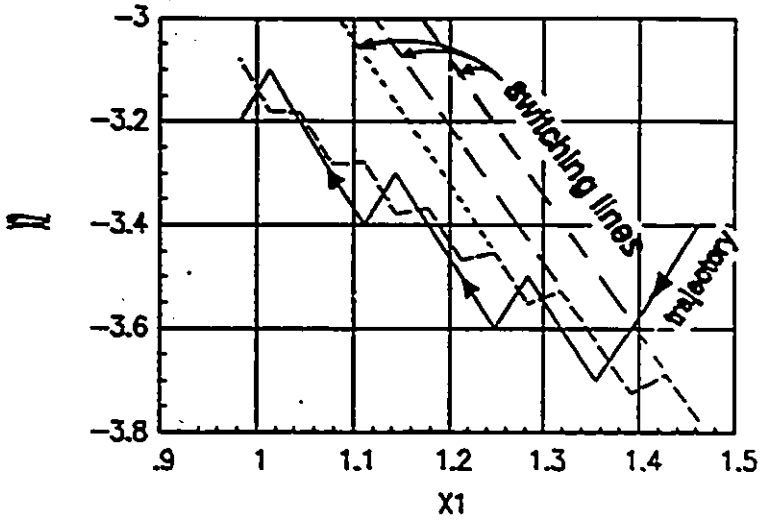

Figure III.2-6 Phase plane representation of the trajectory (detail rectangle A-A).

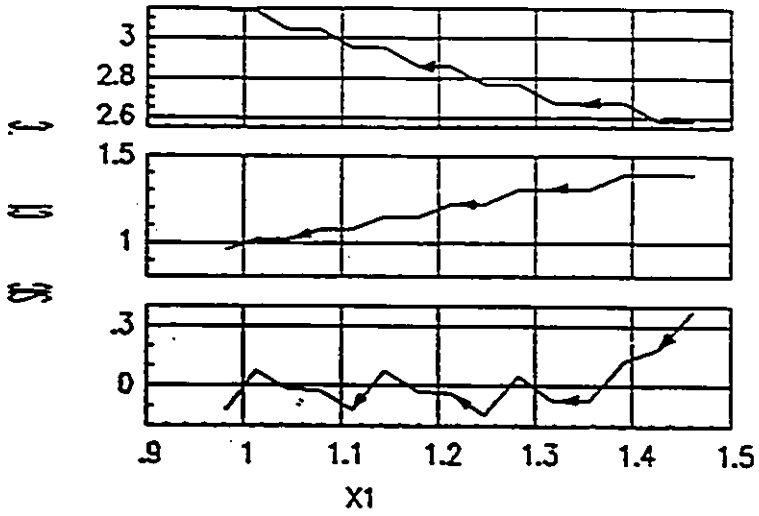

Figure III.2-5 c,c1,s versus $x_1(t)$ (detail rectangle A'-A').

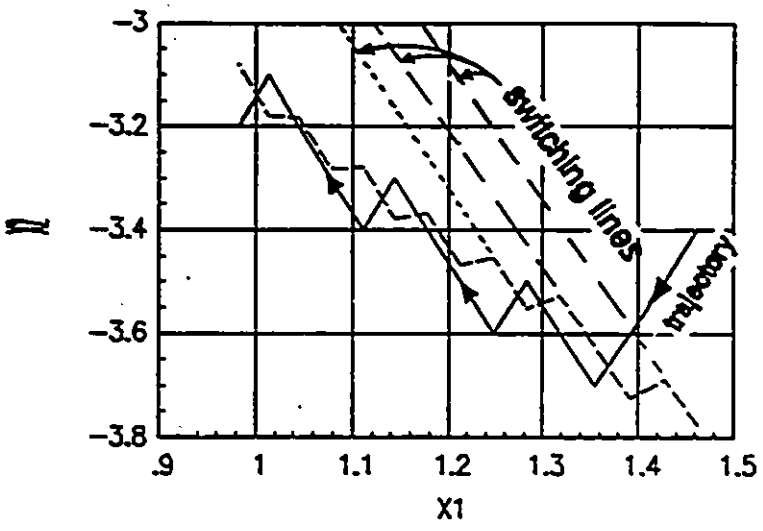

Figure III.2-6 Phase plane representation of the trajectory (detail rectangle A-A).

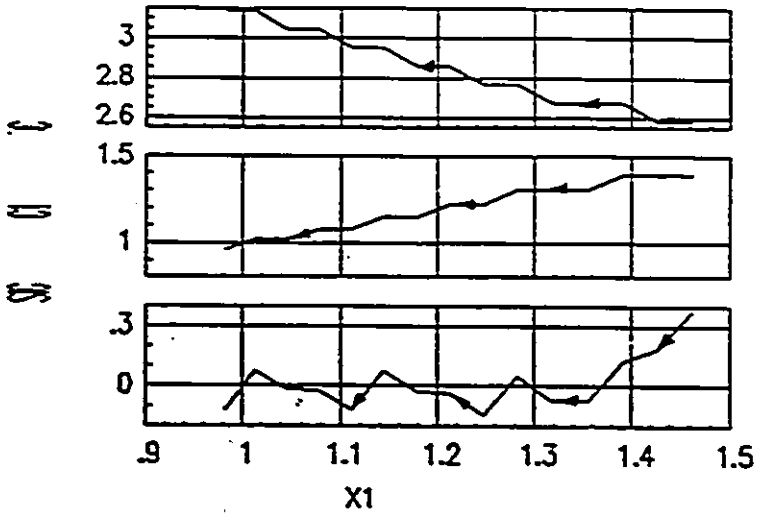

Figure III.2-5 c,c1,s versus $x_1(t)$ (detail rectangle A'-A').

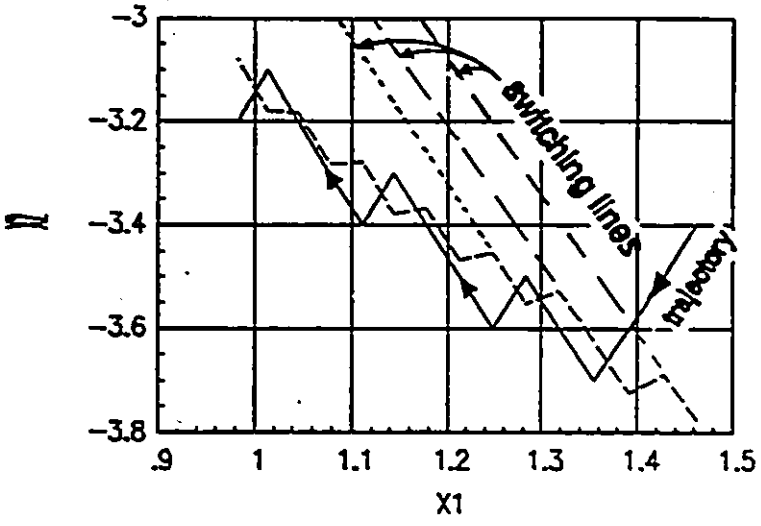

Figure III.2-6 Phase plane representation of the trajectory (detail rectangle A-A).

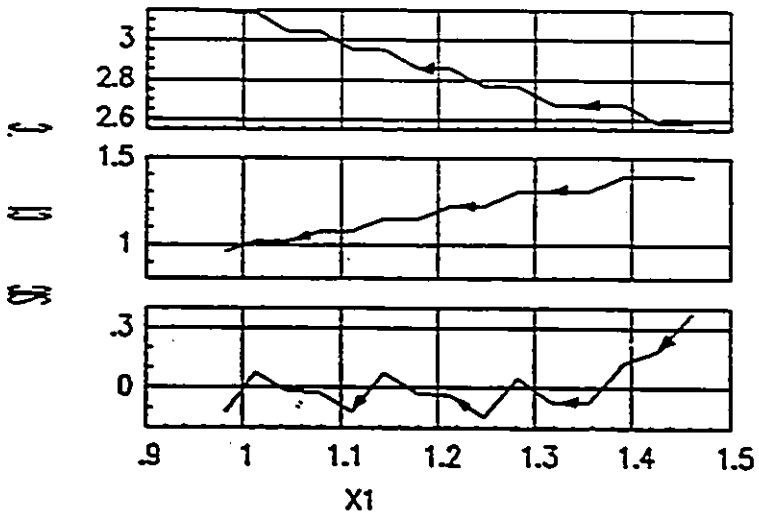

Figure III.2-5 c,c1,s versus $x_1(t)$ (detail rectangle A'-A').

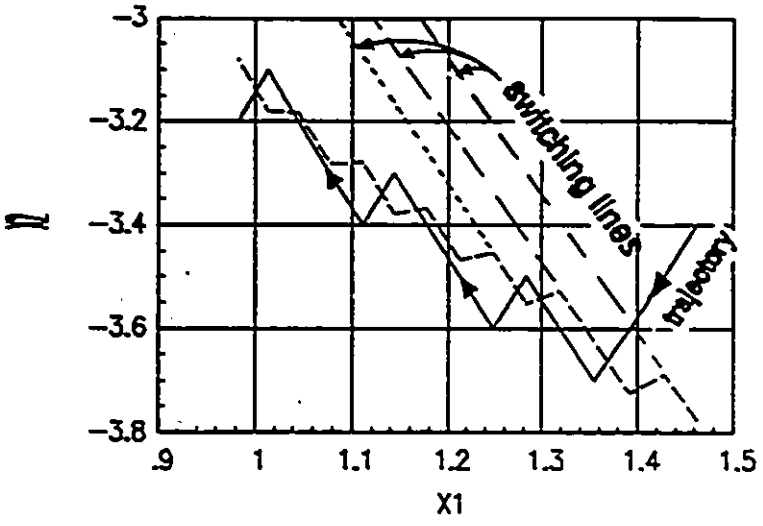

Figure III.2-6 Phase plane representation of the trajectory (detail rectangle A-A).

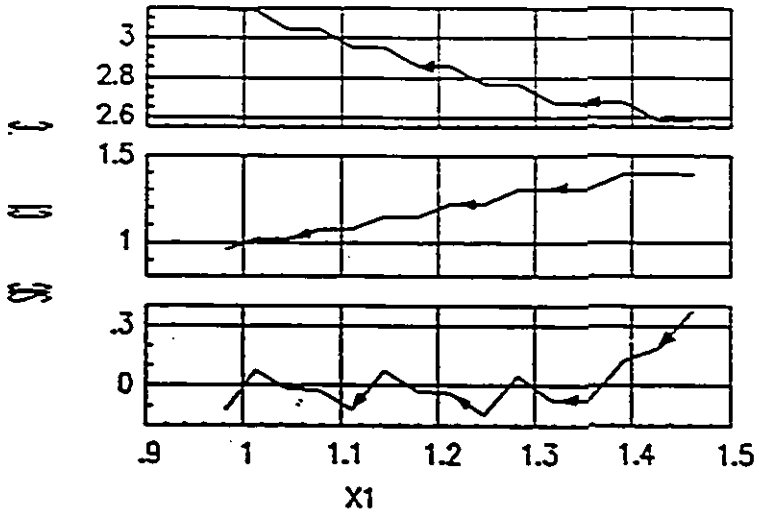

Figure III.2-5 c,c1,s versus $x_1(t)$ (detail rectangle A'-A').

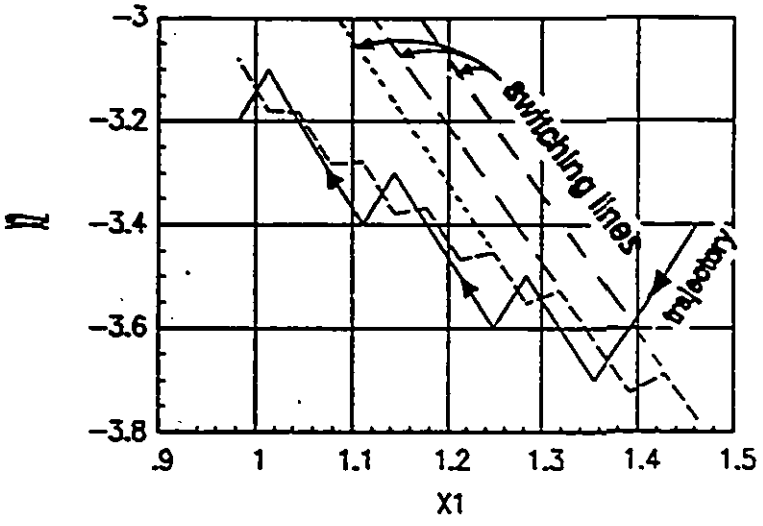

Figure III.2-6 Phase plane representation of the trajectory (detail rectangle A-A).

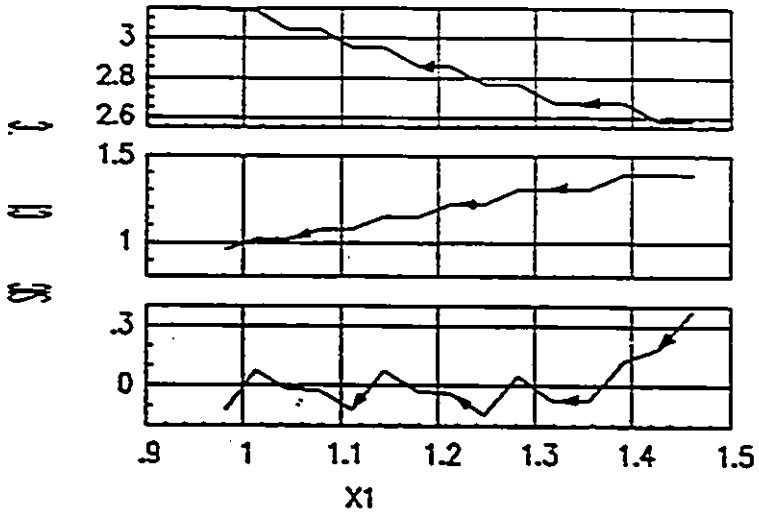

Figure III.2-5 c,c1,s versus $x_1(t)$ (detail rectangle A'-A').

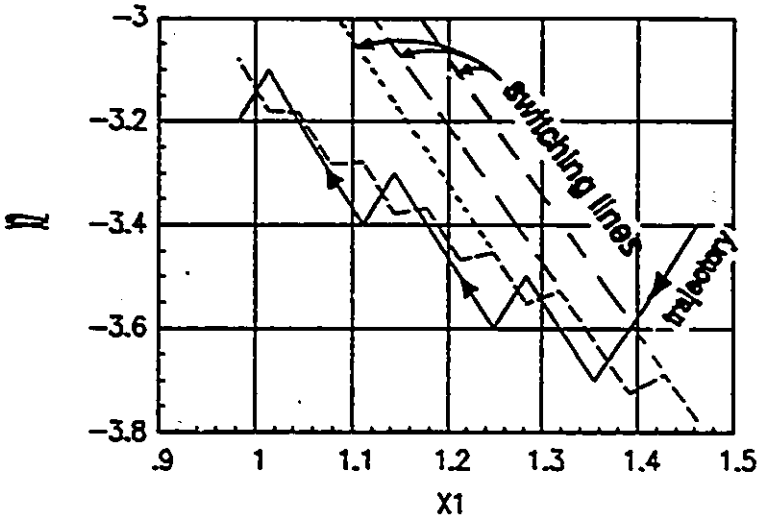

Figure III.2-6 Phase plane representation of the trajectory (detail rectangle A-A).

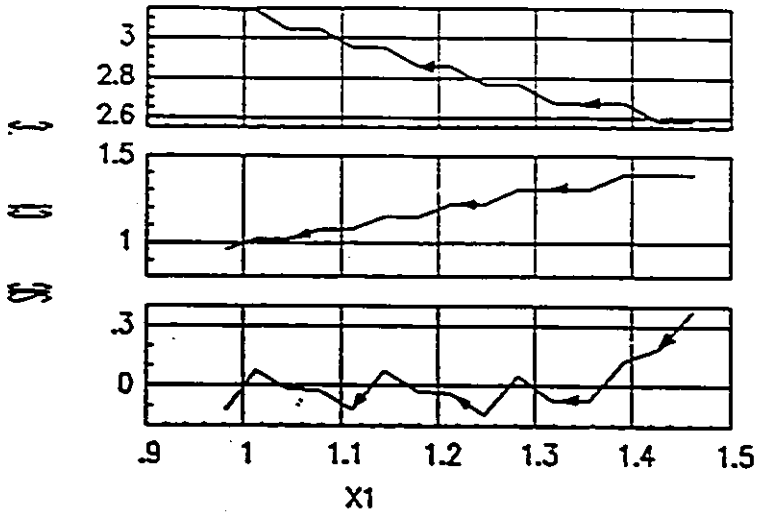

Figure III.2-5 c,c1,s versus $x_1(t)$ (detail rectangle A'-A').

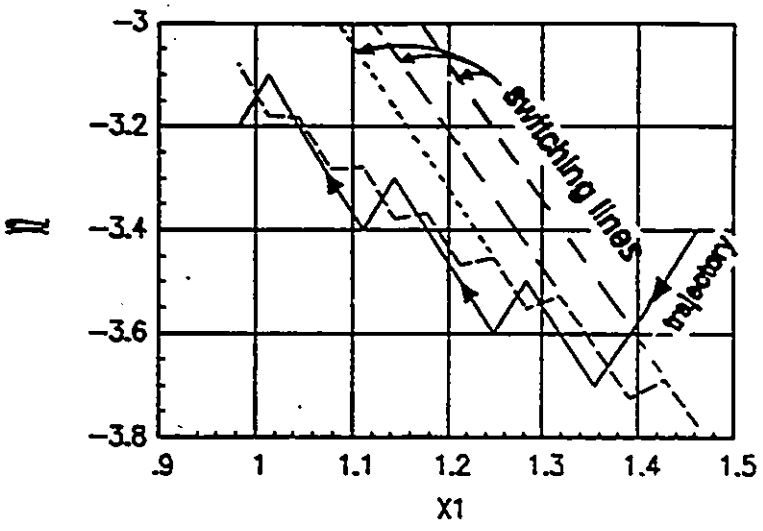

Figure III.2-6 Phase plane representation of the trajectory (detail rectangle A-A).

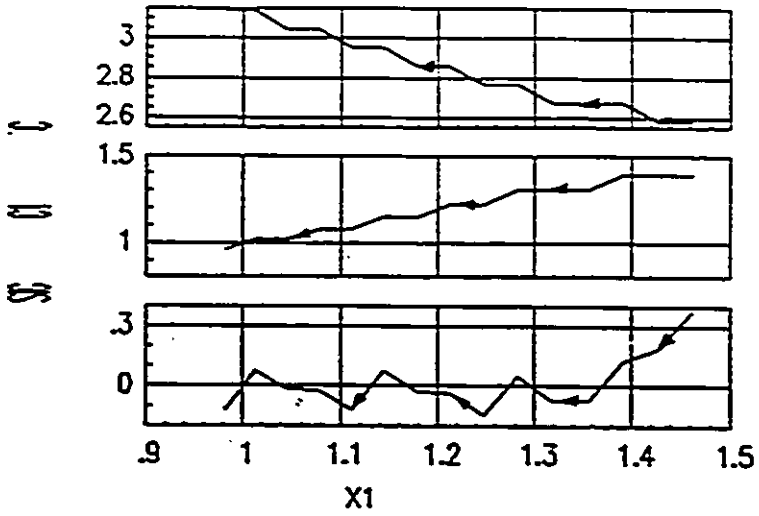

Figure III.2-5 c,c1,s versus $x_1(t)$ (detail rectangle A'-A').

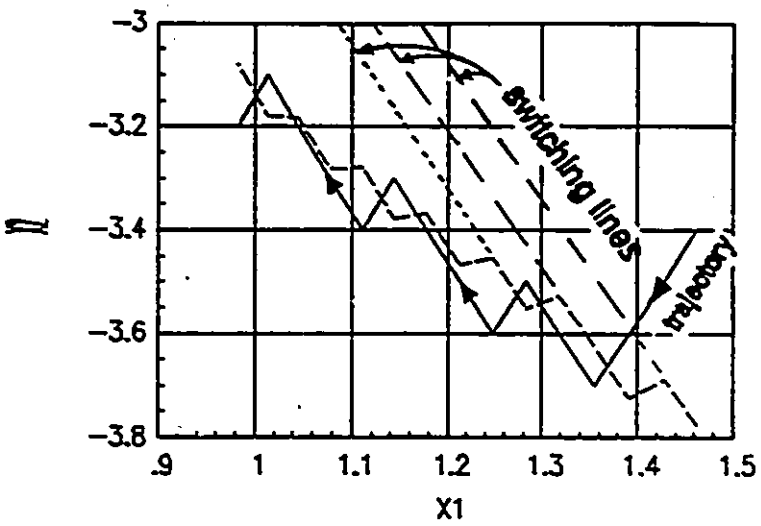

Figure III.2-6 Phase plane representation of the trajectory (detail rectangle A-A).

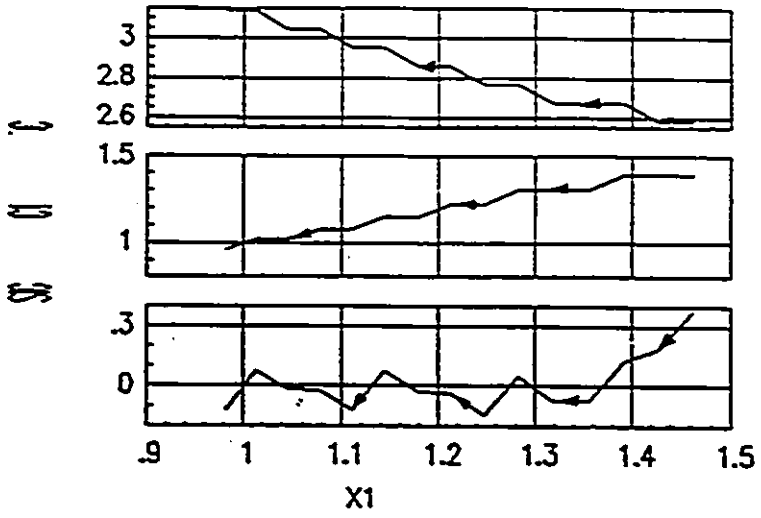

Figure III.2-5 c,c1,s versus $x_1(t)$ (detail rectangle A'-A').

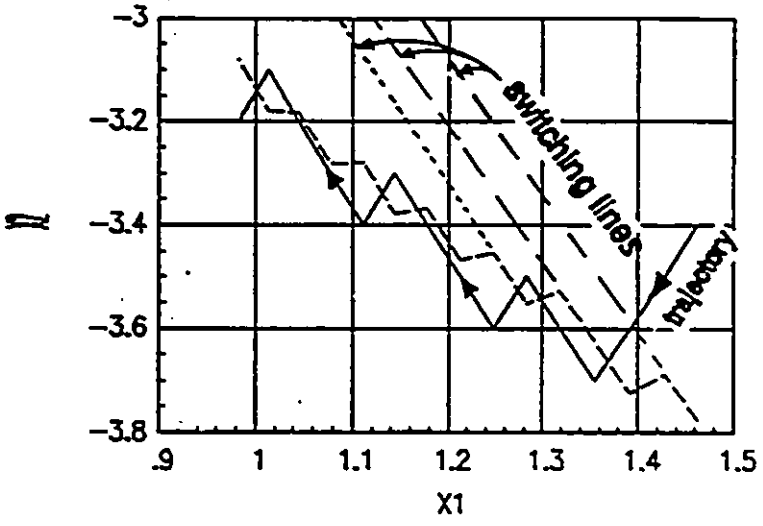

Figure III.2-6 Phase plane representation of the trajectory (detail rectangle A-A).

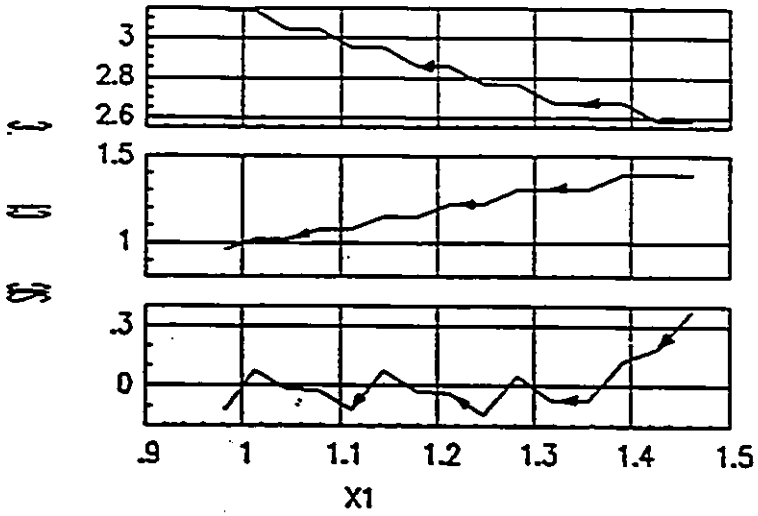

Figure III.2-5 c,c1,s versus $x_1(t)$ (detail rectangle A'-A').

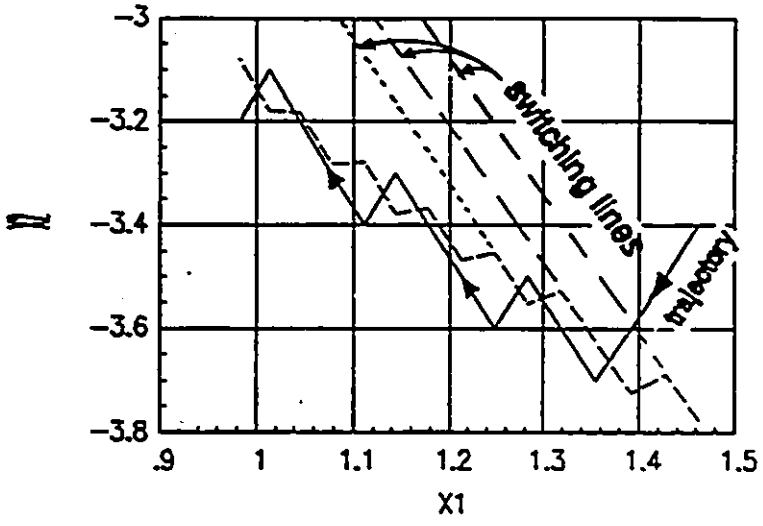

Figure III.2-6 Phase plane representation of the trajectory (detail rectangle A-A).

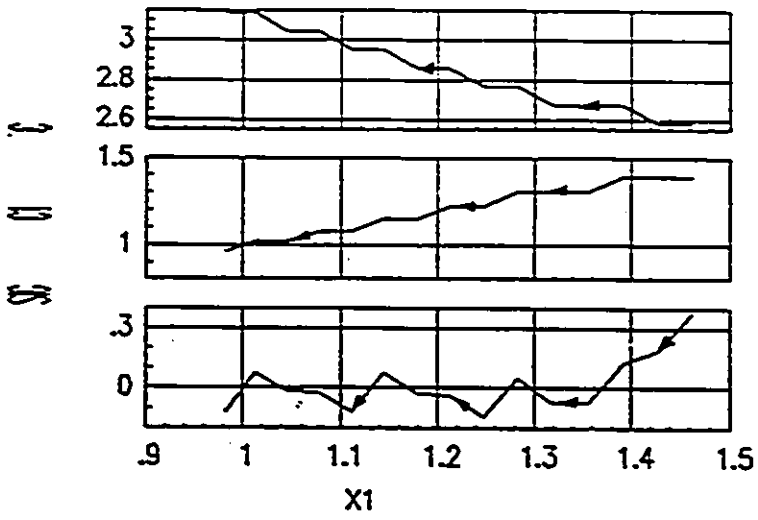

Figure III.2-5 c,c1,s versus $x_1(t)$ (detail rectangle A'-A').

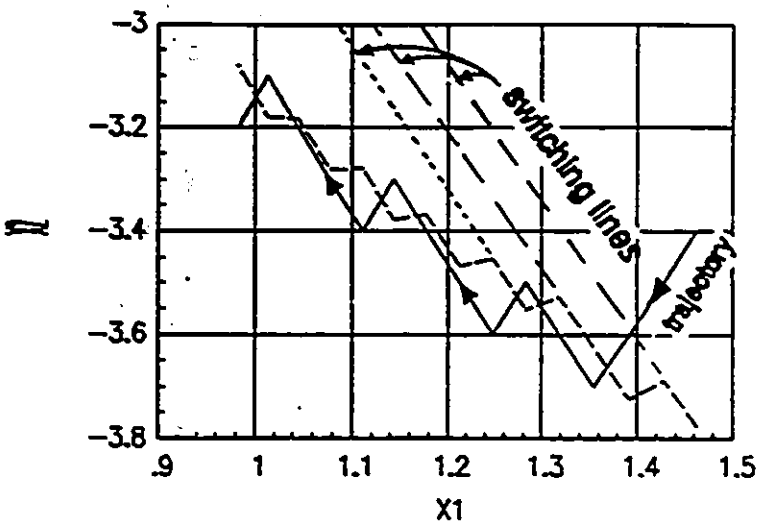

Figure III.2-6 Phase plane representation of the trajectory (detail rectangle A-A).

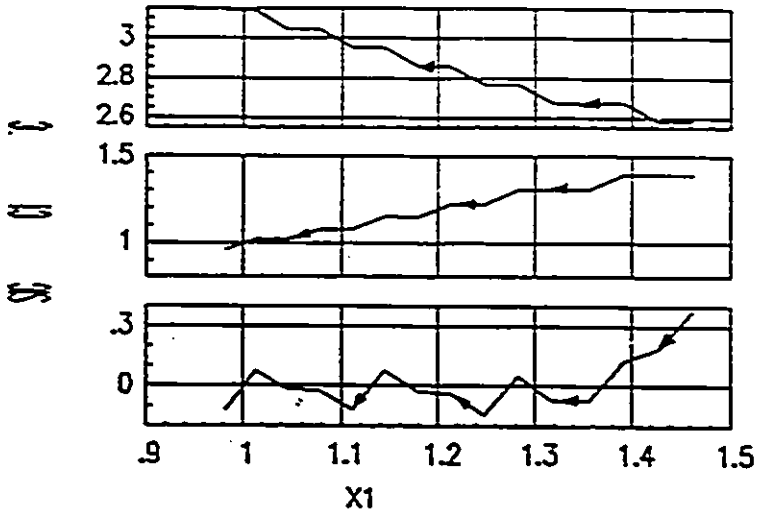

Figure III.2-5 c,c1,s versus $x_1(t)$ (detail rectangle A'-A').

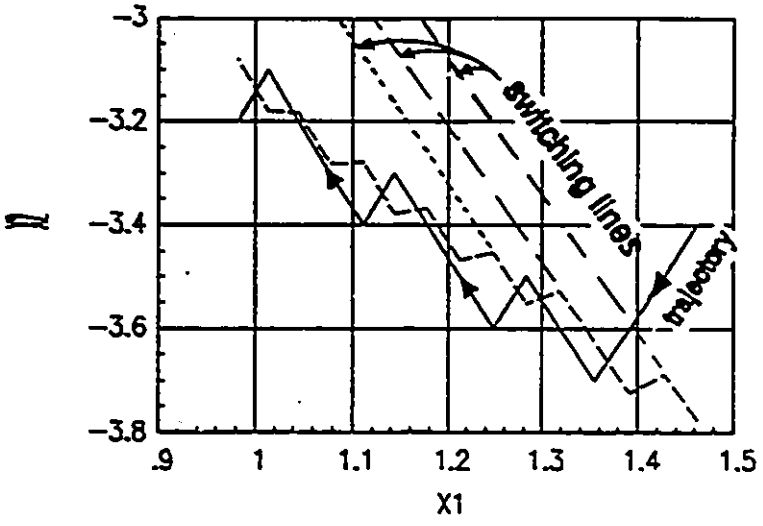

Figure III.2-6 Phase plane representation of the trajectory (detail rectangle A-A).

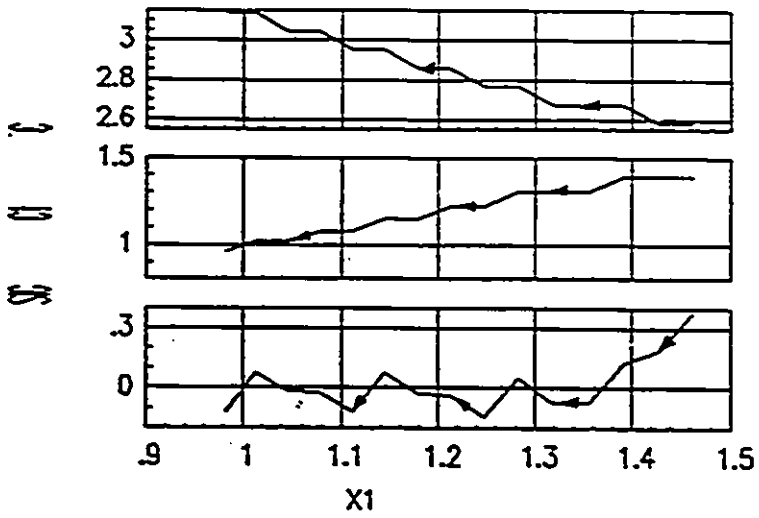

Figure III.2-5 c,c1,s versus $x_1(t)$ (detail rectangle A'-A').

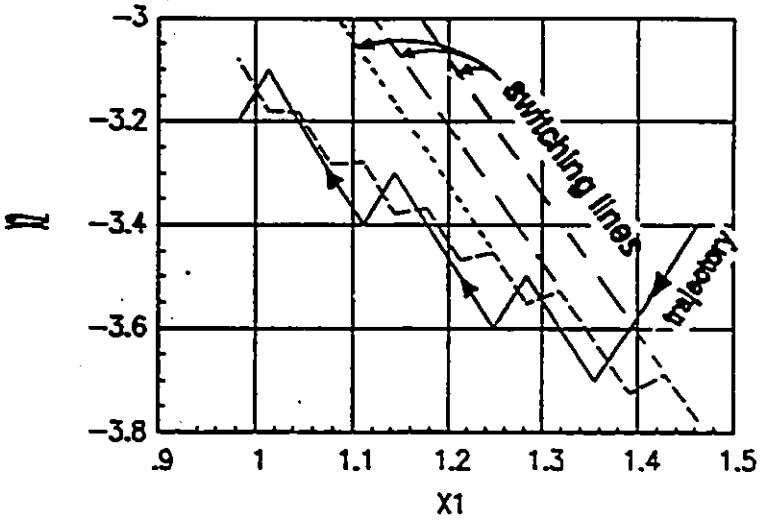

Figure III.2-6 Phase plane representation of the trajectory (detail rectangle A-A).

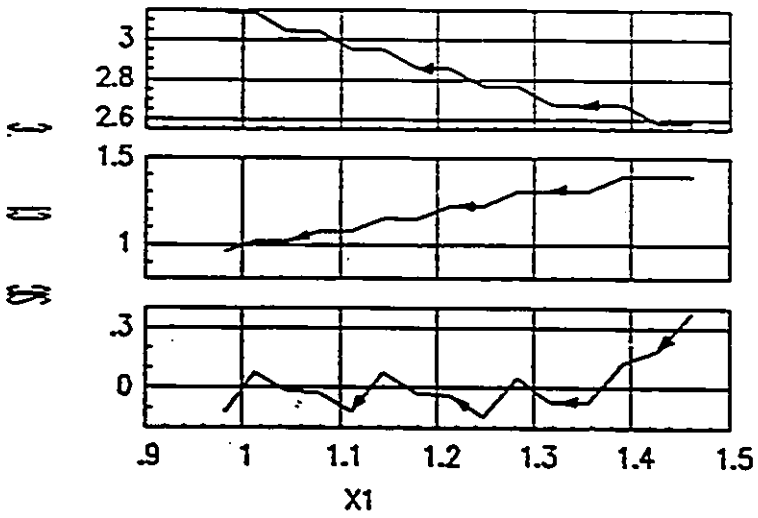

Figure III.2-5 c,c1,s versus $x_1(t)$ (detail rectangle A'-A').

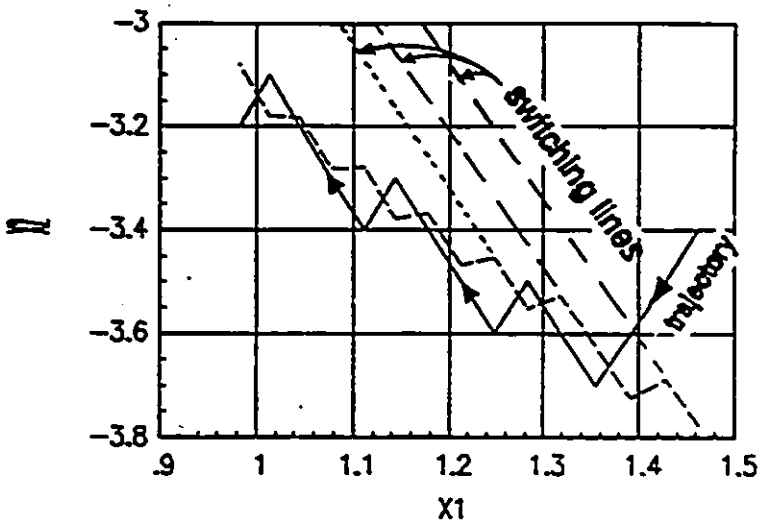

Figure III.2-6 Phase plane representation of the trajectory (detail rectangle A-A).

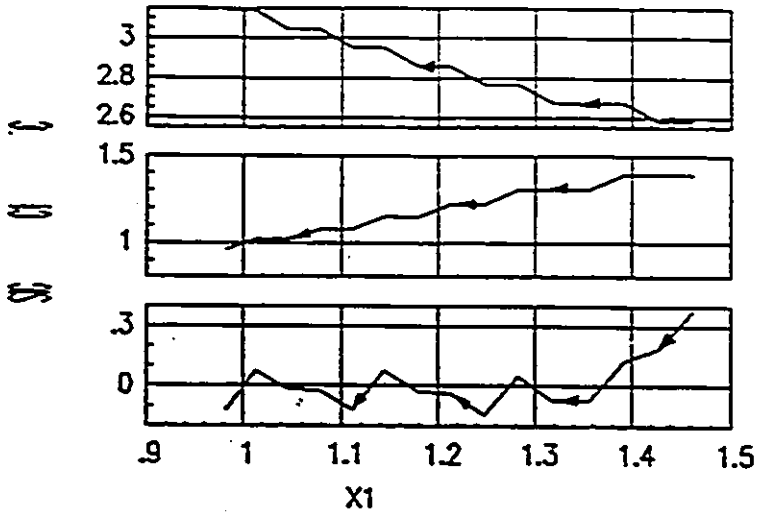

Figure III.2-5 c,c1,s versus $x_1(t)$ (detail rectangle A'-A').

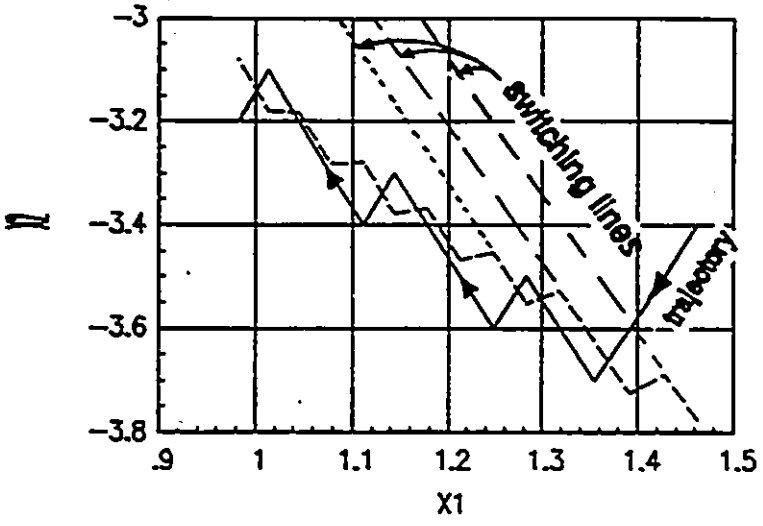

Figure III.2-6 Phase plane representation of the trajectory (detail rectangle A-A).

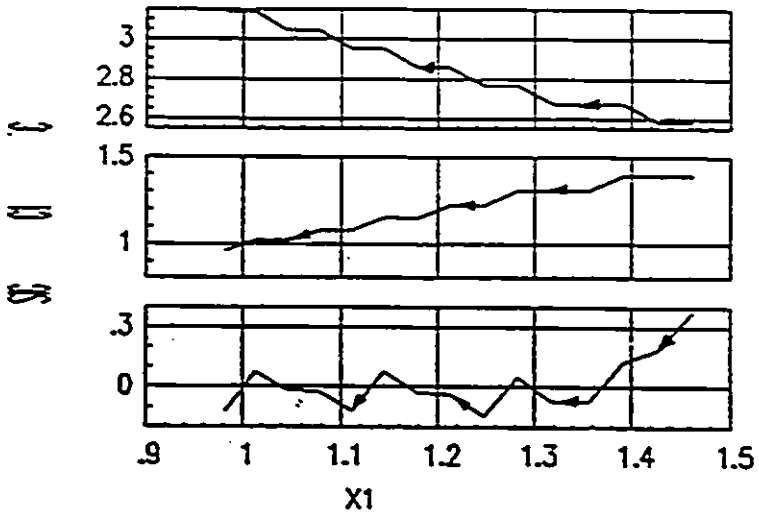

Figure III.2-5 c,c1,s versus $x_1(t)$ (detail rectangle A'-A').

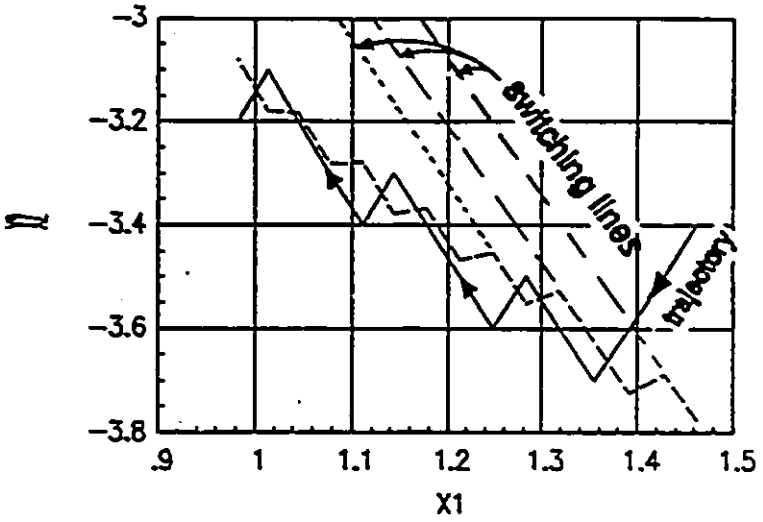

Figure III.2-6 Phase plane representation of the trajectory (detail rectangle A-A).

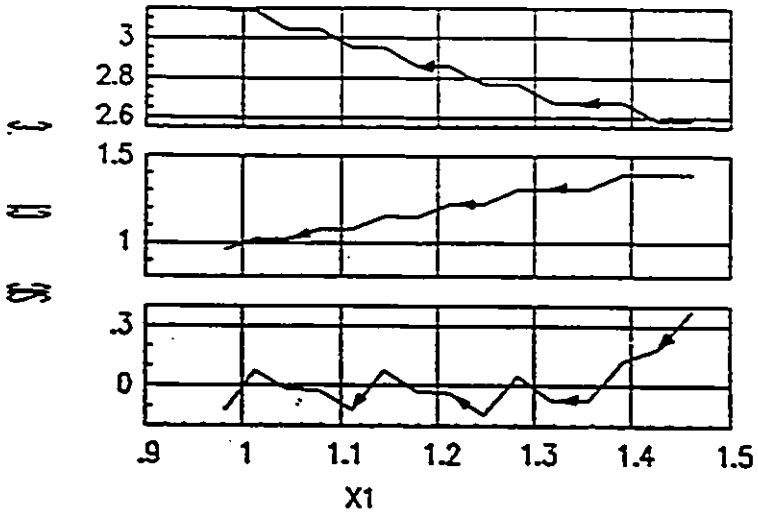

Figure III.2-5 c,c1,s versus $x_1(t)$ (detail rectangle A'-A').

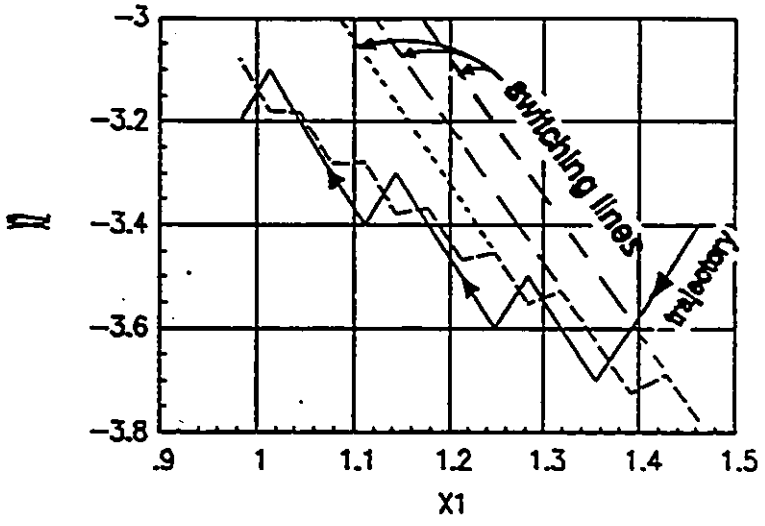

Figure III.2-6 Phase plane representation of the trajectory (detail rectangle A-A).

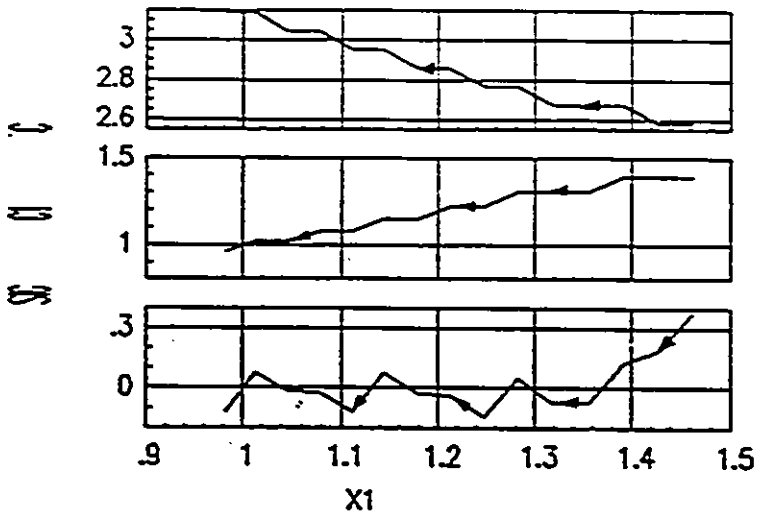

Figure III.2-5 c,c1,s versus $x_1(t)$ (detail rectangle A'-A').

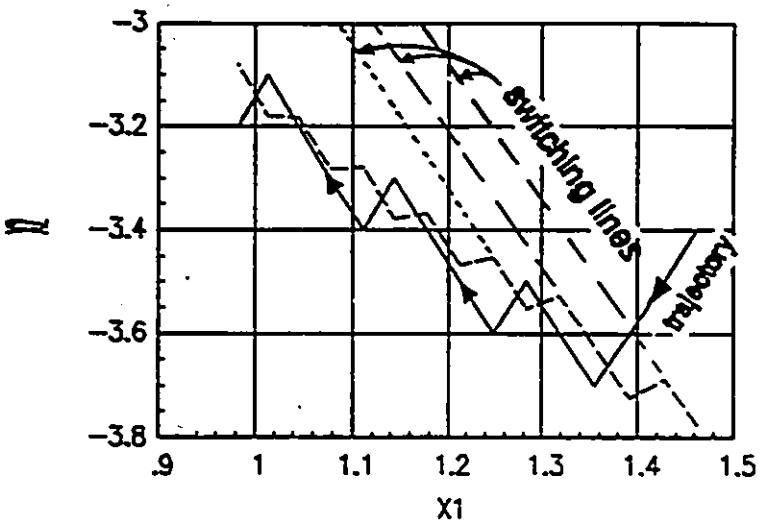

Figure III.2-6 Phase plane representation of the trajectory (detail rectangle A-A).

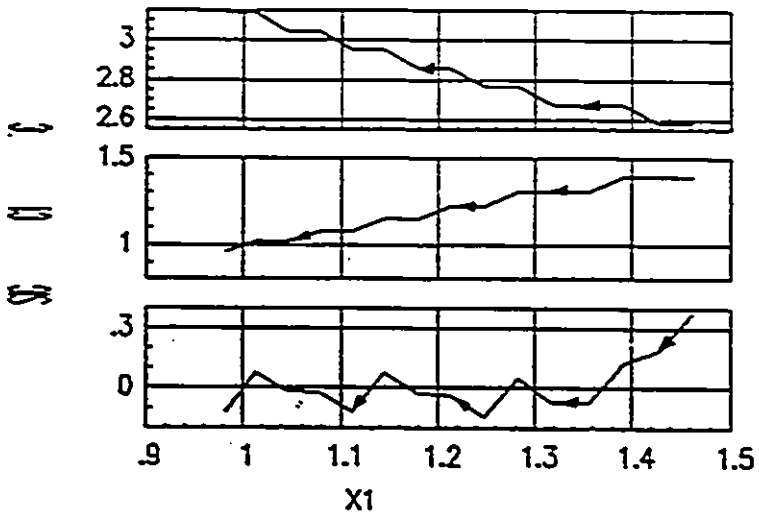

Figure III.2-5 c,c1,s versus $x_1(t)$ (detail rectangle A'-A').

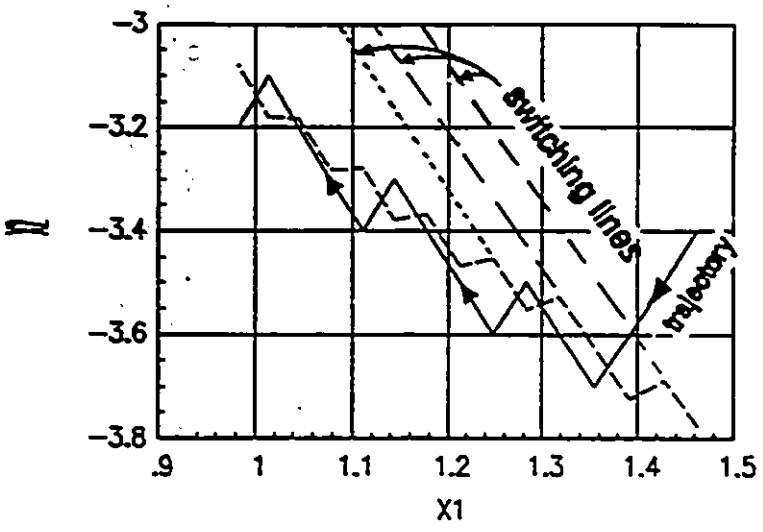

Figure III.2-6 Phase plane representation of the trajectory (detail rectangle A-A).

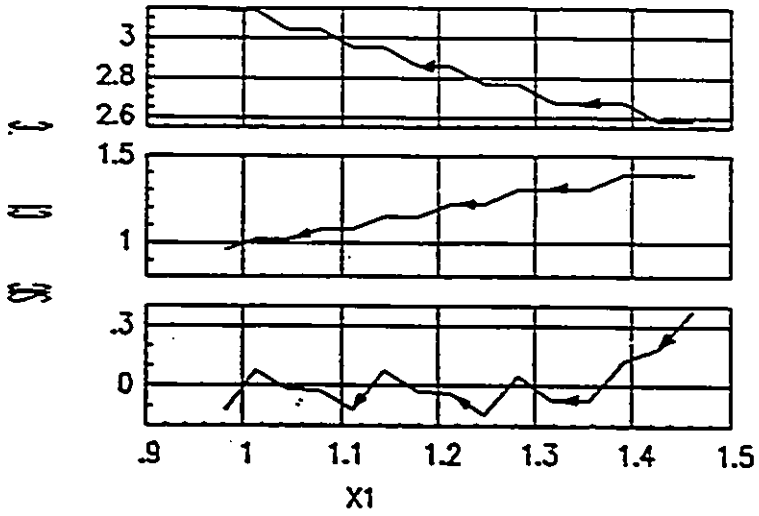

Figure III.2-5 c,c1,s versus $x_1(t)$ (detail rectangle A'-A').

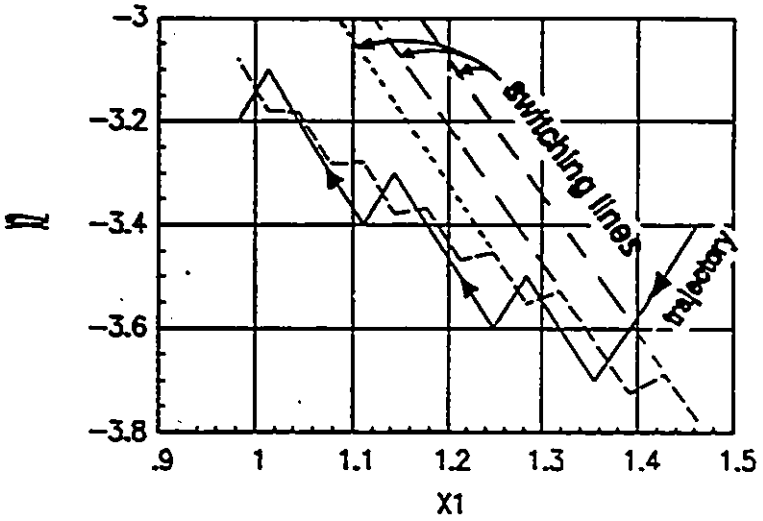

Figure III.2-6 Phase plane representation of the trajectory (detail rectangle A-A).

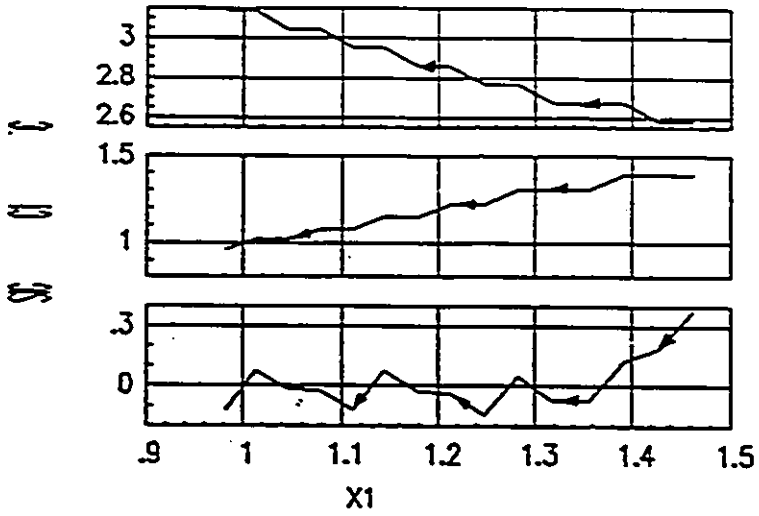

Figure III.2-5 c,c1,s versus $x_1(t)$ (detail rectangle A'-A').

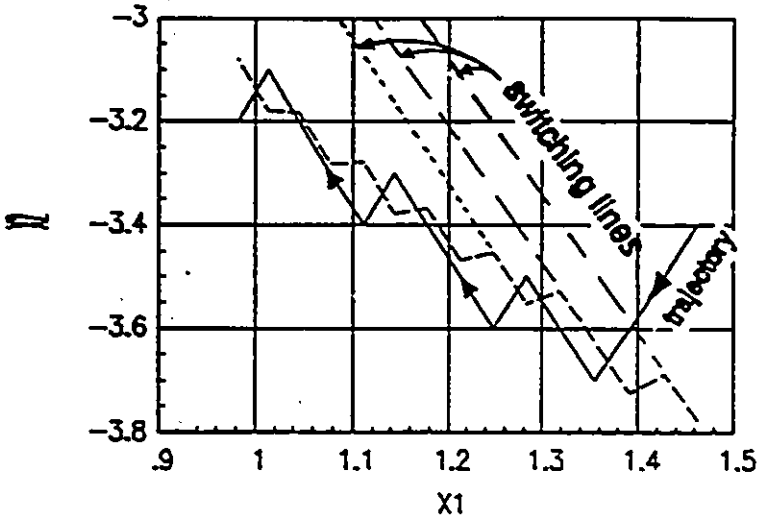

Figure III.2-6 Phase plane representation of the trajectory (detail rectangle A-A).

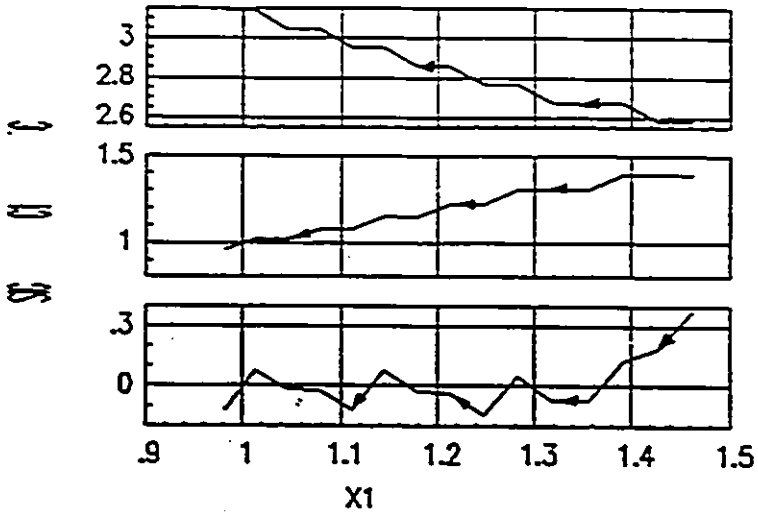

Figure III.2-5 c,c1,s versus $x_1(t)$ (detail rectangle A'-A').

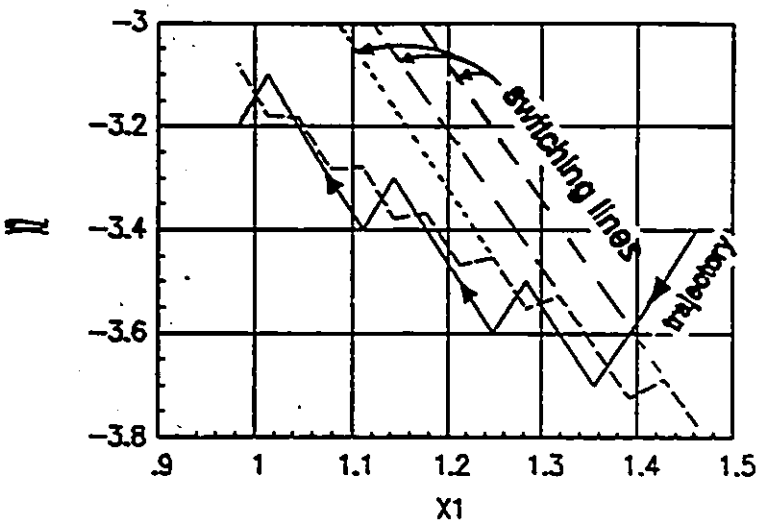

Figure III.2-6 Phase plane representation of the trajectory (detail rectangle A-A).

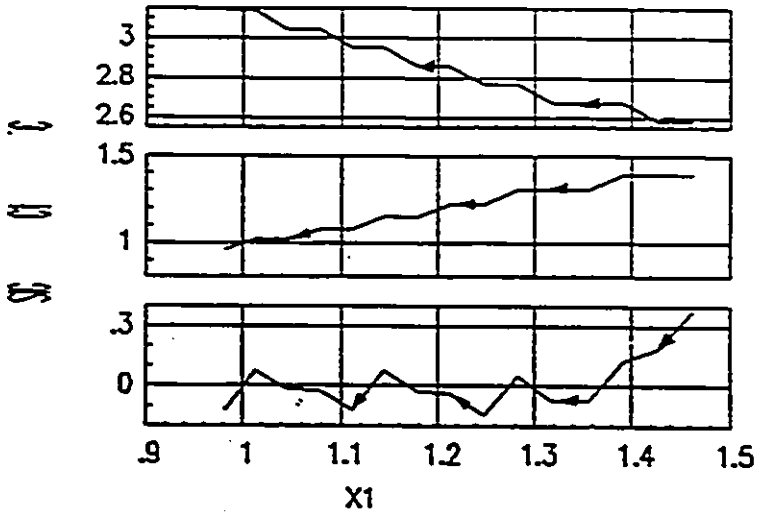

Figure III.2-5 c,c1,s versus $x_1(t)$ (detail rectangle A'-A').

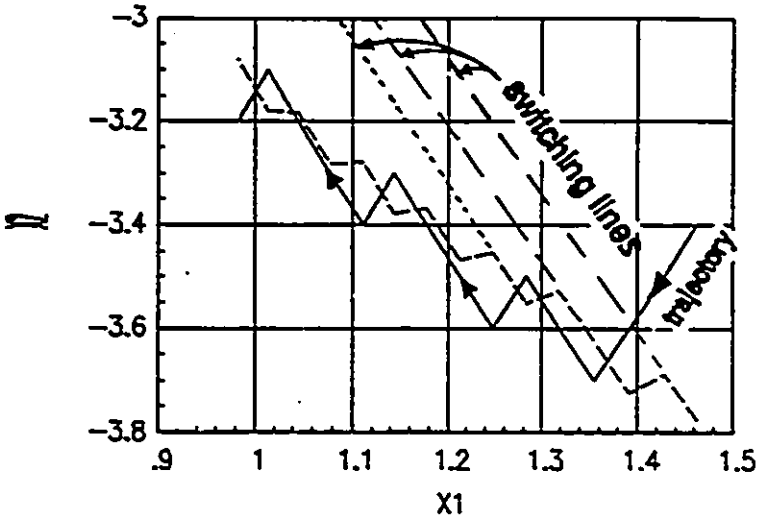

Figure III.2-6 Phase plane representation of the trajectory (detail rectangle A-A).

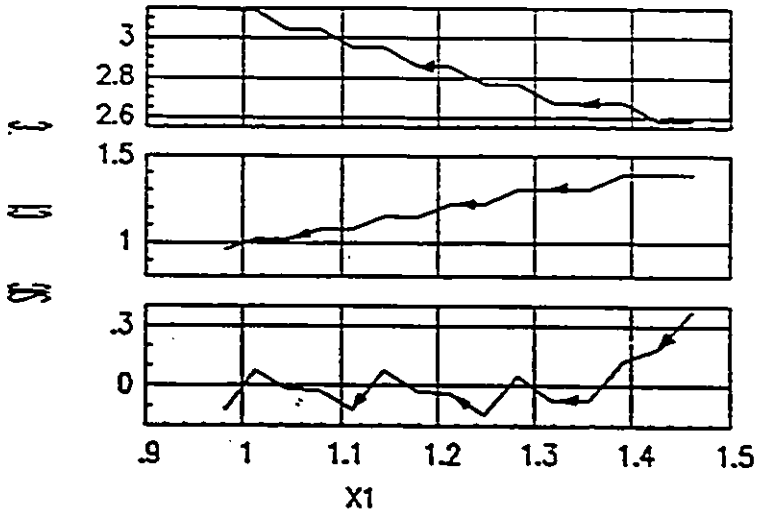

Figure III.2-5 c,c1,s versus $x_1(t)$ (detail rectangle A'-A').

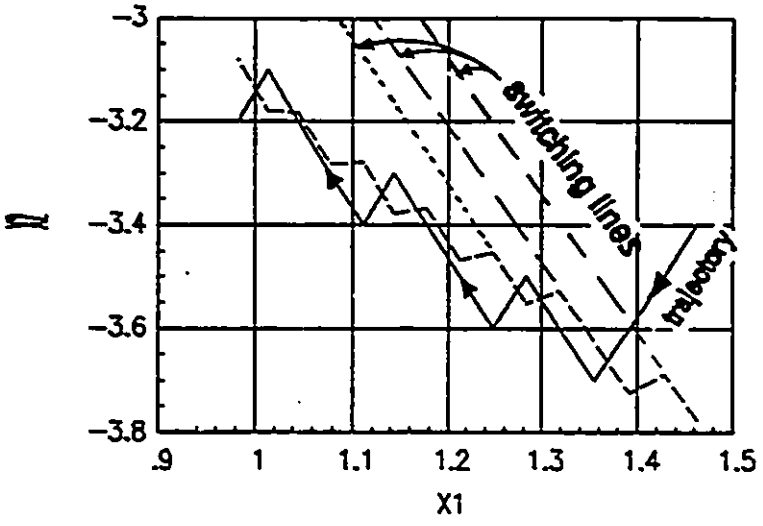

Figure III.2-6 Phase plane representation of the trajectory (detail rectangle A-A).

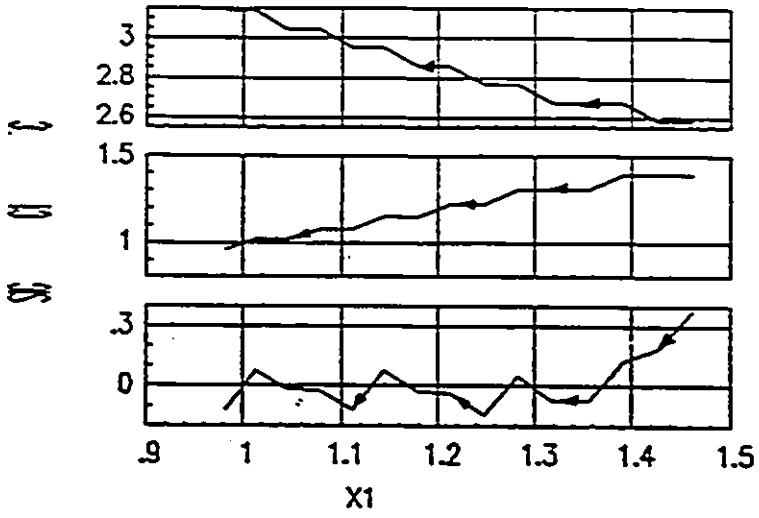

Figure III.2-5 c,c1,s versus $x_1(t)$ (detail rectangle A'-A').

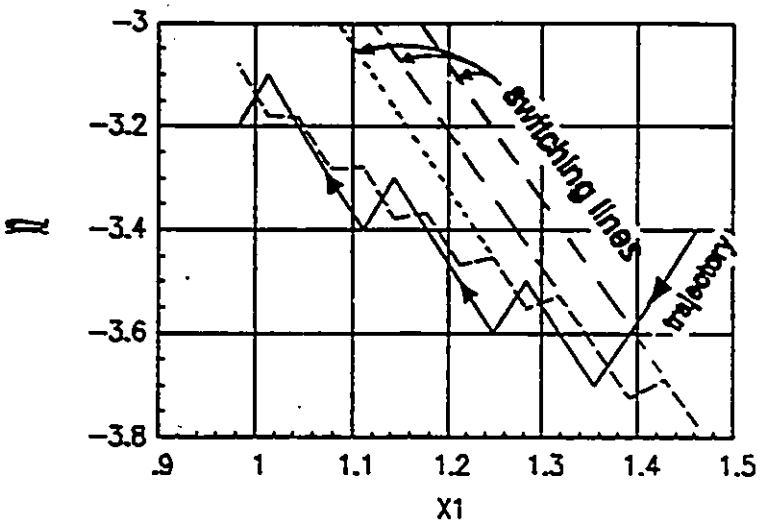

Figure III.2-6 Phase plane representation of the trajectory (detail rectangle A-A).

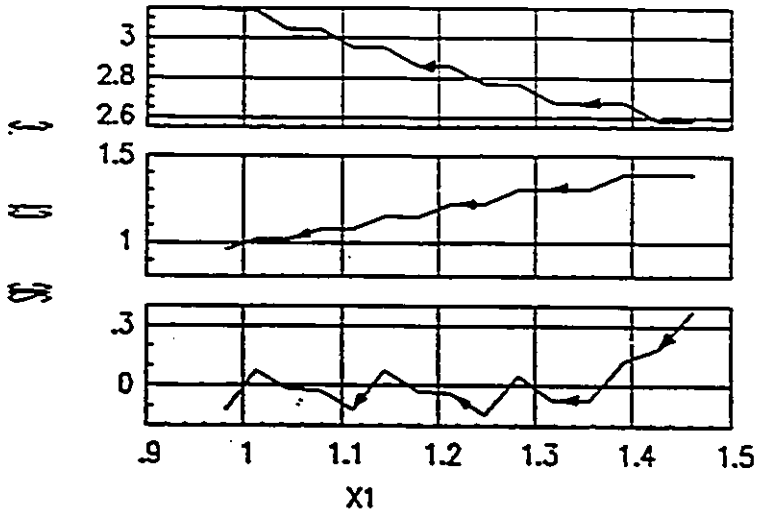

Figure III.2-5 c,c1,s versus $x_1(t)$ (detail rectangle A'-A').

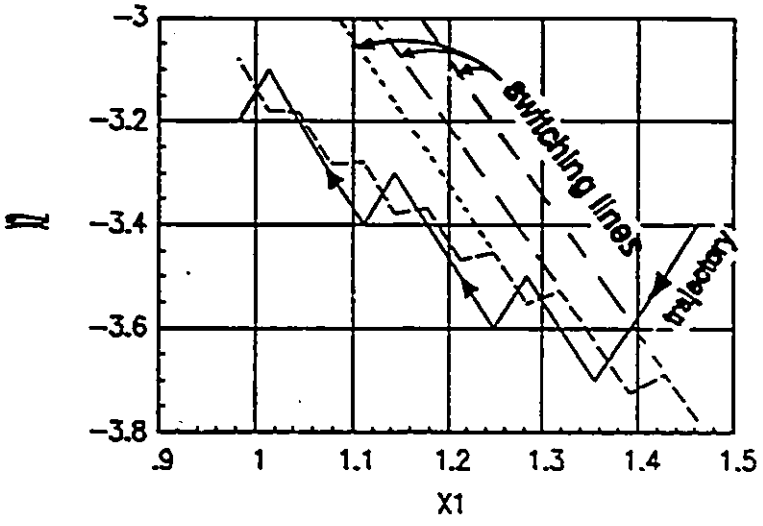

Figure III.2-6 Phase plane representation of the trajectory (detail rectangle A-A).

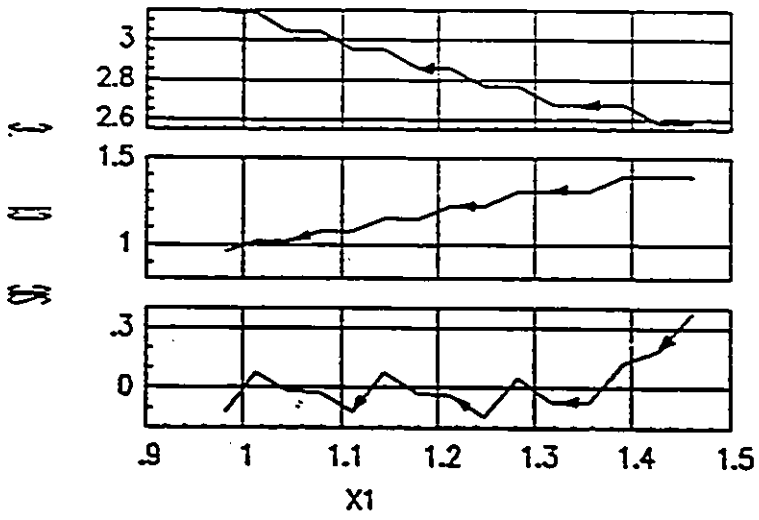

Figure III.2-5 c,c1,s versus $x_1(t)$ (detail rectangle A'-A').

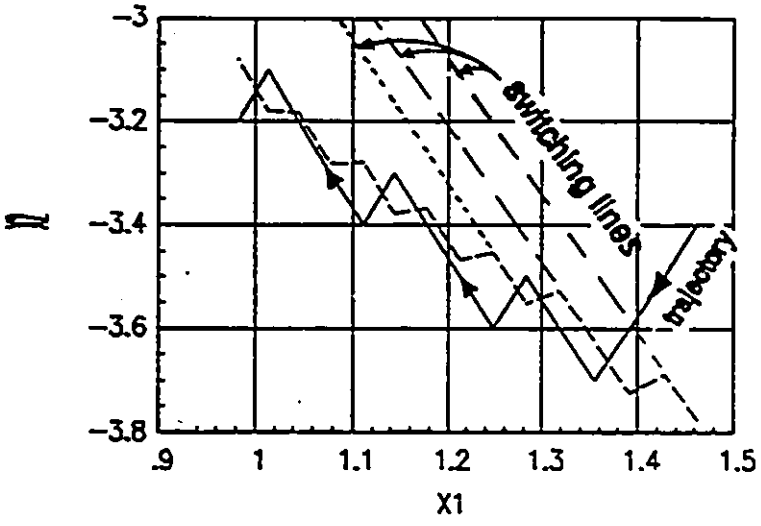

Figure III.2-6 Phase plane representation of the trajectory (detail rectangle A-A).

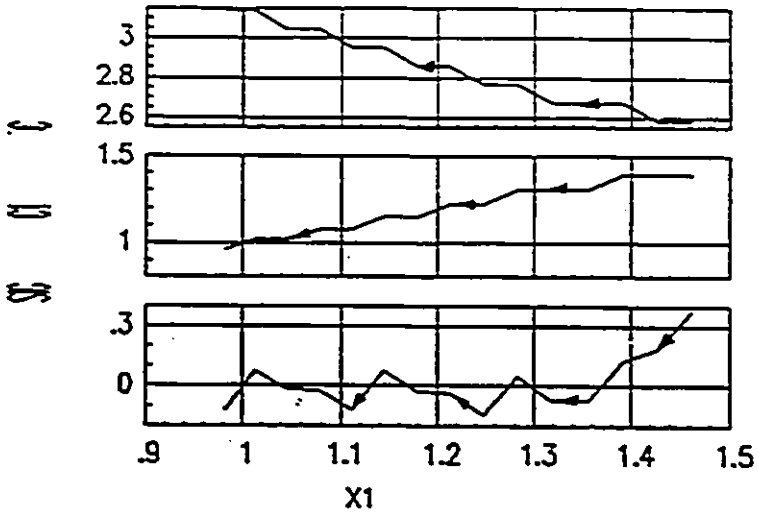

Figure III.2-5 c,c1,s versus $x_1(t)$ (detail rectangle A'-A').

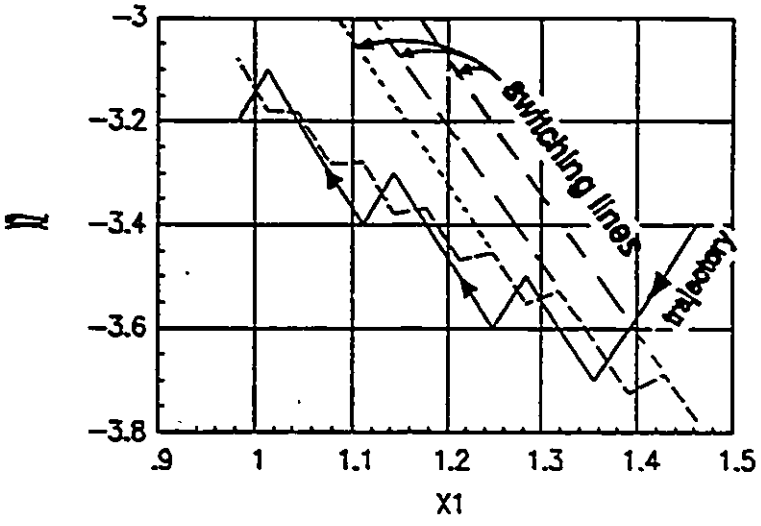

Figure III.2-6 Phase plane representation of the trajectory (detail rectangle A-A).

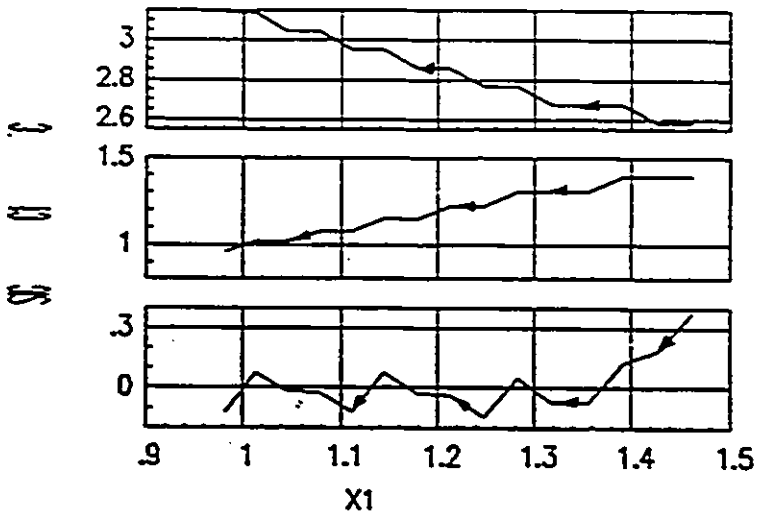

Figure III.2-5 c,c1,s versus $x_1(t)$ (detail rectangle A'-A').

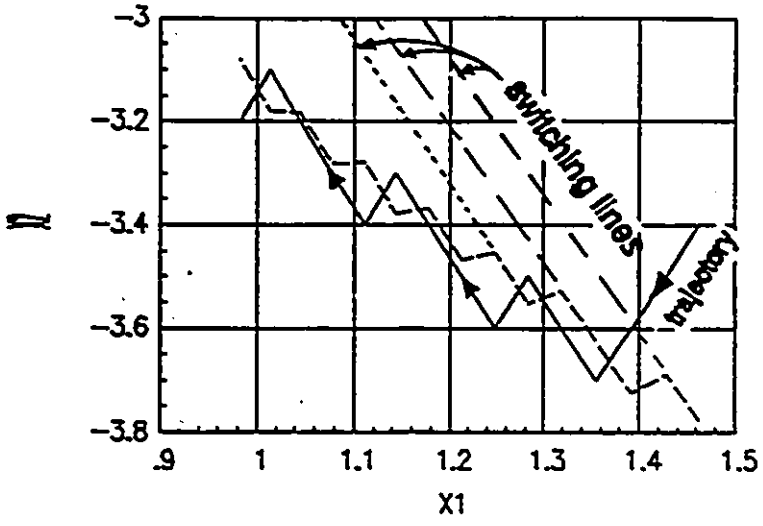

Figure III.2-6 Phase plane representation of the trajectory (detail rectangle A-A).

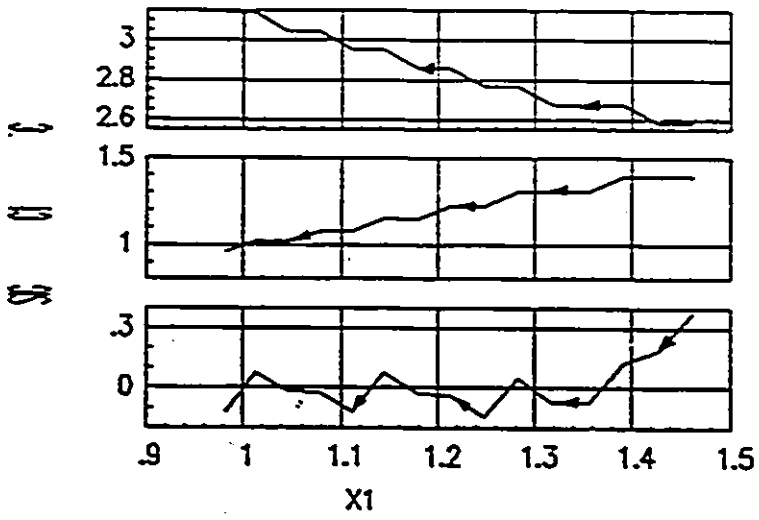

Figure III.2-5 c,c1,s versus $x_1(t)$ (detail rectangle A'-A').

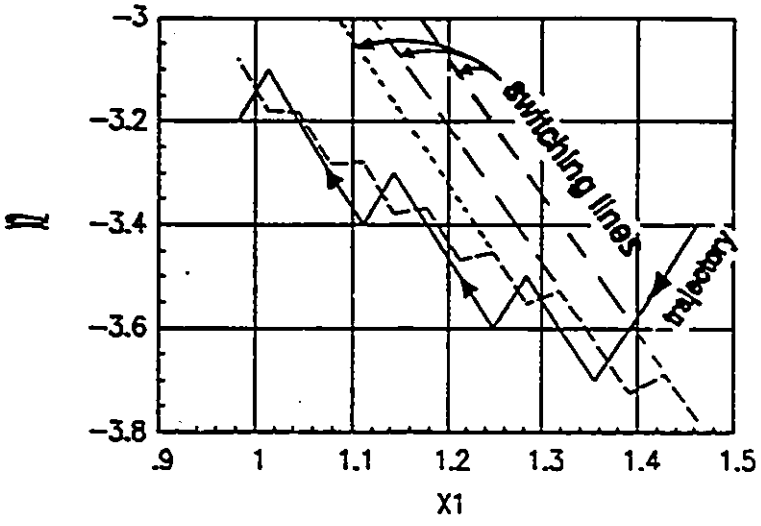

Figure III.2-6 Phase plane representation of the trajectory (detail rectangle A-A).

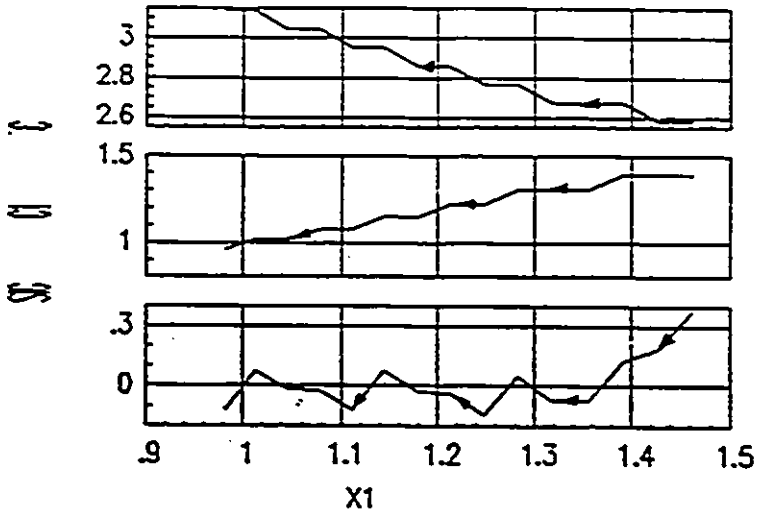

Figure III.2-5 c,c1,s versus $x_1(t)$ (detail rectangle A'-A').

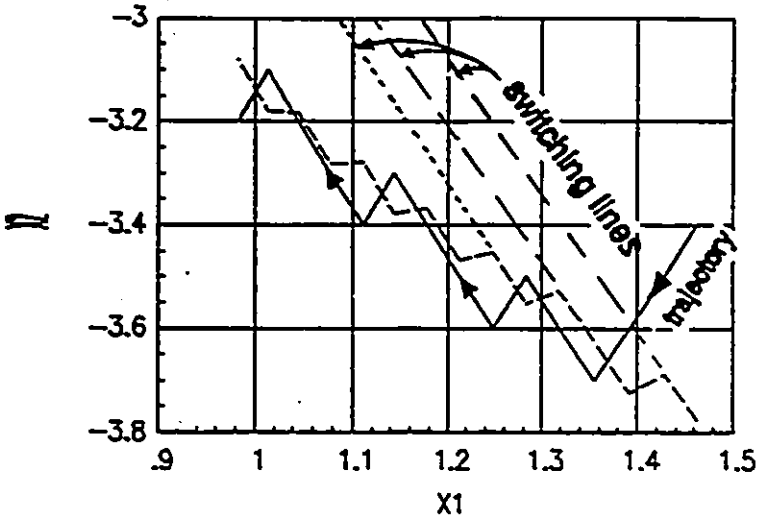

Figure III.2-6 Phase plane representation of the trajectory (detail rectangle A-A).

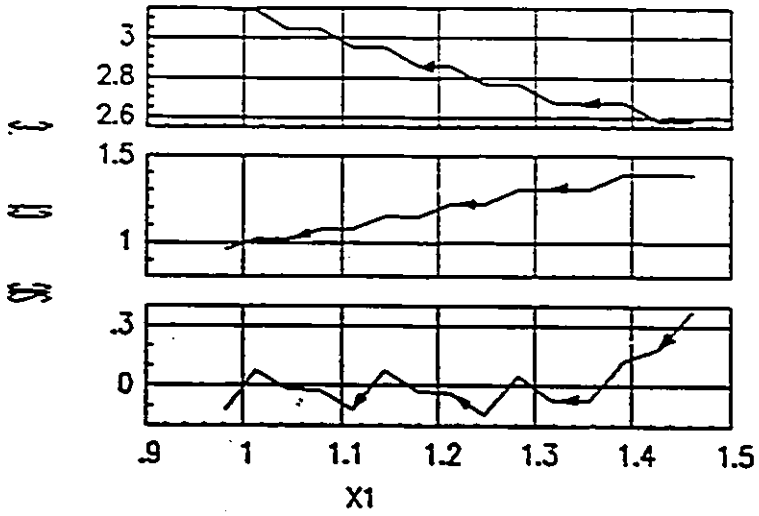

Figure III.2-5 c,c1,s versus $x_1(t)$ (detail rectangle A'-A').

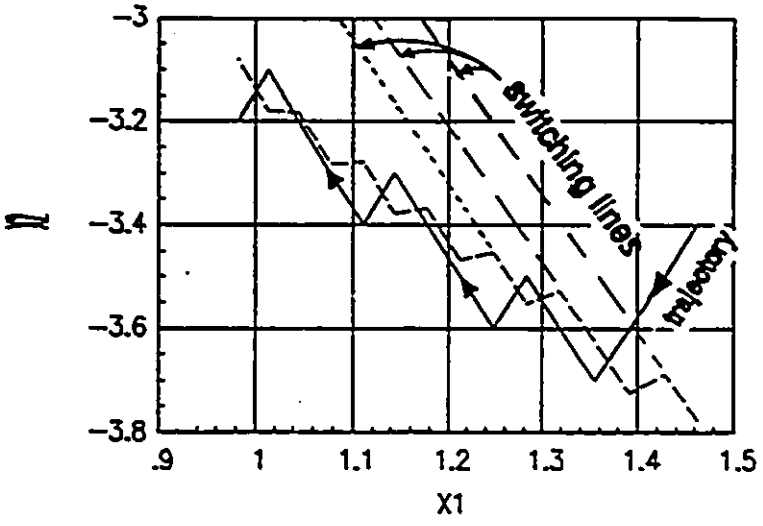

Figure III.2-6 Phase plane representation of the trajectory (detail rectangle A-A).

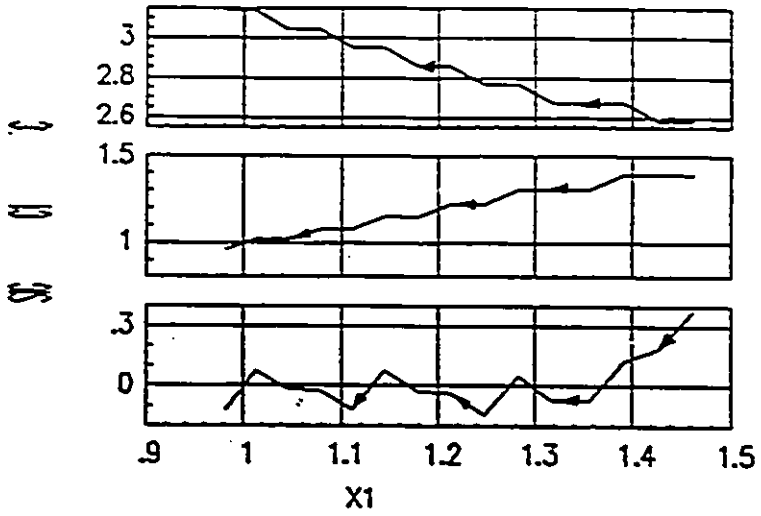

Figure III.2-5 c,c1,s versus $x_1(t)$ (detail rectangle A'-A').

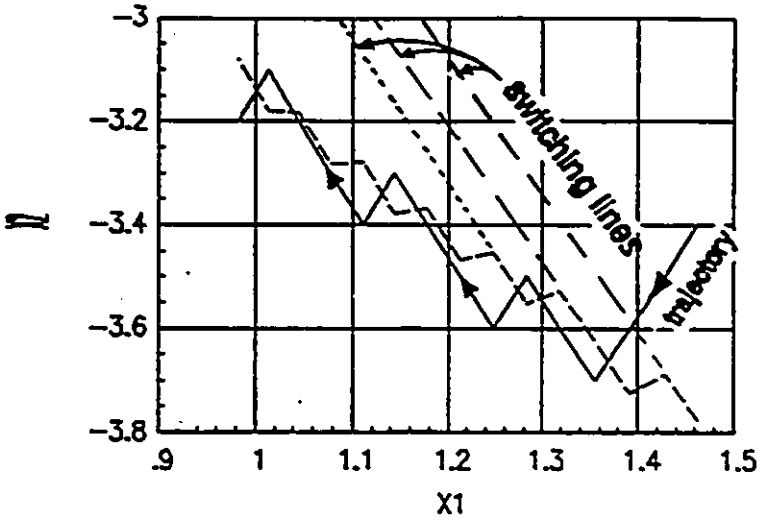

Figure III.2-6 Phase plane representation of the trajectory (detail rectangle A-A).

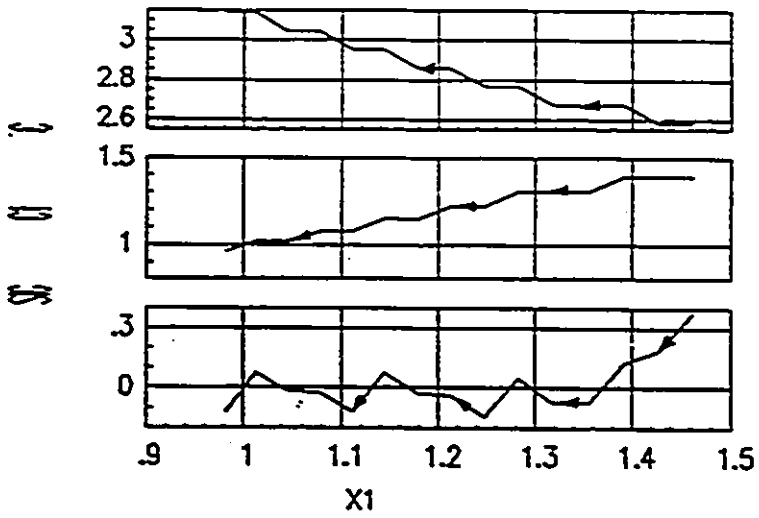

Figure III.2-5 c,c1,s versus $x_1(t)$ (detail rectangle A'-A').

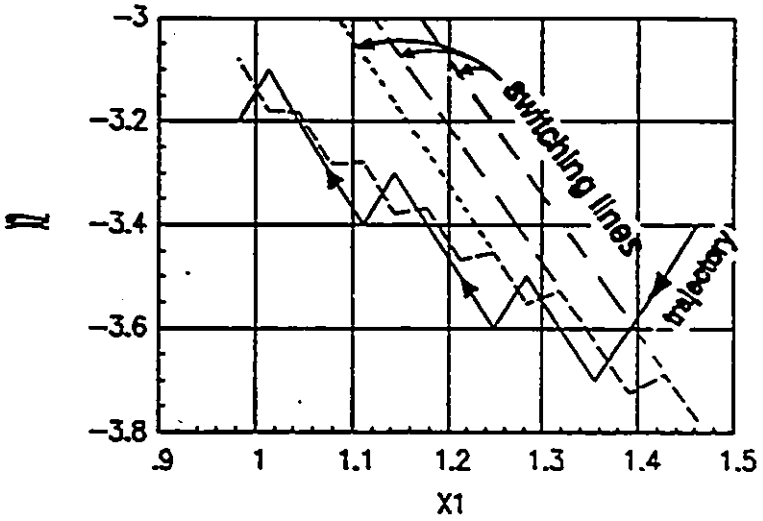

Figure III.2-6 Phase plane representation of the trajectory (detail rectangle A-A).

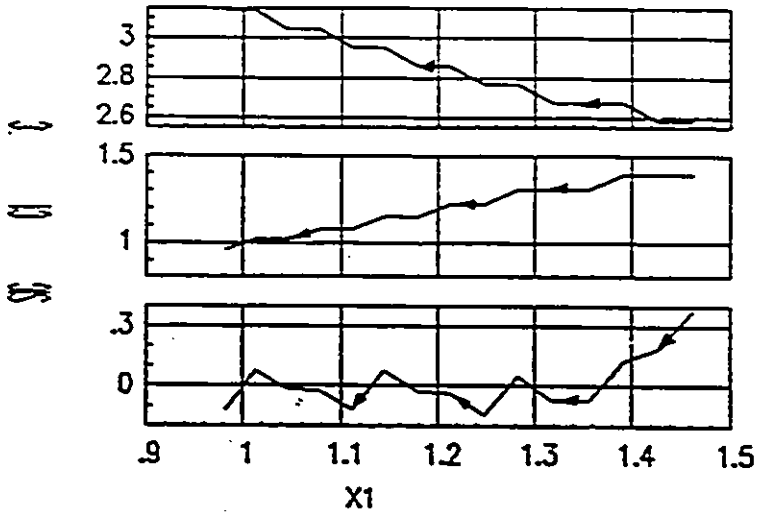

Figure III.2-5 c,c1,s versus $x_1(t)$ (detail rectangle A'-A').

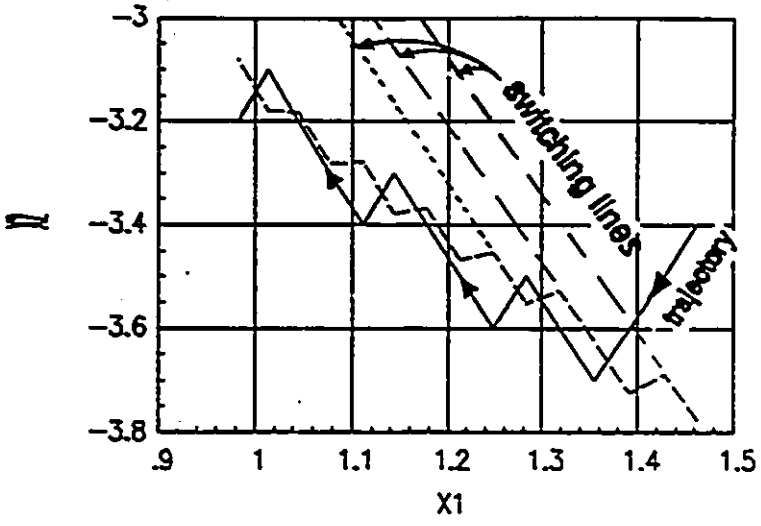

Figure III.2-6 Phase plane representation of the trajectory (detail rectangle A-A).

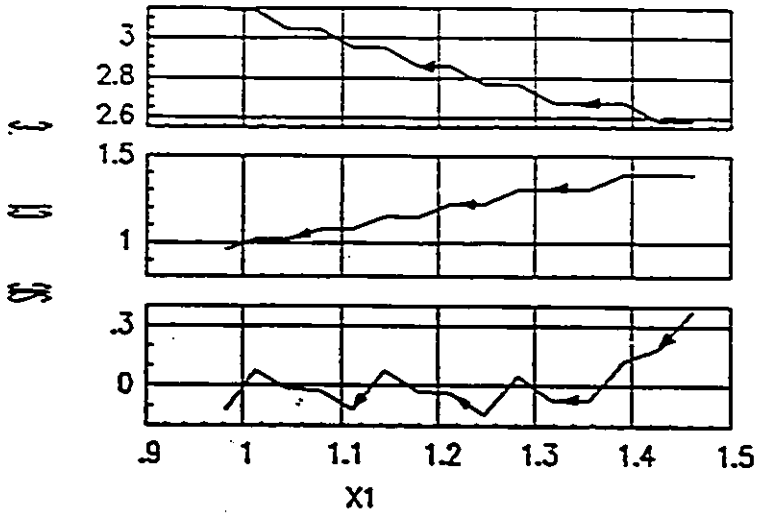

Figure III.2-5 c,c1,s versus $x_1(t)$ (detail rectangle A'-A').

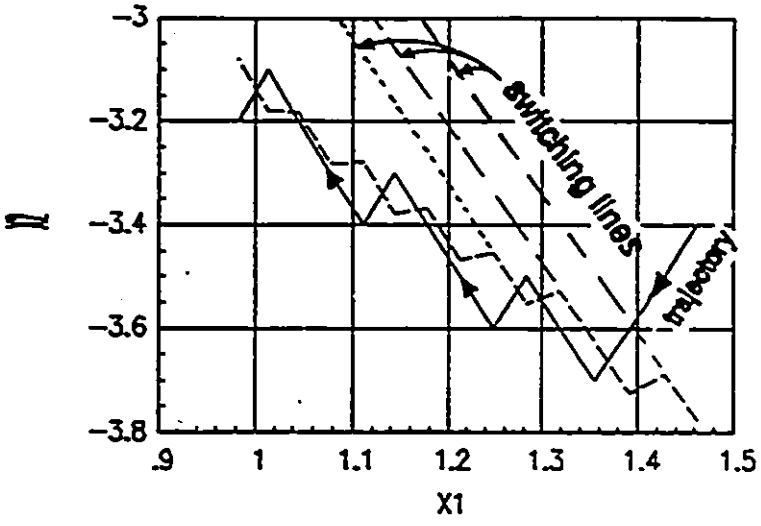

Figure III.2-6 Phase plane representation of the trajectory (detail rectangle A-A).

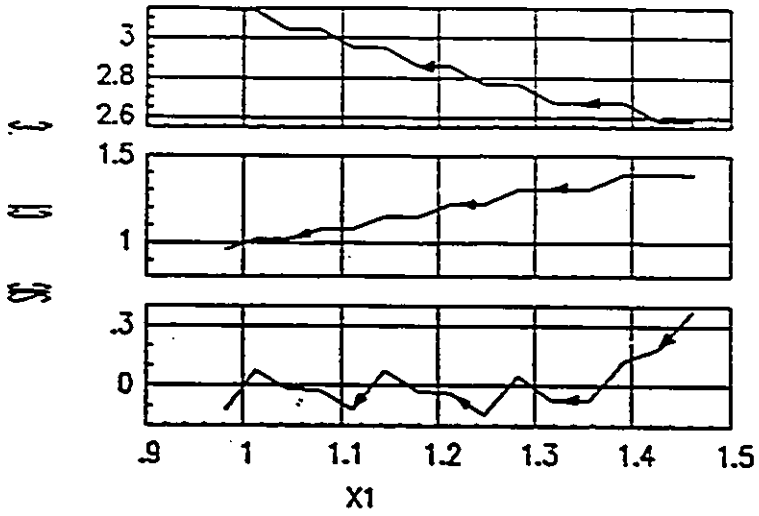

Figure III.2-5 c,c1,s versus $x_1(t)$ (detail rectangle A'-A').

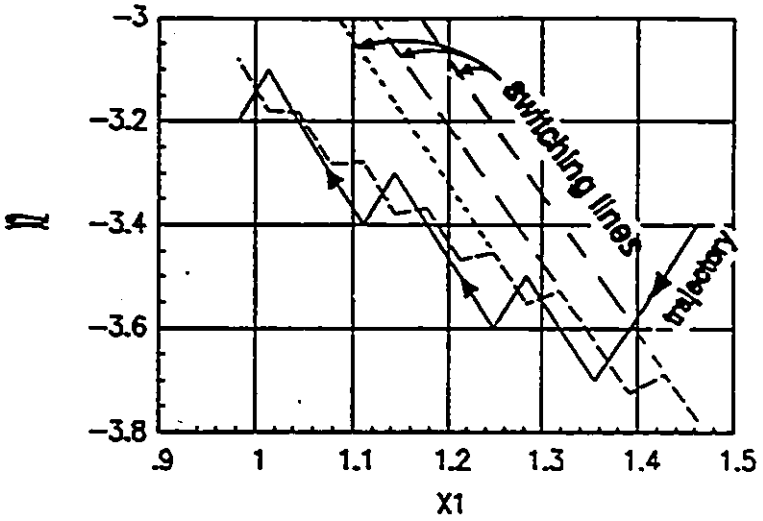

Figure III.2-6 Phase plane representation of the trajectory (detail rectangle A-A).

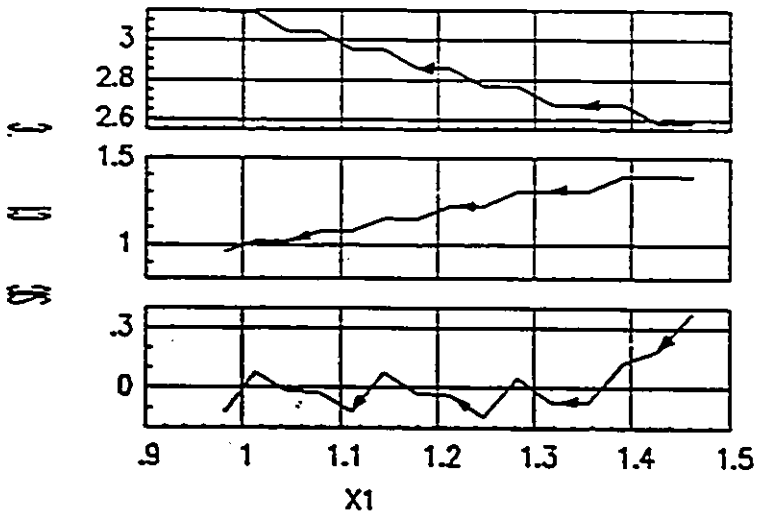

Figure III.2-5 c,c1,s versus $x_1(t)$ (detail rectangle A'-A').

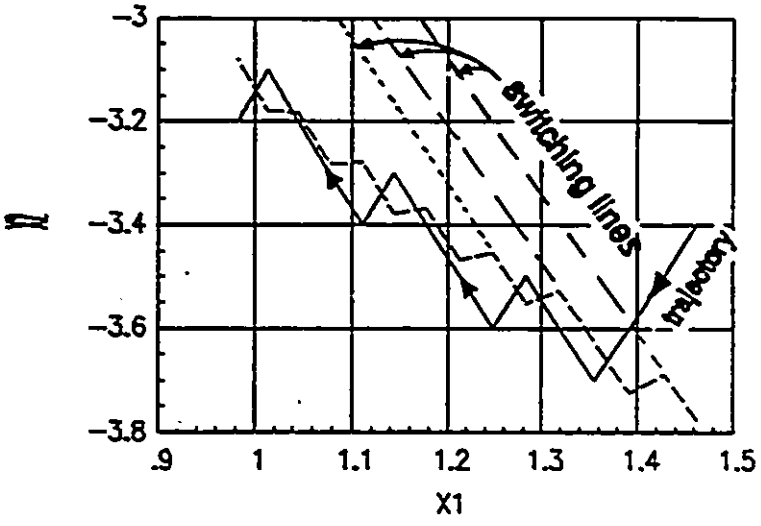

Figure III.2-6 Phase plane representation of the trajectory (detail rectangle A-A).

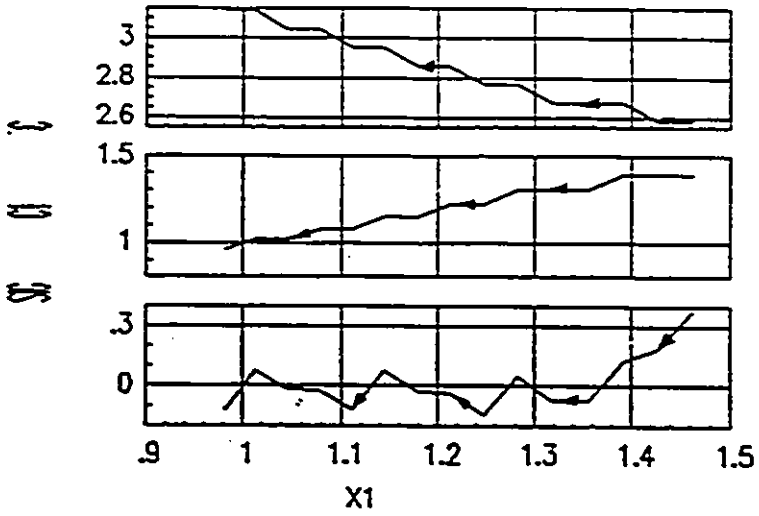

Figure III.2-5 c,c1,s versus $x_1(t)$ (detail rectangle A'-A').

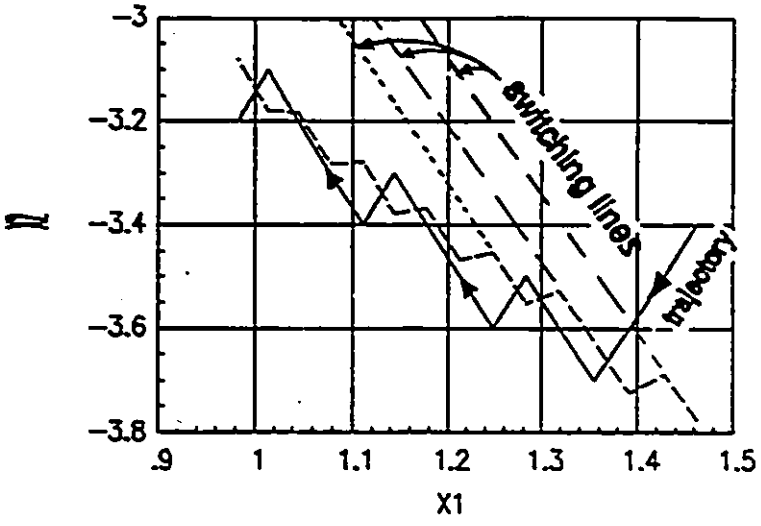

Figure III.2-6 Phase plane representation of the trajectory (detail rectangle A-A).

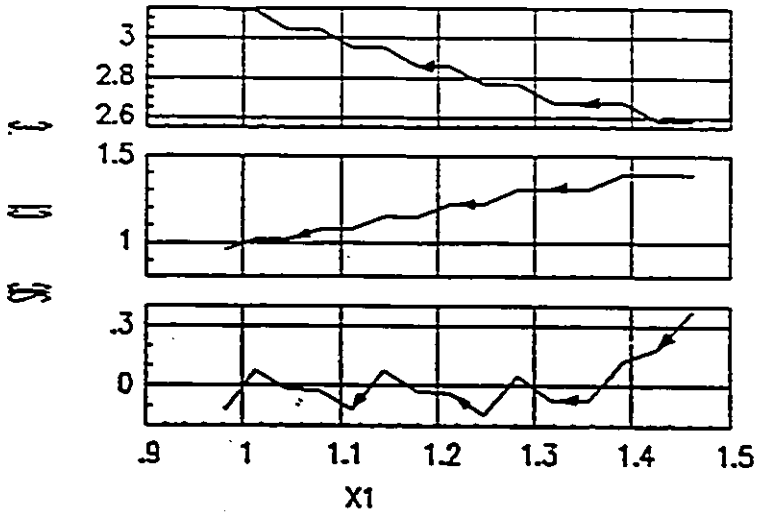

Figure III.2-5 c,c1,s versus $x_1(t)$ (detail rectangle A'-A').

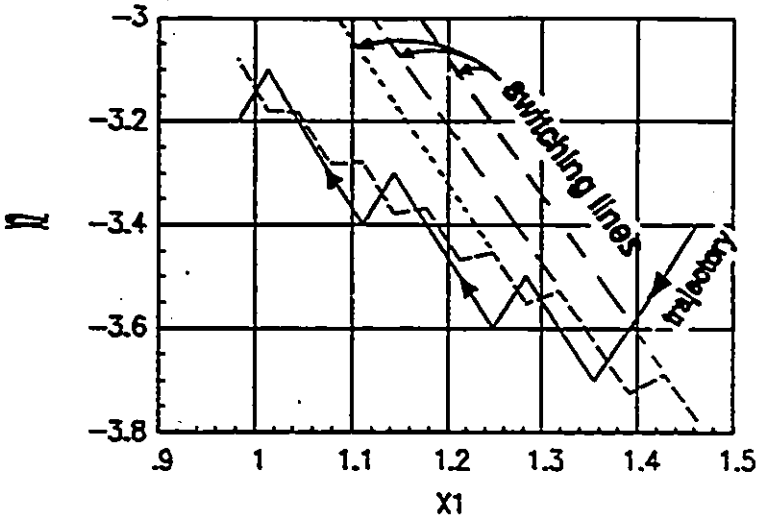

Figure III.2-6 Phase plane representation of the trajectory (detail rectangle A-A).

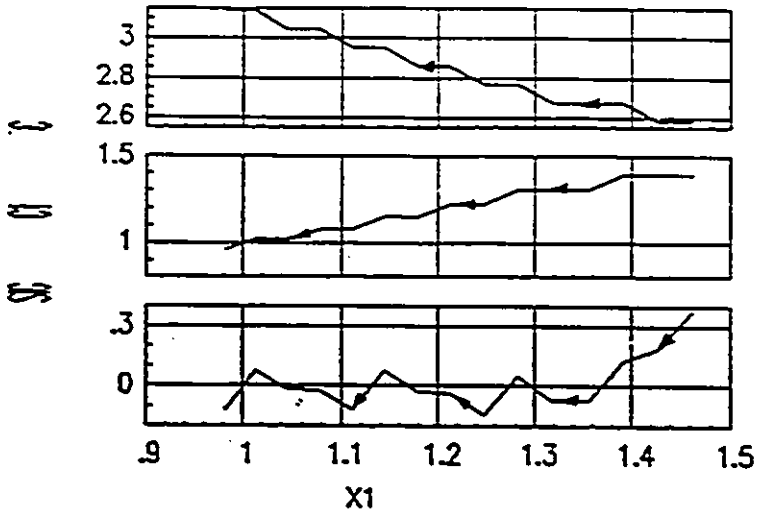

Figure III.2-5 c,c1,s versus $x_1(t)$ (detail rectangle A'-A').

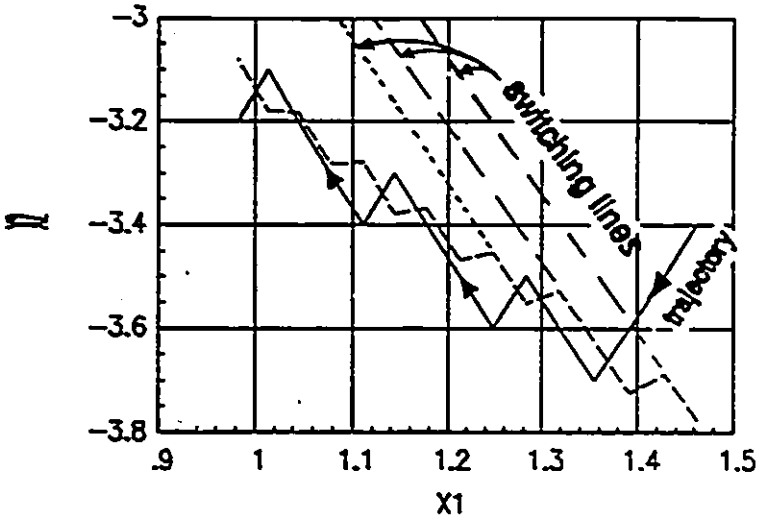

Figure III.2-6 Phase plane representation of the trajectory (detail rectangle A-A).

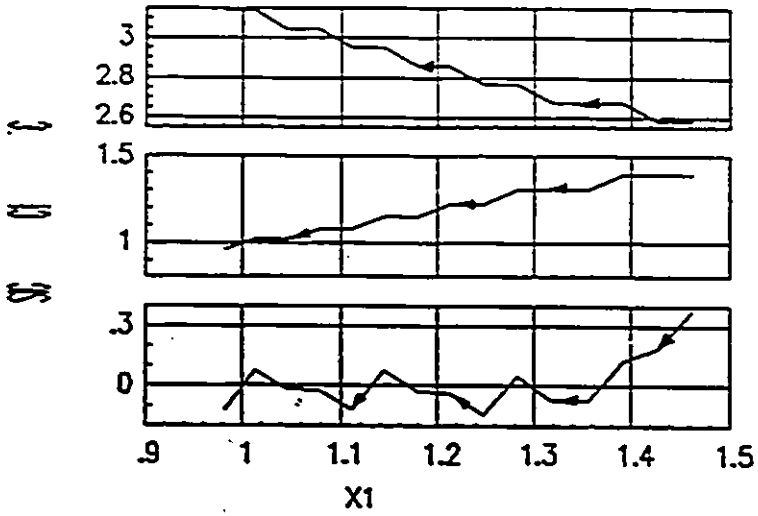

Figure III.2-5 c,c1,s versus $x_1(t)$ (detail rectangle A'-A').

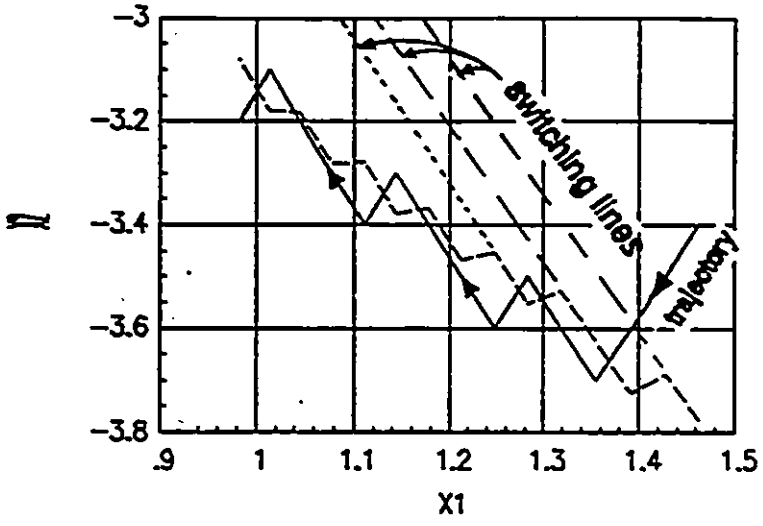

Figure III.2-6 Phase plane representation of the trajectory (detail rectangle A-A).

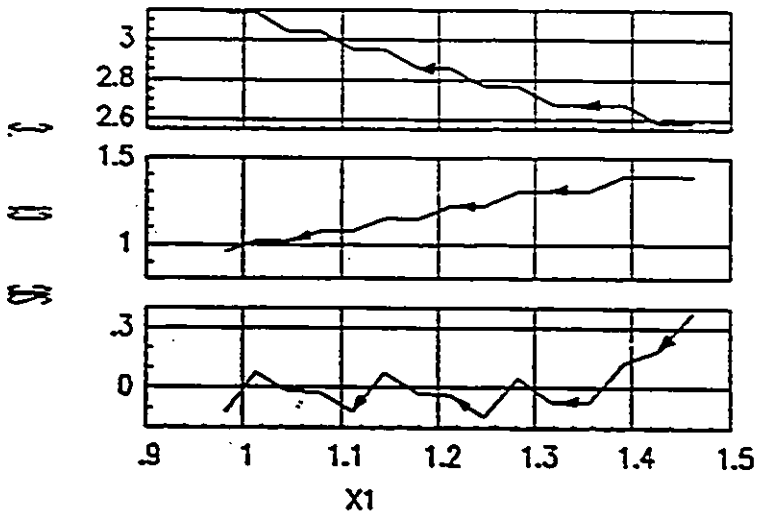

Figure III.2-5 c,c1,s versus $x_1(t)$ (detail rectangle A'-A').

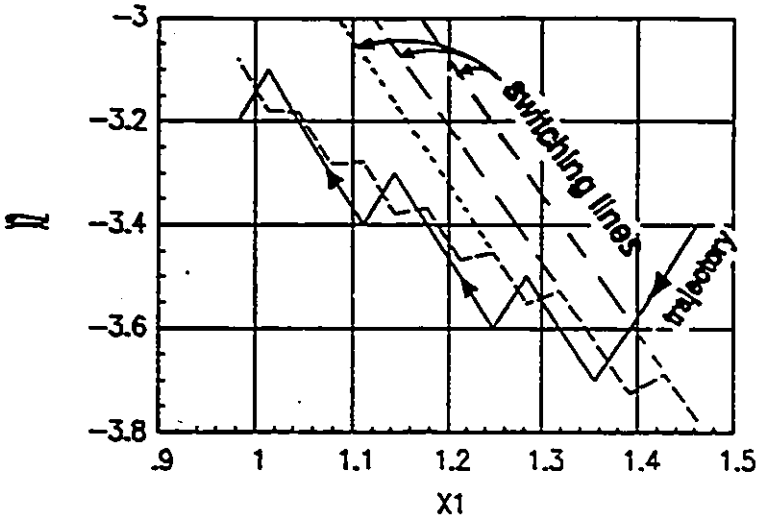

Figure III.2-6 Phase plane representation of the trajectory (detail rectangle A-A).

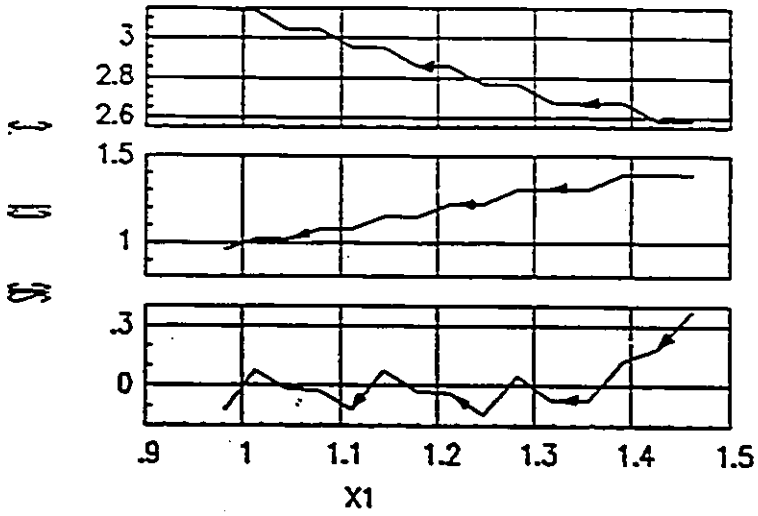

Figure III.2-5 c,c1,s versus $x_1(t)$ (detail rectangle A'-A').

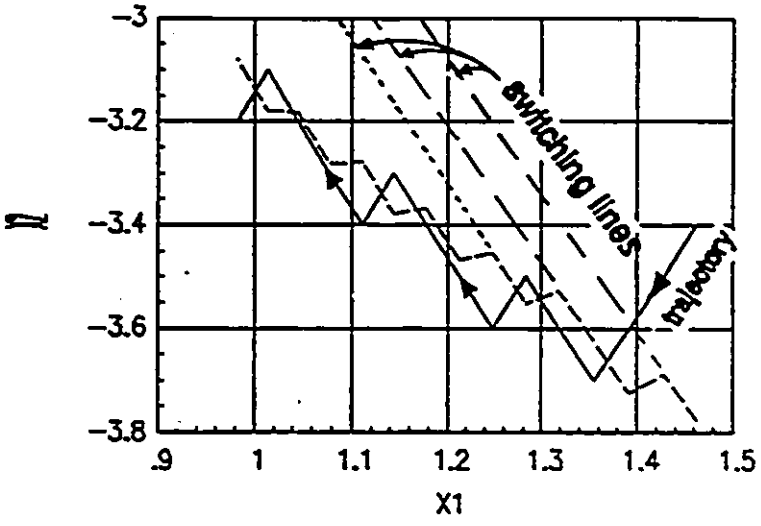

Figure III.2-6 Phase plane representation of the trajectory (detail rectangle A-A).

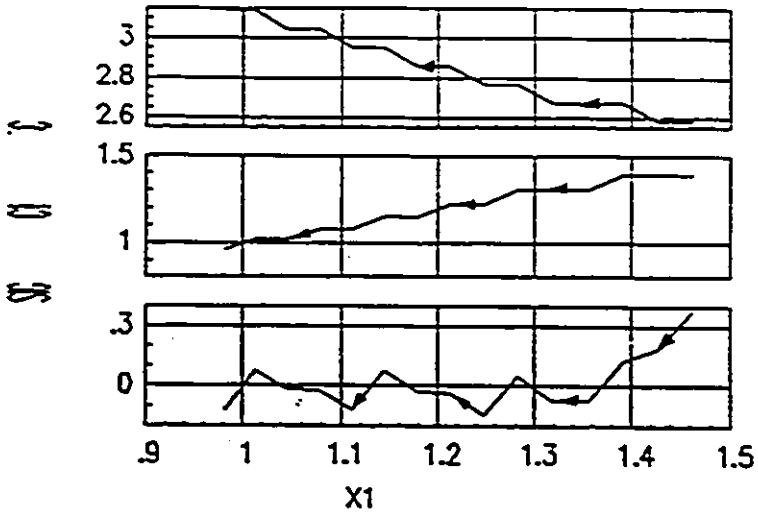

Figure III.2-5 c,c1,s versus $x_1(t)$ (detail rectangle A'-A').

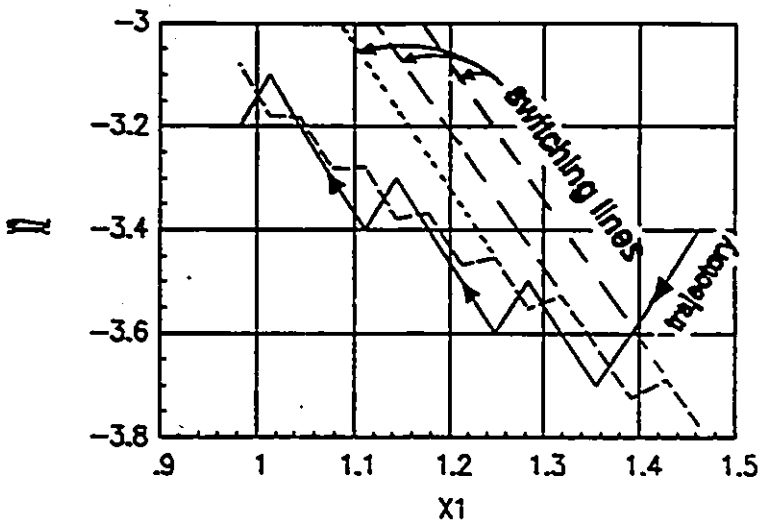

Figure III.2-6 Phase plane representation of the trajectory (detail rectangle A-A).

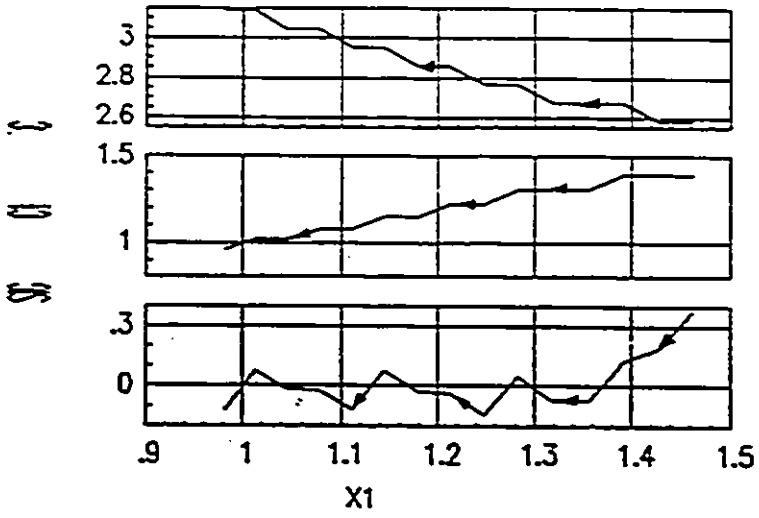

Figure III.2-5 c,c1,s versus $x_1(t)$ (detail rectangle A'-A').

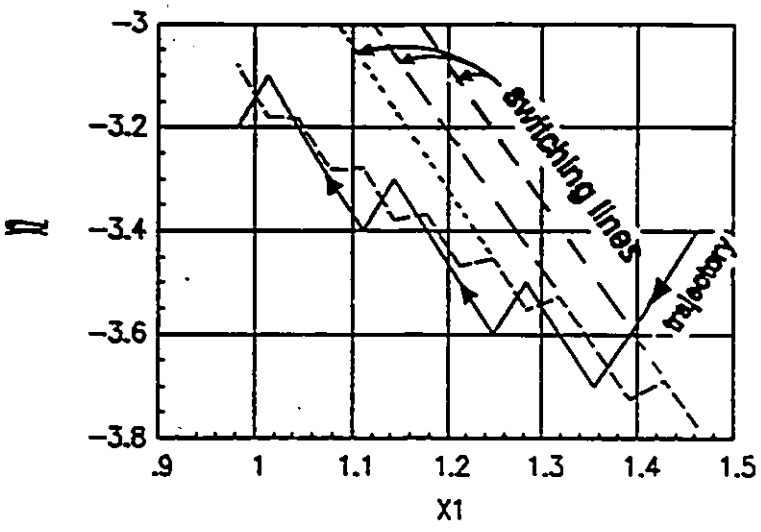

Figure III.2-6 Phase plane representation of the trajectory (detail rectangle A-A).

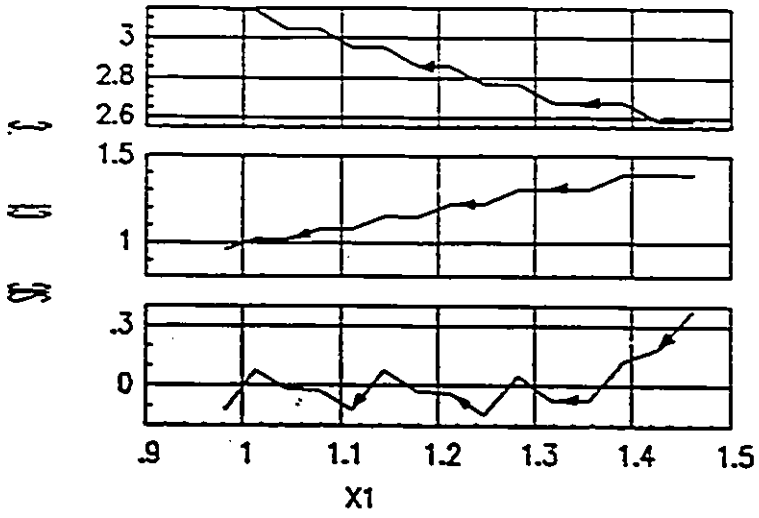

Figure III.2-5 c,c1,s versus $x_1(t)$ (detail rectangle A'-A').

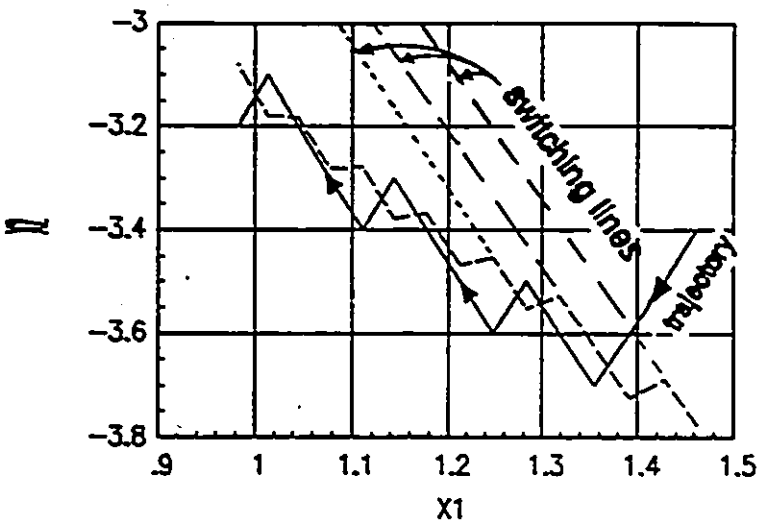

Figure III.2-6 Phase plane representation of the trajectory (detail rectangle A-A).

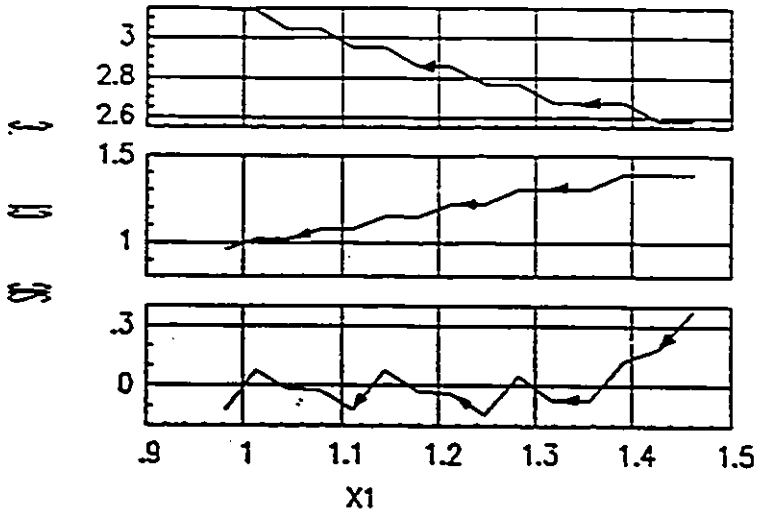

Figure III.2-5 c,c1,s versus $x_1(t)$ (detail rectangle A'-A').

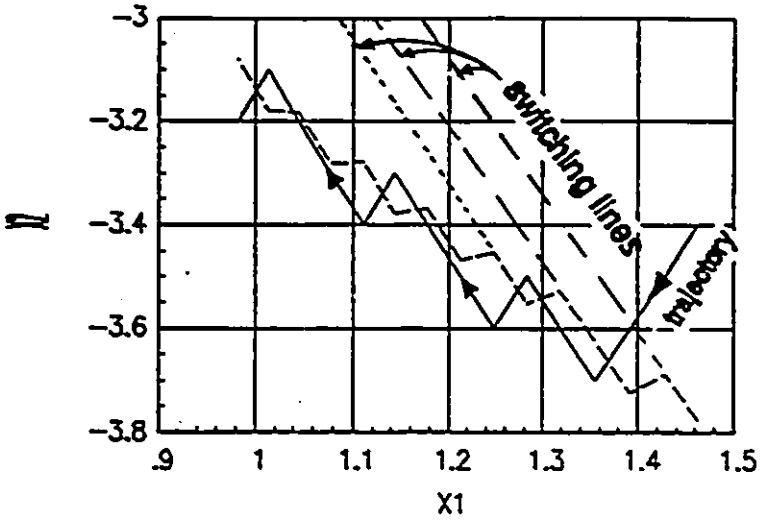

Figure III.2-6 Phase plane representation of the trajectory (detail rectangle A-A).

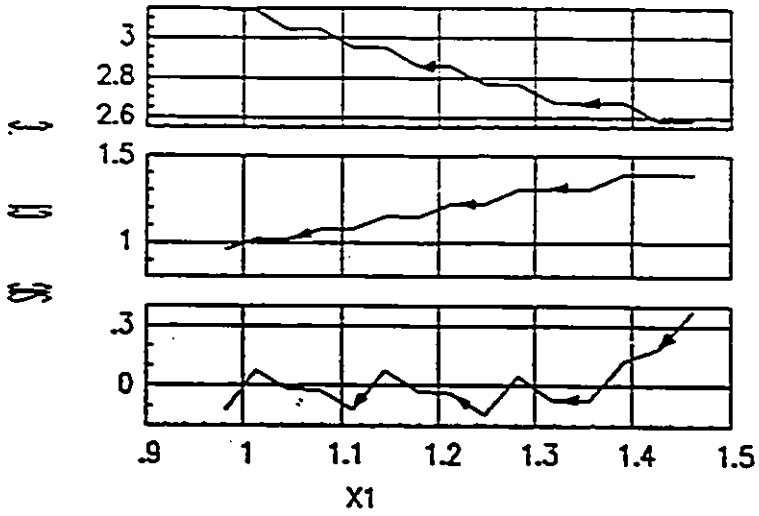

Figure III.2-5 c,c1,s versus $x_1(t)$ (detail rectangle A'-A').

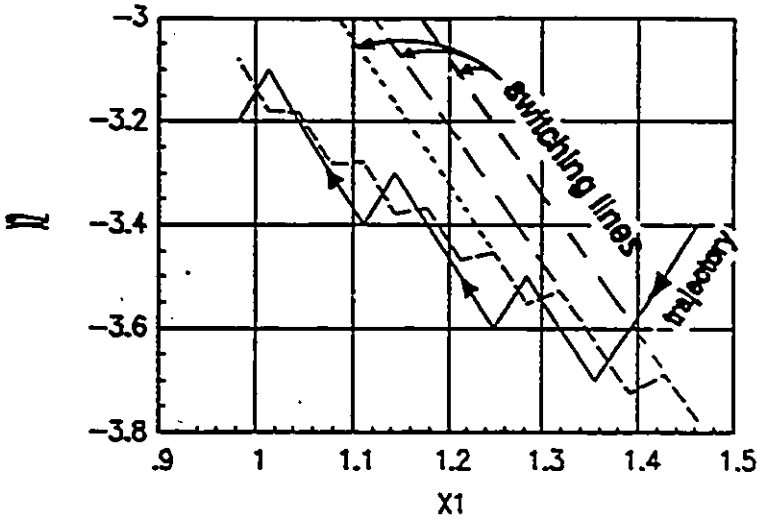

Figure III.2-6 Phase plane representation of the trajectory (detail rectangle A-A).

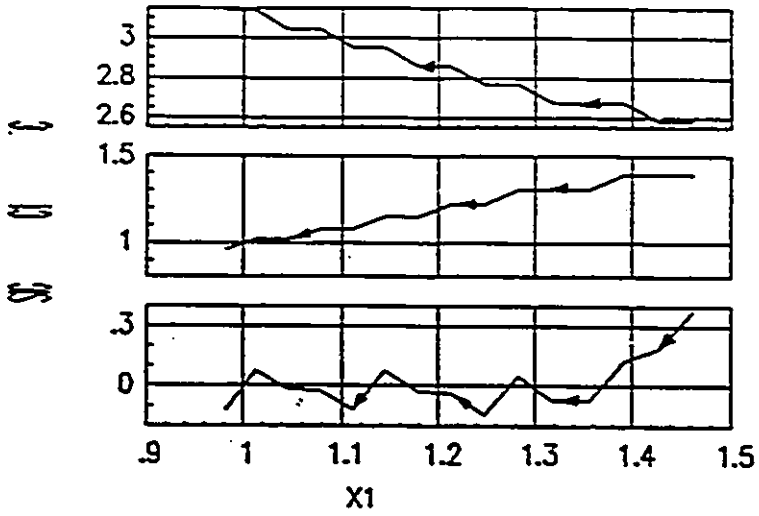

Figure III.2-5 c,c1,s versus $x_1(t)$ (detail rectangle A'-A').

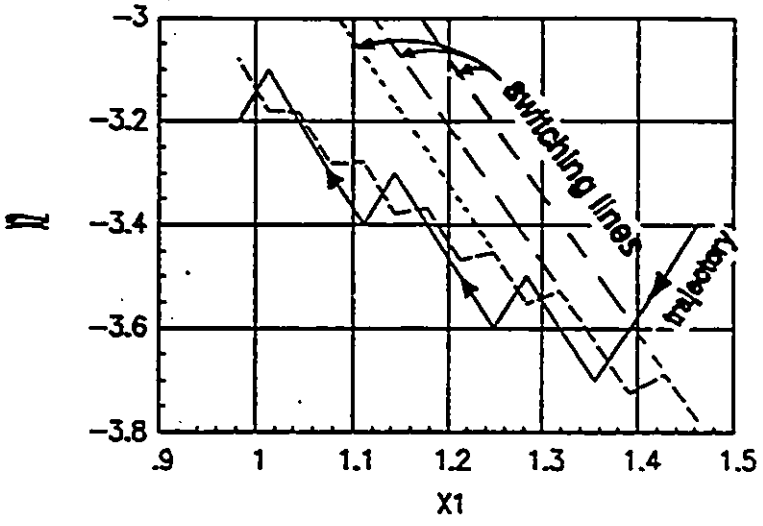

Figure III.2-6 Phase plane representation of the trajectory (detail rectangle A-A).

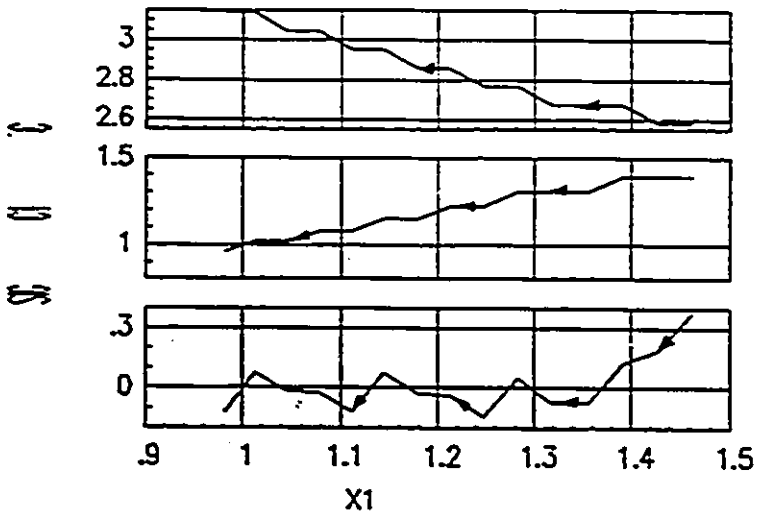

Figure III.2-5 c,c1,s versus $x_1(t)$ (detail rectangle A'-A').

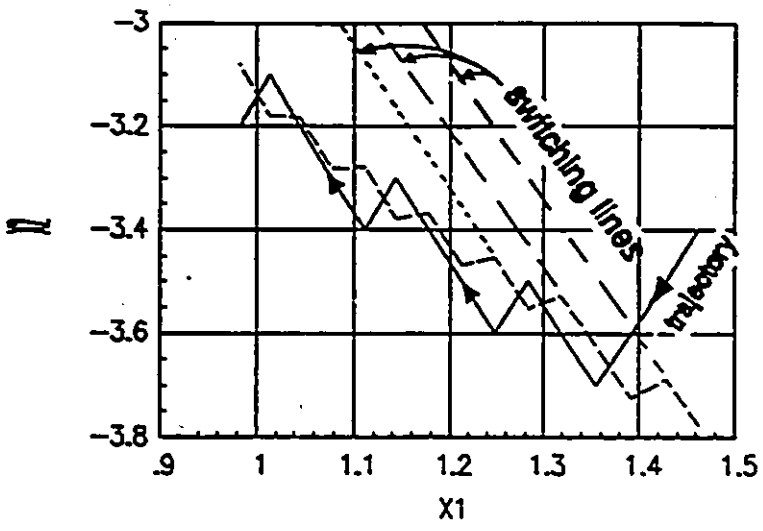

Figure III.2-6 Phase plane representation of the trajectory (detail rectangle A-A).

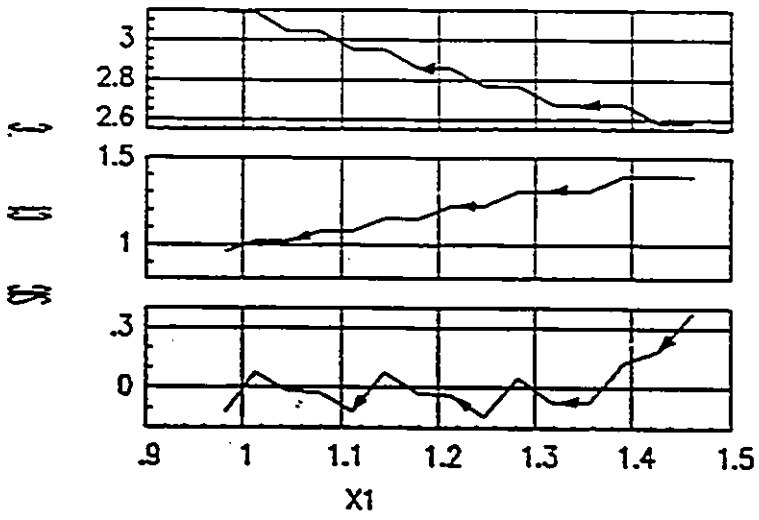

Figure III.2-5 c,c1,s versus $x_1(t)$ (detail rectangle A'-A').

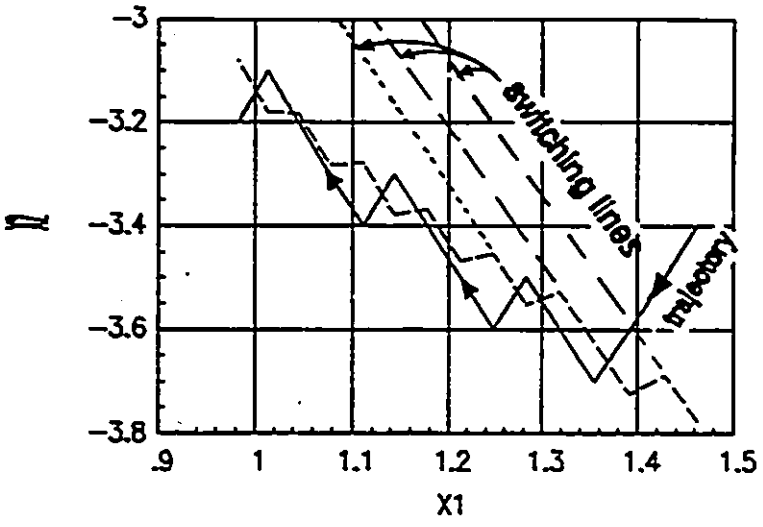

Figure III.2-6 Phase plane representation of the trajectory (detail rectangle A-A).

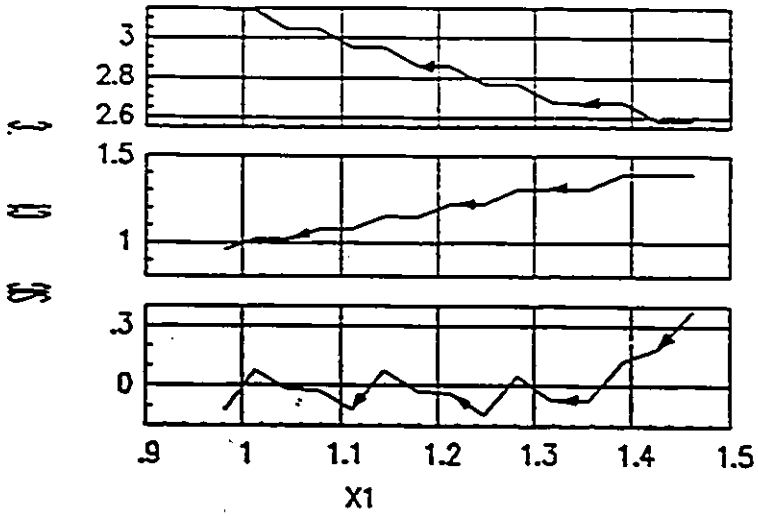

Figure III.2-5 c,c1,s versus $x_1(t)$ (detail rectangle A'-A').

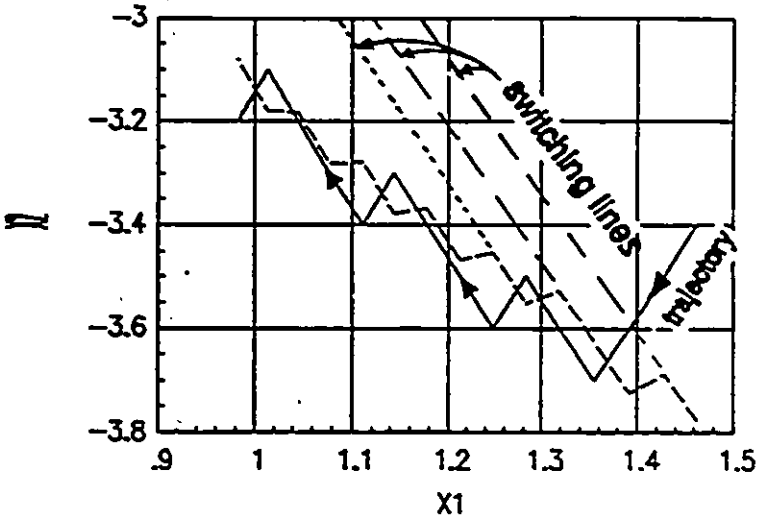

Figure III.2-6 Phase plane representation of the trajectory (detail rectangle A-A).

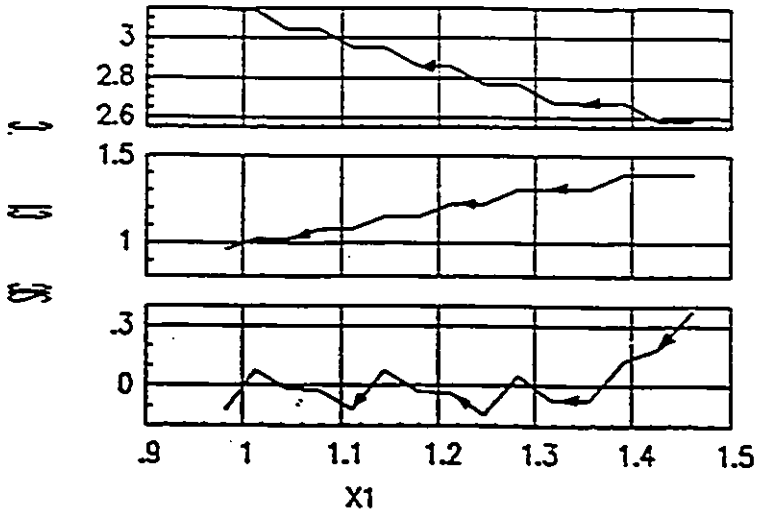

Figure III.2-5 c,c1,s versus $x_1(t)$ (detail rectangle A'-A').

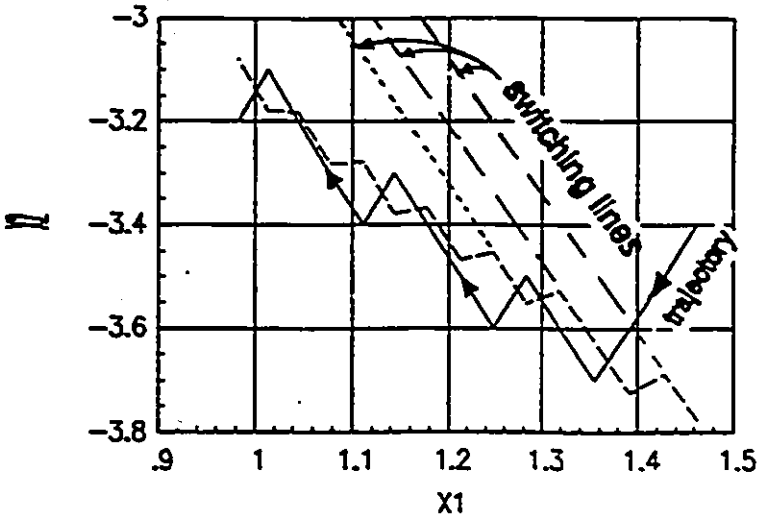

Figure III.2-6 Phase plane representation of the trajectory (detail rectangle A-A).

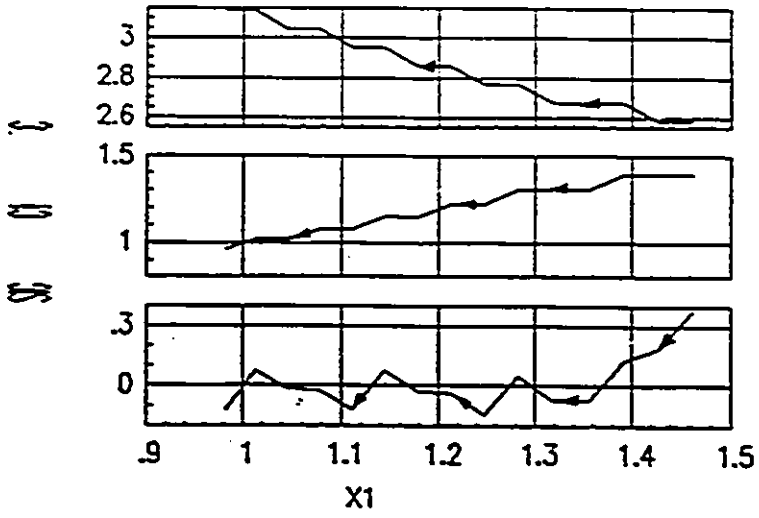

Figure III.2-5 c,c1,s versus $x_1(t)$ (detail rectangle A'-A').

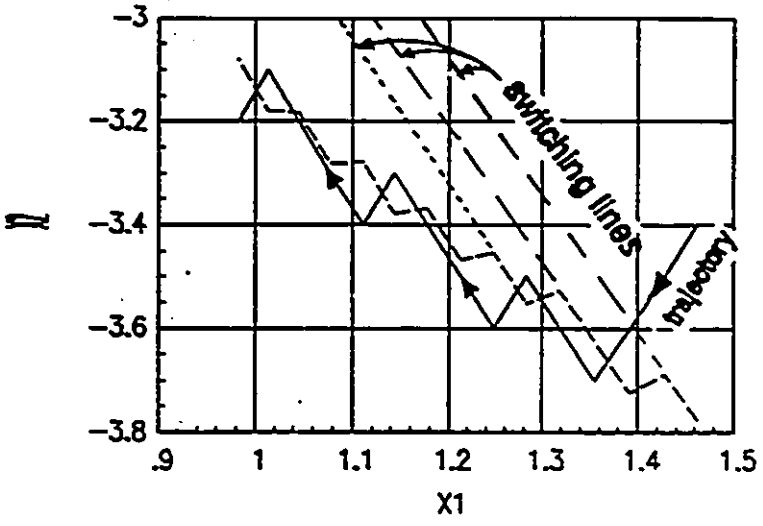

Figure III.2-6 Phase plane representation of the trajectory (detail rectangle A-A).

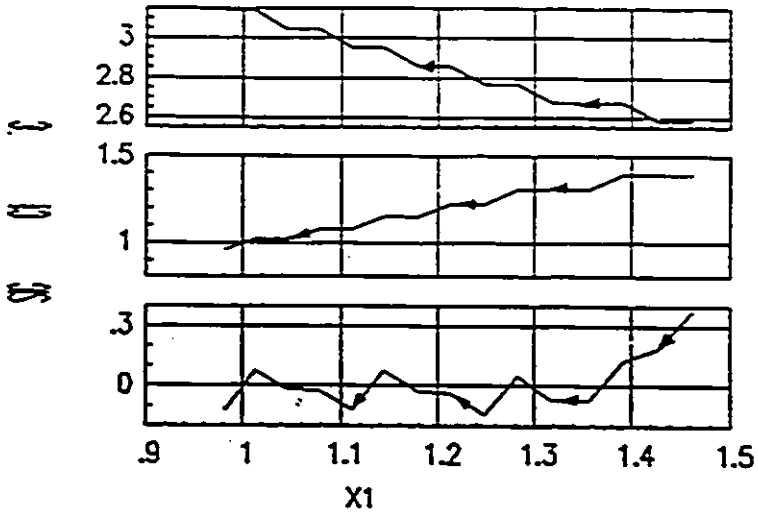

Figure III.2-5 c,c1,s versus $x_1(t)$ (detail rectangle A'-A').

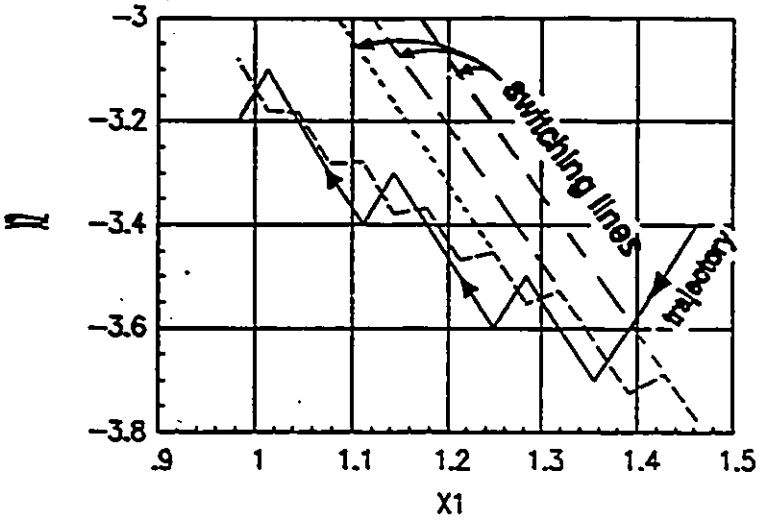

Figure III.2-6 Phase plane representation of the trajectory (detail rectangle A-A).

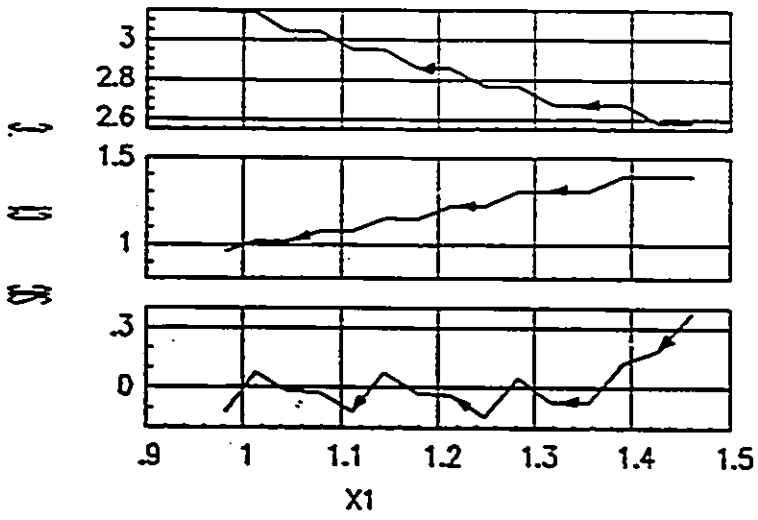

Figure III.2-5 c,c1,s versus $x_1(t)$ (detail rectangle A'-A').

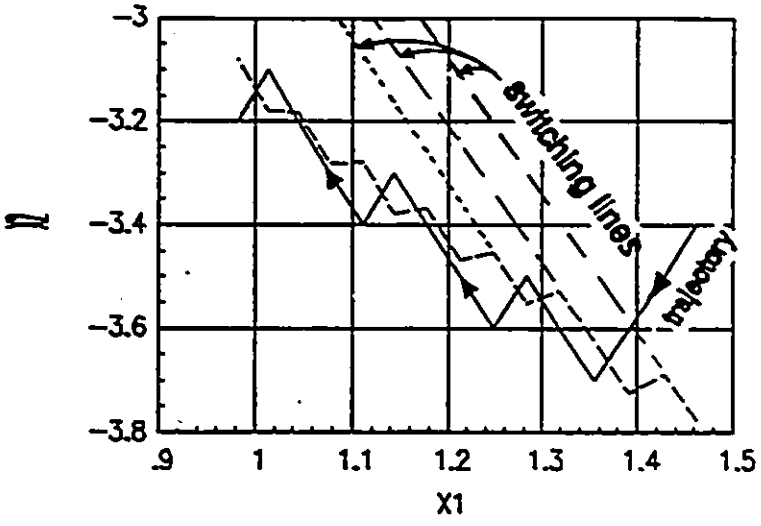

Figure III.2-6 Phase plane representation of the trajectory (detail rectangle A-A).

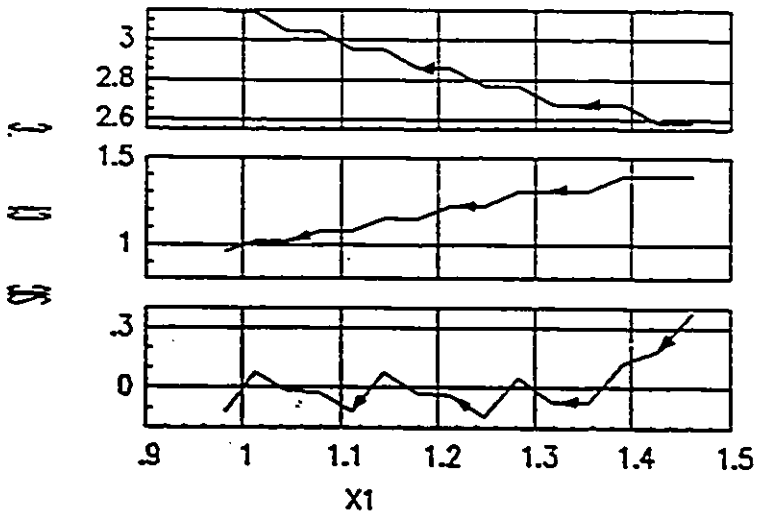

Figure III.2-5 c,c1,s versus $x_1(t)$ (detail rectangle A'-A').

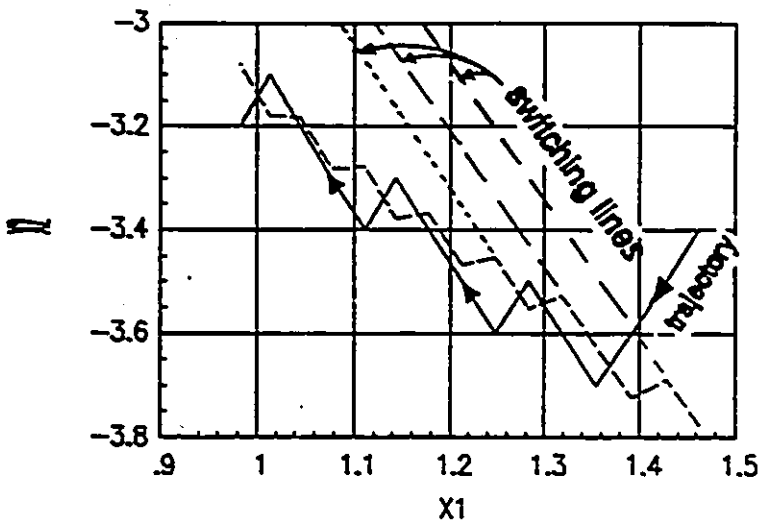

Figure III.2-6 Phase plane representation of the trajectory (detail rectangle A-A).

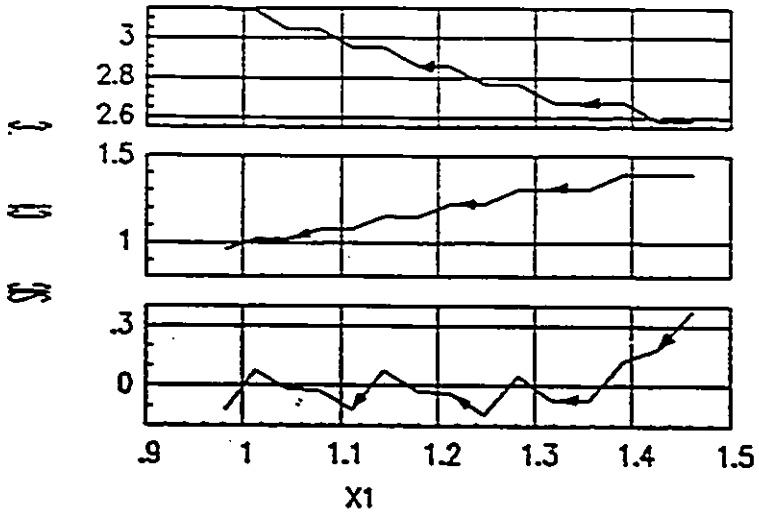

Figure III.2-5 c,c1,s versus $x_1(t)$ (detail rectangle A'-A').

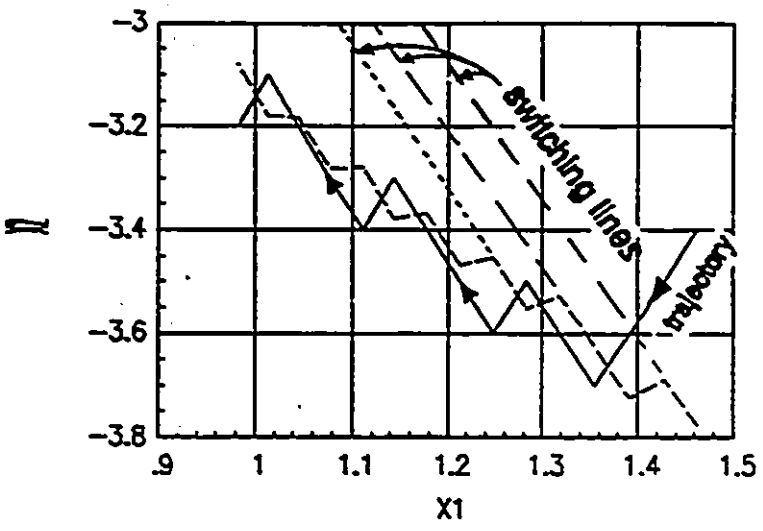

Figure III.2-6 Phase plane representation of the trajectory (detail rectangle A-A).

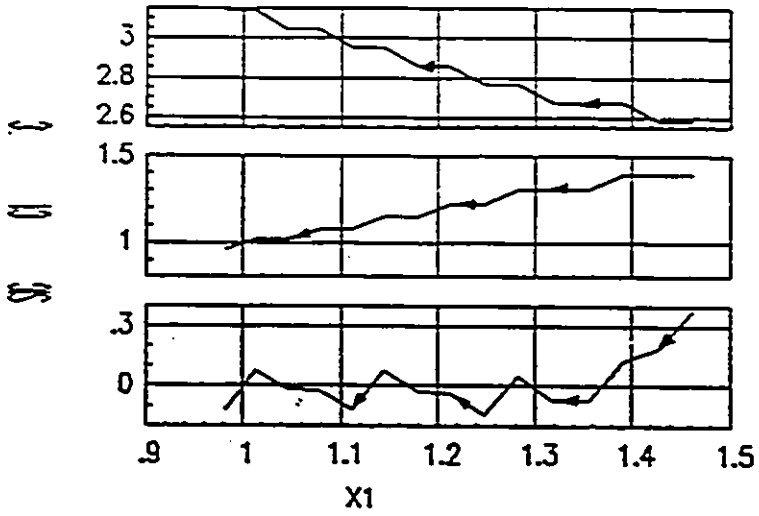

Figure III.2-5 c,c1,s versus $x_1(t)$ (detail rectangle A'-A').

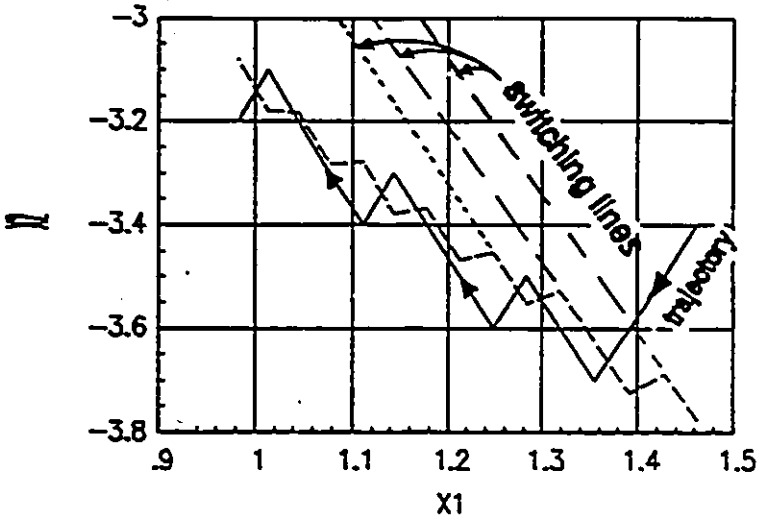

Figure III.2-6 Phase plane representation of the trajectory (detail rectangle A-A).

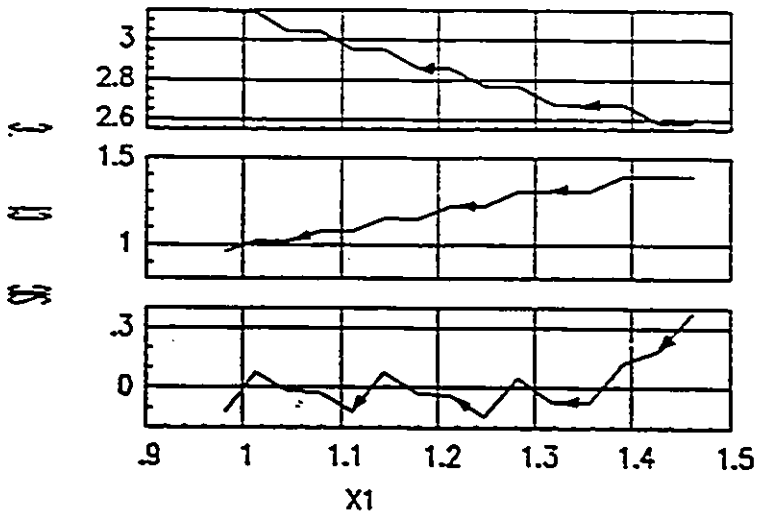

Figure III.2-5 c,c1,s versus $x_1(t)$ (detail rectangle A'-A').

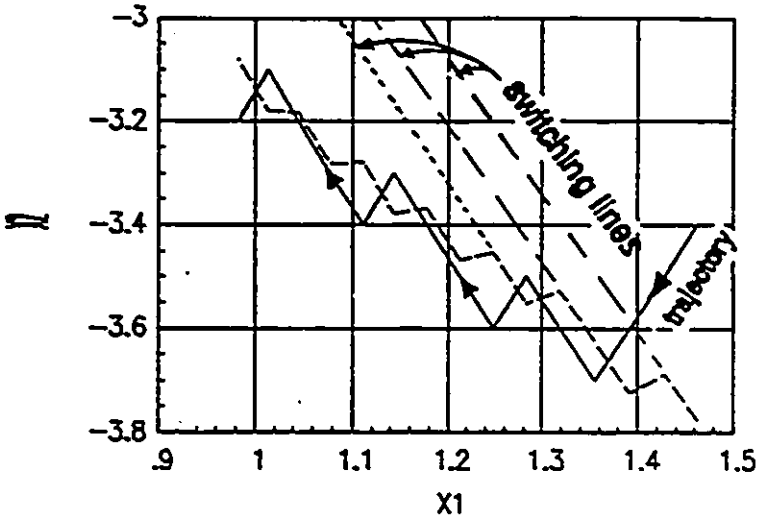

Figure III.2-6 Phase plane representation of the trajectory (detail rectangle A-A).

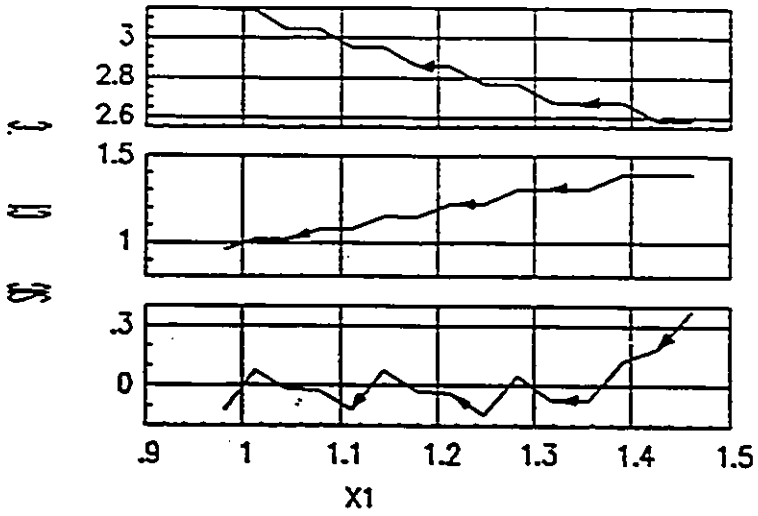

Figure III.2-5 c,c1,s versus $x_1(t)$ (detail rectangle A'-A').

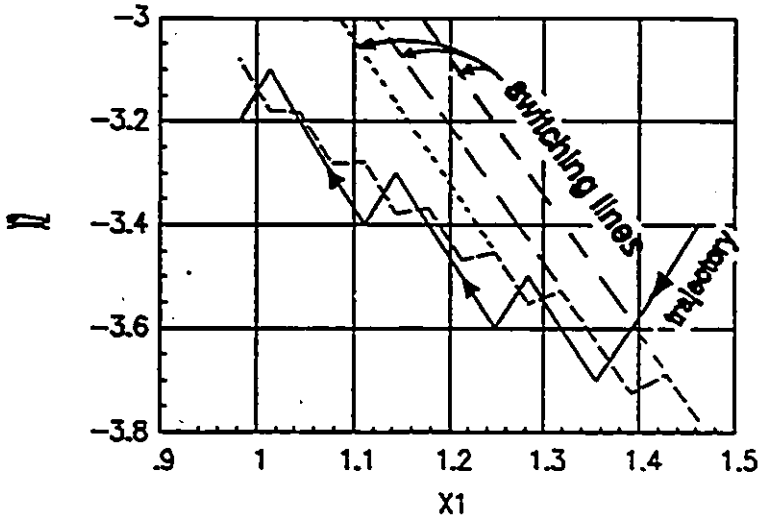

Figure III.2-6 Phase plane representation of the trajectory (detail rectangle A-A).

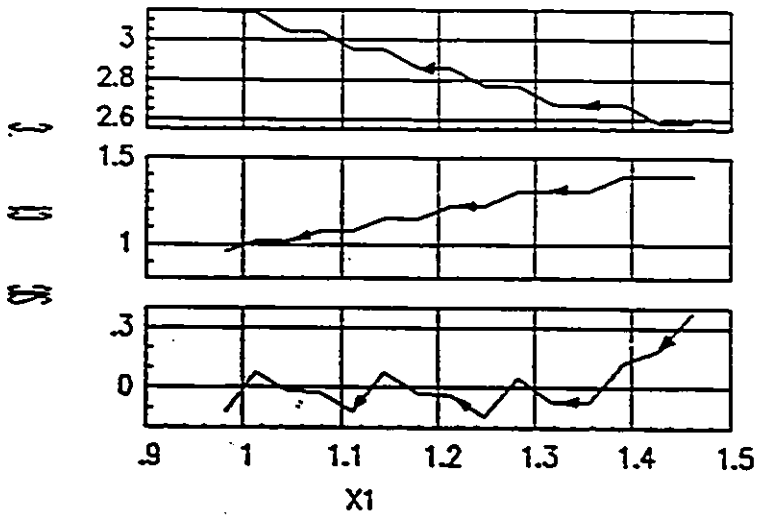

Figure III.2-5 c,c1,s versus $x_1(t)$ (detail rectangle A'-A').

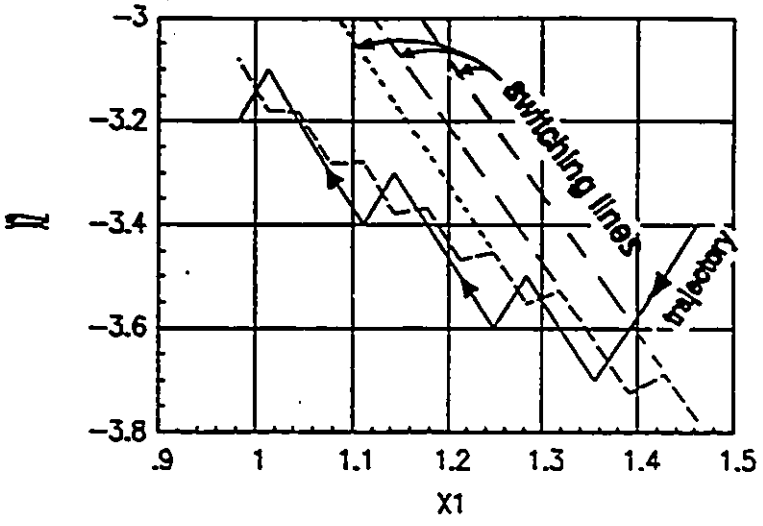

Figure III.2-6 Phase plane representation of the trajectory (detail rectangle A-A).

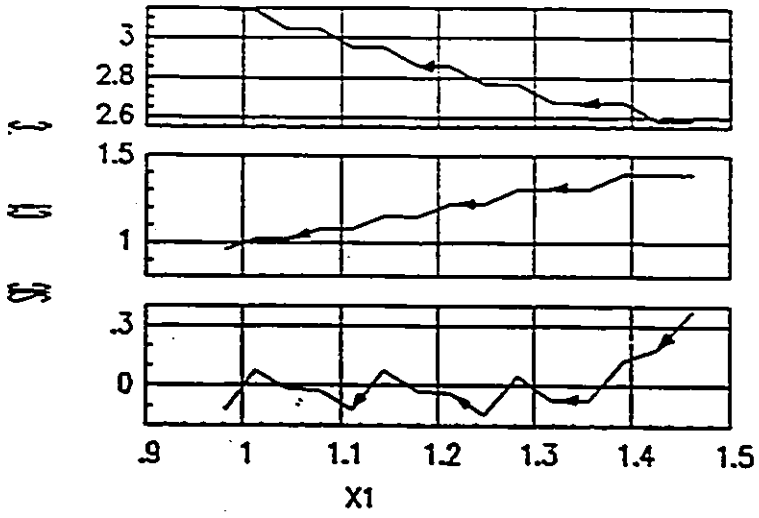

Figure III.2-5 c,c1,s versus $x_1(t)$ (detail rectangle A'-A').

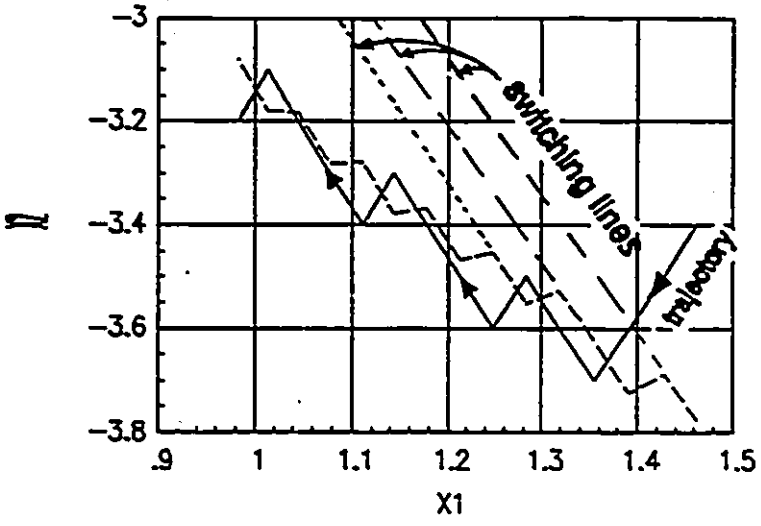

Figure III.2-6 Phase plane representation of the trajectory (detail rectangle A-A).

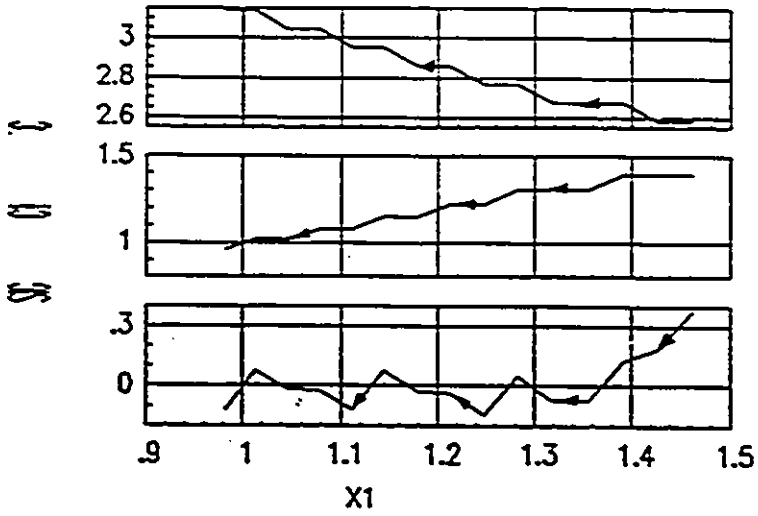

Figure III.2-5 c,c1,s versus $x_1(t)$ (detail rectangle A'-A').

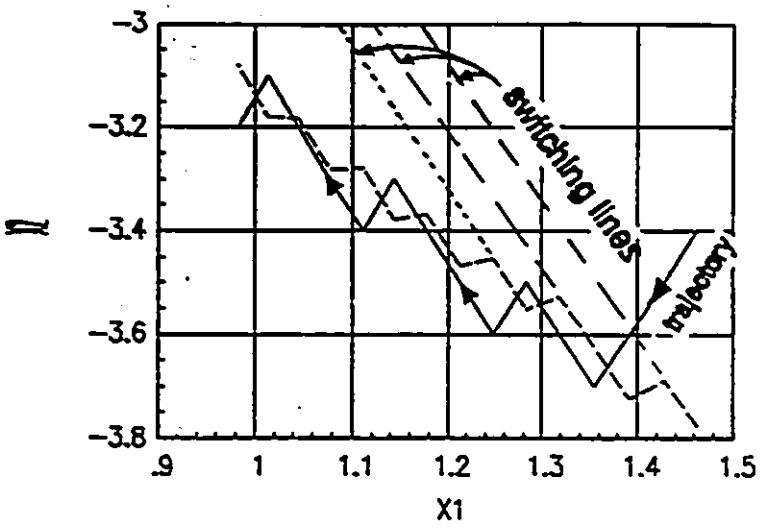

Figure III.2-6 Phase plane representation of the trajectory (detail rectangle A-A).

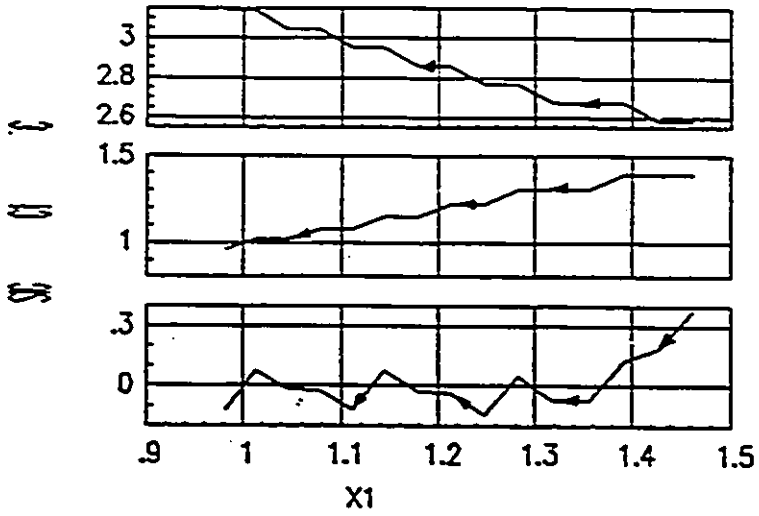

Figure III.2-5 c,c1,s versus $x_1(t)$ (detail rectangle A'-A').

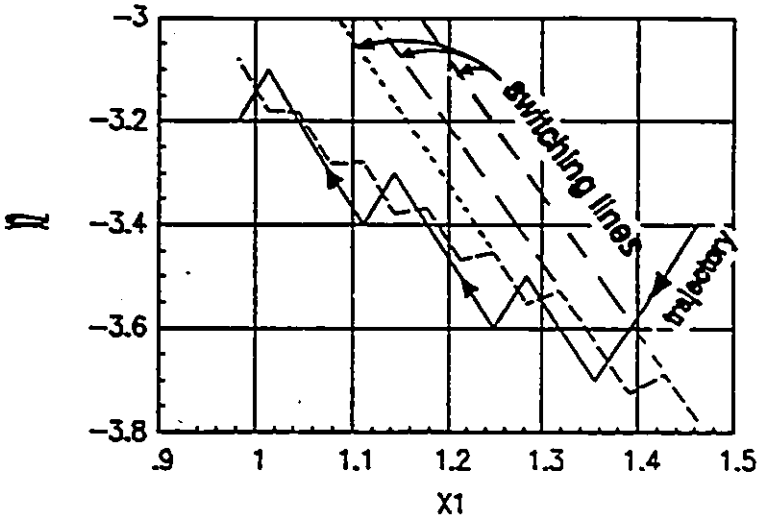

Figure III.2-6 Phase plane representation of the trajectory (detail rectangle A-A).

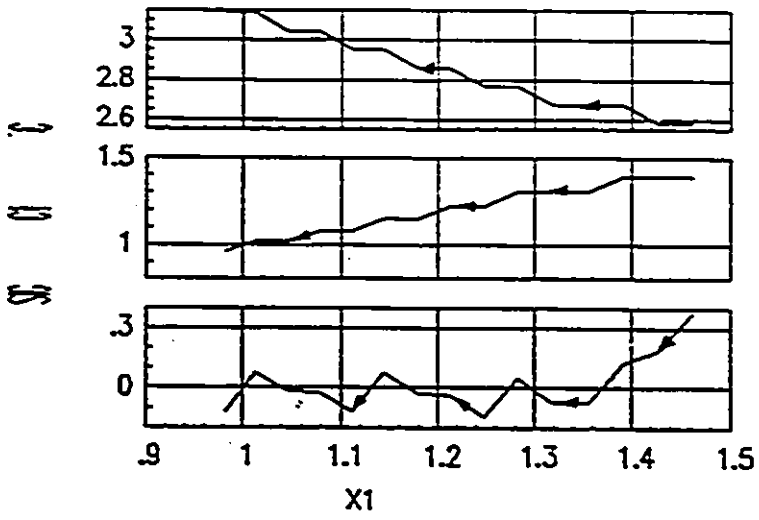

Figure III.2-5 c,c1,s versus $x_1(t)$ (detail rectangle A'-A').

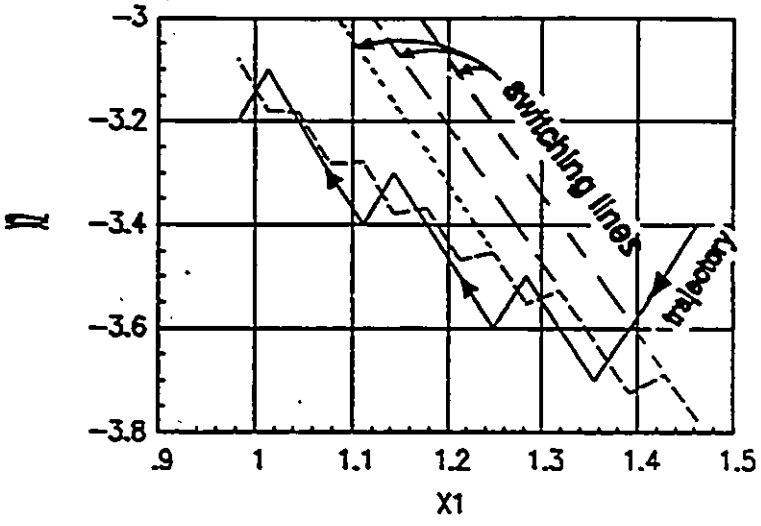

Figure III.2-6 Phase plane representation of the trajectory (detail rectangle A-A).

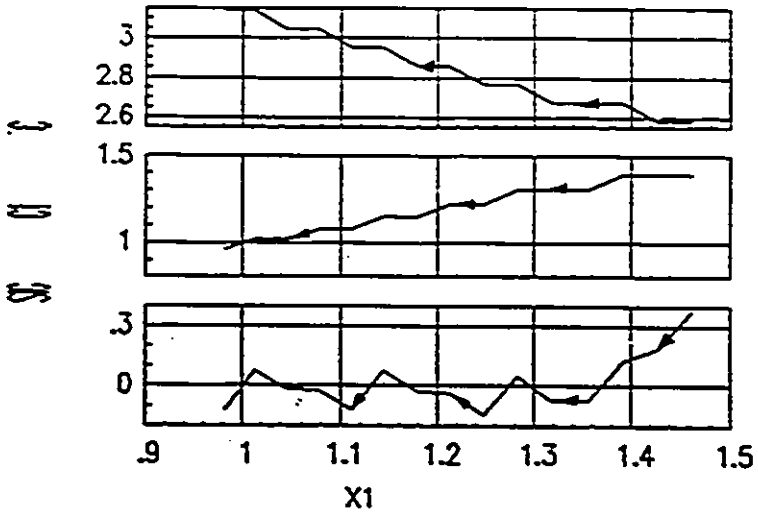

Figure III.2-5 c,c1,s versus $x_1(t)$ (detail rectangle A'-A').

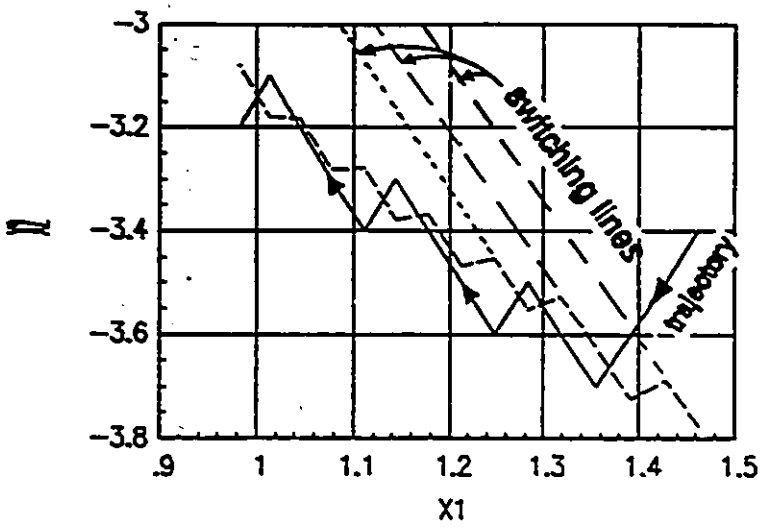

Figure III.2-6 Phase plane representation of the trajectory (detail rectangle A-A).

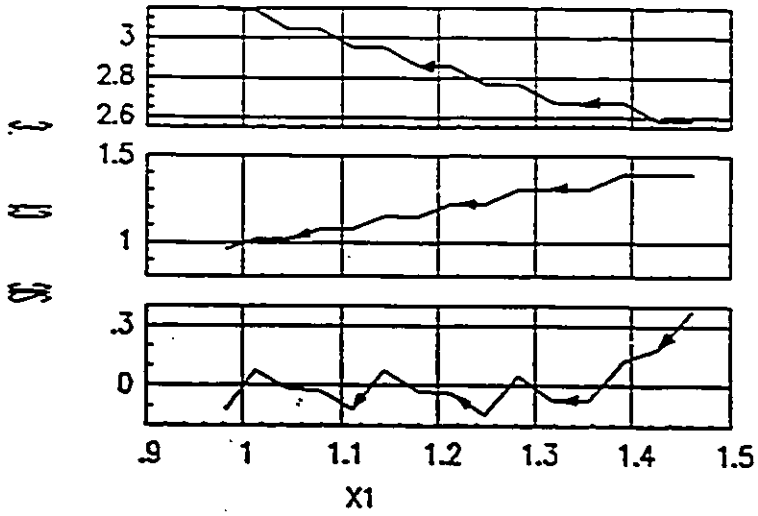

Figure III.2-5 c,c1,s versus $x_1(t)$ (detail rectangle A'-A').

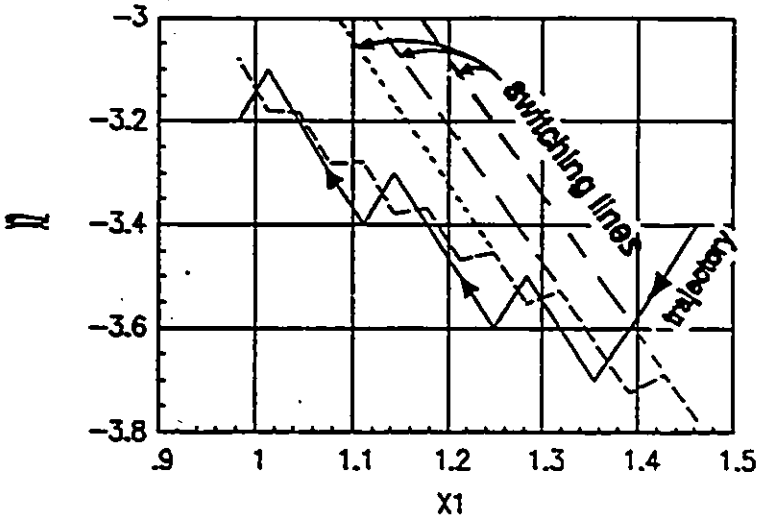

Figure III.2-6 Phase plane representation of the trajectory (detail rectangle A-A).

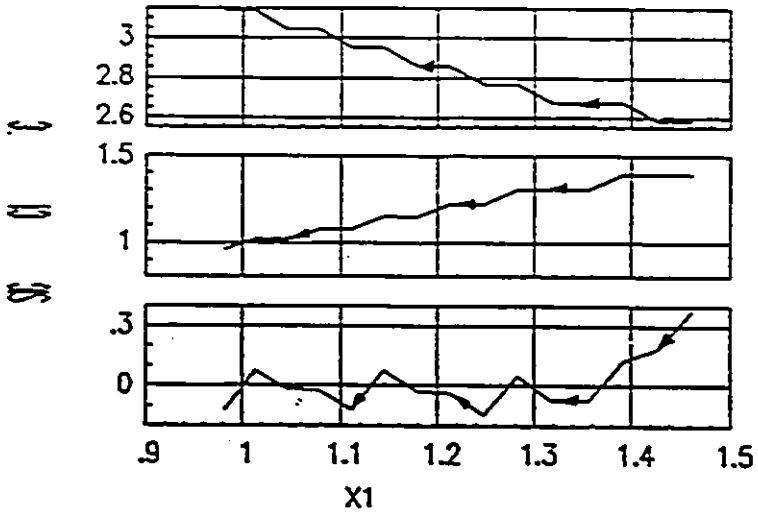

Figure III.2-5 c,c1,s versus $x_1(t)$ (detail rectangle A'-A').

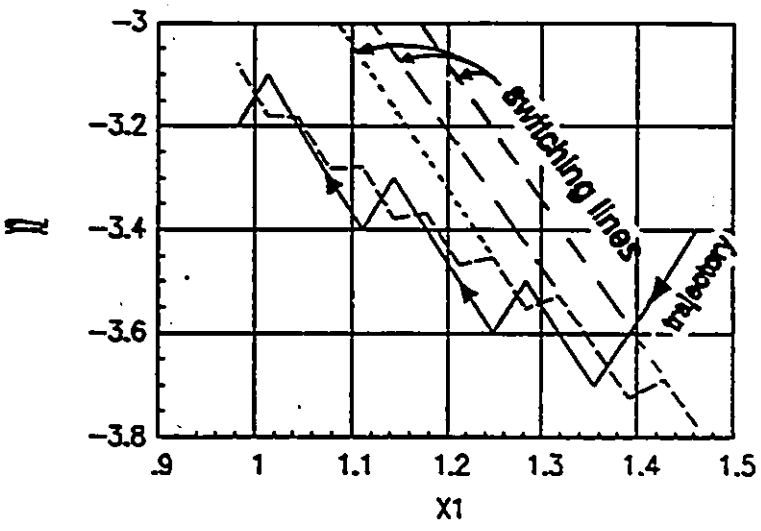

Figure III.2-6 Phase plane representation of the trajectory (detail rectangle A-A).

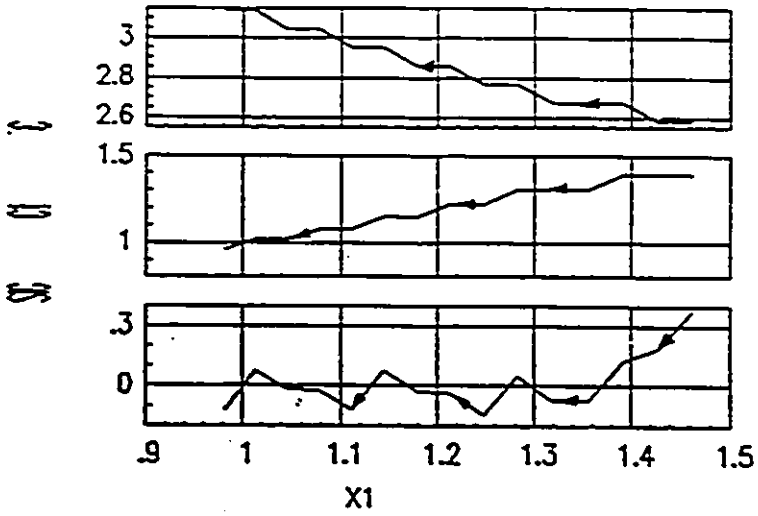

Figure III.2-5 c,c1,s versus $x_1(t)$ (detail rectangle A'-A').

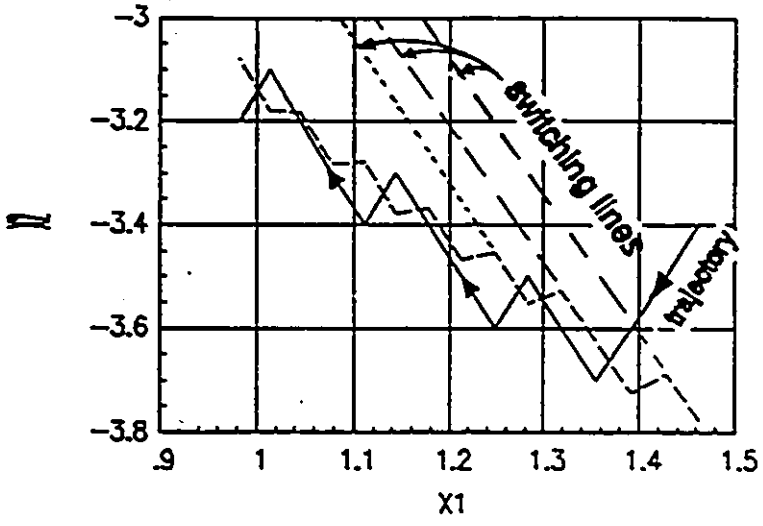

Figure III.2-6 Phase plane representation of the trajectory (detail rectangle A-A).

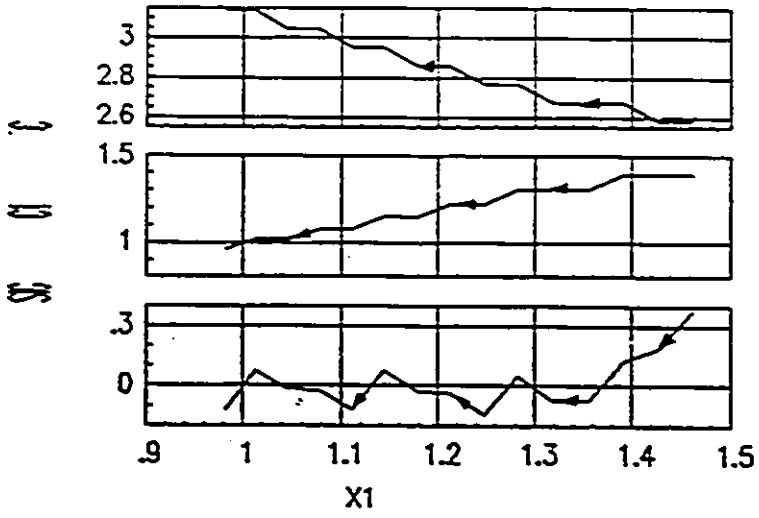

Figure III.2-5 c,c1,s versus $x_1(t)$ (detail rectangle A'-A').

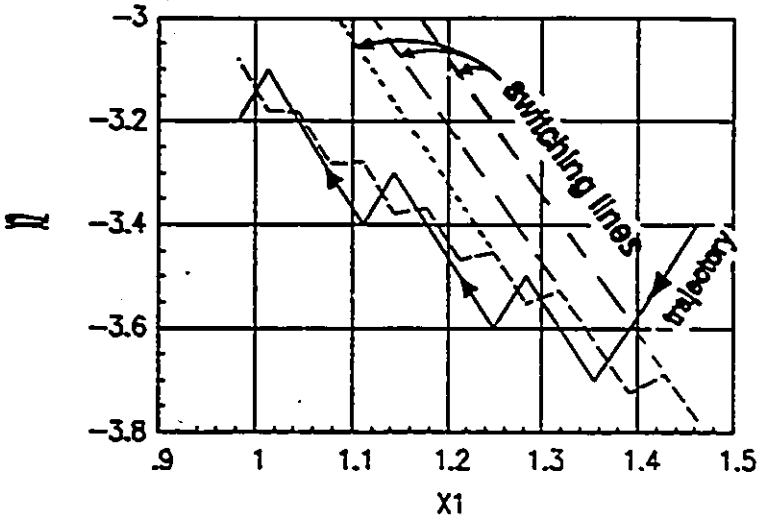

Figure III.2-6 Phase plane representation of the trajectory (detail rectangle A-A).

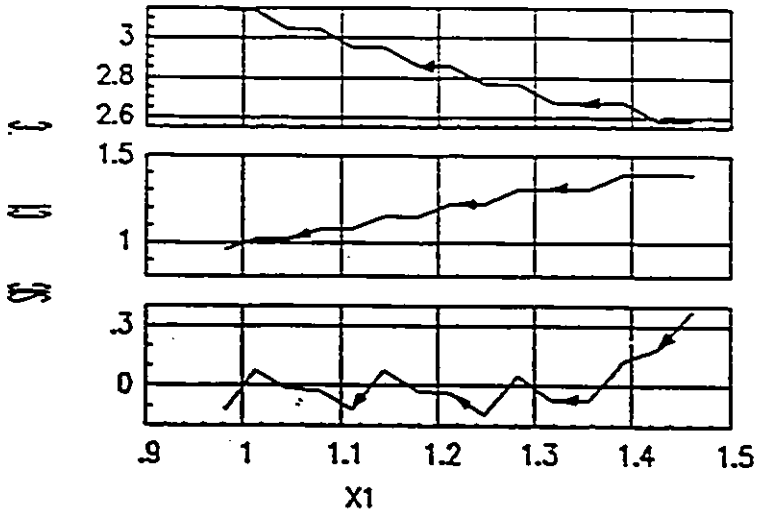

Figure III.2-5 c,c1,s versus $x_1(t)$ (detail rectangle A'-A').

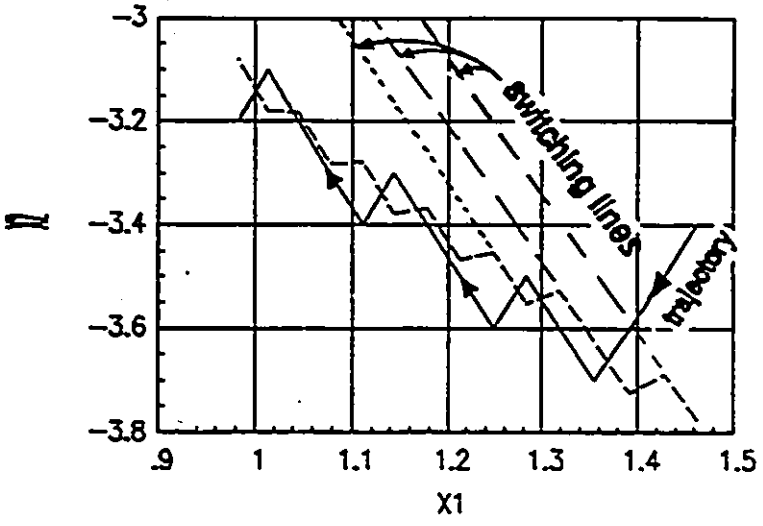

Figure III.2-6 Phase plane representation of the trajectory (detail rectangle A-A).

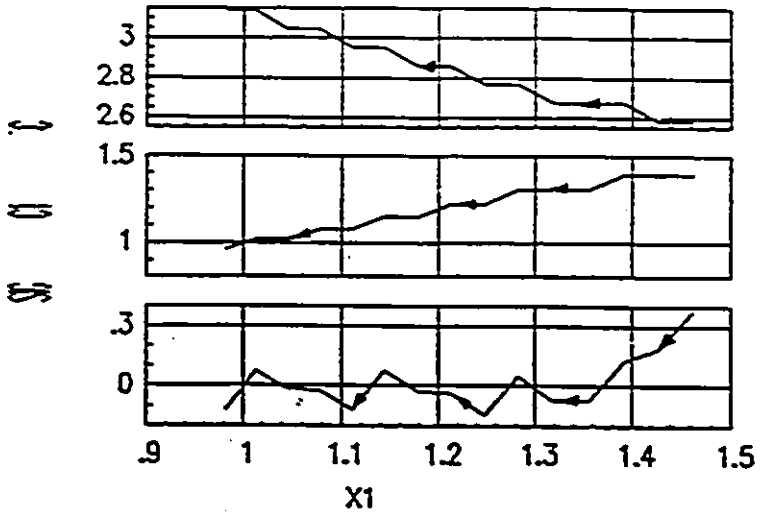

Figure III.2-5 c,c1,s versus $x_1(t)$ (detail rectangle A'-A').

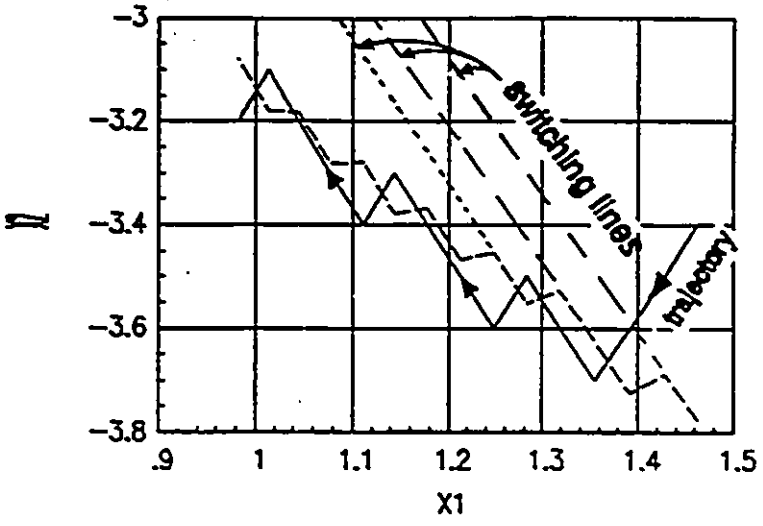

Figure III.2-6 Phase plane representation of the trajectory (detail rectangle A-A).

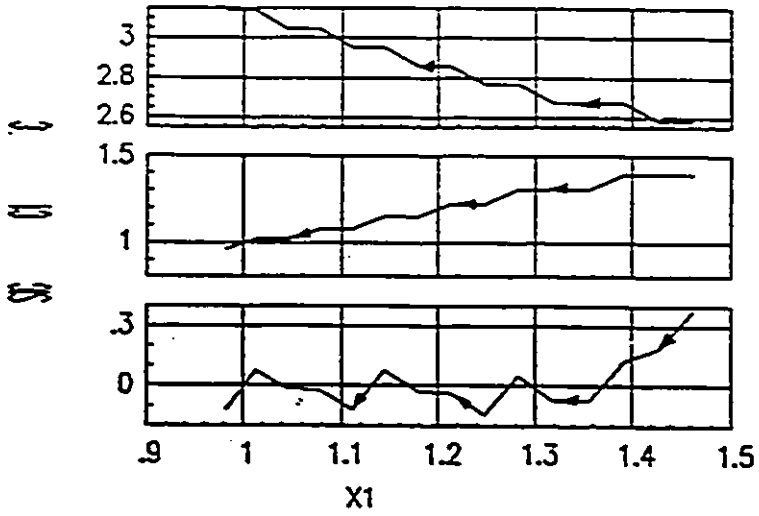

Figure III.2-5 c,c1,s versus $x_1(t)$ (detail rectangle A'-A').

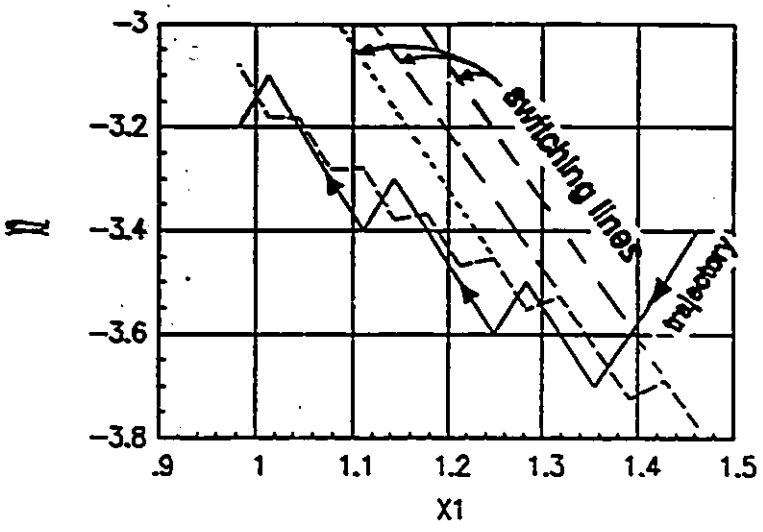

Figure III.2-6 Phase plane representation of the trajectory (detail rectangle A-A).

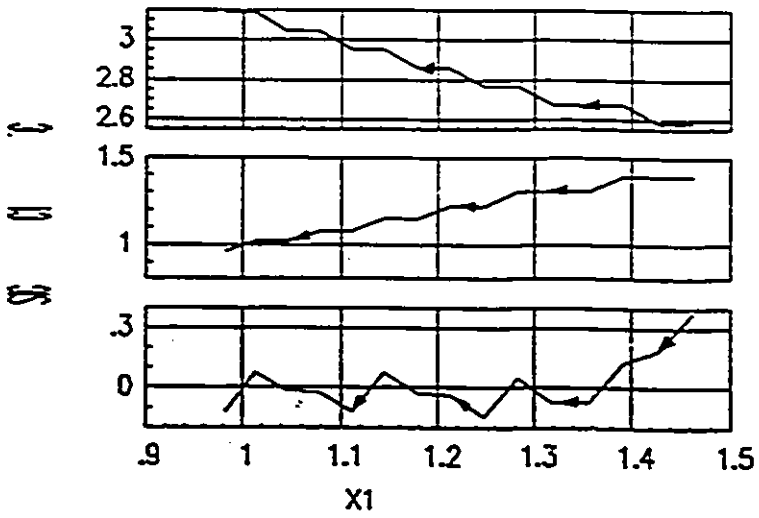

Figure III.2-5 c,c1,s versus $x_1(t)$ (detail rectangle A'-A').

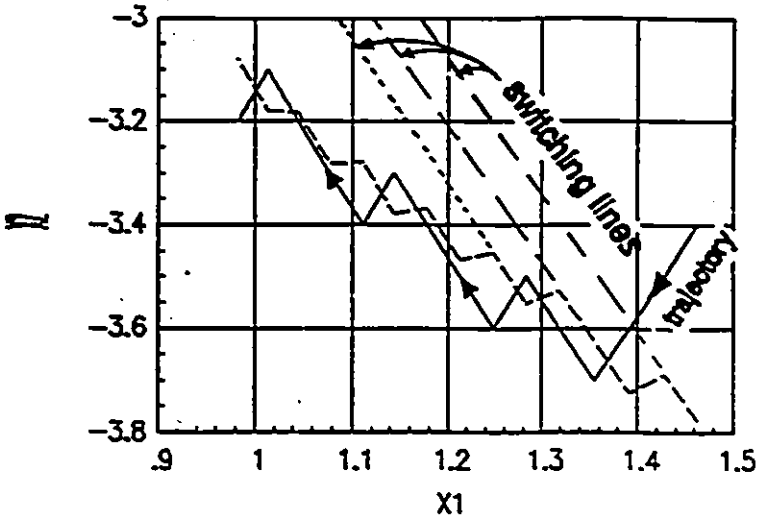

Figure III.2-6 Phase plane representation of the trajectory (detail rectangle A-A).

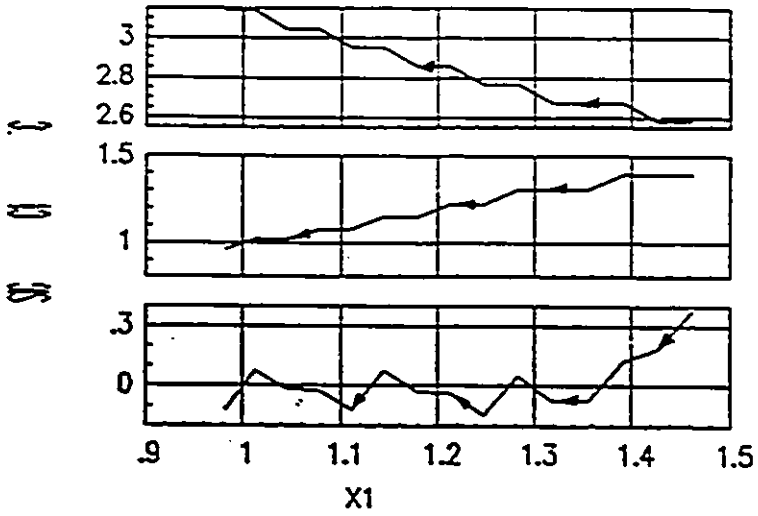

Figure III.2-5 c,c1,s versus $x_1(t)$ (detail rectangle A'-A').

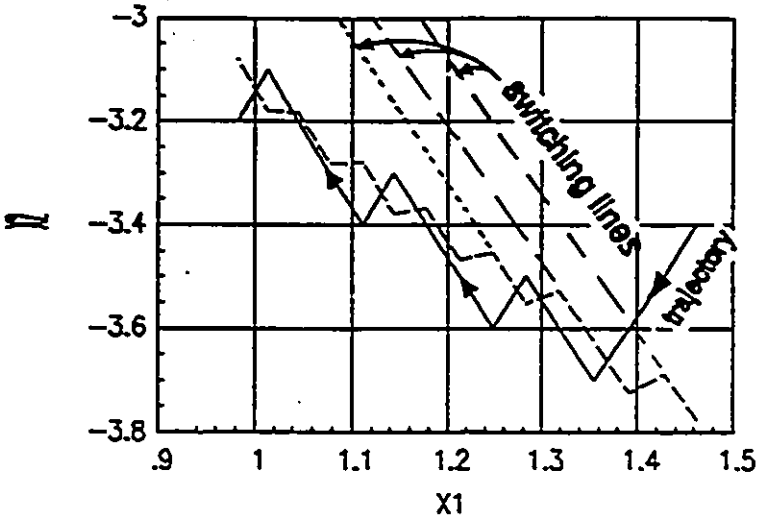

Figure III.2-6 Phase plane representation of the trajectory (detail rectangle A-A).

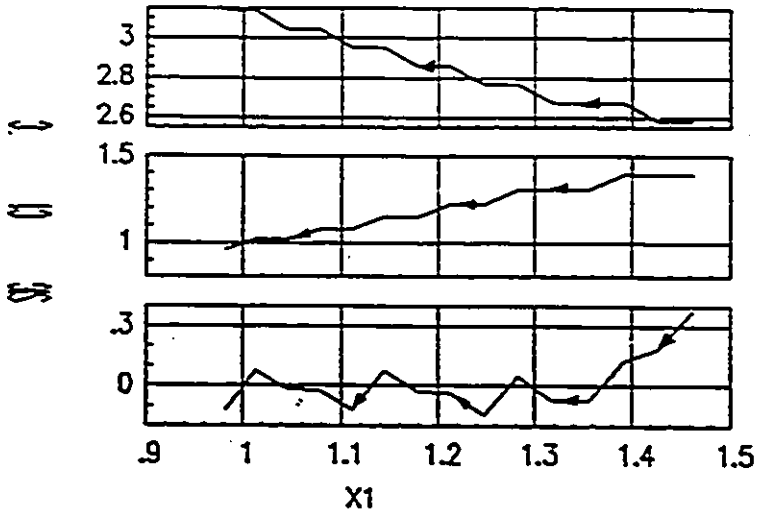

Figure III.2-5 c,c1,s versus $x_1(t)$ (detail rectangle A'-A').

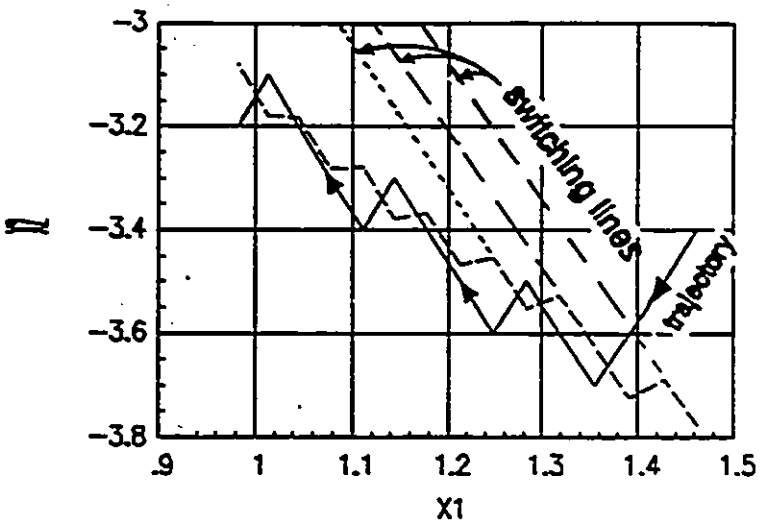

Figure III.2-6 Phase plane representation of the trajectory (detail rectangle A-A).

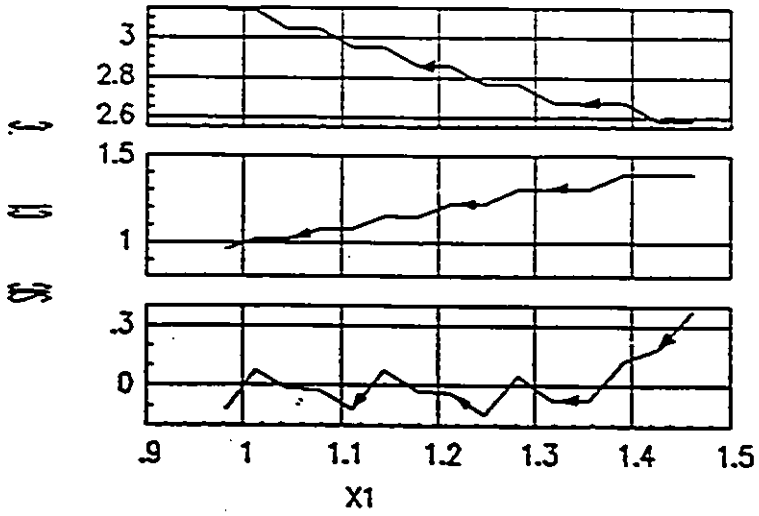

Figure III.2-5 c,c1,s versus $x_1(t)$ (detail rectangle A'-A').

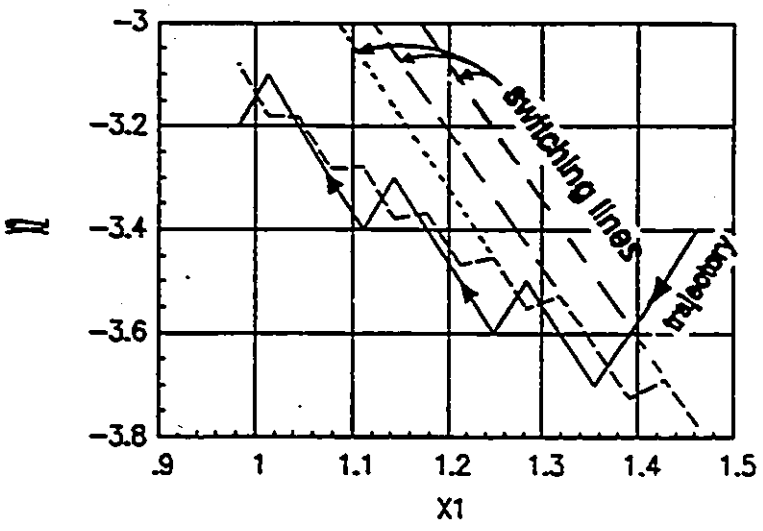

Figure III.2-6 Phase plane representation of the trajectory (detail rectangle A-A).

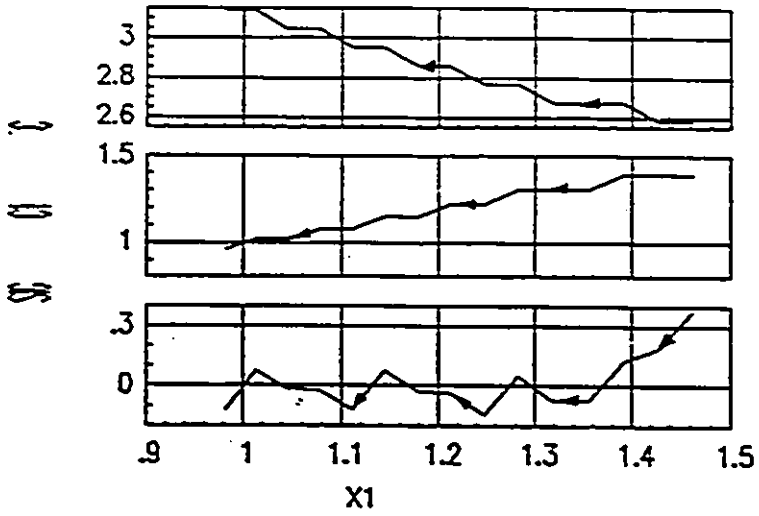

Figure III.2-5 c,c1,s versus $x_1(t)$ (detail rectangle A'-A').

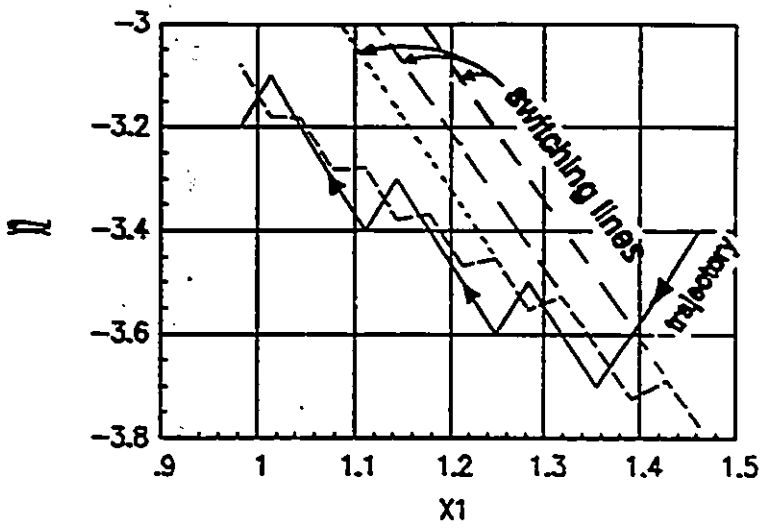

Figure III.2-6 Phase plane representation of the trajectory (detail rectangle A-A).

```
LD %2F,#00   ;REG. 2FH USED FOR THE T1 .1SEC COUNTER
LD %30,#00   ;REG. 30H, DIRECTION SENSOR [SET + DIRECTION]  FOR
          ;THE POSITIVE VOLTAGE [TABLE-A,SECTION IV.1.4]
LD %31,#20   ;AAA=20 AT REG. 31H,[THETA/U]=[AAA/S(S+BBB)]
LD %32,#1    ;BBB AT REG.32H
  ;REG. %33 IS IN USE DURING CALCULATIONS
LD %34,#00   ;CHECK SIGN REG. OF X2 AT REG. %25
LD %35,#00   ;CHECK SIGN REG. OF X1 AT REG. %21
  ; IN computations reg. 32H is not used
;   ********** MAIN PROGRAM **********
EI
CALL CALC
R4R4:
LD FLAGS,#00
CP %25,#00    ;TERMINATION CONDITION, checking reg. 25 [x1=0] in 1e-4 sec.
JP LE,R5R5
LD FLAGS,#00
CP %2F,#10   ;IF VALUE AT REG. 2FH <= 10
JP LE,R4R4   ;JUMP TO R4R4:
LD %2F,#00   ;ELSE, VALUE AT REG. 2FH=ZERO [Ts=.1SEC, T1=.01SEC]
CALL CALC    ;call function CALC
JP R4R4      ;TRY NEXT POINT
R5R5:
DI
LD TMR,#00
LD %F6,#0    ;STOP MOTOR, ENDED
LD %02,#140  ;OPEN PORT-2
OR %03,#%10  ;LATCH OPEN [P34='1']
IRET
;   ********** MAIN PROGRAM ENDED **********
;
;     [FUNCTIONS CALC, MUL, DIV, IRQ2, IRQ5;]
;
CALC:
;-------- X2 COMPUTATIONS ----------
LD %23,%22  ;X1(t-Ts) TO REG. %23
COM %23
INC %23     ;2'S COMPLEMENT OF REG. 23H
LD %21,%25  ;UPDATE X1
LD %34,#00
ADD %23,%21 ;X1(t)-X1(t-Ts) AT REG. %23
LD FLAGS,#00
CP %23,#00
JP GE,PLUS
COM %23
INC %23
```

```
LD %2F,#00   ;REG. 2FH USED FOR THE T1 .1SEC COUNTER
LD %30,#00   ;REG. 30H, DIRECTION SENSOR [SET + DIRECTION]  FOR
          ;THE POSITIVE VOLTAGE [TABLE-A,SECTION IV.1.4]
LD %31,#20   ;AAA=20 AT REG. 31H,[THETA/U]=[AAA/S(S+BBB)]
LD %32,#1    ;BBB AT REG.32H
  ;REG. %33 IS IN USE DURING CALCULATIONS
LD %34,#00   ;CHECK SIGN REG. OF X2 AT REG. %25
LD %35,#00   ;CHECK SIGN REG. OF X1 AT REG. %21
 ; IN computations reg. 32H is not used
;   ********************* MAIN PROGRAM *********************
EI
CALL CALC
R4R4:
LD FLAGS,#00
CP %25,#00    ;TERMINATION CONDITION, checking reg. 25 [x1=0] in 1e-4 sec.
JP LE,R5R5
LD FLAGS,#00
CP %2F,#10   ;IF VALUE AT REG. 2FH <= 10
JP LE,R4R4   ;JUMP TO R4R4:
LD %2F,#00   ;ELSE, VALUE AT REG. 2FH=ZERO [Ts=.1SEC, T1=.01SEC]
CALL CALC    ;call function CALC
JP R4R4      ;TRY NEXT POINT
R5R5:
DI
LD TMR,#00
LD %F6,#0    ;STOP MOTOR, ENDED
LD %02,#140  ;OPEN PORT-2
OR %03,#%10  ;LATCH OPEN [P34='1']
IRET
;   ******************* MAIN PROGRAM ENDED *********************
;
;     [FUNCTIONS CALC, MUL, DIV, IRQ2, IRQ5;]
;
CALC:
;-------- X2 COMPUTATIONS ----------
LD %23,%22  ;X1(t-Ts) TO REG. %23
COM %23
INC %23     ;2'S COMPLEMENT OF REG. 23H
LD %21,%25  ;UPDATE X1
LD %34,#00
ADD %23,%21 ;X1(t)-X1(t-Ts) AT REG. %23
LD FLAGS,#00
CP %23,#00
JP GE,PLUS
COM %23
INC %23
```

```
LD %2F,#00   ;REG. 2FH USED FOR THE T1 .1SEC COUNTER
LD %30,#00   ;REG. 30H, DIRECTION SENSOR [SET + DIRECTION]  FOR
          ;THE POSITIVE VOLTAGE [TABLE-A,SECTION IV.1.4]
LD %31,#20   ;AAA=20 AT REG. 31H,[THETA/U]=[AAA/S(S+BBB)]
LD %32,#1    ;BBB AT REG.32H
  ;REG. %33 IS IN USE DURING CALCULATIONS
LD %34,#00   ;CHECK SIGN REG. OF X2 AT REG. %25
LD %35,#00   ;CHECK SIGN REG. OF X1 AT REG. %21
 ; IN computations reg. 32H is not used
;  ********** MAIN PROGRAM **********
EI
CALL CALC
R4R4:
LD FLAGS,#00
CP %25,#00    ;TERMINATION CONDITION, checking reg. 25 [x1=0] in 1e-4 sec.
JP LE,R5R5
LD FLAGS,#00
CP %2F,#10   ;IF VALUE AT REG. 2FH <= 10
JP LE,R4R4   ;JUMP TO R4R4:
LD %2F,#00   ;ELSE, VALUE AT REG. 2FH=ZERO [Ts=.1SEC, T1=.01SEC]
CALL CALC    ;call function CALC
JP R4R4      ;TRY NEXT POINT
R5R5:
DI
LD TMR,#00
LD %F6,#0    ;STOP MOTOR, ENDED
LD %02,#140  ;OPEN PORT-2
OR %03,#%10  ;LATCH OPEN [P34='1']
IRET
;   ********** MAIN PROGRAM ENDED **********
;
;     [FUNCTIONS CALC, MUL, DIV, IRQ2, IRQ5;]
;
CALC:
;-------- X2 COMPUTATIONS ----------
LD %23,%22  ;X1(t-Ts) TO REG. %23
COM %23
INC %23     ;2'S COMPLEMENT OF REG. 23H
LD %21,%25  ;UPDATE X1
LD %34,#00
ADD %23,%21 ;X1(t)-X1(t-Ts) AT REG. %23
LD FLAGS,#00
CP %23,#00
JP GE,PLUS
COM %23
INC %23
```

```
LD %2F,#00   ;REG. 2FH USED FOR THE T1 .1SEC COUNTER
LD %30,#00   ;REG. 30H, DIRECTION SENSOR [SET + DIRECTION]  FOR
          ;THE POSITIVE VOLTAGE [TABLE-A,SECTION IV.1.4]
LD %31,#20   ;AAA=20 AT REG. 31H,[THETA/U]=[AAA/S(S+BBB)]
LD %32,#1    ;BBB AT REG.32H
  ;REG. %33 IS IN USE DURING CALCULATIONS
LD %34,#00   ;CHECK SIGN REG. OF X2 AT REG. %23
LD %35,#00   ;CHECK SIGN REG. OF X1 AT REG. %21
 ; IN computations reg. 32H is not used
;   ********** MAIN PROGRAM **********
EI
CALL CALC
R4R4:
LD FLAGS,#00
CP %25,#00    ;TERMINATION CONDITION, checking reg. 25 [x1=0] in 1e-4 sec.
JP LE,R5R5
LD FLAGS,#00
CP %2F,#10   ;IF VALUE AT REG. 2FH <= 10
JP LE,R4R4   ;JUMP TO R4R4:
LD %2F,#00   ;ELSE, VALUE AT REG. 2FH=ZERO [Ts=.1SEC, T1=.01SEC]
CALL CALC    ;call function CALC
JP R4R4      ;TRY NEXT POINT
R5R5:
DI
LD TMR,#00
LD %F6,#0    ;STOP MOTOR, ENDED
LD %02,#140  ;OPEN PORT-2
OR %03,#%10  ;LATCH OPEN [P34='1']
IRET
;   ********** MAIN PROGRAM ENDED **********
;
;     [FUNCTIONS CALC, MUL, DIV, IRQ2, IRQ5;]
;
CALC:
;-------- X2 COMPUTATIONS ----------
LD %23,%22  ;X1(t-Ts) TO REG. %23
COM %23
INC %23     ;2'S COMPLEMENT OF REG. 23H
LD %21,%25  ;UPDATE X1
LD %34,#00
ADD %23,%21 ;X1(t)-X1(t-Ts) AT REG. %23
LD FLAGS,#00
CP %23,#00
JP GE,PLUS
COM %23
INC %23
```

```
LD %2F,#00   ;REG. 2FH USED FOR THE T1 .1SEC COUNTER
LD %30,#00   ;REG. 30H, DIRECTION SENSOR [SET + DIRECTION]  FOR
          ;THE POSITIVE VOLTAGE [TABLE-A,SECTION IV.1.4]
LD %31,#20   ;AAA=20 AT REG. 31H,[THETA/U]=[AAA/S(S+BBB)]
LD %32,#1    ;BBB AT REG.32H
  ;REG. %33 IS IN USE DURING CALCULATIONS
LD %34,#00   ;CHECK SIGN REG. OF X2 AT REG. %23
LD %35,#00   ;CHECK SIGN REG. OF X1 AT REG. %21
 ; IN computations reg. 32H is not used
;   ********** MAIN PROGRAM **********
EI
CALL CALC
R4R4:
LD FLAGS,#00
CP %25,#00    ;TERMINATION CONDITION, checking reg. 25 [x1=0] in 1e-4 sec.
JP LE,R5R5
LD FLAGS,#00
CP %2F,#10   ;IF VALUE AT REG. 2FH <= 10
JP LE,R4R4   ;JUMP TO R4R4:
LD %2F,#00   ;ELSE, VALUE AT REG. 2FH=ZERO [Ts=.1SEC, T1=.01SEC]
CALL CALC    ;call function CALC
JP R4R4      ;TRY NEXT POINT
R5R5:
DI
LD TMR,#00
LD %F6,#0    ;STOP MOTOR, ENDED
LD %02,#140  ;OPEN PORT-2
OR %03,#%10  ;LATCH OPEN [P34='1']
IRET
;   ********** MAIN PROGRAM ENDED **********
;
;     [FUNCTIONS CALC, MUL, DIV, IRQ2, IRQ5;]
;
CALC:
;-------- X2 COMPUTATIONS ----------
LD %23,%22  ;X1(t-Ts) TO REG. %23
COM %23
INC %23     ;2'S COMPLEMENT OF REG. 23H
LD %21,%25  ;UPDATE X1
LD %34,#00
ADD %23,%21 ;X1(t)-X1(t-Ts) AT REG. %23
LD FLAGS,#00
CP %23,#00
JP GE,PLUS
COM %23
INC %23
```

```
LD %2F,#00   ;REG. 2FH USED FOR THE T1 .1SEC COUNTER
LD %30,#00   ;REG. 30H, DIRECTION SENSOR [SET + DIRECTION]  FOR
          ;THE POSITIVE VOLTAGE [TABLE-A,SECTION IV.1.4]
LD %31,#20   ;AAA=20 AT REG. 31H,[THETA/U]=[AAA/S(S+BBB)]
LD %32,#1    ;BBB AT REG.32H
  ;REG. %33 IS IN USE DURING CALCULATIONS
LD %34,#00   ;CHECK SIGN REG. OF X2 AT REG. %25
LD %35,#00   ;CHECK SIGN REG. OF X1 AT REG. %21
 ; IN computations reg. 32H is not used
;   ********** MAIN PROGRAM **********
EI
CALL CALC
R4R4:
LD FLAGS,#00
CP %25,#00    ;TERMINATION CONDITION, checking reg. 25 [x1=0] in 1e-4 sec.
JP LE,R5R5
LD FLAGS,#00
CP %2F,#10   ;IF VALUE AT REG. 2FH <= 10
JP LE,R4R4   ;JUMP TO R4R4:
LD %2F,#00   ;ELSE, VALUE AT REG. 2FH=ZERO [Ts=.1SEC, T1=.01SEC]
CALL CALC    ;call function CALC
JP R4R4      ;TRY NEXT POINT
R5R5:
DI
LD TMR,#00
LD %F6,#0    ;STOP MOTOR, ENDED
LD %02,#140  ;OPEN PORT-2
OR %03,#%10  ;LATCH OPEN [P34='1']
IRET
;   ********** MAIN PROGRAM ENDED **********
;
;     [FUNCTIONS CALC, MUL, DIV, IRQ2, IRQ5;]
;
CALC:
;-------- X2 COMPUTATIONS ----------
LD %23,%22  ;X1(t-Ts) TO REG. %23
COM %23
INC %23     ;2'S COMPLEMENT OF REG. 23H
LD %21,%25  ;UPDATE X1
LD %34,#00
ADD %23,%21 ;X1(t)-X1(t-Ts) AT REG. %23
LD FLAGS,#00
CP %23,#00
JP GE,PLUS
COM %23
INC %23
```

```
LD %2F,#00   ;REG. 2FH USED FOR THE T1 .1SEC COUNTER
LD %30,#00   ;REG. 30H, DIRECTION SENSOR [SET + DIRECTION]  FOR
          ;THE POSITIVE VOLTAGE [TABLE-A,SECTION IV.1.4]
LD %31,#20   ;AAA=20 AT REG. 31H,[THETA/U]=[AAA/S(S+BBB)]
LD %32,#1    ;BBB AT REG.32H
  ;REG. %33 IS IN USE DURING CALCULATIONS
LD %34,#00   ;CHECK SIGN REG. OF X2 AT REG. %23
LD %35,#00   ;CHECK SIGN REG. OF X1 AT REG. %21
 ; IN computations reg. 32H is not used
;  ********** MAIN PROGRAM **********
EI
CALL CALC
R4R4:
LD FLAGS,#00
CP %25,#00    ;TERMINATION CONDITION, checking reg. 25 [x1=0] in 1e-4 sec.
JP LE,R5R5
LD FLAGS,#00
CP %2F,#10   ;IF VALUE AT REG. 2FH <= 10
JP LE,R4R4   ;JUMP TO R4R4:
LD %2F,#00   ;ELSE, VALUE AT REG. 2FH=ZERO [Ts=.1SEC, T1=.01SEC]
CALL CALC    ;call function CALC
JP R4R4      ;TRY NEXT POINT
R5R5:
DI
LD TMR,#00
LD %F6,#0    ;STOP MOTOR, ENDED
LD %02,#140  ;OPEN PORT-2
OR %03,#%10  ;LATCH OPEN [P34='1']
IRET
;   ********** MAIN PROGRAM ENDED **********
;
;     [FUNCTIONS CALC, MUL, DIV, IRQ2, IRQ5;]
;
CALC:
;-------- X2 COMPUTATIONS ----------
LD %23,%22  ;X1(t-Ts) TO REG. %23
COM %23
INC %23     ;2'S COMPLEMENT OF REG. 23H
LD %21,%25  ;UPDATE X1
LD %34,#00
ADD %23,%21 ;X1(t)-X1(t-Ts) AT REG. %23
LD FLAGS,#00
CP %23,#00
JP GE,PLUS
COM %23
INC %23
```

```
LD %2F,#00   ;REG. 2FH USED FOR THE T1 .1SEC COUNTER
LD %30,#00   ;REG. 30H, DIRECTION SENSOR [SET + DIRECTION]  FOR
          ;THE POSITIVE VOLTAGE [TABLE-A,SECTION IV.1.4]
LD %31,#20   ;AAA=20 AT REG. 31H,[THETA/U]=[AAA/S(S+BBB)]
LD %32,#1    ;BBB AT REG.32H
  ;REG. %33 IS IN USE DURING CALCULATIONS
LD %34,#00   ;CHECK SIGN REG. OF X2 AT REG. %23
LD %35,#00   ;CHECK SIGN REG. OF X1 AT REG. %21
 ; IN computations reg. 32H is not used
;   ********** MAIN PROGRAM **********
EI
CALL CALC
R4R4:
LD FLAGS,#00
CP %25,#00    ;TERMINATION CONDITION, checking reg. 25 [x1=0] in 1e-4 sec.
JP LE,R5R5
LD FLAGS,#00
CP %2F,#10   ;IF VALUE AT REG. 2FH <= 10
JP LE,R4R4   ;JUMP TO R4R4:
LD %2F,#00   ;ELSE, VALUE AT REG. 2FH=ZERO [Ts=.1SEC, T1=.01SEC]
CALL CALC    ;call function CALC
JP R4R4      ;TRY NEXT POINT
R5R5:
DI
LD TMR,#00
LD %F6,#0    ;STOP MOTOR, ENDED
LD %02,#140  ;OPEN PORT-2
OR %03,#%10  ;LATCH OPEN [P34='1']
IRET
;   ********** MAIN PROGRAM ENDED **********
;
;     [FUNCTIONS CALC, MUL, DIV, IRQ2, IRQ5;]
;
CALC:
;-------- X2 COMPUTATIONS ----------
LD %23,%22  ;X1(t-Ts) TO REG. %23
COM %23
INC %23     ;2'S COMPLEMENT OF REG. 23H
LD %21,%25  ;UPDATE X1
LD %34,#00
ADD %23,%21 ;X1(t)-X1(t-Ts) AT REG. %23
LD FLAGS,#00
CP %23,#00
JP GE,PLUS
COM %23
INC %23
```

```
LD %2F,#00   ;REG. 2FH USED FOR THE T1 .1SEC COUNTER
LD %30,#00   ;REG. 30H, DIRECTION SENSOR [SET + DIRECTION]  FOR
          ;THE POSITIVE VOLTAGE [TABLE-A,SECTION IV.1.4]
LD %31,#20   ;AAA=20 AT REG. 31H,[THETA/U]=[AAA/S(S+BBB)]
LD %32,#1    ;BBB AT REG.32H
  ;REG. %33 IS IN USE DURING CALCULATIONS
LD %34,#00   ;CHECK SIGN REG. OF X2 AT REG. %23
LD %35,#00   ;CHECK SIGN REG. OF X1 AT REG. %21
 ; IN computations reg. 32H is not used
;   ********** MAIN PROGRAM **********
EI
CALL CALC
R4R4:
LD FLAGS,#00
CP %25,#00    ;TERMINATION CONDITION, checking reg. 25 [x1=0] in 1e-4 sec.
JP LE,R5R5
LD FLAGS,#00
CP %2F,#10   ;IF VALUE AT REG. 2FH <= 10
JP LE,R4R4   ;JUMP TO R4R4:
LD %2F,#00   ;ELSE, VALUE AT REG. 2FH=ZERO [Ts=.1SEC, T1=.01SEC]
CALL CALC    ;call function CALC
JP R4R4      ;TRY NEXT POINT
R5R5:
DI
LD TMR,#00
LD %F6,#0    ;STOP MOTOR, ENDED
LD %02,#140  ;OPEN PORT-2
OR %03,#%10  ;LATCH OPEN [P34='1']
IRET
;   ********** MAIN PROGRAM ENDED **********
;
;     [FUNCTIONS CALC, MUL, DIV, IRQ2, IRQ5;]
;
CALC:
;-------- X2 COMPUTATIONS ----------
LD %23,%22  ;X1(t-Ts) TO REG. %23
COM %23
INC %23     ;2'S COMPLEMENT OF REG. 23H
LD %21,%25  ;UPDATE X1
LD %34,#00
ADD %23,%21 ;X1(t)-X1(t-Ts) AT REG. %23
LD FLAGS,#00
CP %23,#00
JP GE,PLUS
COM %23
INC %23
```

```
LD %2F,#00   ;REG. 2FH USED FOR THE T1 .1SEC COUNTER
LD %30,#00   ;REG. 30H, DIRECTION SENSOR [SET + DIRECTION]  FOR
          ;THE POSITIVE VOLTAGE [TABLE-A,SECTION IV.1.4]
LD %31,#20   ;AAA=20 AT REG. 31H,[THETA/U]=[AAA/S(S+BBB)]
LD %32,#1    ;BBB AT REG.32H
  ;REG. %33 IS IN USE DURING CALCULATIONS
LD %34,#00   ;CHECK SIGN REG. OF X2 AT REG. %23
LD %35,#00   ;CHECK SIGN REG. OF X1 AT REG. %21
 ; IN computations reg. 32H is not used
;   ********** MAIN PROGRAM **********
EI
CALL CALC
R4R4:
LD FLAGS,#00
CP %25,#00    ;TERMINATION CONDITION, checking reg. 25 [x1=0] in 1e-4 sec.
JP LE,R5R5
LD FLAGS,#00
CP %2F,#10   ;IF VALUE AT REG. 2FH <= 10
JP LE,R4R4   ;JUMP TO R4R4:
LD %2F,#00   ;ELSE, VALUE AT REG. 2FH=ZERO [Ts=.1SEC, T1=.01SEC]
CALL CALC    ;call function CALC
JP R4R4      ;TRY NEXT POINT
R5R5:
DI
LD TMR,#00
LD %F6,#0    ;STOP MOTOR, ENDED
LD %02,#140  ;OPEN PORT-2
OR %03,#%10  ;LATCH OPEN [P34='1']
IRET
;   ********** MAIN PROGRAM ENDED **********
;
;     [FUNCTIONS CALC, MUL, DIV, IRQ2, IRQ5;]
;
CALC:
;-------- X2 COMPUTATIONS ----------
LD %23,%22  ;X1(t-Ts) TO REG. %23
COM %23
INC %23     ;2'S COMPLEMENT OF REG. 23H
LD %21,%25  ;UPDATE X1
LD %34,#00
ADD %23,%21 ;X1(t)-X1(t-Ts) AT REG. %23
LD FLAGS,#00
CP %23,#00
JP GE,PLUS
COM %23
INC %23
```

```
LD %2F,#00   ;REG. 2FH USED FOR THE T1 .1SEC COUNTER
LD %30,#00   ;REG. 30H, DIRECTION SENSOR [SET + DIRECTION]  FOR
          ;THE POSITIVE VOLTAGE [TABLE-A,SECTION IV.1.4]
LD %31,#20   ;AAA=20 AT REG. 31H,[THETA/U]=[AAA/S(S+BBB)]
LD %32,#1    ;BBB AT REG.32H
  ;REG. %33 IS IN USE DURING CALCULATIONS
LD %34,#00   ;CHECK SIGN REG. OF X2 AT REG. %25
LD %35,#00   ;CHECK SIGN REG. OF X1 AT REG. %21
 ; IN computations reg. 32H is not used
;  ********** MAIN PROGRAM **********
EI
CALL CALC
R4R4:
LD FLAGS,#00
CP %25,#00    ;TERMINATION CONDITION, checking reg. 25 [x1=0] in 1e-4 sec.
JP LE,R5R5
LD FLAGS,#00
CP %2F,#10   ;IF VALUE AT REG. 2FH <= 10
JP LE,R4R4   ;JUMP TO R4R4:
LD %2F,#00   ;ELSE, VALUE AT REG. 2FH=ZERO [Ts=.1SEC, T1=.01SEC]
CALL CALC    ;call function CALC
JP R4R4      ;TRY NEXT POINT
R5R5:
DI
LD TMR,#00
LD %F6,#0    ;STOP MOTOR, ENDED
LD %02,#140  ;OPEN PORT-2
OR %03,#%10  ;LATCH OPEN [P34='1']
IRET
;   ********** MAIN PROGRAM ENDED **********
;
;     [FUNCTIONS CALC, MUL, DIV, IRQ2, IRQ5;]
;
CALC:
;-------- X2 COMPUTATIONS ----------
LD %23,%22  ;X1(t-Ts) TO REG. %23
COM %23
INC %23     ;2'S COMPLEMENT OF REG. 23H
LD %21,%25  ;UPDATE X1
LD %34,#00
ADD %23,%21 ;X1(t)-X1(t-Ts) AT REG. %23
LD FLAGS,#00
CP %23,#00
JP GE,PLUS
COM %23
INC %23
```

```
LD %2F,#00   ;REG. 2FH USED FOR THE T1 .1SEC COUNTER
LD %30,#00   ;REG. 30H, DIRECTION SENSOR [SET + DIRECTION]  FOR
          ;THE POSITIVE VOLTAGE [TABLE-A,SECTION IV.1.4]
LD %31,#20   ;AAA=20 AT REG. 31H,[THETA/U]=[AAA/S(S+BBB)]
LD %32,#1    ;BBB AT REG.32H
  ;REG. %33 IS IN USE DURING CALCULATIONS
LD %34,#00   ;CHECK SIGN REG. OF X2 AT REG. %25
LD %35,#00   ;CHECK SIGN REG. OF X1 AT REG. %21
  ; IN computations reg. 32H is not used
;   ********************* MAIN PROGRAM *********************
EI
CALL CALC
R4R4:
LD FLAGS,#00
CP %25,#00    ;TERMINATION CONDITION, checking reg. 25 [x1=0] in 1e-4 sec.
JP LE,R5R5
LD FLAGS,#00
CP %2F,#10   ;IF VALUE AT REG. 2FH <= 10
JP LE,R4R4   ;JUMP TO R4R4:
LD %2F,#00   ;ELSE, VALUE AT REG. 2FH=ZERO [Ts=.1SEC, T1=.01SEC]
CALL CALC    ;call function CALC
JP R4R4      ;TRY NEXT POINT
R5R5:
DI
LD TMR,#00
LD %F6,#0    ;STOP MOTOR, ENDED
LD %02,#140  ;OPEN PORT-2
OR %03,#%10  ;LATCH OPEN [P34='1']
IRET
;   ******************* MAIN PROGRAM ENDED *********************
;
;     [FUNCTIONS CALC, MUL, DIV, IRQ2, IRQ5;]
;
CALC:
;------- X2 COMPUTATIONS ------------
LD %23,%22  ;X1(t-Ts) TO REG. %23
COM %23
INC %23     ;2'S COMPLEMENT OF REG. 23H
LD %21,%25  ;UPDATE X1
LD %34,#00
ADD %23,%21 ;X1(t)-X1(t-Ts) AT REG. %23
LD FLAGS,#00
CP %23,#00
JP GE,PLUS
COM %23
INC %23
```

```
LD %2F,#00   ;REG. 2FH USED FOR THE T1 .1SEC COUNTER
LD %30,#00   ;REG. 30H, DIRECTION SENSOR [SET + DIRECTION]  FOR
          ;THE POSITIVE VOLTAGE [TABLE-A,SECTION IV.1.4]
LD %31,#20   ;AAA=20 AT REG. 31H,[THETA/U]=[AAA/S(S+BBB)]
LD %32,#1    ;BBB AT REG.32H
  ;REG. %33 IS IN USE DURING CALCULATIONS
LD %34,#00   ;CHECK SIGN REG. OF X2 AT REG. %25
LD %35,#00   ;CHECK SIGN REG. OF X1 AT REG. %21
 ; IN computations reg. 32H is not used
;   ********** MAIN PROGRAM **********
EI
CALL CALC
R4R4:
LD FLAGS,#00
CP %25,#00    ;TERMINATION CONDITION, checking reg. 25 [x1=0] in 1e-4 sec.
JP LE,R5R5
LD FLAGS,#00
CP %2F,#10   ;IF VALUE AT REG. 2FH <= 10
JP LE,R4R4   ;JUMP TO R4R4:
LD %2F,#00   ;ELSE, VALUE AT REG. 2FH=ZERO [Ts=.1SEC, T1=.01SEC]
CALL CALC    ;call function CALC
JP R4R4      ;TRY NEXT POINT
R5R5:
DI
LD TMR,#00
LD %F6,#0    ;STOP MOTOR, ENDED
LD %02,#140  ;OPEN PORT-2
OR %03,#%10  ;LATCH OPEN [P34='1']
IRET
;   ********** MAIN PROGRAM ENDED **********
;
;     [FUNCTIONS CALC, MUL, DIV, IRQ2, IRQ5;]
;
CALC:
;-------- X2 COMPUTATIONS ----------
LD %23,%22  ;X1(t-Ts) TO REG. %23
COM %23
INC %23     ;2'S COMPLEMENT OF REG. 23H
LD %21,%25  ;UPDATE X1
LD %34,#00
ADD %23,%21 ;X1(t)-X1(t-Ts) AT REG. %23
LD FLAGS,#00
CP %23,#00
JP GE,PLUS
COM %23
INC %23
```

```
LD %2F,#00   ;REG. 2FH USED FOR THE T1 .1SEC COUNTER
LD %30,#00   ;REG. 30H, DIRECTION SENSOR [SET + DIRECTION]  FOR
          ;THE POSITIVE VOLTAGE [TABLE-A,SECTION IV.1.4]
LD %31,#20   ;AAA=20 AT REG. 31H,[THETA/U]=[AAA/S(S+BBB)]
LD %32,#1    ;BBB AT REG.32H
  ;REG. %33 IS IN USE DURING CALCULATIONS
LD %34,#00   ;CHECK SIGN REG. OF X2 AT REG. %25
LD %35,#00   ;CHECK SIGN REG. OF X1 AT REG. %21
 ; IN computations reg. 32H is not used
;   ********** MAIN PROGRAM **********
EI
CALL CALC
R4R4:
LD FLAGS,#00
CP %25,#00    ;TERMINATION CONDITION, checking reg. 25 [x1=0] in 1e-4 sec.
JP LE,R5R5
LD FLAGS,#00
CP %2F,#10   ;IF VALUE AT REG. 2FH <= 10
JP LE,R4R4   ;JUMP TO R4R4:
LD %2F,#00   ;ELSE, VALUE AT REG. 2FH=ZERO [Ts=.1SEC, T1=.01SEC]
CALL CALC    ;call function CALC
JP R4R4      ;TRY NEXT POINT
R5R5:
DI
LD TMR,#00
LD %F6,#0    ;STOP MOTOR, ENDED
LD %02,#140  ;OPEN PORT-2
OR %03,#%10  ;LATCH OPEN [P34='1']
IRET
;   ********** MAIN PROGRAM ENDED **********
;
;     [FUNCTIONS CALC, MUL, DIV, IRQ2, IRQ5;]
;
CALC:
;-------- X2 COMPUTATIONS ----------
LD %23,%22  ;X1(t-Ts) TO REG. %23
COM %23
INC %23     ;2'S COMPLEMENT OF REG. 23H
LD %21,%25  ;UPDATE X1
LD %34,#00
ADD %23,%21 ;X1(t)-X1(t-Ts) AT REG. %23
LD FLAGS,#00
CP %23,#00
JP GE,PLUS
COM %23
INC %23
```

```
LD %2F,#00   ;REG. 2FH USED FOR THE T1 .1SEC COUNTER
LD %30,#00   ;REG. 30H, DIRECTION SENSOR [SET + DIRECTION]  FOR
          ;THE POSITIVE VOLTAGE [TABLE-A,SECTION IV.1.4]
LD %31,#20   ;AAA=20 AT REG. 31H,[THETA/U]=[AAA/S(S+BBB)]
LD %32,#1    ;BBB AT REG.32H
  ;REG. %33 IS IN USE DURING CALCULATIONS
LD %34,#00   ;CHECK SIGN REG. OF X2 AT REG. %25
LD %35,#00   ;CHECK SIGN REG. OF X1 AT REG. %21
 ; IN computations reg. 32H is not used
;   ********** MAIN PROGRAM **********
EI
CALL CALC
R4R4:
LD FLAGS,#00
CP %25,#00    ;TERMINATION CONDITION, checking reg. 25 [x1=0] in 1e-4 sec.
JP LE,R5R5
LD FLAGS,#00
CP %2F,#10   ;IF VALUE AT REG. 2FH <= 10
JP LE,R4R4   ;JUMP TO R4R4:
LD %2F,#00   ;ELSE, VALUE AT REG. 2FH=ZERO [Ts=.1SEC, T1=.01SEC]
CALL CALC    ;call function CALC
JP R4R4      ;TRY NEXT POINT
R5R5:
DI
LD TMR,#00
LD %F6,#0    ;STOP MOTOR, ENDED
LD %02,#140  ;OPEN PORT-2
OR %03,#%10  ;LATCH OPEN [P34='1']
IRET
;   ********** MAIN PROGRAM ENDED **********
;
;     [FUNCTIONS CALC, MUL, DIV, IRQ2, IRQ5;]
;
CALC:
;-------- X2 COMPUTATIONS ----------
LD %23,%22  ;X1(t-Ts) TO REG. %23
COM %23
INC %23     ;2'S COMPLEMENT OF REG. 23H
LD %21,%25  ;UPDATE X1
LD %34,#00
ADD %23,%21 ;X1(t)-X1(t-Ts) AT REG. %23
LD FLAGS,#00
CP %23,#00
JP GE,PLUS
COM %23
INC %23
```

```
LD %2F,#00   ;REG. 2FH USED FOR THE T1 .1SEC COUNTER
LD %30,#00   ;REG. 30H, DIRECTION SENSOR [SET + DIRECTION]  FOR
          ;THE POSITIVE VOLTAGE [TABLE-A,SECTION IV.1.4]
LD %31,#20   ;AAA=20 AT REG. 31H,[THETA/U]=[AAA/S(S+BBB)]
LD %32,#1    ;BBB AT REG.32H
  ;REG. %33 IS IN USE DURING CALCULATIONS
LD %34,#00   ;CHECK SIGN REG. OF X2 AT REG. %23
LD %35,#00   ;CHECK SIGN REG. OF X1 AT REG. %21
 ; IN computations reg. 32H is not used
;  ********** MAIN PROGRAM **********
EI
CALL CALC
R4R4:
LD FLAGS,#00
CP %25,#00    ;TERMINATION CONDITION, checking reg. 25 [x1=0] in 1e-4 sec.
JP LE,R5R5
LD FLAGS,#00
CP %2F,#10   ;IF VALUE AT REG. 2FH <= 10
JP LE,R4R4   ;JUMP TO R4R4:
LD %2F,#00   ;ELSE, VALUE AT REG. 2FH=ZERO [Ts=.1SEC, T1=.01SEC]
CALL CALC    ;call function CALC
JP R4R4      ;TRY NEXT POINT
R5R5:
DI
LD TMR,#00
LD %F6,#0    ;STOP MOTOR, ENDED
LD %02,#140  ;OPEN PORT-2
OR %03,#%10  ;LATCH OPEN [P34='1']
IRET
;   ********** MAIN PROGRAM ENDED **********
;
;     [FUNCTIONS CALC, MUL, DIV, IRQ2, IRQ5;]
;
CALC:
;-------- X2 COMPUTATIONS ----------
LD %23,%22  ;X1(t-Ts) TO REG. %23
COM %23
INC %23     ;2'S COMPLEMENT OF REG. 23H
LD %21,%25  ;UPDATE X1
LD %34,#00
ADD %23,%21 ;X1(t)-X1(t-Ts) AT REG. %23
LD FLAGS,#00
CP %23,#00
JP GE,PLUS
COM %23
INC %23
```

```
LD %2F,#00   ;REG. 2FH USED FOR THE T1 .1SEC COUNTER
LD %30,#00   ;REG. 30H, DIRECTION SENSOR [SET + DIRECTION]  FOR
          ;THE POSITIVE VOLTAGE [TABLE-A,SECTION IV.1.4]
LD %31,#20   ;AAA=20 AT REG. 31H,[THETA/U]=[AAA/S(S+BBB)]
LD %32,#1    ;BBB AT REG.32H
  ;REG. %33 IS IN USE DURING CALCULATIONS
LD %34,#00   ;CHECK SIGN REG. OF X2 AT REG. %23
LD %35,#00   ;CHECK SIGN REG. OF X1 AT REG. %21
 ; IN computations reg. 32H is not used
;   ********** MAIN PROGRAM **********
EI
CALL CALC
R4R4:
LD FLAGS,#00
CP %25,#00    ;TERMINATION CONDITION, checking reg. 25 [x1=0] in 1e-4 sec.
JP LE,R5R5
LD FLAGS,#00
CP %2F,#10   ;IF VALUE AT REG. 2FH <= 10
JP LE,R4R4   ;JUMP TO R4R4:
LD %2F,#00   ;ELSE, VALUE AT REG. 2FH=ZERO [Ts=.1SEC, T1=.01SEC]
CALL CALC    ;call function CALC
JP R4R4      ;TRY NEXT POINT
R5R5:
DI
LD TMR,#00
LD %F6,#0    ;STOP MOTOR, ENDED
LD %02,#140  ;OPEN PORT-2
OR %03,#%10  ;LATCH OPEN [P34='1']
IRET
;   ********** MAIN PROGRAM ENDED **********
;
;     [FUNCTIONS CALC, MUL, DIV, IRQ2, IRQ5;]
;
CALC:
;-------- X2 COMPUTATIONS ----------
LD %23,%22  ;X1(t-Ts) TO REG. %23
COM %23
INC %23     ;2'S COMPLEMENT OF REG. 23H
LD %21,%25  ;UPDATE X1
LD %34,#00
ADD %23,%21 ;X1(t)-X1(t-Ts) AT REG. %23
LD FLAGS,#00
CP %23,#00
JP GE,PLUS
COM %23
INC %23
```

```
LD %2F,#00   ;REG. 2FH USED FOR THE T1 .1SEC COUNTER
LD %30,#00   ;REG. 30H, DIRECTION SENSOR [SET + DIRECTION]  FOR
          ;THE POSITIVE VOLTAGE [TABLE-A,SECTION IV.1.4]
LD %31,#20   ;AAA=20 AT REG. 31H,[THETA/U]=[AAA/S(S+BBB)]
LD %32,#1    ;BBB AT REG.32H
  ;REG. %33 IS IN USE DURING CALCULATIONS
LD %34,#00   ;CHECK SIGN REG. OF X2 AT REG. %25
LD %35,#00   ;CHECK SIGN REG. OF X1 AT REG. %21
 ; IN computations reg. 32H is not used
;   ********** MAIN PROGRAM **********
EI
CALL CALC
R4R4:
LD FLAGS,#00
CP %25,#00    ;TERMINATION CONDITION, checking reg. 25 [x1=0] in 1e-4 sec.
JP LE,R5R5
LD FLAGS,#00
CP %2F,#10   ;IF VALUE AT REG. 2FH <= 10
JP LE,R4R4   ;JUMP TO R4R4:
LD %2F,#00   ;ELSE, VALUE AT REG. 2FH=ZERO [Ts=.1SEC, T1=.01SEC]
CALL CALC    ;call function CALC
JP R4R4      ;TRY NEXT POINT
R5R5:
DI
LD TMR,#00
LD %F6,#0    ;STOP MOTOR, ENDED
LD %02,#140  ;OPEN PORT-2
OR %03,#%10  ;LATCH OPEN [P34='1']
IRET
;   ********** MAIN PROGRAM ENDED **********
;
;     [FUNCTIONS CALC, MUL, DIV, IRQ2, IRQ5;]
;
CALC:
;-------- X2 COMPUTATIONS ----------
LD %23,%22  ;X1(t-Ts) TO REG. %23
COM %23
INC %23     ;2'S COMPLEMENT OF REG. 23H
LD %21,%25  ;UPDATE X1
LD %34,#00
ADD %23,%21 ;X1(t)-X1(t-Ts) AT REG. %23
LD FLAGS,#00
CP %23,#00
JP GE,PLUS
COM %23
INC %23
```

```
LD %2F,#00   ;REG. 2FH USED FOR THE T1 .1SEC COUNTER
LD %30,#00   ;REG. 30H, DIRECTION SENSOR [SET + DIRECTION]  FOR
          ;THE POSITIVE VOLTAGE [TABLE-A,SECTION IV.1.4]
LD %31,#20   ;AAA=20 AT REG. 31H,[THETA/U]=[AAA/S(S+BBB)]
LD %32,#1    ;BBB AT REG.32H
  ;REG. %33 IS IN USE DURING CALCULATIONS
LD %34,#00   ;CHECK SIGN REG. OF X2 AT REG. %25
LD %35,#00   ;CHECK SIGN REG. OF X1 AT REG. %21
 ; IN computations reg. 32H is not used
;   ********** MAIN PROGRAM **********
EI
CALL CALC
R4R4:
LD FLAGS,#00
CP %25,#00    ;TERMINATION CONDITION, checking reg. 25 [x1=0] in 1e-4 sec.
JP LE,R5R5
LD FLAGS,#00
CP %2F,#10   ;IF VALUE AT REG. 2FH <= 10
JP LE,R4R4   ;JUMP TO R4R4:
LD %2F,#00   ;ELSE, VALUE AT REG. 2FH=ZERO [Ts=.1SEC, T1=.01SEC]
CALL CALC    ;call function CALC
JP R4R4      ;TRY NEXT POINT
R5R5:
DI
LD TMR,#00
LD %F6,#0    ;STOP MOTOR, ENDED
LD %02,#140  ;OPEN PORT-2
OR %03,#%10  ;LATCH OPEN [P34='1']
IRET
;   ********** MAIN PROGRAM ENDED **********
;
;     [FUNCTIONS CALC, MUL, DIV, IRQ2, IRQ5;]
;
CALC:
;-------- X2 COMPUTATIONS ----------
LD %23,%22  ;X1(t-Ts) TO REG. %23
COM %23
INC %23     ;2'S COMPLEMENT OF REG. 23H
LD %21,%25  ;UPDATE X1
LD %34,#00
ADD %23,%21 ;X1(t)-X1(t-Ts) AT REG. %23
LD FLAGS,#00
CP %23,#00
JP GE,PLUS
COM %23
INC %23
```

```
LD %2F,#00   ;REG. 2FH USED FOR THE T1 .1SEC COUNTER
LD %30,#00   ;REG. 30H, DIRECTION SENSOR [SET + DIRECTION]  FOR
          ;THE POSITIVE VOLTAGE [TABLE-A,SECTION IV.1.4]
LD %31,#20   ;AAA=20 AT REG. 31H,[THETA/U]=[AAA/S(S+BBB)]
LD %32,#1    ;BBB AT REG.32H
  ;REG. %33 IS IN USE DURING CALCULATIONS
LD %34,#00   ;CHECK SIGN REG. OF X2 AT REG. %25
LD %35,#00   ;CHECK SIGN REG. OF X1 AT REG. %21
  ; IN computations reg. 32H is not used
;   ********** MAIN PROGRAM **********
EI
CALL CALC
R4R4:
LD FLAGS,#00
CP %25,#00    ;TERMINATION CONDITION, checking reg. 25 [x1=0] in 1e-4 sec.
JP LE,R5R5
LD FLAGS,#00
CP %2F,#10   ;IF VALUE AT REG. 2FH <= 10
JP LE,R4R4   ;JUMP TO R4R4:
LD %2F,#00   ;ELSE, VALUE AT REG. 2FH=ZERO [Ts=.1SEC, T1=.01SEC]
CALL CALC    ;call function CALC
JP R4R4      ;TRY NEXT POINT
R5R5:
DI
LD TMR,#00
LD %F6,#0    ;STOP MOTOR, ENDED
LD %02,#140  ;OPEN PORT-2
OR %03,#%10  ;LATCH OPEN [P34='1']
IRET
;   ********** MAIN PROGRAM ENDED **********
;
;     [FUNCTIONS CALC, MUL, DIV, IRQ2, IRQ5;]
;
CALC:
;-------- X2 COMPUTATIONS ----------
LD %23,%22  ;X1(t-Ts) TO REG. %23
COM %23
INC %23     ;2'S COMPLEMENT OF REG. 23H
LD %21,%25  ;UPDATE X1
LD %34,#00
ADD %23,%21 ;X1(t)-X1(t-Ts) AT REG. %23
LD FLAGS,#00
CP %23,#00
JP GE,PLUS
COM %23
INC %23
```

```
LD %2F,#00   ;REG. 2FH USED FOR THE T1 .1SEC COUNTER
LD %30,#00   ;REG. 30H, DIRECTION SENSOR [SET + DIRECTION]  FOR
          ;THE POSITIVE VOLTAGE [TABLE-A,SECTION IV.1.4]
LD %31,#20   ;AAA=20 AT REG. 31H,[THETA/U]=[AAA/S(S+BBB)]
LD %32,#1    ;BBB AT REG.32H
  ;REG. %33 IS IN USE DURING CALCULATIONS
LD %34,#00   ;CHECK SIGN REG. OF X2 AT REG. %25
LD %35,#00   ;CHECK SIGN REG. OF X1 AT REG. %21
 ; IN computations reg. 32H is not used
;  ********** MAIN PROGRAM **********
EI
CALL CALC
R4R4:
LD FLAGS,#00
CP %25,#00    ;TERMINATION CONDITION, checking reg. 25 [x1=0] in 1e-4 sec.
JP LE,R5R5
LD FLAGS,#00
CP %2F,#10   ;IF VALUE AT REG. 2FH <= 10
JP LE,R4R4   ;JUMP TO R4R4:
LD %2F,#00   ;ELSE, VALUE AT REG. 2FH=ZERO [Ts=.1SEC, T1=.01SEC]
CALL CALC    ;call function CALC
JP R4R4      ;TRY NEXT POINT
R5R5:
DI
LD TMR,#00
LD %F6,#0    ;STOP MOTOR, ENDED
LD %02,#140  ;OPEN PORT-2
OR %03,#%10  ;LATCH OPEN [P34='1']
IRET
;   ********** MAIN PROGRAM ENDED **********
;
;     [FUNCTIONS CALC, MUL, DIV, IRQ2, IRQ5;]
;
CALC:
;------- X2 COMPUTATIONS ----------
LD %23,%22  ;X1(t-Ts) TO REG. %23
COM %23
INC %23     ;2'S COMPLEMENT OF REG. 23H
LD %21,%25  ;UPDATE X1
LD %34,#00
ADD %23,%21 ;X1(t)-X1(t-Ts) AT REG. %23
LD FLAGS,#00
CP %23,#00
JP GE,PLUS
COM %23
INC %23
```

```
LD %2F,#00   ;REG. 2FH USED FOR THE T1 .1SEC COUNTER
LD %30,#00   ;REG. 30H, DIRECTION SENSOR [SET + DIRECTION]  FOR
          ;THE POSITIVE VOLTAGE [TABLE-A,SECTION IV.1.4]
LD %31,#20   ;AAA=20 AT REG. 31H,[THETA/U]=[AAA/S(S+BBB)]
LD %32,#1    ;BBB AT REG.32H
  ;REG. %33 IS IN USE DURING CALCULATIONS
LD %34,#00   ;CHECK SIGN REG. OF X2 AT REG. %25
LD %35,#00   ;CHECK SIGN REG. OF X1 AT REG. %21
 ; IN computations reg. 32H is not used
;   ********** MAIN PROGRAM **********
EI
CALL CALC
R4R4:
LD FLAGS,#00
CP %25,#00    ;TERMINATION CONDITION, checking reg. 25 [x1=0] in 1e-4 sec.
JP LE,R5R5
LD FLAGS,#00
CP %2F,#10   ;IF VALUE AT REG. 2FH <= 10
JP LE,R4R4   ;JUMP TO R4R4:
LD %2F,#00   ;ELSE, VALUE AT REG. 2FH=ZERO [Ts=.1SEC, T1=.01SEC]
CALL CALC    ;call function CALC
JP R4R4      ;TRY NEXT POINT
R5R5:
DI
LD TMR,#00
LD %F6,#0    ;STOP MOTOR, ENDED
LD %02,#140  ;OPEN PORT-2
OR %03,#%10  ;LATCH OPEN [P34='1']
IRET
;   ********** MAIN PROGRAM ENDED **********
;
;     [FUNCTIONS CALC, MUL, DIV, IRQ2, IRQ5;]
;
CALC:
;-------- X2 COMPUTATIONS ----------
LD %23,%22  ;X1(t-Ts) TO REG. %23
COM %23
INC %23     ;2'S COMPLEMENT OF REG. 23H
LD %21,%25  ;UPDATE X1
LD %34,#00
ADD %23,%21 ;X1(t)-X1(t-Ts) AT REG. %23
LD FLAGS,#00
CP %23,#00
JP GE,PLUS
COM %23
INC %23
```

```
LD %2F,#00   ;REG. 2FH USED FOR THE T1 .1SEC COUNTER
LD %30,#00   ;REG. 30H, DIRECTION SENSOR [SET + DIRECTION]  FOR
          ;THE POSITIVE VOLTAGE [TABLE-A,SECTION IV.1.4]
LD %31,#20   ;AAA=20 AT REG. 31H,[THETA/U]=[AAA/S(S+BBB)]
LD %32,#1    ;BBB AT REG.32H
  ;REG. %33 IS IN USE DURING CALCULATIONS
LD %34,#00   ;CHECK SIGN REG. OF X2 AT REG. %25
LD %35,#00   ;CHECK SIGN REG. OF X1 AT REG. %21
 ; IN computations reg. 32H is not used
;   ********************* MAIN PROGRAM *********************
EI
CALL CALC
R4R4:
LD FLAGS,#00
CP %25,#00    ;TERMINATION CONDITION, checking reg. 25 [x1=0] in 1e-4 sec.
JP LE,R5R5
LD FLAGS,#00
CP %2F,#10   ;IF VALUE AT REG. 2FH <= 10
JP LE,R4R4   ;JUMP TO R4R4:
LD %2F,#00   ;ELSE, VALUE AT REG. 2FH=ZERO [Ts=.1SEC, T1=.01SEC]
CALL CALC    ;call function CALC
JP R4R4      ;TRY NEXT POINT
R5R5:
DI
LD TMR,#00
LD %F6,#0    ;STOP MOTOR, ENDED
LD %02,#140  ;OPEN PORT-2
OR %03,#%10  ;LATCH OPEN [P34='1']
IRET
;   ******************* MAIN PROGRAM ENDED *********************
;
;     [FUNCTIONS CALC, MUL, DIV, IRQ2, IRQ5;]
;
CALC:
;-------- X2 COMPUTATIONS ----------
LD %23,%22  ;X1(t-Ts) TO REG. %23
COM %23
INC %23     ;2'S COMPLEMENT OF REG. 23H
LD %21,%25  ;UPDATE X1
LD %34,#00
ADD %23,%21 ;X1(t)-X1(t-Ts) AT REG. %23
LD FLAGS,#00
CP %23,#00
JP GE,PLUS
COM %23
INC %23
```

```
LD %2F,#00   ;REG. 2FH USED FOR THE T1 .1SEC COUNTER
LD %30,#00   ;REG. 30H, DIRECTION SENSOR [SET + DIRECTION]  FOR
          ;THE POSITIVE VOLTAGE [TABLE-A,SECTION IV.1.4]
LD %31,#20   ;AAA=20 AT REG. 31H,[THETA/U]=[AAA/S(S+BBB)]
LD %32,#1    ;BBB AT REG.32H
  ;REG. %33 IS IN USE DURING CALCULATIONS
LD %34,#00   ;CHECK SIGN REG. OF X2 AT REG. %25
LD %35,#00   ;CHECK SIGN REG. OF X1 AT REG. %21
 ; IN computations reg. 32H is not used
;   ********** MAIN PROGRAM **********
EI
CALL CALC
R4R4:
LD FLAGS,#00
CP %25,#00    ;TERMINATION CONDITION, checking reg. 25 [x1=0] in 1e-4 sec.
JP LE,R5R5
LD FLAGS,#00
CP %2F,#10   ;IF VALUE AT REG. 2FH <= 10
JP LE,R4R4   ;JUMP TO R4R4:
LD %2F,#00   ;ELSE, VALUE AT REG. 2FH=ZERO [Ts=.1SEC, T1=.01SEC]
CALL CALC    ;call function CALC
JP R4R4      ;TRY NEXT POINT
R5R5:
DI
LD TMR,#00
LD %F6,#0    ;STOP MOTOR, ENDED
LD %02,#140  ;OPEN PORT-2
OR %03,#%10  ;LATCH OPEN [P34='1']
IRET
;   ********** MAIN PROGRAM ENDED **********
;
;     [FUNCTIONS CALC, MUL, DIV, IRQ2, IRQ5;]
;
CALC:
;-------- X2 COMPUTATIONS ----------
LD %23,%22  ;X1(t-Ts) TO REG. %23
COM %23
INC %23     ;2'S COMPLEMENT OF REG. 23H
LD %21,%25  ;UPDATE X1
LD %34,#00
ADD %23,%21 ;X1(t)-X1(t-Ts) AT REG. %23
LD FLAGS,#00
CP %23,#00
JP GE,PLUS
COM %23
INC %23
```